THE GEOCHEMICAL EVOLUTION OF THE CERRO UTURUNCU MAGMA CHAMBER, SW BOLIVIA AND ITS RELATION TO THE ANDEAN CENTRAL VOLCANIC ZONE

by

Gary Scott Michelfelder

A dissertation submitted in partial fulfillment
of the requirements for the degree

of

Doctor of Philosophy

in

Earth Sciences

MONTANA STATE UNIVERSITY
Bozeman, Montana

January, 2015

DEDICATION

This work is dedicated to my wife, Breanna, for the support, motivation, and insightful discussions.

ACKNOWLEDGEMENTS

First and foremost, I would like to thank my advisor, Todd C. Feeley, for his guidance, support and inspirational enthusiasm for the fields of igneous petrology and volcanology. My committee members, David Mogk, Colin Shaw, and Shanaka (Shan) de Silva provided insightful comments, suggestions and valuable reviews of this research, and participation of David Young (MSU Extended University) as graduate representative is gratefully acknowledged.

Funding for this study was provided by the National Science Foundation Continental Dynamics Program administered by Dr. Feeley. This combined with generous support from the Department of Earth Sciences at MSU and the Veterans Memorial Scholarship from the Rocky Mountain Association of Geologists supported four years of enrollment in the doctoral program. I am thankful for the opportunity to focus on coursework and research and gain experience teaching in this time period and grateful to the people and professional organizations that made it possible.

A special thanks to the other members of the PLUTONS Research Group for insightful discussions, help in the field, and overall collaboration during the project.

Within the department of Earth Sciences, a special thank you my friends and colleagues for sharing their time and helping me in the labs and the field: Alicia Wilder, Jacob Thacker, Jamie Kern, Nick Atwood, Mort Larsen, Dan Ross, Eric Easley, Gillian Arnoux, Helen Lynn, and Whitney Treadway.

TABLE OF CONTENTS

TABLE OF CONTENTS- CONTINUED

TABLE OF CONTENTS- CONTINUED

LIST OF TABLES

LIST OF FIGURES

LIST OF FIGURES – CONTINUED

Figure Page

LIST OF FIGURES – CONTINUED

ABSTRACT

Cerro Uturuncu is a composite volcano located in the back-arc of the Andean Central Volcanic Zone (22.27°S, 67.18°W). The volcano has exclusively erupted crystal-rich andesite and dacite lava flows over the ~800,000 year life span of eruptive activity. This study provides new bulk-rock major- and trace- element, $^{18}O/^{16}O$ isotope ratios, Sr, Nd, and Pb radiogenic isotopic ratios of lava flows, domes, magmatic inclusions and xenoliths. The study also adds major and trace element and Sr isotopic ratios of plagioclase phenocrysts in order to examine the evolution of the magmatic plumbing system beneath Cerro Uturuncu and place the volcanic center in the regional context of the CVZ.

Plagioclase crystals from silicic (andesitic to dacitic) lavas and domes at Volcán Uturuncu exhibit large variations in An contents, textures, and core to rim $^{87}Sr/^{86}Sr$ ratios. Many of the isotopic variations cannot have existed at magmatic temperatures for more than a few thousand years. The crystals likely derived from different locations in the crustal magmatic system and mixed just prior to eruption. Uturuncu magmas initially assimilated crustal rocks with high $^{87}Sr/^{86}Sr$ ratios. The magmas were subsequently modified by frequent recharge of more mafic magmas with lower $^{87}Sr/^{86}Sr$ ratios. A typical Uturuncu silicic magma therefore only attains its final composition just prior to or during eruption.

On an arc-wide scale silicic lavas erupted from three well-characterized composite volcanoes between 21°S and 22°S (Aucanquilcha, Ollagüe, and Uturuncu) display systematically higher K_2O, LILE, REE and HFSE contents and $^{87}Sr/^{86}Sr$ ratios with increasing distance from the arc-front. In contrast, the lavas have systematically lower Al_2O_3, Na_2O, Sr, and Ba contents; LILE/HFSE ratios; $^{143}Nd/^{144}Nd$ ratios; and more negative Eu anomalies. Silicic magmas along the arc-front apparently reflect melting of relatively young, mafic composition amphibolitic source rocks with the continental crust becoming increasingly older with a more felsic bulk composition toward the east. This results from progressively smaller degrees of mantle partial melting, primary melt generation, and crustal hybridization with distance from the arc-front.

CHAPTER ONE

INTRODUCTION

In recent years, the ties between plutonism and volcanism have been hotly debated (Glazner et al., 2004; Bachman et al., 2007; de Silva and Gosnold, 2007; Huber et al., 2011; and the reference therein). This debate has focused on whether plutonism related to volcanism is different from plutonism without volcanism. Crustal magmatism plays a fundamental role in the generation of continental crust and the thermal and rheological evolution of mountain belts and plateaus. Large-scale melting of the continental crust is manifest as both granite batholith intrusions and large-volume volcanic eruptions (ignimbrites). While there is compelling evidence that at least some large ignimbrites are the erupted upper parts of pluton-scale silicic magma chambers (e.g., Lipman, 2007), there is a long history of controversy over whether the intrusive and extrusive records of magmatism occur simultaneously, or indeed, are related at all (e.g., Bachmann et al., 2007).

The debate about the relationship between pluton growth and volcanism exists because it is rare to find geologic evidence of both systems of similar age in the same area. Granite plutons are the integrated result of intrusion over hundreds of thousands to millions of years, and typically studied as fossil systems exposed by erosion. Volcanic rocks record information on magma bodies at a single moment in time (although the system may have been perturbed by the eruption process), but typically are eroded away by the time that the intrusions are exposed.

The question of how magma accumulates in intrusions or extrusions is of more than academic interest. For example, a common style of volcanism in the central Andes is the eruption of large volume ignimbrites (VEI = 7 to 8; hundreds to thousands of km^3) and formation of calderas (e.g., de Silva, 1989; de Silva et al., 2006a). Fortunately, these super-eruptions (defined as more than 300 km^3 of magma erupted; Sparks et al., 2005) are extremely rare, with a global recurrence interval of more than 10,000 years, such that there is less than a 1% chance of such an eruption occurring in the 21st century (Mason et al., 2004; Self, 2006). On the other hand, an eruption does not have to be "super" to have a strong impact on regional or global climate. For example, a repeat of the VEI = 6 Tambora, Indonesia eruption of 1815 (30-40 km^3), has the potential for global catastrophe (e.g., Self, 2006) and a 10-50% chance of occurrence in the 21st century (Sparks et al., 2005). While current technology may be able to detect evidence of an impending large eruption months to years in advance, it is not clear whether it is possible to forecast the magnitude or exact timing of such an eruption (Lowenstern et al., 2006).

Research Goals

The objectives of this project were to characterize the location, size and potentially the percent melt of the potential magma chamber(s) beneath Cerro Uturuncu located in the back-arc of the Central Volcanic Zone (CVZ) in SW Bolivia. The following chapters examine the processes occurring in and the evolution of the magma chamber feeding Cerro Uturuncu and its relationship to the CVZ through focused isotopic and petrologic investigations. The specific goals of this work answered three primary

questions. First, how did the magma chamber evolve over time and what processes affected magma composition during the magmatic evolution of the system? Second, what extent does Uturuncu represents a manifestation of Altiplano- Puna Volcanic Complex (APVC) magmatism, and is large-scale hybridization of the continental crust by intrusion beneath long-lived volcanic centers a continental dynamic phenomenon of general importance? Finally, how does this volcanic center relate to the big picture of magmatism in the CVZ?

Manuscript Summaries

The following three manuscripts describe the processes timescales and evolution of Cerro Uturuncu and places the center in the context of the CVZ. The first manuscript, titled "*The volcanic evolution of Cerro Uturuncu: A high-K, composite volcano in the back-arc of the central Andes of SW Bolivia*," was submitted and accepted to a special issue of the *International Journal of Geosciences* focusing on volcanic eruption research. This manuscript discusses the volcanic evolution of Cerro Uturuncu and the phases of volcanism that produced the cone that is present today.

The lack of comprehensive studies on individual back-arc composite volcanoes in the CVZ prompted a detailed field, petrologic and geochemical study of Uturuncu. The objectives of this manuscript are to discuss the volcanic evolution of an individual back-arc composite volcano and broadly assess petrogenetic processes affecting magma composition in the back-arc of the CVZ. This study of Uturuncu results from a reconnaissance petrologic and geophysical investigation by Sparks et al. (2008).

Currently, the system is in a period of dormancy as the most recent eruption occurred at ~270 ka. Relatively long periods of quiescence are common at composite volcanoes, as they have been observed at other intermediate composition systems in the CVZ. In this paper, we build on the reconnaissance investigation of Sparks et al. (2008) by furthering discussion of the volcanic history, field relationships, and petrography of volcanic rocks at Uturuncu. The final objective of the manuscript presents a broad geochemical model to account for the restricted compositional diversity of magmas erupted at the volcano.

The second manuscript, titled "*Crustal differentiation processes at Cerro Uturuncu, Andean Central Volcanic Zone, SW Bolivia*," has been prepared for submission to a special issue of *Geosphere* focusing on the NSF and NERC PLUTONS research project. The focus of the manuscript is to determine the petrologic processes, sources of contaminants and time-scales of magmatic processes that occurred during migration from source to eruption. This was completed by studies of crystal isotope stratigraphy (CIS; Davidson et al., 2007) of mineral phases found in the lava flows and domes.

Linear trends in bulk-rock compositions of volcanic rocks from Cerro Uturuncu represent the sum of the components and the integrated effects that define the system from the magmatic source to final crystallization and eruption (Tepley et al., 1999; 2000). However, bulk-rock compositions impose inherent limitations on petrologic interpretations. While it is straightforward to distinguish components in a suite with bulk-mineral or bulk-rock data, it is difficult to determine where in the crust a process

occurred, time-scales of the process, and order of events when multiple processes/ events are suspected (Ramos and Tepley, 2008).

Differentiated and hybridized magmas often-record isotopic signatures prior to and during differentiation and hybridization in early formed, well-preserved crystal cores and growth rims (Davidson et al., 2007; Ramos and Tepley, 2008). Studies of crystal-isotope stratigraphy (textural, chemical, and isotopic analysis of single crystals and growth zones within crystals) have shown that sub-mineral scale trace element compositions and isotopic ratios express more variation within a single unit than is seen in the entire suite of rocks (Davidson et al., 2007). Isotopic and trace element analyses of individual mineral components in volcanic rocks have been shown to be extremely valuable in identifying and isolating the effects of magmatic processes (Davidson et al., 2007; Ginibre and Davidson, 2014), and record detailed information on the processes affecting crystallization that are in contrast to bulk-rock analyses.

At Cerro Uturuncu, textures, major element and Sr isotopic data of plagioclase phenocrysts suggests that while magma mixing was an important process that possibly triggered eruption, and created limited compositional diversity in bulk-rock trends, the process played a limited role in the differentiation of the magma. One-dimensional diffusion modeling suggests that observed isotopic crystal heterogeneities could not have existed for more than a few thousand years at inferred magmatic temperatures. The chemical and isotopic variability observed in Uturuncu phenocrysts within a single lava flow or dome suggest that although shallow crustal assimilation and magma mixing appear to have had limited effect on whole rock chemistry, a complex late-stage

petrogenetic history is recorded within the magmatic cargo of crystals and magmatic inclusions.

The final manuscript, titled "*Modification of the continental crust by subduction zone magmatism and vice-versa: Across-strike geochemical variations of silicic lavas from individual eruptive centers in the Andean Central Volcanic Zone*," was submitted and accepted to a special issue of *Geosciences* focusing on continental accretion and evolution. This manuscript places Cerro Uturuncu into the regional context of the CVZ and examines the similarities and differences of magma differentiation between young silicic volcanic centers from the arc-front to the back-arc. This information is used to shed light on how the continental crust may influence across-arc trends in magma chemistry. Associated with active eastward subduction of the oceanic Nazca plate beneath the continental South American plate, the CVZ represents an end member in subduction zone systems on Earth because the continental crust is thicker (70–80 km) than at any other convergent margin setting (Beck et al., 1996; Allmendinger et al., 1997; McGlashan et al., 2008). The centers examined in this manuscript were selected because of the young and limited range in ages (<1 Ma), quality and availability of comprehensive data sets (including isotopic data), and similarity in eruptive histories (*i.e.*, effusive eruptions from andesitic to dacitic composite cones). In addition, we selected centers that span the range of volcanic activity in the arc, but show a small N-S coverage area, in order to minimize potential along-arc variations in magma sources and processes. These restrictions allow for a more focused examination relative to larger regional studies. Previous regional-scale studies of magmatism in the southern Altiplano

region documented eastward increases in K_2O and related incompatible trace elements virtually identical to across-strike geochemical trends observed at many oceanic island arcs and continental arcs constructed on thin crust (Feeley, 1993).

References

Allmendinger, R. W., Jordan, T. E., Kay, S. M., and Isacks, B. L., 1997, The evolution of the Altiplano-Puna plateau of the Central Andes: Annual Review of Earth and Planetary Sciences, v. 25, p. 139-174.

Bachmann, O., Charlier, B. L. A., and Lowenstern, J. B., 2007, Zircon crystallization and recycling in the magma chamber of the rhyolitic Kos Plateau Tuff (Aegean arc): Geology, v. 35, no. 1, p. 73-76.

Beck, S. L., and Zandt, G., 2002, The nature of orogenic crust in the central Andes: Journal of Geophysical Research-Solid Earth, v. 107, no. B10.

Davidson, J. P., Morgan, D. J., and Charlier, B. L. A., 2007, Isotopic microsampling of magmatic rocks: Elements, v. 3, no. 4, p. 253-259.

de Silva, S. L., and Gosnold, W. D., 2007, Episodic construction of batholiths: Insights from the spatiotemporal development of an ignimbrite flare-up: Journal of Volcanology and Geothermal Research, v. 167, no. 1-4, p. 320-335.

de Silva, S. L., 1989, Altiplano-Puna Volcanic Complex of the Central Andes: Geology, v. 17, no. 12, p. 1102-1106.

de Silva, S. L., Zandt, G., Trumbull, R., Viramonte, J., Salas, G., Jiminez, N., 2006, Large ignimbrite eruptions and volcano-tectonic depressions in the Central Andes: a thermomechanical perspective, *in* Troise, C., De Natale, G., Kilburn, C.R.J. , ed., Mechanisms of activity and unrest at large calderas, Geological Society Special Publication No. 269, Volume 269: London, The Geologic Society, p. 47-63.

Feeley, T. C., 1993, Crustal Modification during Subduction-Zone Magmatism: Evidence from the Southern Salar De Uyuni Region (20^o-22^o S), Central Andes: Geology, v. 21, no. 11, p. 1019-1022.

Ginibre, C., and Davidson, J.P., 2014, Sr isotope zoning in plagioclase from Prainacota Volcano (Northern Chile): Quantifying magma mixing and crustal contamination: Journal of Petrology, v. 55, no. 6, p. 1203-1238.

Glazner, A., Bartley, J. M., Coleman, D. S., Gray, W., and Taylor, R. Z., 2004, Are plutons assembled over millions of years by amalgamation from small magma chambers?: GSA Today, v. 14, no. 4/5, p. 4-11.

Huber, C., Bachmann, O., and Dufek, J., 2011, Thermo-mechanical reactivation of locked crystal mushes: Melting-induced internal fracturing and assimilation

processes in magmas: Earth and Planetary Science Letters, v. 304, no. 3-4, p. 443-454.

Lipman, P. W., 2007, Incremental assembly and prolonged consolidation of Cordilleran magma chambers: Evidence from the Southern Rocky Mountain volcanic field: Geosphere, v. 3, no. 1, p. 42-70.

Lowenstern, J. B., Charlier, B. L. A., Clynne, M. A., and Wooden, J. L., 2006, Extreme U-Th disequilibrium in rift-related basalts, rhyolites and granophyric granite and the timescale of rhyolite generation, intrusion and crystallization at Alid volcanic center, Eritrea: Journal of Petrology, v. 47, no. 11, p. 2105-2122.

Mason, B. G., Pyle, D. M., and Oppenheimer, C., 2004, The size and frequency of the largest explosive eruptions on Earth: Bulletin of Volcanology, v. 66, no. 8, p. 735-748.

McGlashan, N., Brown, L., and Kay, S. M., 2008, Crustal thickness in the central Andes from teleseismically recorded depth phase precursors: Geophysical Journal International, v. 175, no. 3, p. 1013-1022.

Ramos, F. C., and Tepley, F. J., 2008, Inter- and Intracrystalline Isotopic Disequilibria: Techniques and Applications, *in* Putirka, K.D, and Tepley, F.J., eds., Minerals, Inclusions and Volcanic Processes: Reviews in Mineralogy and Geochemistry v. 69, p. 403-443.

Self, S., 2006, The effects and consequences of very large explosive volcanic eruptions: Philosophical Transactions of the Royal Society A: Mathematical, Physical and Engineering Sciences, v. 364, no. 1845, p. 2073-2097.

Sparks, R.S.J., Self, S., Grattan, J.P., Oppenheimer, C., Pyle, D.M., and Rymer, H., 2005, Super-eruptions: Global effects and future threats. Report of a Geological Society of London working group, v. 24, London, UK: The Geological Society.

Sparks, R. S. J., Folkes, C. B., Humphreys, M. C. S., Barfod, D. N., Clavero, J., Sunagua, M. C., McNutt, S. R., and Pritchard, M. E., 2008, Uturuncu volcano, Bolivia: Volcanic unrest due to mid-crustal magma intrusion: American Journal of Science, v. 308, no. 6, p. 727-769.

Tepley, F. J., Davidson, J. P., and Clynne, M. A., 1999, Magmatic Interactions as Recorded in Plagioclase Phenocrysts of Chaos Crags, Lassen Volcanic Center, California: Journal of Petrology, v. 40, no. 5, p. 787-806.

Tepley, F. J., Davidson, J. P., Tilling, R. I., and Arth, J. G., 2000, Magma mixing, recharge and eruption histories recorded in plagioclase phenocrysts from El Chichon Volcano, Mexico: Journal of Petrology, v. 41, no. 9, p. 1397-1411.

CHAPTER TWO

BACKGROUND GEOLOGY OF THE ANDEAN CENTRAL VOLCANIC ZONE

The Andean Central Volcanic Zone

The Andean Central Volcanic Complex (CVZ; Fig. 1) provides an excellent location to observe and characterize volcanic deposits. Volcanism within the Andes range is associated with the subduction of the Nazca plate beneath South America. Variations in dip angle and crustal thickness have created three distinct zones: the Northern Volcanic Zone (NVZ), ranging from Columbia to Peru; the Central Volcanic Zone, ranging from Peru to central Chile; and the Southern Volcanic Zone (SVZ), ranging from central Chile to southern Chile. The CVZ is the zone in which the Cerro Uturuncu is constructed.

The CVZ back-arc is the type-locality for continental arc volcanism (Feeley and Davidson, 1994; de Silva, 1989; de Silva and Francis, 1991; de Silva and Gosnold, 2007; de Silva et al., 2006, 2008; Davidson et al,. 1991; Sparks et al. 2008). The modern central Andes at 19°–24° S latitude are divided into three north- to north-west striking geological and upper crustal provinces. From west to east these are: (1) the Western Cordillera: an active volcanic arc bounded on the west by a westward dipping monocline; (2) the Altiplano: a broad, elevated plateau (>3800 m) where undeformed late-Miocene and younger volcanic rocks overlie variably folded and faulted mid-Miocene and older sedimentary and volcanic rocks; and (3) the Eastern Cordillera: a major east-verging thrust complex involving Paleozoic to Mesozoic sedimentary and metamorphic rocks.

The youngest rocks in the southern Altiplano region of the CVZ were erupted following relatively recent changes in the subduction history of the CVZ. These changes are related to breakup of the Farallon plate into the Cocos and the Nazca plates, which increased the rate of subduction beneath the South American plate (Kay et al., 1999; Somoza and Ghidella, 2005; 2012). Between 15° and 28° S latitude the present day subduction angle of ~30° allows for an expression of magmatism that is absent from 2° to 15° S where the subduction angle is between 5° and 10° (Somoza and Ghidella, 2005; 2012). Uplift of the Altiplano and thickening of the CVZ crust are believed to be related, in part, to the recent steepening of the subducting slab (Isacks, 1988; Kay et al., 1999; 2009).

Late Cenozoic to modern volcanic rocks in the CVZ are divided into three groups based on similarities in composition and eruptive style (Thorpe et al., 1982; Feeley et al., 1993). First, between 21-24° S, large-volume, regionally extensive ignimbrites erupted from large caldera complexes on the Altiplano and Western Cordillera in a volcanic complex known as the Altiplano- Puna Volcanic Complex (APVC; ~10 Ma- 1 Ma;Coira et al., 1982; de Silva, 1989a; 1989b). These rocks are calc-alkaline, homogeneous dacites to rhyolites. Second, basaltic andesite to dacite lava flows erupted from 23 Ma to the present. At 21°–22° S, the largest volumes of these magmas erupted from composite volcanoes that form the peaks of the Western Cordillera. Baker and Francis (1978) estimated that the Western Cordillera contains ~3000 km^3 of these lava flows. Lava flows associated with composite volcanoes extend for ~200 km eastward onto the Altiplano, although volumes decrease sharply to <800 km^3. Third, volumetrically minor alkali

basalts erupted from small monogenetic centers to the east of the arc-front on the Altiplano north of 21° S (de Silva et al., 1993; Davidson and de Silva, 1995).

The CVZ back-arc volcanic rocks contain a distinct isotopic and geochemical signature from the arc front. They present with strongly enriched incompatible trace elements compositions and lower $^{143}Nd/^{144}Nd$ ratio (<0.5123) and higher $^{87}Sr/^{86}Sr$ (<0.705) ratios compared to the arc-front (Fig. 2; Davidson and de Silva, 1995). Isotopic variation within CVZ is abundant at a local scale suggesting that control of geochemical variation is basement material and supports a crustal contamination hypothesis creating the compositional diversity observed in the CVZ (Wörner et al., 1992; Mamani et al., 2008; 2010).

The Altiplano-Puna Volcanic Complex (APVC) extends from 21^{o}-24^{o}S covering more than 70,000 km^2. It composes the largest young ignimbrite complex on earth (de Silva, 1989). The APVC has a complex magmatic history. Between the late Tertiary and the late Miocene, magmatism was dominated by effusive andesitic eruptions. The second phase (late Miocene to present) produced the large ignimbrite complex erupting an estimated 15,000 km^3 of dacitic ignimbrite (de Silva et al., 2006). The ignimbrites of the APVC are considered a “monotonous intermediate” genre (Hildreth, 1981) in that they are crystal-rich, high-K, calc-alkaline dacite to rhyodacite with occasional rhyolites and andesites. Models proposed for the production of these ignimbrites using radiogenic isotopes and trace elements require at least 30% mantle derived melt mixed with crustal material between 15-30 km depth (de Silva and Gosnold, 2007; de Silva, 1989a; de Silva

et al., 2006a; Coira et al., 1993; Ort et al., 1996; Schmitt et al., 2001; Lindsay et al., 2001a; 2001b).

Cerro Uturuncu

Cerro Uturuncu is an andesite to dacite composite volcano located in the southern Altiplano region of the CVZ, approximately 120 km east of the arc-front (Fig.1). The volcano was primarily active between 1Ma and 250 ka (Muir, personal communication). Volcanic activity remains active at Uturuncu through degassing at the summit, but the most recent eruption was dated at 250 ka (Muir, personal communication). Construction of the cone took place in one phase of volcanism erupting approximately 89km^3 of material. Most flows and domes sampled by Sparks et al. (2008) and in this study contain undercooled andesitic magmatic inclusions that compose no more than a few volume percent of the host rocks. In many older rocks, magmatic inclusions are rarer (Sparks et al. 2008). This relationship is similar to that seen at Volcán Aucanquilcha (Klemetti and Grunder, 2008) and Volcán Ollagüe (Feeley et al., 1993) where magmatic inclusions are typically more abundant in younger lavas.

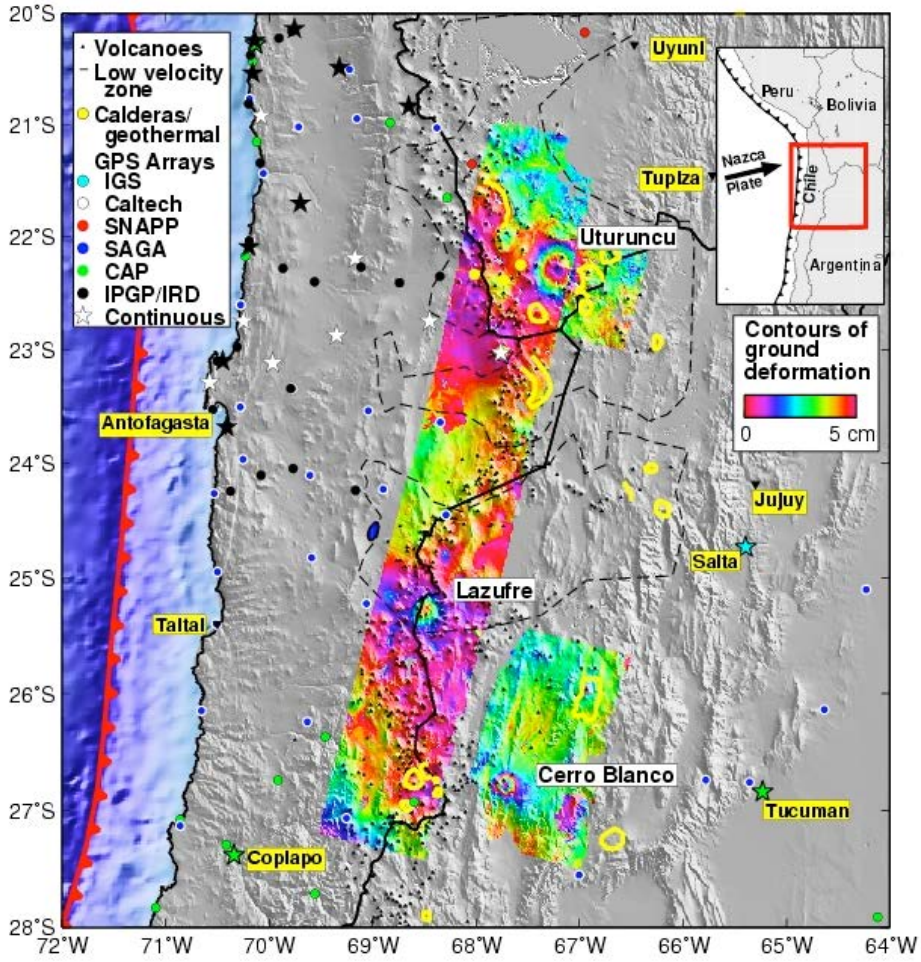

Figure 1. Context map showing the location of Cerro Uturuncu in the Andean Central Volcanic Zone. Interferograms from interference synthetic aperture radar (InSAR) are shown in color and correspond to contours of ground deformation in the line of sight of the satellite radar beam between 1996-2000. The approximate location of the seismic low velocity zone is shown as the black dotted line (Yuan et al., 2000), but the area of inferred partial melt is spatially smaller (e.g., Zandt et al., 2003). GPS stations are shown as blue circles (e.g., Klotz et al., 2001; Kendrick et al., 2001; Chlieh et al., 2004). Small black dots show the 1113 volcanoes from the de Silva and Francis (1991) database. Some calderas from the last 10 Ma and active geothermal fields are shown in yellow (de Silva and Francis, 1991). Selected cities are labeled in yellow.

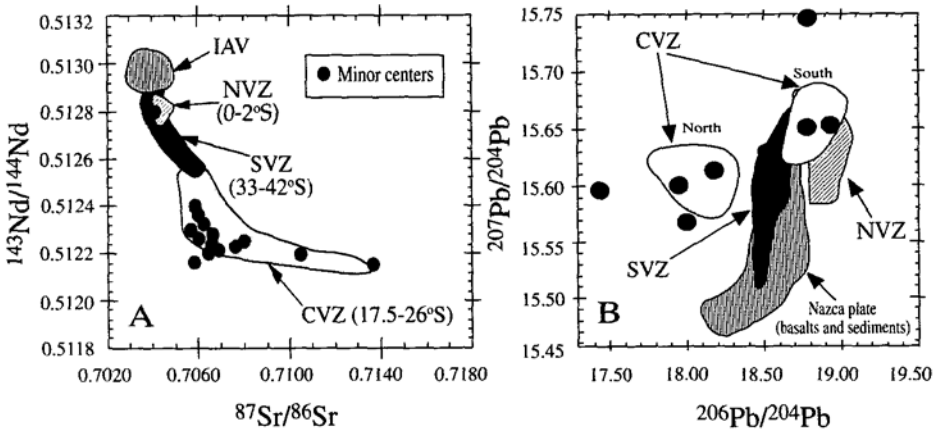

Figure 2. Sr and Nd isotope ratios of CVZ volcanic centers excluding calderas. Centers are compared to island-arc volcanic rocks (IAV) and the northern and southern Andes volcanic zones (NVZ; SVZ). Pb isotopes of the same volcanic centers compared to volcanic material within the North and South Volcanic Arc and subducted Nazca plate material. From Davidson and de Silva (1992).

References

Chlieh, M., De Chabalier, J., Ruegg, J., Armijo, R., Dmowska, R., Campos, J., and Feigl, K., 2004, Crustal deformation and fault slip during the seismic cycle in the North Chile subduction zone, from GPS and InSAR observations: Geophysical Journal International, v. 158, no. 2, p. 695-711.

Coira, B., Kay, S. M., and Viramonte, J., 1993, Upper Cenozoic magmatic evolution of the Argentine Puna—a model for changing subduction geometry: International Geology Review, v. 35, no. 8, p. 677-720.

Davidson, J. P., and de Silva, S. L., 1992, Volcanic-Rocks from the Bolivian Altiplano - Insights into Crustal Structure, Contamination, and Magma Genesis - Reply: Geology, v. 21, no. 12, p. 1148-1148.

-, 1995, Late Cenozoic Magmatism of the Bolivian Altiplano: Contributions to Mineralogy and Petrology, v. 119, no. 4, p. 387-408.

Davidson, J. P., Hannon, R.S., and Womer, G., 1991, The source of central Andean magmas; some considerations, *in* Hannon, R. S., and Rapela, C.W., ed., Andean magmatism and its tectonic setting, Volume 265: Denver, Geological Society of America, p. 825-843.

de Silva, S., Salas, G., and Schubring, S., 2008, Triggering explosive eruptions—The case for silicic magma recharge at Huaynaputina, southern Peru: Geology, v. 36, no. 5, p. 387-390.

de Silva, S. L., 1989a, Altiplano-Puna Volcanic Complex of the Central Andes: Geology, v. 17, no. 12, p. 1102-1106.

De Silva, S.L., 1989b, Geochronology and stratigraphy of the ignimbrites from the 21° 30’ S to 23°30’ S portion of the Central Andes of northern Chile. Journal of Volcanology and Geothermal Research: v. 37, 93-131.

de Silva, S. L., Davidson, J. P., Croudace, I. W., and Escobar, A., 1993, Volcanological and Petrological Evolution of Volcan Tata Sabaya, Sw Bolivia: Journal of Volcanology and Geothermal Research, v. 55, no. 3-4, p. 305-335.

de Silva, S. L., and Francis, P. W., 1991, Volcanoes of the Central Andes, New York, Springer-Verlag, p. 216.

de Silva, S. L., and Gosnold, W. D., 2007, Episodic construction of batholiths: Insights from the spatiotemporal development of an ignimbrite flare-up: Journal of Volcanology and Geothermal Research, v. 167, no. 1-4, p. 320-335.

de Silva, S. L., Zandt, G., Trumbull, R., Viramonte, J., Salas, G., Jiminez, N., 2006, Large ignimbrite eruptions and volcano-tectonic depressions in the Central Andes: a thermomechanical perspective, *in* Troise, C., De Natale, G., Kilburn, C.R.J. , ed., Mechanisms of activity and unrest at large calderas, Geological Society Special Publication No. 269, Volume 269: London, The Geologic Society, p. 47-63.

Feeley, T. C., and Davidson, J. P., 1994, Petrology of Calc-Alkaline Lavas at Volcan-Ollague and the Origin of Compositional Diversity at Central Andean Stratovolcanoes: Journal of Petrology, v. 35, no. 5, p. 1295-1340.

Feeley, T. C., Davidson, J. P., and Armendia, A., 1993, The Volcanic and Magmatic Evolution of Volcan Ollague, a High-K, Late Quaternary Stratovolcano in the Andean Central Volcanic Zone: Journal of Volcanology and Geothermal Research, v. 54, no. 3-4, p. 221-245.

Feeley, T. C., and Sharp, Z. D., 1995, $^{18}O/^{16}O$ Isotope Geochemistry of Silicic Lava Flows Erupted from Volcan Ollague, Andean Central Volcanic Zone: Earth and Planetary Science Letters, v. 133, no. 3-4, p. 239-254.

Gregory-Wodzicki, K. M., 2000, Uplift history of the Central and Northern Andes: a review: Geological Society of America Bulletin, v. 112, no. 7, p. 1091-1105.

Hildreth, W., 1981, Gradients in Silicic Magma Chambers - Implications for Lithospheric Magmatism: Journal of Geophysical Research, v. 86, no. Nb11, p. 153-192.

Isacks, B. L., 1988, Uplift of the Central Andean Plateau and Bending of the Bolivian Orocline: Journal of Geophysical Research-Solid Earth and Planets, v. 93, no. B4, p. 3211-3231.

Kay, S. M., Coira, B. L., and Kay, R. W., 2009, Central Andean Galan Ignimbrites: Magma evolution from the mantle to eruption in a thickened crust: Geochimica Et Cosmochimica Acta, v. 73, no. 13, p. A630-A630.

Kay, S. M., Mpodzis, C., and Coria, B., 1999, Neogene magmatism, tectonism, and mineral deposits of the Central Andes (22° to 33°S latitude), *in* Skinner, B. J., ed., Geology and Ore deposits of the Central Andes, Volume 7, Society of Economic Geologists, p. 27-59.

Kendrick, E., Bevis, M., Smalley, R., and Brooks, B., 2001, An integrated crustal velocity field for the central Andes: Geochemistry, Geophysics, Geosystems, v. 2, no. 11.

Klemetti, E. W., and Grunder, A. L., 2008, Volcanic evolution of Volcan Aucanquilcha: a long-lived dacite volcano in the Central Andes of northern Chile: Bulletin of Volcanology, v. 70, no. 5, p. 633-650.

Klotz, J., Khazaradze, G., Angermann, D., Reigber, C., Perdomo, R., and Cifuentes, O., 2001, Earthquake cycle dominates contemporary crustal deformation in Central and Southern Andes: Earth and Planetary Science Letters, v. 193, no. 3, p. 437-446.

Lindsay, J. M., de Silva, S., Trumbull, R., Emmermann, R., and Wemmer, K., 2001a, La Pacana caldera, N. Chile: a re-evaluation of the stratigraphy and volcanology of one of the world's largest resurgent calderas: Journal of Volcanology and Geothermal Research, v. 106, no. 1-2, p. 145-173.

Lindsay, J. M., Schmitt, A. K., Trumbull, R. B., De Silva, S. L., Siebel, W., and Emmermann, R., 2001b, Magmatic evolution of the La Pacana caldera system, Central Andes, Chile: Compositional variation of two cogenetic, large-volume felsic ignimbrites: Journal of Petrology, v. 42, no. 3, p. 459-486.

Mamani, M., Tassara, A., and Woerner, G., 2008, Composition and structural control of crustal domains in the central Andes: Geochemistry Geophysics Geosystems, v. 9.

Mamani, M., Worner, G., and Sempere, T., 2010, Geochemical variations in igneous rocks of the Central Andean orocline (13^{o} S to 18^{o} S): Tracing crustal thickening and magma generation through time and space: Geological Society of America Bulletin, v. 122, no. 1-2, p. 162-182.

Mason, B. G., Pyle, D. M., and Oppenheimer, C., 2004, The size and frequency of the largest explosive eruptions on Earth: Bulletin of Volcanology, v. 66, no. 8, p. 735-748.

Neufeld, L., and Roy, J., 2004, Laser ablation solid sampling plasma spectrochemistry - The importance of matching the hardware to the application: Spectroscopy, v. 19, no. 1, p. 16-+.

Ort, M. H., Coira, B. L., and Mazzoni, M. M., 1996, Generation of a crust-mantle magma mixture: Magma sources and contamination at Cerro Panizos, central Andes: Contributions to Mineralogy and Petrology, v. 123, no. 3, p. 308-322.

Schmitt, A. K., de Silva, S. L., Trumbull, R. B., and Emmermann, R., 2001, Magma evolution in the Purico ignimbrite complex, northern Chile: evidence for zoning of a dacitic magma by injection of rhyolitic melts following mafic recharge: Contributions to Mineralogy and Petrology, v. 140, no. 6, p. 680-700.

Somoza, R., and Ghidella, M.E., 2005, Convergencia en el margen occidental de América del Sur durante el Cenozoico: subducción de las placas de Nazca, Farallon y Phoenix: Rev. Asoc. Geol. Argent, v. 60, p. 797-809.

Somoza R., G., M.E., 2012, Late Cretaceous to recent plate motioins in western South America revisited: Earth and Planetary Science Letters, v. 331-332, p. 152-163.

Sparks, R. S. J., Folkes, C. B., Humphreys, M. C. S., Barfod, D. N., Clavero, J., Sunagua, M. C., McNutt, S. R., and Pritchard, M. E., 2008, Uturuncu volcano, Bolivia: Volcanic unrest due to mid-crustal magma intrusion: American Journal of Science, v. 308, no. 6, p. 727-769.

Thorpe, R. S., Francis, P.W., Hammill, M. and Baker. M.C.W., 1982, The Andes, *in* Thorpe, R. S., ed., Andesites: New York, Wiley, p. 187-205.

Worner, G., Moorbath, S., and Harmon, R. S., 1992, Andean Cenozoic Volcanic Centers Reflect Basement Isotopic Domains: Geology, v. 20, no. 12, p. 1103-1106.

CHAPTER THREE

GENERAL METHODS

In order to address the questions discussed above this study employed a variety of geochemical methods to characterize Uturuncu magmas and their crystal cargo, on a variety of scales. These data, combined with existing major and trace element data from Sparks et al. (2008), was used in the generation of models for magma genesis and eruption. Bulk-rock isotopic ratios tied to petrogenetic models were used to assess the overall proportions of magma derived from mantle-derived parental melts by crystallization differentiation and crustal melting processes. Bulk-rock samples of Uturuncu volcanic rocks were analyzed for major and trace element compositions at Washington State University, Pullman. Major and trace element compositions for 121 samples were acquired by X-ray fluorescence spectrometry (XRF) on a ThermoARL Advant'XP+ automated sequential wavelength spectrometer. Methods and errors for XRF analyses are described in Johnson et al. (1999). Additional trace element compositions, including the rare earth elements, for 45 samples, were acquired by inductively coupled plasma mass spectrometry (ICP-MS) on an Agilent 7700 ICP-MS. Methods and errors for trace element analyses are presented in detail in Jarvis (1988).

Bulk-rock Nd and Sr isotopic analyses of 30 samples were acquired by Thermal Ionization Mass Spectrometry (TIMS) on a VG Sector 54, and analyzed by five Faraday collectors in dynamic mode at New Mexico State University, Las Cruces. Calibration of $^{87}Sr/^{86}Sr$ ratios was calculated using the $^{86}Sr/^{88}Sr$ ratio analyzed at 3.0 V aiming

intensity and normalized to 0.1194 using NBS 987 Standard (0.710298 + 0.000010) to monitor the precision of the analyses. Sr was isolated using Sr-Spec resin column chromatography by the method described in Ramos and Reid (2005). Nd was separated using REE resin column chromatography using the digested split of prepared sample for Sr chromatography. Nd isotopes were normalized to $^{146}Nd/^{144}Nd = 0.7219$ and results for JNDi-1 were $^{146}Nd/^{144}Nd = 0.512137 \pm 0.000009$ for five analyses. Pb isotopes were separated from the same digested samples used for Sr and Nd isotope ratios. Pb separations used ~2 mL of anion exchange resin in a high-aspect ratio glass column with an eluent of 1*N* HBr and 7*N* HNO_3. Purified samples were then dried and re-dissolved in 1 mL of 2% HNO_3 containing 0.01 ppm Tl. Samples were analyzed on a ThermoFinnigan Neptune multi-collector ICP-MS equipped with nine Faraday collectors and an ion counter. The standard NBS 981 ($^{208}Pb/^{204}Pb \approx 36.662 \pm 0.002$, $^{207}Pb/^{204}Pb \approx 15.462 \pm 0.001$, $^{206}Pb/^{204}Pb \approx 16.928 \pm 0.001$) was used for accuracy corrections and to monitor precision of the analyses. The values measured for NBS 981 were within the error of published ratios for NBS 981 (Todt et al., 1996) and therefore corrections were not applied to unknown sample ratios. Given the young ages of all rocks examined in this study, no age corrections were performed for the radiogenic isotope data.

$\delta^{18}O$ values were determined for 30 Uturuncu samples by the laser fluorination method described by Takeuchi and Larsen (2005) at Washington State University, Pullman. Quartz and plagioclase phenocryst separates were analyzed twice to insure reproducibility. The standard UWG-2 was measured with a difference of 0.2‰ from the published value of 5.89‰ (Valley et al., 1995; Takeuchi and Larsen, 2005). The oxygen

isotope data for Uturuncu rocks was particularly informative as comprehensive phenocryst based laser-fusion data exist for Aucanquilcha and Ollagüe volcanoes on and just east of the arc front (Feeley and Sharp, 1995; Klemetti and Grunder, 2008). Oxygen isotope values of lavas from the arc front volcanoes demonstrate, on a local scale, the strong influence that intrusion of mantle-derived mafic magmas can have on modifying the composition of pre-existing continental crust in lower and upper crustal regions of melt production.

Major and trace element compositions of plagioclase micro-phenocrysts and phenocrysts were determined on a JEOL JXA-8500F field emission electron microprobe/scanning electron microscope (EMPA) with an acceleration voltage of 15 KV at Washington State University, Pullman using the methods described in Ellis et al. (2010). Ten to fifteen phenocrysts and five to ten micro-phenocrysts from 30 lava flows and domes were selected to reduce sample bias. Transects included the core and any rim 15 microns or larger.

Laser ablation multi-collector inductively coupled plasma mass spectrometry (LA-MC-ICPMS) analysis to determine in situ Sr isotopic ratios of plagioclase phenocrysts were performed at Washington State University, Pullman. The analyses were performed using a New Wave^{TM} UP 213 nm Nd: YAG laser ablation system (Jackson, 2001; Neufeld and Roy, 2004) in conjunction with a double focusing Thermo-Finnegan Neptune^{TM} MC-ICPMS equipped with nine Faraday collectors and 10^{-11} Ω resistors. Ablation trenches of 80 microns in diameter and 800 microns long by approximately 15 microns deep for each analysis. Precision of Sr isotopic ratios is within 0.00001 (Ramos

et al., 2004). An in-house reference sample, SRP-1 ($^{87}Sr/^{86}Sr$= 0.70671) was used for calibration and corrections. Analytical procedures for in situ Sr isotope analysis and discussion of data quality and corrections have been addressed by Ramos et al. (2004). EPMA of zones within plagioclase larger than 80 micron in width containing Sr concentrations between 300 and 1000 ppm allowed analysis of zones for the highest quality data (Ramos et al., 2004; Ramos and Tepley, 2008). Whenever possible we combined NDIC imaging (Anderson, 1983; Feeley and Davidson, 1994; Pearce et al., 1987a; 1987b) and electron micro-probe traverses with laser ablation pits to relate textural features, major element chemistry and isotopic compositions.

In chapter 5, we describe the results of crystal- isotope stratigraphy studies performed on plagioclase phenocrysts in rocks spanning the eruptive history of Uturuncu. We focused on plagioclase phenocrysts from lava flows and domes for the following reasons. First, plagioclase is a ubiquitous mineral phase in Uturuncu rocks. Second, the phase typically crystallizes over a broad temperature range, and, therefore, potentially records a significant part of the cooling history of the magmas. Third, plagioclase commonly has high Sr contents (partitioning coefficient of 2.84 to 5.28 for dacite and andesite respectively; Ewart and Griffin, 1994) allowing for isotopic analysis by laser ablation inductively coupled plasma mass spectrometry. Lastly, plagioclase crystals are usually large and display textural features such as growth zones, dissolution surfaces, and overgrowths that are readily identifiable allowing for detailed micro-sampling strategies (Sparks et al., 2008; Charlier et al., 2006; Davidson et al., 2007; Ramos and Tepley, 2008).

References

Anderson, A. T., 1983, Oscillatory Zoning of Plagioclase - Nomarski Interference Contrast Microscopy of Etched Polished Sections: American Mineralogist, v. 68, no. 1-2, p. 125-129.

Charlier, B. L. A., Ginibre, C., Morgan, D., Nowell, G. M., Pearson, D. G., Davidson, J. P., and Ottley, C. J., 2006, Methods for the microsampling and high-precision analysis of strontium and rubidium isotopes at single crystal scale for petrological and geochronological applications: Chemical Geology, v. 232, no. 3-4, p. 114-133.

Davidson, J. P., Morgan, D. J., and Charlier, B. L. A., 2007, Isotopic microsampling of magmatic rocks: Elements, v. 3, no. 4, p. 253-259.

Ellis, B. S., Barry, T., Branney, M. J., Wolff, J. A., Bindeman, I., Wilson, R., and Bonnichsen, B., 2010, Petrologic constraints on the development of a large-volume, high temperature, silicic magma system: The Twin Falls eruptive centre, central Snake River Plain: Lithos, v. 120, no. 3, p. 475-489.

Ewart, A., and Griffin, W., 1994, Application of proton-microprobe data to trace-element partitioning in volcanic rocks: Chemical Geology, v. 117, no. 1, p. 251-284.

Feeley, T. C., and Davidson, J. P., 1994, Petrology of Calc-Alkaline Lavas at Volcan-Ollague and the Origin of Compositional Diversity at Central Andean Stratovolcanoes: Journal of Petrology, v. 35, no. 5, p. 1295-1340.

Feeley, T. C., and Sharp, Z. D., 1995, $^{18}O/^{16}O$ Isotope Geochemistry of Silicic Lava Flows Erupted from Volcan Ollague, Andean Central Volcanic Zone: Earth and Planetary Science Letters, v. 133, no. 3-4, p. 239-254.

Jackson, S. E., 2001, The application of Nd:YAG lasers in LA-ICPMS, *in* Sylvester, P. J., ed., Laser Ablation ICP- Mass Spectrometry in the Earth Sciences: Principles and Application, Volume 29, Mineralogical Association of Canada, p. 29-45.

Jarvis, K. E., 1988, Inductively Coupled Plasma Mass-Spectrometry - a New Technique for the Rapid or Ultra-Trace Level Determination of the Rare-Earth Elements in Geological-Materials: Chemical Geology, v. 68, no. 1-2, p. 31-39.

Johnson, D. M., Hooper P.R., and Conrey, R.M., 1999, GeoAnalytical Lab, Washington State University: Advances in X-ray Analysis, v. 41, p. 843-867.

Klemetti, E. W., and Grunder, A. L., 2008, Volcanic evolution of Volcan Aucanquilcha: a long-lived dacite volcano in the Central Andes of northern Chile: Bulletin of Volcanology, v. 70, no. 5, p. 633-650.

Neufeld, L., and Roy, J., 2004, Laser ablation solid sampling plasma spectrochemistry - The importance of matching the hardware to the application: Spectroscopy, v. 19, no. 1, p. 16-+.

Pearce, T. H., Griffin, M. P., and Kolisnik, A. M., 1987a, Magmatic Crystal Stratigraphy and Constraints on Magma Chamber Dynamics - Laser Interference Results on Individual Phenocrysts: Journal of Geophysical Research-Solid Earth and Planets, v. 92, no. B13, p. 13745-13752.

Pearce, T. H., Russell, J. K., and Wolfson, I., 1987b, Laser-Interference and Nomarski Interference Imaging of Zoning Profiles in Plagioclase Phenocrysts from the May 18, 1980, Eruption of Mount-St-Helens, Washington: American Mineralogist, v. 72, no. 11-12, p. 1131-1143.

Ramos, F. C., and Reid, M. R., 2005, Distinguishing melting of heterogeneous mantle sources from crustal contamination: Insights from Sr isotopes at the phenocryst scale, Pisgah Crater, California: Journal of Petrology, v. 46, no. 5, p. 999-1012.

Ramos, F. C., and Tepley, F. J., 2008, Inter- and Intracrystalline Isotopic Disequilibria: Techniques and Applications: Minerals, Inclusions and Volcanic Processes, v. 69, p. 403-443.

Ramos, F. C., Wolff, J. A., and Tollstrup, D. L., 2004, Measuring Sr-87/Sr-86 variations in minerals and groundmass from basalts using LA-MC-ICPMS: Chemical Geology, v. 211, no. 1-2, p. 135-158.

Takeuchi, A., and Larson, P. B., 2005, Oxygen isotope evidence for the late Cenozoic development of an orographic rain shadow in eastern Washington, USA: Geology, v. 33, no. 4, p. 313-316.

Thorpe, R. S., Francis, P.W., Hammill, M. and Baker. M.C.W., 1982, The Andes, *in* Thorpe, R. S., ed., Andesites: New York, Wiley, p. 187-205.

Todt, W., Cliff, R.A., Hanser, A., and Hofmann, A.W., 1996, Evaluation of a ^{202}Pb- ^{205}Pb double spike for high-precision lead isotope analysis, *in* Hart, S. R., and Basu, A. , ed., Earth processes: Reading the isotope code, Volume 95: Washington D.C., American Geophysical Union, p. 429-437.

Valley, J. W., Kitchen, N., Kohn, M. J., Niendorf, C. R., and Spicuzza, M. J., 1995, UWG-2, a garnet standard for oxygen isotope ratios: Strategies for high precision and accuracy with laser heating: Geochimica Et Cosmochimica Acta, v. 59, no. 24, p. 5223-5231.

CHAPTER FOUR

THE VOLCANIC EVOLUTION OF CERRO UTURUNCU: A HIGH-K, COMPOSITE VOLCANO IN THE BACK-ARC OF THE CENTRAL ANDES OF SW BOLIVIA

Contribution of Authors and Co-Authors

Manuscript in Chapter 4

Author: Gary S. Michelfelder

Contributions: Performed geochemical analyses, field work sample preparation, and performed computer modeling. Wrote manuscript with input on data from co-authors.

Co-Author: Todd C. Feeley

Contributions: Aided in the preparation of the manuscript and figures.

Co-Author: Alicia D. Wilder

Contributions: Alicia worked in the field with me as my assistant and contributed by performing geochemical analyses.

Manuscript Information Page

Michelfelder, G.S., Feeley, T.C., and Wilder, A.D.
International Journal of Geosciences
Status of Manuscript:
___ Prepared for submission to a peer-reviewed journal
____ Officially submitted to a peer-review journal
____ Accepted by a peer-reviewed journal
__x_ Published in a peer-reviewed journal

Citation:

Michelfelder, G.S., Feeley, T.C., and Wilder, A.D., 2014, The Volcanic Evolution of Cerro Uturuncu: A High-K, Composite Volcano in the Back-Arc of the Central Andes of SW Bolivia: International Journal of Geosciences, v. 5, no. 11, p. 1263-1281.

International Journal of Geosciences, 2014, 5, 1263-1281
Published Online October 2014 in SciRes. http://www.scirp.org/journal/ijg
http://dx.doi.org/10.4236/ijg.2014.511105

Scientific Research

The Volcanic Evolution of Cerro Uturuncu: A High-K, Composite Volcano in the Back-Arc of the Central Andes of SW Bolivia

Gary S. Michelfelder[1,2*], Todd C. Feeley[1], Alicia D. Wilder[1]

[1]Department of Earth Sciences, Montana State University, Bozeman, USA
[2]Department of Geography, Geology and Planning, Missouri State University, Springfield, USA
Email: *gary.michelfelder@msu.montana.edu

Received 19 June 2014; revised 15 July 2014; accepted 12 August 2014

Abstract

Cerro Uturuncu, southwest Bolivia, is a high-K, calc-alkaline, composite volcano constructed upon extremely thick continental crust approximately 125 km behind the arc-front of the Andean Central Volcanic Zone (CVZ). Eruptive activity occurred between 890 - 271 ka in a single phase of volcanism lasting ~620,000 years. The edifice consists of a central cone and several flank vents where dacitic and andesitic lava flows and domes erupted. Volumes of individual eruptive units range from 0.1 to ~10 km^3; the composite volume of Uturuncu is ~89 km^3. In this paper, we present new field, petrographic, and geochemical data in an effort to understand the volcanic and magmatic evolution of Uturuncu. Lava flows and domes have a restricted range in whole rock compositions ranging from 61 wt% - 67 wt% SiO_2; magmatic inclusions contained within these units have a larger range from 53 wt% - 64 wt% SiO_2. Typical phenocryst assemblages are plagioclase > orthopyroxene > biotite >> quartz and Fe-Ti oxides. Pb isotope ratios are characteristic of the southern CVZ by containing high $^{207}Pb/^{204}Pb$ and $^{206}Pb/^{204}Pb$ and moderate to high $^{208}Pb/^{204}Pb$. Sr and Nd isotope ratios indicate that Uturuncu magmas were modified by high $^{87}Sr/^{86}Sr$ and low $^{143}Nd/^{144}Nd$ felsic basement lithology during magma migration and differentiation. In all eruptive units, there is petrographic and geochemical evidence for magma mixing and mingling. In this regard, magma mixing and mingling is considered to be responsible for the small range in lava flow and dome compositions throughout the eruptive history of the center.

Keywords

Utrunucu, Volcanic Evolution, Central Volcanic Zone, Magmatic Inclusion

*Corresponding author.

How to cite this paper: Michelfelder, G.S., Feeley, T.C. and Wilder, A.D. (2014) The Volcanic Evolution of Cerro Uturuncu: A High-K, Composite Volcano in the Back-Arc of the Central Andes of SW Bolivia. *International Journal of Geosciences*, 5, 1263-1281. http://dx.doi.org/10.4236/ijg.2014.511105

1. Introduction

Volcanism in the Central Volcanic Zone (CVZ) of the Andes is a prime example of active continental arc magmatism. Young (e.g., <6 Ma) volcanic rocks in the CVZ are dominantly andesitic to dacitic in composition with geochemical and petrographic features indicative of extensive crustal contamination during magma differentiation (e.g., [1]-[3]). Previous studies of CVZ volcanic rocks have greatly contributed to our understanding of the regional setting of the magmas [4] [5]; and references therein in addition to ignimbrite forming eruptions [6]-[9]; among others and volcanism along the modern arc-front [3] [10]. However, comprehensive studies of back-arc composite volcanoes are scarce, due in part, to their rarity and remote locations. As a result, studies of these systems are typically reconnaissance in nature and associated with regional studies [4] [5] [11]-[13].

The lack of comprehensive studies on individual back-arc composite volcanoes in the CVZ prompted a detailed field, petrologic and geochemical study of the back-arc center Cerro Uturuncu (6010 m; 22˚15'S, **Figure 1**). The objectives of this study are to discuss the volcanic evolution of an individual back-arc composite volcano and broadly assess petrogenetic processes affecting magma composition in the back-arc of the CVZ. This study of Uturuncu results from a reconnaissance petrologic and geophysical investigation by Sparks *et al*. [16]. These authors concluded Uturuncu exhibits stages of volcanism separated by periods of quiescence common at other intermediate composite centers in the CVZ. Currently, the system is in a period of dormancy as the most recent eruption occurred at ~270 ka. Relatively long periods of quiescence are common at composite volcanoes as they been observed at other intermediate composition systems in the CVZ and elsewhere such as at Soufrière Hills Volcano, Montserrat [3] [17] [18]. In this paper, we build on the reconnaissance investigation of Sparks *et al*. [16] by furthering discussion of the volcanic history, field relationships, and petrography of volcanic rocks at Uturuncu. We also present a broad geochemical model to account for the restricted compositional diversity of magmas erupted at the volcano. More detailed discussion of the petrology and petrogenesis of Uturuncu magmas will ensue in a forth-coming paper.

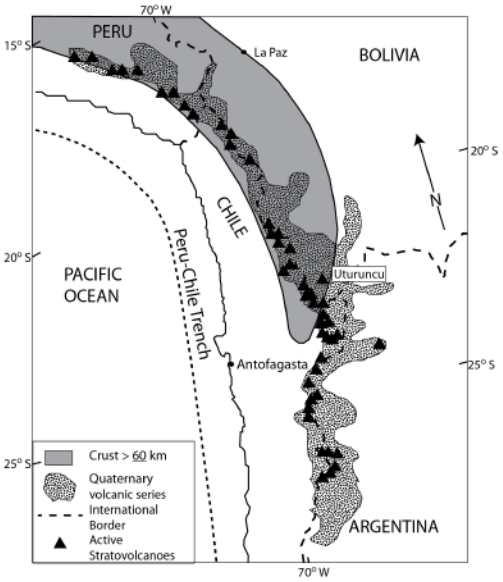

Figure 1. Map showing location of Andean Central Volcanic Zone (CVZ). Shaded area shows the region where crustal thickness exceeds 60 km [14] [15]; stippled region illustrates distribution of Quaternary volcanic rocks. Modified from Feeley and Hacker [2].

2. Regional and Tectonic Setting

The Andes are considered the classic example of a modern Cordilleran-type orogen formed by long-term subduction of oceanic lithosphere beneath continental lithosphere. The central Andes represents the type locality for this process owing to the great width of the orogen, immense crustal thickness (up to 70 - 80 km) [19] and high elevations (~4 - 6 km above sea level) [19] that occur over a vast area (**Figure 1**). The region composes one of the youngest and largest active silicic volcanic provinces with recent caldera formation. The CVZ contains ~20 calderas that have erupted ignimbrites (large ash flow sheets) less than 10 Ma and over 1100 late Cenozoic volcanic edifices [6] [7] [20].

The southern central Andes between 21˚S - 24˚S is divided into three NW to SE trending geologic provinces based on structural similarities [19]. From east to west, these are the Eastern Cordillera (Cordillera Oriental), the Altiplano, and the Western Cordillera (Cordillera Occidental). The Eastern Cordillera comprises a classic thin-skinned fold and thrust belt. The Altiplano is a broad plateau where undeformed late Miocene and younger ignimbrites overlie variably deformed mid-Miocene and older volcanic and sedimentary rocks. The Western Cordillera consists of a westward dipping monocline and the modern volcanic arc-front [19] [21]. Depths to the subducting slab at these latitudes range from 130 km at the arc-front to ~250 km along the eastern boundary of the Altiplano [22] [23].

Late Cenozoic to modern volcanic rocks in the CVZ is divided into three groups based on similarities in composition and eruptive style [21] [24]. First, between 21˚S - 24˚S, large-volume, regionally extensive ignimbrites erupted from large caldera complexes on the Altiplano and Western Cordillera [6] [7] [25]. These rocks are calc-alkaline, homogeneous dacites to rhyolites. Second, basaltic andesitic to dacitic lava flows erupted from 23 Ma to the present. At 21˚S - 22˚S, the largest volumes of these magmas erupted from composite volcanoes forming the peaks of the Western Cordillera. Baker and Francis [12] estimated the Western Cordillera contains ~3000 km^3 of these lavas between 21˚S and 22˚S latitude. Lavas associated with composite volcanoes extend for ~200 km eastward onto the Altiplano, although volumes decrease sharply to <800 km^3. Uturuncu is associated with this group. Third, volumetrically minor alkali basalts erupted from small monogenetic centers to the east of the arc-front on the Altiplano north of 21˚S [13] [26].

3. Methods

New whole rock samples of Uturuncu volcanic rocks were analyzed for major and trace element compositions at Washington State University, Pullman. Major and trace element compositions for 121 samples were acquired by X-ray fluorescence spectrometry (XRF) on a ThermoARL Advant'XP+ automated sequential wavelength spectrometer. Methods and errors for XRF analyses are described in Johnson *et al.* [27]. Additional trace element compositions, including the rare earth elements, for 45 samples, were acquired by inductively coupled plasma mass spectrometry (ICP-MS) on an Agilent 7700 ICP-MS. Methods and errors for trace element analyses are presented in detail in Jarvis [28]. Whole rock Nd and Sr isotopic ratios, for 30 samples, were acquired by thermal ionization mass spectrometry (TIMS) on a VG Sector 54, analyzed by five Faraday collectors in dynamic mode at New Mexico State University, Las Cruces. Pb isotopes were analyzed on a Thermo Finnigan Neptune multi-collector ICP-MS equipped with nine Faraday collectors and an ion counter at the University of California at Santa Barbara. Michelfelder *et al.* [29] describe in detail the methods for radiogenic isotopic analyses. Geologic mapping was performed using commercially purchased ASTER satellite imagery and field mapping.

4. Geology and Eruptive History of Cerro Uturuncu

In this section, we summarize the volcanic and petrographic features of the lava flows and domes at Cerro Uturuncu. Cerro Uturuncu is classified as a composite volcano [20] resulting from volcanism over ~620,000 years [16]. Construction of the edifice of Cerro Uturuncu took place the back-arc of the CVZ approximately 125 km behind the modern arc front in the Altiplano region (**Figure 1**). The volcano is built upon a series of 5 Ma to 1 Ma ignimbrites erupted from large calderas complexes in the area [8] [9] [30] [31]. The eruptive history of Uturuncu is dominantly effusive with no evidence of explosive activity. Eruptive activity at Uturuncu predates the last glacial episode (~11,000 ky [26]) in the area as evident by glacial valleys incising lava flows and the reformed southern and northern flanks mantled in places by moraines (**Figure 2**). Glacial incision has allowed for access to the potentially oldest lava flows erupted from Uturuncu.

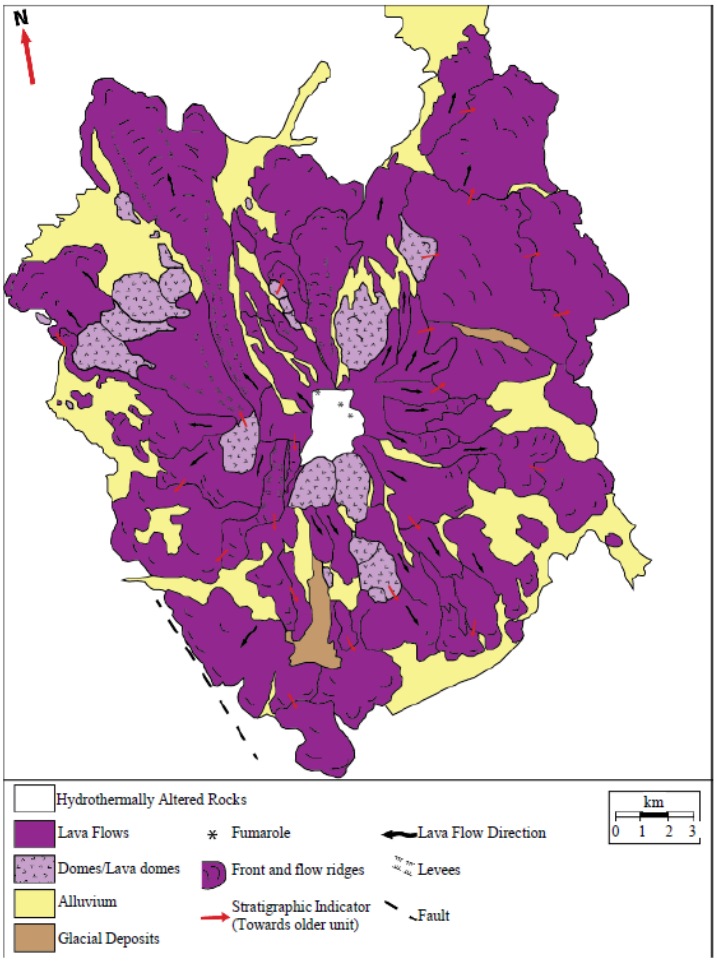

Figure 2. Simplified geologic map of Cerro Uturuncu based on field mapping and satellite imagery interpretation. Modified from Sparks *et al.* [16].

Active fumaroles producing hydrothermally altered volcanic rocks are present in the saddle between the two peaks of Uturuncu. Hydrothermal alteration, mining of altered rocks for sulfur and erosion of the stratigraphically youngest volcanic rocks has removed the interpreted location of the central vent. The presence of fumaroles suggests current activity beneath Cerro Uturuncu. Pritchard and Simmons [32] identified a 70 km diameter regional uplift centered on Uturuncu. This uplift, suggested to be the result of diapiric rise of new magma into a shallow chamber beneath the center [33], could lead to new activity at Uturuncu in the future.

Relatively few radiometric ages are available for Uturuncu lavas and domes. The available ages suggest two stages of volcanism between 890 - 271 ka [16] and a period of quiescence from 540 - 470 ka. The stages described by Sparks *et al.* [16] are compositionally and petrographically similar, though erupted volumes of vol-

canic rocks decrease with younger age.

4.1. Morphology and Volume of Cerro Utrunucu

Considered dormant, Cerro Uturuncu has not been the focus of intense study until recently. Fernandez *et al.* [34], Kussmaul *et al.* [11], Baker and Francis [12] and Hildreth and Moorebath [35] included Uturuncu in regional studies but did not investigate the volcanic history. Reconnaissance geologic mapping performed by Sparks *et al.* [16] identified ~50 lava flows and domes with volumes ranging from 0.1 - 10 km^3. Based on new mapping (**Figure 2**), as well as geochemical and stratigraphic criteria, the eruptive history of Uturuncu represents a single stage of activity spanning ~620,000 years with an additional 45 lava flows and 10 domes identified as part of this study. Newly identified lava flows and domes observed during mapping and verified geochemically are stratigraphically between the 540 ka and the 470 ka lava flows. Volumes of these newly identified lava flows and domes are similar to those reported by Sparks *et al.* [16] with a total estimated volume of ~89 km^3. The suggested repose interval based on radiometric age dates and the number of erupted units is between 6000 and 8000 years.

The predominant rock types at Cerro Uturuncu are medium-grey, blocky to platy, orthopyroxene, biotite andesites and dacites. Dacites of relatively uniform compositions were the dominant magmas erupted, although significant volumes of andesite lava flows were erupted throughout the life span of the volcano. Flow fronts of lava flows range in thickness from <5 m to over 200 m thick. Widths of flows vary with slope and are wider than thick for gentler slopes (**Figure 2** & **Figure 3**). Some lava flows extend for more than 10 km and traced back to the central vent (**Figure 2**), while smaller volume flows rarely extend more than 2 - 3 km from the vent. Many flows have internal flow folds and are autobrecciated at the terminus showing several meters of oxidation (**Figure 3**).

Domes occur throughout the volcano and suggest the activity was not restricted to a central vent, though lava flows cannot be trace to these flank vents. Piles of glassy, prismatically jointed blocks making up the exterior walls identified domes. Rare exposures of the interiors of domes are vesiculated ranging from 8% - 23% of the total volume (**Figure 3**). Vesicles ranged in size from millimeter to centimeter scale.

4.2. Petrography

Mineralogically and petrographically, Uturuncu lava flows and domes are porphyritic to seriate. Domes are occasionally hiatal. Some lava flows have ophitic and poikilitic textures. Glomerocrysts containing orthopyroxene (OPX) and plagioclase common with occasional olivine observed in some lava flows. Modal compositions of Uturuncu volcanic rocks are variable in crystal content, but similar in mineral assemblage (**Figure 4**). Crystal contents range from 30% - 53% total volume for all lava flows and domes with domes containing the highest crystal volumes. Phenocryst phases include plagioclase (An_{42-94}) > OPX (En_{45-83}) > biotite >> quartz, Fe-Ti oxides, and trace clinopyroxene (CPX), hornblende and olivine in micro-inclusions (**Figure 4**).

Plagioclase and OPX phenocrysts exhibit multiple textures. In the same eruptive unit, plagioclase phenocrysts textures include a combination of sieving, dissolution surfaces, growth zones, and clean crystals (**Figure 5**). Sieving occurs in both cores and rims of phenocrysts and dissolution surfaces commonly separate clear or sieved cores from zoned rims (**Figure 5(B)** & **Figure 5(C)**). Large plagioclase phenocrysts (>0.5 mm) are interpreted as xenocrysts because they contain cores riddled with abundant, irregular shaped glass inclusions and euhedral to subeuhedral rims with oscillatory chemical zoning from core to rim (An_{core} = 46 - 92; An_{rims} = 44 - 88). Nearly all OPX crystals show some zoning. Chemically unzoned OPX are only associated with glomerocrysts and in groundmass crystals (**Figure 5(A)** & **Figure 5(D)**). OPX crystals are Ca-poor at (Wo_{06} or less) and represent two zoned populations [16]. The first contains Mg-poor cores (En_{55}) and reverse zoned rims (En_{65-75}), and the second population contains Mg-rich cores (En_{65-80}) and normally zoned rims (En_{50-705}). Reaction rims of Fe-Ti oxides and OPX typically surrounds biotite phenocrysts over 0.5 mm. Quartz and olivine phenocrysts, and microphenocrysts typically exhibit resorption textures suggesting they are most likely xenocrysts or antecrysts.

Groundmass of the lava flows and domes are hyalopilitic with mineral phases similar to phenocryst phases. Additional phases in the groundmass include glass, trace zircon, apatite, and occasional olivine. Groundmass plagioclase (An_{45-85}) crystals do not exhibit sieving seen in phenocrysts. Groundmass plagioclase and OPX (En_{46-75}) crystals occasionally show zoning and dissolution surfaces. Vesicles comprise approximately 8% - 23% of the mode in domes interiors and 0% - 12 % in lava flows.

Figure 3. Representative views of Cerro Uturuncu geology. (A) View southeast towards the edifice of Uturuncu; (B) Typical flow folding in lava flows; (C) Hydrothermally altered remains of the edifice of Uturuncu produced by fumaroles; (D) Typical prismatically jointed block from exterior wall of a collapsed dome; (E) Andesite inclusions in an Uturuncu lava flow; (F) Typical flow front of an Uturuncu lava flow overlying APVC ignimbrite; (G) Oxidized autobrecciation found at the terminus of lava flows; (H) Pressure ridge found commonly found in lava flows over 20 m thick.

4.3. Magmatic Inclusions

A common occurrence in Uturuncu volcanic rocks is the presence of magmatic inclusions. Individual lava flows vary greatly in the volume of magmatic inclusions ranging from ~0% - 4%. Three general populations of inclusions exist in Uturuncu lava flows and domes. Mineralogically and petrographically inclusions exhibit similar modes to the lavas and domes. With the exception of inclusions defining population 3, inclusions typically lack quartz and biotite and contain a higher volume of CPX and olivine compared to the host lava flows and domes.

The first population of inclusions is ellipsoidal with a porphyritic to hiatal texture and contains a thick, vesicle-free, glassy rim with vesiculated interiors. These inclusions are characterized by euhedral to subhedral parageneitcally early phenocrysts of OPX and plagioclase in varying proportions. Plagioclase phenocrysts range in

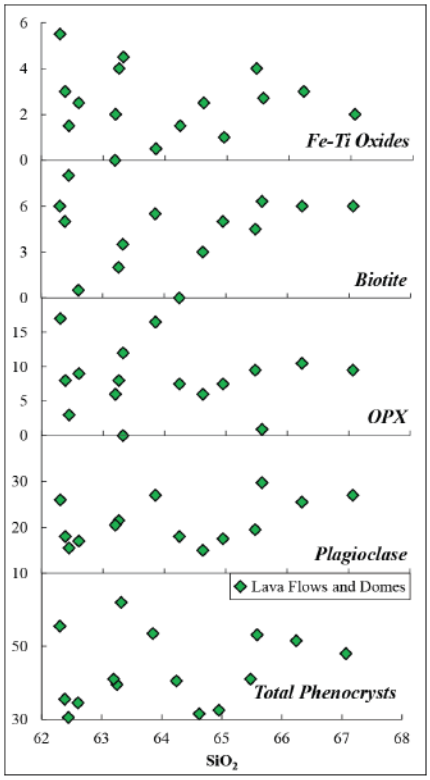

Figure 4. Modal percent phenocrysts versus SiO_2 for representative Ututuncu lava and domes.

size from 0.25 mm to 1.5 mm along the long axis. Large plagioclase phenocrysts are interpreted as xenocrysts or antecrysts because they contain cores riddled with abundant, irregular shaped glass inclusions and euhedral rims and oscillatory zoning patterns similar to those observed in the host lava flows and domes. The groundmasses of these inclusions are hyalopilitic and are composed of microlite-sized (<0.25 mm) plagioclase crystals and Fe-Ti oxides in a glassy matrix. These inclusions are the most common type observed, and range in size from micro-inclusions (<3 mm) to ~5 cm in diameter although occasional larger inclusions were observed.

The second population of inclusions are non-vesiculated basaltic andesite clots, containing plagioclase > OPX > Fe-Ti oxides > olivine > amphibole ± clinopyroxene. Hiatal to intergranular crystal sizes dominate this population of inclusions. The second population of inclusions lack glassy rims in contact with the host lava flow or dome as described above. The contacts of the inclusions are angular and defined by crystal boundaries. Crystal sizes range from microlite-size to crystals ~1.5 mm along the long axis. Inclusion size varies from micro-inclusions (~3 mm) to ~10 cm in diameter. Hand specimen size samples of this inclusion population was only observed in two lava flows, although these inclusions may have been overlooked due to their similarity in color to the host lavas when weathered. Two additional lava flows and one dome contain micro-inclusions of this population.

Non-vesiculated micro-inclusions are distinct from the glomerocrysts observed lava flows and domes due to their crystal size and presence of rare amphibole. OPX phenocrysts are similar in size to the plagioclase though

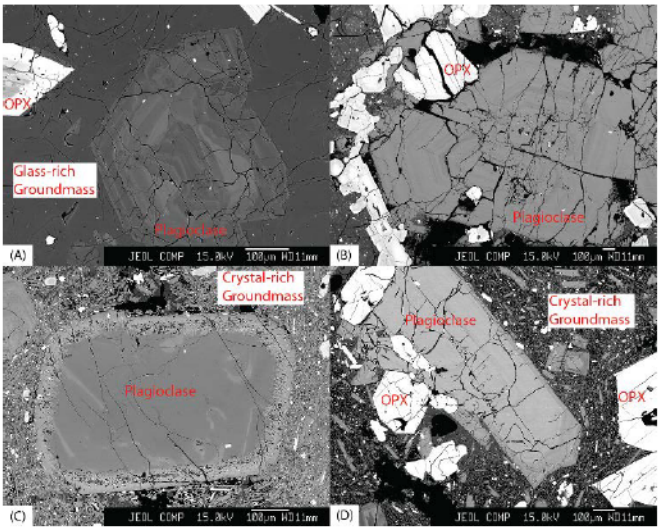

Figure 5. Back-scattered electron micrographs of Uturuncu volcanic rocks. (A) Plagioclase phenocryst exhibiting resoption surfaces and growth zones; (B) Glomerocryst composed of zoned OPX phenocrysts around a single sieved and zoned plagioclase phenocryst; (C) Dacite lava flow with a sieved, unzoned plagioclase phenocryst; and (D) a glomerocryst composed of unzoned OPX phenocrysts around zoned and unzoned plagioclase phenocrysts.

chemical zoning is not present. Some plagioclase phenocrysts show sieving and dissolution surfaces and all crystals over 0.5 mm contain growths zones. A reaction rim of OPX typically surrounds olivine phenocrysts. The groundmasses of the non-vesiculated inclusions are intergranular to hyalopilitic and are composed of microlite-sized acicular lath of plagioclase and blocky OPX.

Vesiculated and non-vesiculated magmatic inclusions (population 1 and 2) are common features observed in CVZ volcanic rocks as well as at other intermediate composition volcanic systems around the world [21] [36]-[38]. Magmatic inclusions, with or without vesiculation, represent blobs of mafic magma quenched in cooler, more silicic magma [36] due to the processes of magma mixing and mingling. This is our interpretation of inclusion populations 1 and 2 observed in Uturuncu lavas and domes.

The third population of inclusions observed does not exhibit the same mineralogy as the host lavas and domes. This population is dominantly hypidiomorphic to allotriomorphic granular with trace to rare glass (0% - 0.5%). Plagioclase and quartz dominate the mode of these inclusions with trace OPX and biotite. Plagioclase crystals are clear with no growth zones or dissolution surfaces observed. Quartz crystals show resorption along the corners of the crystals. Margins of these inclusions are angular and defined by the crystal boundaries. Textures observed in this population of inclusions suggest the same process does not produce these inclusions as populations 1 and 2. It is likely that inclusions in population 3 are xenoliths.

Sparks *et al.* [16] described two xenolith populations have a similar petrographic description to inclusions in population 3 of this study. These authors interpreted observed quartz-rich xenoliths to represent crustal partial melting of rocks trapped in a MASH zone [35]. It is our interpretation that xenoliths observed in this study represent basement rocks interacting with Uturuncu magmas during migration and differentiation. These xenoliths may represent the residue of a granodiorite crustal contaminant beneath Uturuncu.

A fourth inclusion population described by Sparks *et al.* [16] and was not observed in this study. These authors describe a noritic composition xenolith population found in multiple lava flows sampled in the study. These xenoliths contain mineral assemblages and similar mineral compositions to those observed in the lava flows and domes [16]. The adcumulate textures observed in these xenoliths suggested to these authors that these

xenoliths represent adcumulates of early-formed crystals that segregated from hotter, less evolved residual magma related to the Uturuncu magmas [16].

5. Whole Rock Geochemistry

5.1. Major and Trace Elements

Figures 6-8 illustrate major- and trace-element compositions of lava flows, domes and inclusions. Table 1 and Table 2 present representative analyses of these data. These compositions define a high-K, calc-alkaline suite (Figure 6). SiO_2 ranges from 61 wt% - 67 wt% for the lava flows and domes, 53 wt% - 64 wt% for the magmatic inclusions (population 1 & 2), and 78 wt% - 79 wt% for the xenoliths (inclusion population 3). For the suite as a whole, contents of CaO, FeO^*, MgO, TiO_2, MnO, Yb, Sr and Cr decrease, and concentrations of Na_2O, K_2O, P_2O_5, La, Zr, Ba and Rb increase with increasing SiO_2 concentrations (Figure 7 & Figure 8). Compared to other centers in the CVZ [29], higher concentrations of are observed in LIL-element concentrations for Uturuncu volcanic rocks.

Consistent with petrography, xenolith samples do not exhibit the same geochemical trends observed in the lavas, domes, or inclusions (Figure 7 & Figure 8) suggesting these xenoliths are trapped residue in a MASH zone or represent a crustal contaminant. Compared to other volcanic rock compositions at Uturuncu, compositions of the xenoliths are significantly lower for elements not compatible with quartz or plagioclase (Figure 7 & Figure 8).

The compositional variation and trends observed versus SiO_2 highlight the petrologic processes affecting the evolution of Uturuncu magmas. The linear trends observed in all major element compositions and the divergent linear trends in MgO, La, Sr, Y and Yb suggest multiple components in magma evolution. These linear trends reflect magma mixing as a dominant process in the generation of the limited compositional diversity observed of lavas and domes at Uturuncu. Magmatic inclusion compositions are an extension of this trend at lower SiO_2 contents.

5.2. Radiogenic Isotopes

Table 1 and Table 2 present, and Figure 9 illustrate radiogenic isotopic ratios for $^{87}Sr/^{86}Sr$, $^{143}Nd/^{144}Nd$, and Pb isotopes of lavas and domes, inclusions and xenoliths. The range in $^{87}Sr/^{86}Sr$ and $^{143}Nd/^{144}Nd$ isotopic ratios for Uturuncu rocks is small compared to the range observed across the CVZ (Figure 9(B)) [4] [37]. In comparison with other individual CVZ composite cones, Uturuncu rocks have higher $^{87}Sr/^{86}Sr$ ratios and lower $^{143}Nd/^{144}Nd$ ratios and are more similar in comparison to ignimbrites erupted from Cerro Panizos on the eastern Altiplano or the 5 Ma to 1 Ma Altiplano ignimbrites Uturuncu overlies (Figure 9(B)) [30] [39]. When compared to previously report isotopic analyses in reconnaissance or regional studies including volcanic rocks from Uturuncu, this study reports more isotopic variation [11] [12]. The $^{87}Sr/^{86}Sr$ isotopic compositions for the inclusions overlap the lowest ratios measured in the host lavas and domes (Figure 9(A) & Figure 9(B)) suggesting extensive crustal contamination of the most mafic magmas observed in this study.

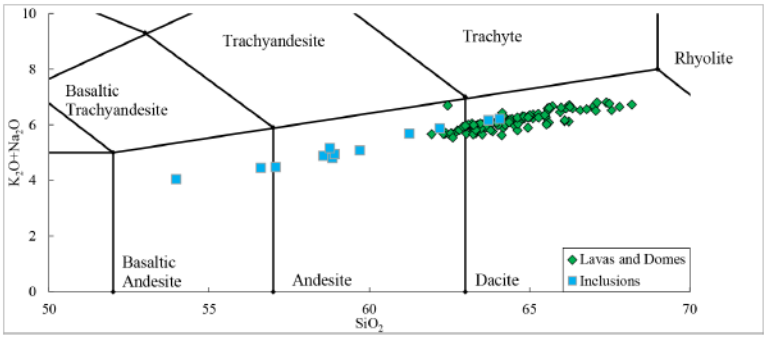

Figure 6. Total alkali concentrations versus SiO_2 for Uturuncu lavas, domes and inclusions.

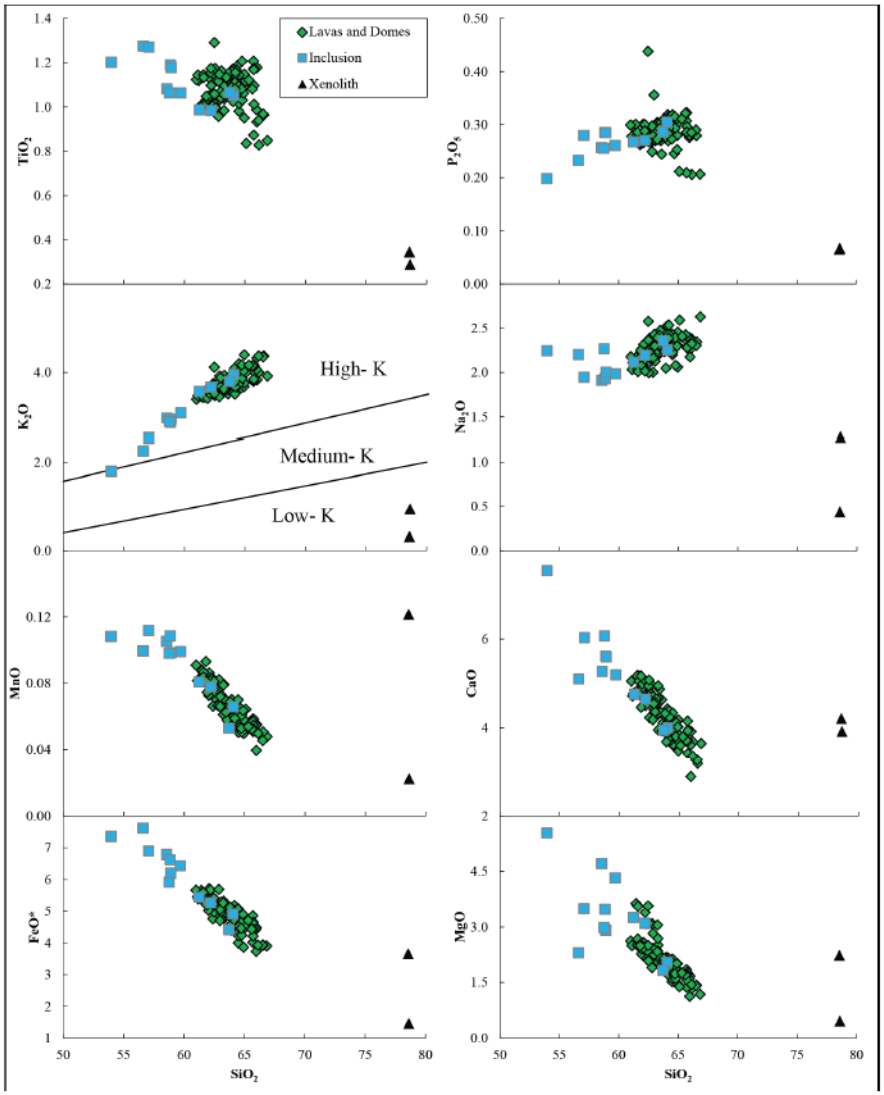

Figure 7. Major-element oxide concentrations versus SiO_2 for Uturuncu lavas and domes, inclusions and xenoliths.

6. Petrogenesis of Cerro Uturuncu Magmas

In this section, we describe a simple working model to explain the limited compositional diversity observed in Uturuncu volcanic rocks. The intent of the proposed model is not a rigorous description of the petrogenesis of the magmas nor is the variables and compositions selected for assimilation-fractional crystallization and mag-

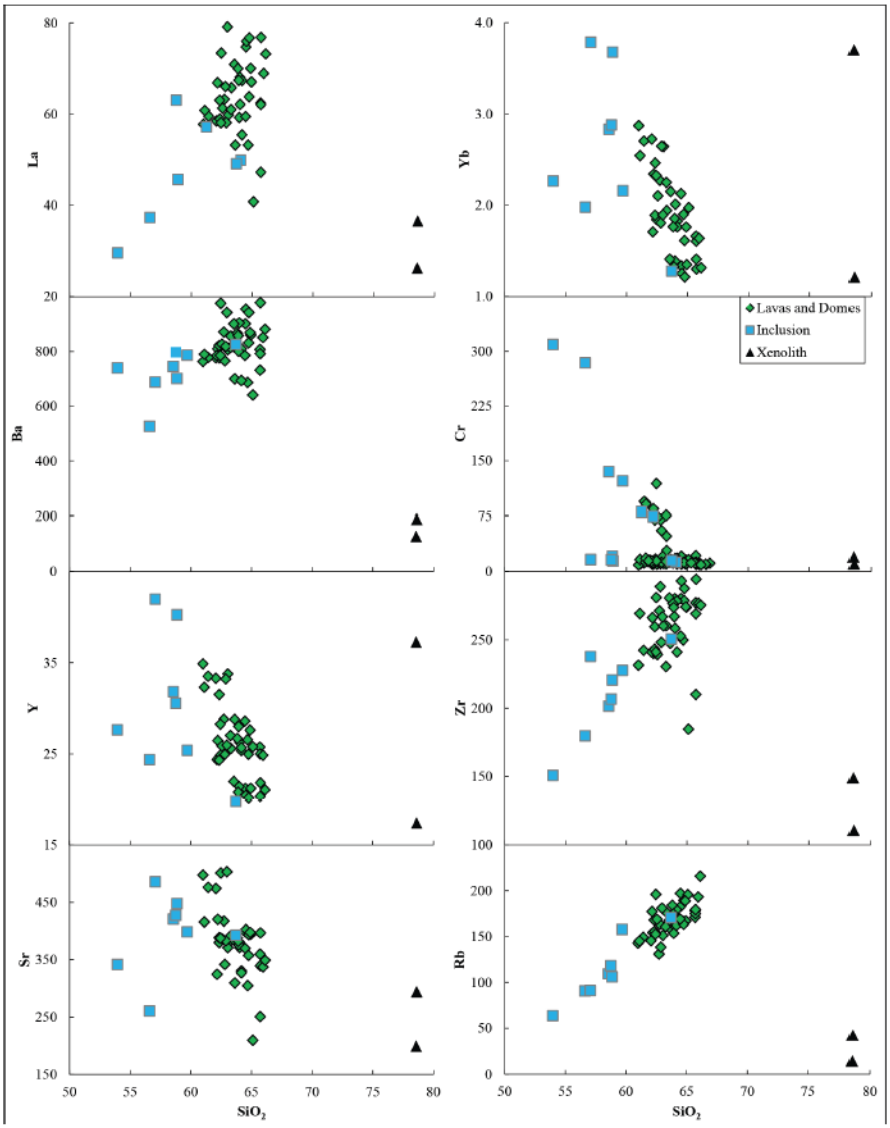

Figure 8. Trace-element concentrations versus SiO_2 for Ututuncu lavas and domes, inclusions and xenoliths.

mamixing models intended to quantify the magmatic system beneath Ututuncu. The intent is to constrain the processes affecting compositional diversity of the rocks and serve as a point of reference in future studies of Ututuncu volcanic rocks.

Table 1. Representative whole rock major-, trace-element concentrations and isotopic ratios analyses of Ururuncu lava flows and domes.

	DM10A	DM28A	DM58A2	DM73A2	DM101A2	GSM14	GSM22	GSM-49	GSM-50
SiO_2	65.55	63.33	62.30	63.04	65.61	66.10	65.00	64.15	64.84
TiO_2	1.08	1.16	1.13	1.17	1.21	1.18	1.12	1.09	1.08
Al_2O_3	16.16	17.26	17.19	17.10	15.90	15.89	16.24	16.37	16.25
FeO^*	4.81	5.29	5.73	5.57	4.85	4.65	5.10	4.79	4.93
MnO	0.07	0.08	0.09	0.08	0.06	0.06	0.07	0.07	0.07
MgO	1.87	2.27	2.60	2.46	1.85	1.73	1.86	2.30	2.11
CaO	4.14	4.65	4.95	4.63	4.14	3.95	4.05	4.44	4.11
Na_2O	2.37	2.15	2.21	2.07	2.28	2.29	2.46	2.48	2.29
K_2O	3.70	3.54	3.49	3.61	3.79	3.87	3.81	3.95	4.01
P_2O_5	0.25	0.27	0.30	0.28	0.31	0.29	0.28	0.36	0.32
LOI (%)	0.99	0.65	0.43	1.47	0.00	0.30	0.93	1.24	0.95
Total	100.00	100.00	100.00	100.00	100.00	100.00	100.00	100.00	100.00
La	53.18	63.26	58.50	66.88	62.42	62.12	67.41	79.14	70.02
Ce	108.68	126.92	118.34	138.06	129.40	128.55	137.37	154.36	141.18
Pr	13.05	15.17	13.96	16.62	15.65	15.23	16.73	17.80	16.69
Nd	49.52	56.99	52.67	62.32	59.33	57.58	62.93	65.53	62.11
Sm	9.64	10.84	10.19	11.50	11.41	11.08	11.43	11.71	11.42
Eu	1.80	2.10	1.98	1.88	2.04	2.01	1.88	2.13	1.97
Gd	7.68	8.36	8.23	7.95	8.48	8.25	8.16	8.44	8.36
Tb	1.11	1.22	1.25	1.11	1.17	1.15	1.11	1.14	1.18
Dy	5.89	6.50	6.96	5.59	5.96	5.83	5.62	5.76	6.07
Ho	1.03	1.15	1.31	0.94	0.99	0.96	0.97	1.00	1.04
Er	2.44	2.84	3.29	2.24	2.28	2.18	2.29	2.42	2.40
Tm	0.33	0.38	0.45	0.30	0.29	0.29	0.30	0.32	0.31
Yb	1.90	2.27	2.72	1.71	1.66	1.60	1.76	1.89	1.76
Lu	0.27	0.33	0.40	0.24	0.23	0.22	0.25	0.28	0.25
Ba	686	870	776	784	807	791	809	942	866
Th	19.4	21.4	18.7	24.7	21.9	21.8	24.5	25.2	24.9
Nb	18.2	20.7	20.8	18.4	22.1	21.7	18.3	26.5	22.1
Y	27	29	33	24	26	25	26	26	27
Hf	6.6	7.2	6.4	7.4	7.3	7.1	7.3	7.1	7.3
Ta	1.4	1.5	1.5	1.3	1.6	1.5	1.3	1.6	1.5
U	4.4	3.7	3.7	4.5	3.9	4.0	4.4	4.7	4.5
Pb	20.9	21.7	20.4	23.4	21.7	21.8	22.5	21.6	22.7
Rb	167	131	146	177	171	175	179	181	184
Cs	7.9	4.3	5.2	6.3	5.2	4.9	5.4	6.5	6.4
Sr	305	417	474	325	360	340	327	503	388
Zr	249.8	271.0	241.1	266.0	277.0	268.9	278.2	266.7	276.4
$^{87}Sr/^{86}Sr$	0.714570	0.712956	0.711294	0.712738	0.714300	0.714519	0.713692	0.711002	0.712468
$^{144}Nd/^{143}Nd$	0.512148	0.512246	0.512179	0.512159	0.512172	0.512163	0.512202	0.512247	0.512163

Table 2. Representative whole rock major-, trace-element concentrations and isotopic ratios analyses of Ututuncu magmatic inclusions and xenoliths.

	UTU 13N	UTU 17N	UTU 28N1	UTU 28N3	UTU 56N	UTU 58N1	UTU 69N3	UTU 28X	UTU 56N3
	Inclusion	Inclusion	Inclusion	Inclusion	Inclusion	Inclusion	Inclusion	Xenolith	Xenolith
SiO_2	54.0	56.6	59.7	58.6	58.9	57.1	63.7	78.6	78.6
TiO_2	1.20	1.28	1.06	1.08	1.19	1.27	1.07	0.29	0.34
Al_2O_3	15.59	16.81	16.41	16.26	17.24	18.28	15.81	10.00	8.62
FeO^*	7.35	7.62	6.43	6.78	6.62	6.89	4.41	1.46	3.66
MnO	0.11	0.10	0.10	0.11	0.11	0.11	0.05	0.02	0.12
MgO	5.54	2.31	4.33	4.71	3.48	3.49	1.83	0.46	2.24
CaO	7.55	5.10	5.19	5.27	5.61	6.03	3.94	3.91	4.21
Na_2O	2.25	2.20	1.99	1.91	1.93	1.95	2.36	1.28	0.44
K_2O	1.79	2.24	3.09	2.97	2.87	2.53	3.80	0.94	0.32
P_2O_5	0.20	0.23	0.26	0.26	0.29	0.28	0.29	0.07	0.07
Total	95.55	94.50	98.56	97.92	98.19	97.91	97.28	97.03	98.58
La	29.55	37.30	57.16	49.82	45.62	49.09	63.06	36.54	26.25
Ce	51.98	64.02	113.16	98.03	91.52	98.21	130.97	79.27	56.05
Pr	7.50	8.62	13.47	11.92	11.13	12.11	15.01	10.10	7.31
Nd	29.71	32.90	50.06	45.50	43.26	46.75	55.64	38.70	27.64
Sm	6.62	6.80	9.60	8.92	8.77	9.65	10.38	8.06	6.77
Eu	1.52	1.86	1.78	1.87	1.92	2.07	1.85	1.38	0.91
Gd	6.21	6.00	7.25	7.61	8.01	8.59	7.32	5.85	6.10
Tb	0.97	0.91	1.03	1.12	1.30	1.39	0.98	0.84	1.13
Dy	5.55	5.02	5.41	6.30	7.85	8.30	4.80	4.21	6.98
Ho	1.08	0.93	1.00	1.22	1.58	1.67	0.79	0.71	1.43
Er	2.69	2.26	2.50	3.20	4.18	4.41	1.72	1.63	3.90
Tm	0.37	0.33	0.36	0.46	0.60	0.62	0.23	0.21	0.59
Yb	2.26	1.98	2.16	2.83	3.68	3.79	1.28	1.21	3.70
Lu	0.34	0.31	0.33	0.44	0.56	0.59	0.18	0.17	0.55
Ba	739	525	786	745	701	687	825	189	126
Th	7	9	21	14	13	15	23	14	13
Nb	14	16	18	17	18	19	19	10	10
Y	28	24	25	32	40	42	20	17	37
Hf	4.06	4.89	6.24	5.48	5.99	6.38	6.96	3.13	4.30
Ta	1.07	1.22	1.29	1.11	1.19	1.29	1.29	1.12	1.12
U	3.07	3.42	4.06	2.59	2.26	2.30	4.44	3.48	5.63
Pb	10	10	18	15	15	16	22	12	4
Rb	64	91	158	109	106	91	170	42	14
Cs	4.49	6.12	6.08	2.68	2.44	2.80	5.89	1.91	0.55
Sr	341	260	399	421	448	485	393	294	199
Zr	151	180	228	202	221	238	251	111	149
$^{87}Sr/^{86}Sr$			0.710339	0.710456				0.713682	0.714553

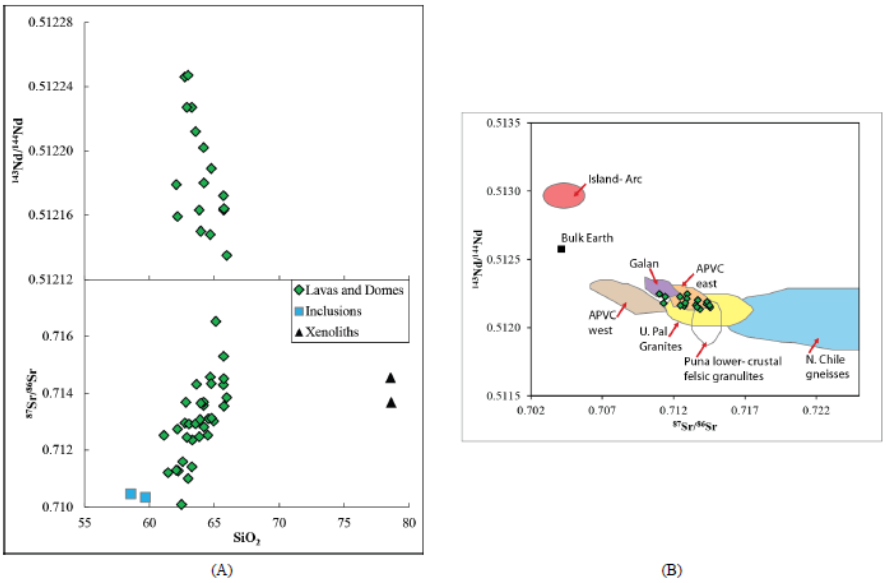

Figure 9. (A) Nd isotope and Sr isotope ratios for Uturuncu lavas and domes; (B) $^{143}Nd/^{144}Nd$ ratios versus $^{87}Sr/^{86}Sr$ ratios for Uturuncu volcanic rocks.

The lavas and domes have a large range of $^{87}Sr/^{86}Sr$ ratios for a narrow range of $^{143}Nd/^{144}Nd$ ratios (**Figure 9(B)**). Assimilation of crustal rocks with high $^{87}Sr/^{86}Sr$ ratios but similar $^{143}Nd/^{144}Nd$ ratios explains the observed trend. **Figure 10** illustrates six scenarios using different composition contaminants and different partition coefficients dependent on the crustal composition. The lower crustal contaminant is a garnet-sillimanite-gneiss xenolith described by McLeod *et al.* [40] from the southern CVZ. We selected this composition because of petrographic similarities to a sillimanite-gneiss xenolith described by Sparks *et al.* [16] from Uturuncu lavas. The upper crustal contaminant used in the models is Paleozoic granite from Sierra de Moreno described by Lucassen *et al.* [41]. These granites are petrographically similar to the xenolith observed in this study. We contaminate two primitive basalt compositions with lower and upper crustal contaminants: one from Davidson and de Silva [13] for basalts from the central Altiplano, and a second from Hernando *et al.* [42] for pre-caldera basalts from the Payún Matrú volcanic field in western Argentina's Southern Volcanic Zone. **Table 3** presents concentrations and isotopic ratios of the contaminants and basalts.

Model curves labeled AFC (D = 1.7) and AFC (D = 1.5) were constructed to simulate the effects of differentiation on two potential parental magmas compositions contaminated by a highly evolved crustal contaminant (**Figure 10**). Bulk distribution coefficients of 1.5 and 1.7 are high for andesites, but the decrease of Sr content with increasing SiO_2 content and in increase of Rb/Sr ratios with increasing $^{87}Sr/^{86}Sr$ ratios suggest Sr was compatible during differentiation. The curve AFC (D = 0.1) was constructed to simulate the effects of differentiation in the lower crust compared to curves for the upper crust. A bulk distribution coefficient of 0.1 is considered appropriate for this composition based on regional studies that have shown an increase in Sr/Y ratio with a decrease in $^{87}Sr/^{86}Sr$ ratios reflects incompatibility of Sr in garnet-stable/plagioclase-unstable-hybridized crust [29] [44] [45].

$^{87}Sr/^{86}Sr$ and $^{143}Nd/^{144}Nd$ ratios for Uturuncu lavas and domes create an array consistent with assimilation of old radiogenic basement rocks with relatively non-radiogenic Nd and radiogenic Sr. High Rb/Sr ratios suggest these basement rocks were also felsic in composition as opposed to noritic as could be interpreted from the presence of noritic composition xenoliths described by Sparks *et al.* [16]. High silica, quartz-feldspathic xeno-

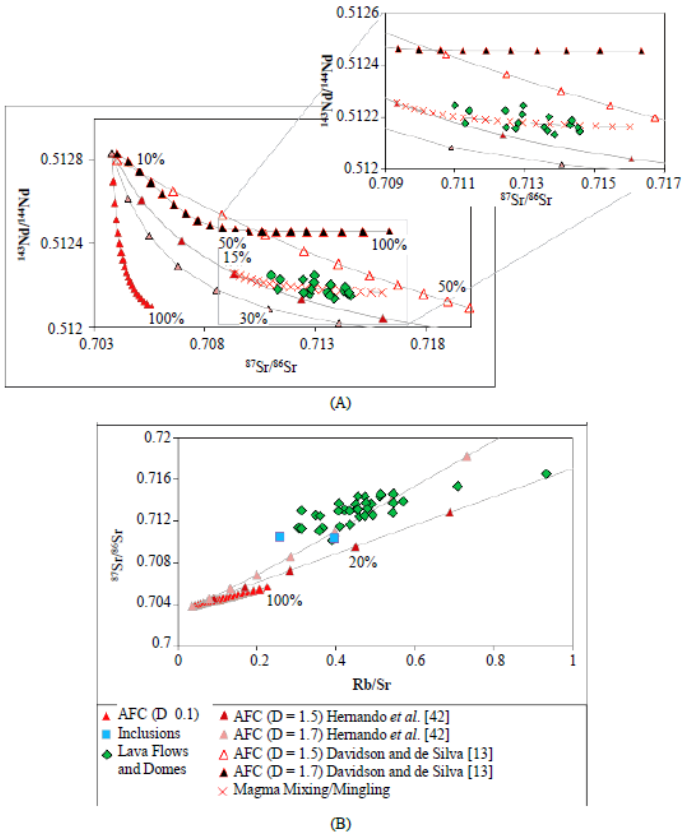

Figure 10. (A) Nd Isotope and Sr isotope constraints on bulk mixing and assimilation fractional crystallization (AFC) [43] models for Uturuncu lava flows and domes. (B) $^{87}Sr/^{86}Sr$ ratios versus Rb/Sr ratios for Uturuncu lava flows, domes and inclusions with AFC models of primary melts discussed in text and in Table 3.

Table 3. Trace element concentrations and isotopic ratios of basement rocks and primary basalts used in geochemical modeling.

	Sample Type	Location	Rb	Sr	Nd	$^{87}Sr/^{86}Sr$	$^{143}Nd/^{144}Nd$	Reference
Py-5	Basalt	PayúnMatrú volcanic field	27	751	24.4	0.703813	0.512834	Hernando *et al.* [42]
4/23	Granite	Sierra de Moreno	173	40	11.65	0.76261	0.512456	Lucassen *et al.* [41]
BC93PAX12	Grt-sill gneiss	Bolivia	27.3	18.5	22.8	0.717314	0.511966	McLeod *et al.* [40]
BC9016a	Basalt	Central Altiplano	23	936	40.1	0.704052	0.512801	Davidson and de Silva [13]

liths, observed in this study, and similar to xenoliths interpreted by Sparks *et al.* [16] to be remnants of a crustal hot zone could represent this contaminant.

7. Volcanic Hazards

Cerro Uturuncu has historically been inactive and glacial erosion suggests that the volcano is in a period of dormancy. However, new geophysical data has shown a concentric uplift centered on Uturuncu for the past 20 years with the potential to initiate future eruptions [32] [33]. According to the spatial distribution of previously erupted lava flows, it is difficult to predict the likeliness of where a lava flow will occur during a future potential eruption. In addition, the injection of new magma beneath the central vent could cause instability of the highly altered hydrothermal rocks composing the summit potentially leading to partial collapse of the vent and debris avalanches towards the north. This event has precedence in other CVZ composite cones [10] [21] [26], but has not been described in volcanic history of Cerro Uturuncu. These events at other intermediate centers have also been associated with pyroclastic flows and volcanic blasts [46]-[48]. The only village within the possibly affected area is Quetena Chico approximately 30 km to the northeast potentially affecting the community with ash fall in the event of one of these more explosive eruptions.

8. Conclusions

In this study we combine field, petrographic and geochemical data to describe the volcanic evolution of Cerro Uturuncu, at 22˚15'S, in the CVZ. The volcano has erupted uniform, crystal-rich orthopyroxene, biotite dacite and andesite lavas for ~620,000 years. Hydrothermal activity and glaciation resulted in the removal of the main vent suggesting a long period of dormancy since the last eruption. Field relationships between the lava flows and domes suggest eruptions are effusive with an average repose interval between 6000 and 8000 years. Sparks *et al.* [16] identified 50 lava flows; we have identified an additional 45 lava flows and 10 domes with the total number of erupted units to 105. Erupted volumes ranged between 0.1 km^3 and ~10 km^3 per eruption with a total volume erupted of ~89 km^3. Construction of the edifice took place in one stage in the volcanic history.

Typical phenocryst assemblage is plagioclase > OPX > biotite >> Fe-Ti oxides and quartz. Micro-inclusions and glomerocrysts contain trace olivine. Phenocrysts of plagioclase and OPX show multiple textures consistent with thermal disequilibrium. Lava flows and domes were erupted with a limited compositional range (61 wt% - 67 wt% SiO_2) of magma for ~620,000 years. Magmatic inclusions and xenoliths observed in nearly all lava flows and domes record the magmatic system beneath Uturuncu. Repeated injections of contaminated parental magma produce the compositional diversity observed in these magmatic inclusions. Xenocrysts/antecrysts of olivine and quartz in both the magmatic inclusion and the lava flows and domes, and the presence of quartz-rich xenoliths suggests crustal contamination is an important process in magma genesis.

Lavas and domes at Uturuncu show abundant evidence for thermal and chemical disequilibrium through the presence of sieved and zoned phenocryst phases and magmatic inclusions. Magma mixing controlled the limited compositional range observed in Uturuncu volcanic rocks. It is possible to explain the geochemical trends of the andesite and dacite volcanic rocks by differentiation in old, Sr radiogenic, Nd non-radiogenic felsic basement rock. The variation in isotopic composition suggests large amounts of assimilation fractional crystallization during differentiation.

Acknowledgements

The authors wish to thank Frank Ramos for use of and assistance with the thermal ionization mass spectrometer at New Mexico State University; the staff at the Geoanalyitical lab at Washington State University and all members of the PLUTONS Research group for insightful discussions. Jamie Kern for assistance mapping and collecting samples in the field, and the residents of Quetena Chico, Bolivia and Lipiko Tours for logistical support and hospitality. We thank the anonymous reviews for detailed comments that substantially improved this manuscript. Support for this work came from the U.S. National Science Foundation EAR-0901148 to TCF and grants to GSM from the Department of Earth Sciences at Montana State University.

References

[1] Davidson, J.P., Harmon, R.S. and Worner, G. (1991) The Source of Central Andean Magmas: Some Considerations. In: Harmon, R.S. and Rapela, C.W., Eds., *Andean Magmatism and Its Tectonic Setting*, *Geological Society of America Special Paper* 265, 233-244. http://dx.doi.org/10.1130/SPE265-p233

[2] Feeley, T.C. and Hacker, M.D. (1995) Intracrustal Derivation of Na-Rich Andesitic and Dacitic Magmas: An Example

from Volcán Ollagüe, Andean Central Volcanic Zone. *Geology*, **103**, 213-215.

[3] Klemetti, E.W. and Grunder, A.L. (2008) Volcanic Evolution of Volcan Aucanquilcha: A Long-Lived Dacite Volcano in the Central Andes of Northern Chile. *Bulletin of Volcanology*, **70**, 633-650. http://dx.doi.org/10.1007/s00445-007-0158-x

[4] Mamani, M., Tassara, A. and Wörner, G. (2008) Composition and Structural Control of Crustal Domains in the Central Andes. *Geochemistry Geophysics and Geosystems*, **9**, 3. http://dx.doi.org/10.1029/2007GC001925

[5] Mamani, M., Wörner, G. and Sempere, T. (2010) Geochemical Variation in Igneous Rocks of the Central Andean Orocline (13˚ to 18˚S): Tracing Crustal Thickening and Magma Generation through Time and Space. *Geological Society of America Bulletin*, **122**, 163-182. http://dx.doi.org/10.1130/B26538.1

[6] de Silva, S.L. (1989) Altiplano-Puna Volcanic Complex of the Central Andes. *Geology*, **17**, 1102-1106. http://dx.doi.org/10.1130/0091-7613(1989)017<1102:APVCOT>2.3.CO;2

[7] de Silva, S.L., Zandt, G., Trumbull, R., Viramonte, J., Salas, G. and Jiminez, N. (2006) Large Ignimbrite Eruptions and Volcano-Tectonic Depressions in the Central Andes: A Thermomechanical Perspective. In: Troise, C., De Natale, G. and Kilburn, C.R.J., Eds., *Mechanisms of Activity and Unrest at Large Calderas*, *Geological Society Special Publication No.* 269, The Geological Society, London, 47-63.

[8] Lindsay, J.M., de Silva, S.L., Trumbull, R. and Emmermann, R. (2001) La Pacana Caldera, N. Chile: A Re-Evaluation of the Stratigraphy and Volcanology of One of the World's Largest Resurgent Calderas. *Journal of Volcanology and Geothermermal Research*, **106**, 145-173. http://dx.doi.org/10.1016/S0377-0273(00)00270-5

[9] Lindsay, J.M., Schmitt, A.K., Trumbull, R.B., de Silva, S.L., Siebel, W. and Emmermann, R. (2001) Magmatic Evolution of the La Pacana Caldera System, Central Andes, Chile: Compositional Variation of Two Cogenetic Large-Volume Felsic Ignimbrites. *Journal of Petrology*, **42**, 459-486. http://dx.doi.org/10.1093/petrology/42.3.459

[10] Grunder, A.L., Klemetti, E.W., Feeley, T.C. and McKee, C.M. (2008) Eleven Million Years of Arc Volcanism at the Aucanquilcha Volcanic Cluster, Northern Chilean Andes: Implications for the Life Span and Emplacement of Plutons. *Transactions of the Royal Society of Edinburgh*: *Earth Sciences*, **97**, 415-436.

[11] Kussmaul, S., Hormann, P.K., Ploskonka, E. and Subieta, T. (1977) Volcanism and Structure of Southwestern Bolivia. *Journal of Volcanology and Geothermal Research*, **2**, 73-111. http://dx.doi.org/10.1016/0377-0273(77)90016-6

[12] Baker, M.C.W. and Francis, P.W. (1978) Upper Cenozoic Volcanism in Central Andes—Ages and Volumes. *Earth and Planetary Science Letters*, **41**, 175-187. http://dx.doi.org/10.1016/0012-821X(78)90008-0

[13] Davidson, J.P. and de Silva, S.L. (1995) Late Cenozoic Magmatism of the Bolivian Altiplano. *Contributions to Mineralogy and Petrology*, **119**, 387-408. http://dx.doi.org/10.1007/BF00286937

[14] James, D.E. (1971) Plate Tectonic Model for the Evolution of the Central Andes. *Geological Society of America Bulletin*, **82**, 3325-3346. http://dx.doi.org/10.1130/0016-7606(1971)82[3325:PTMFTE]2.0.CO;2

[15] Beck, S.L. and Zandt, G. (2002) The Nature of Orogenic Crust in the Central Andes. *Journal of Geophysical Research*: *Solid Earth*, **107**, ESE710-ESE716.

[16] Sparks, R.S.J., Folkes, C.B., Humphreys, M.C.S., Barfod, D.N., Clavero, J., Sunagua, M.C., McNutt, S.R. and Pritchard, M.E. (2008) Uturuncu Volcano, Bolivia: Volcanic Unrest Due to Mid-Crustal Magma Intrusion. *American Journal of Science*, **308**, 727-769. http://dx.doi.org/10.2475/06.2008.01

[17] Harford, C.L., Pringle, M.S., Sparks, R.S. and Young, S.R. (2002) The Volcanic Evolution of Montserrat Using $^{40}Ar/^{39}Ar$ Geochronology. In: Druitt, T.H. and Kokelaar, B.P., Eds., *The Eruption of Soufriere Hills Volcano*, *Montserrat* 1995 *to* 1999, Geological Society Memoir, London, 93-113.

[18] Le Friant, A., Lock, E.J., Hart, M.B., Boudon, G., Sparks, R.S., Leng, M.J., Smart, C.W., Komorowski, J.C., Deplus, C. and Fisher, J.K. (2008) Late Pleistocene Tephrochronology of Marine Sediments Adjacent to Montserrat, Lesser Antilles Volcanic Arc. *Journal of the Geological Society*, **165**, 279-289. http://dx.doi.org/10.1144/0016-76492007-019

[19] Allmendinger, R.W., Jordan, T.E., Kay, S.M. and Isacks, B.L. (1997) The Evolution of the Altiplano-Puna Plateau of the Central Andes. *Annual Reviews in Earth and Planetary Science*, **25**, 139-174. http://dx.doi.org/10.1146/annurev.earth.25.1.139

[20] de Silva, S.L. and Francis, P.W. (1991) Volcanoes of the Central Andes. Springer-Verlag, New York.

[21] Feeley, T.C., Davidson, J.P. and Armendia, A. (1993) The Volcanic and Magmatic Evolution of Volcán Ollagüe, a High-K, Late Quaternary Stratovolcano in the Andean Central Volcanic Zone. *Journal of Volcanology and Geothermal Research*, **54**, 221-245. http://dx.doi.org/10.1016/0377-0273(93)90065-Y

[22] Hayes, G.P., Wald, J.D. and Johnson, R.L. (2012) Slab1.0: A Three-Dimensional Model of Global Subduction Zone Geometries. *Journal of Geophysical Research*: *Solid Earth*, **117**, 1-15. http://dx.doi.org/10.1029/2011JB008524

[23] Muir, D.D., Blundy, J., Hutchinson, M.C. and Rust, A.C. (2014) Petrological Imaging of an Active Pluton beneath Cerro Uturuncu, Bolivia. *Contributions to Mineralogy and Petrology*, **167**, 980.

http://dx.doi.org/10.1007/s00410-014-0980-z

[24] Thorpe, R.S., Potts, P.J., Hammill, M. and Baker, M.C.W. (1982) The Andes. In: Thorpe, R.S., Ed., *Andesites*, Wiley, New York, 187-205.

[25] Coira, B., Davidson, J., Mpodozis, C. and Ramos, V. (1982) Tectonic and Magmatic Evolution of the Andes of Northern Argentina and Chile. *Earth-Science Reviews*, **18**, 303-332.

[26] de Silva, S.L., Davidson, J.P., Croudace, I.W. and Escobar, A. (1993) Volcanological and Petrological Evolution of Volcán Tata Sabaya, SW Bolivia. *Journal of Volcanology and Geothermal Research*, **55**, 305-335.

[27] Johnson, D.M., Hooper, P.R. and Conrey, R.M. (1999) GeoAnalytical Lab, Washington State University. *Advances in X-Ray Analysis*, **41**, 843-867.

[28] Jarvis, K.E. (1988) Inductively Coupled Plasma Mass Spectrometry: A New Technique for the Rapid or Ultra-Trace Level Determination of the Rare-Earth Elements in Geological Materials. *Chemical Geology*, **68**, 31-39. http://dx.doi.org/10.1016/0009-2541(88)90084-8

[29] Michelfelder, G.S., Feeley, T.C., Wilder, A.D. and Klemetti, E.W. (2013) Modification of the Continental Crust by Subduction Zone Magmatism and *Vice-Versa*: Across-Strike Geochemical Variation of Silicic Lavas from Individual Eruptive Centers in the Andean Central Volcanic Zone. *Geosciences*, **3**, 633-667. http://dx.doi.org/10.3390/geosciences3040633

[30] Schmitt, A.K., de Silva, S.L., Trumbull, R. and Emmermann, R. (2001) Magma Evolution in the Purico Ignimbrite Complex, Northern Chile: Evidence for Zoning of a Dacitic Magma by Injection of Rhyolitic Melts Following Mafic Recharge. *Contributions to Mineralogy and Petrology*, **140**, 680-700. http://dx.doi.org/10.1007/s004100000214

[31] Iriarte, R. (2012) The Cerro Guacha Caldera Complex: An Upper Miocene-Pliocene Polycyclic Volcano-Tectonic Structure in the Altiplano Puna Volcanic Complex of the Central Andes of Bolivia. M.S., Oregon State University, Corvallis, 127 p.

[32] Pritchard, M.E. and Simons, M. (2002) A Satellite Geodetic Survey of Large-Scale Deformation of Volcanic Centres in the Central Andes. *Nature*, **418**, 167-171. http://dx.doi.org/10.1038/nature00872

[33] Henderson, S.T. and Pritchard, M.E. (2013) Decadal Volcanic Deformation in the Central Andes Volcanic Zone Revealed by InSAR Time Series. *Geochemistry, Geophysics, Geosystems*, **15**, 1358-1374. http://dx.doi.org/10.1002/ggge.20074

[34] Fernandez, A.C., Hormann, P.K., Kussmaul, S., Meave, J., Pichler, H. and Subieta, T. (1973) First Petrologic Data on Young Volcanic Rocks of SW-Bolivia. *Mineralogy and Petrology*, **19**, 149.

[35] Hildreth, W.S. and Moorbath, S. (1988) Crustal Contribution to Arc Magmatism in the Andes of Central Chile. *Contributions to Mineralogy and Petrology*, **98**, 455-489. http://dx.doi.org/10.1007/BF00372365

[36] Bacon, C.J. (1986) Magmatic Inclusions in Silicic and Intermediate Volcanic Rocks. *Journal of Geophysical Research: Solid Earth*, **91**, 6091-6112. http://dx.doi.org/10.1029/JB091iB06p06091

[37] Davidson, J.P., McMillan, N.J., Moorbath, S., Wörner, G., Harmon, R.S. and Lopez-Escobar, L. (1990) The Nevados de Payachata Volcanic Region (18°S, 69°W, N. Chile) II: Evidence or Widespread Crustal Involvement in Andean Magmatism. *Contributions to Mineralogy and Petrology*, **105**, 412-432. http://dx.doi.org/10.1007/BF00286829

[38] Feeley, T.C., Wilson, L.F. and Underwood, S.J. (2008) Distribution and Composition of Magmatic Inclusions in the Mount Helen Dome, Lassen Volcanic Center, California: Insight into Magma Chamber Processes. *Lithos*, **106**, 173-189. http://dx.doi.org/10.1016/j.lithos.2008.07.010

[39] Ort, M.H., Coira, B.L. and Mazzoni, M.M. (1996) Generation of a Crust-Mantle Mixture; Magma Sources and Contamination at Cerro Panizos Central Andes. *Contributions to Mineralogy and Petrology*, **123**, 308-322. http://dx.doi.org/10.1007/s004100050158

[40] McLeod, C.L., Davidson, J.P., Nowell, G.M., de Silva, S.L. and Schmitt, A.K. (2013) Characterizing the Continental Basement of the Central Andes: Constraints Form Bolivian Crustal Xenoliths. *Geological Society of America Bulletin*, **125**, 985-997. http://dx.doi.org/10.1130/B30721.1

[41] Lucassen, F., Franz, G., Thirlwall, M.F. and Mezger, K. (1999) Crustal Recycling of Metamorphic Basement: Late Paleozoic Granites of Northern Chile (~22°S). Implications for the Composition of the Andean Crust. *Journal of Petrology*, **40**, 1527-1551. http://dx.doi.org/10.1093/petroj/40.10.1527

[42] Hernando, I.R., Aragon, E., Frei, R., González, P.D. and Spakman, W. (2014) Constraints on the Origin and Evolutions of Magmas in the Payún Matrú Volcanic Field, Quaternary Andean Back-Arc of Western Argentina. *Journal of Petrology*, **55**, 209-239. http://dx.doi.org/10.1093/petrology/egt066

[43] De Paolo, D.J. (1981) Trace Element and Isotopic Effects of Combined Wallrock Assimilation and Fractional Crystallization. *Earth and Planetary Science Letters*, **53**, 189-202. http://dx.doi.org/10.1016/0012-821X(81)90153-9

[44] Feeley, T.C. (1993) Crustal Modification during Subduction-Zone Magmatism: Evidence from the Southern Salar de

Uyuni Region (20˚-22˚S), Central Andes. *Geology*, **21**, 1019-1022. http://dx.doi.org/10.1130/0091-7613(1993)021<1019:CMDSZM>2.3.CO;2

[45] Kay, S.M., Coira, B.L., Caffe, P.J. and Chen, C.H. (2010) Regional Chemical Diversity, Crustal and Mantle Sources and Evolution of Central Andean Puna Plateau Ignimbrites. *Journal of Volcanology and Geothermal Research*, **198**, 81-111. http://dx.doi.org/10.1016/j.jvolgeores.2010.08.013

[46] Clavero, J.E., Sparks, R.S.J., Pringle, M.S., Polanco, E. and Gardeweg, M.C. (2004) Evolution and Volcanic Hazards of Taapaca Volcanic Complex, Central Andes of Northern Chile. *Journal of the Geologic Society*, **161**, 603-618. http://dx.doi.org/10.1144/0016-764902-065

[47] Voight, B., Komorowski, J. and Norton, G. (2002) The 26 December (Boxing Day) 1997 Sector Collapse and Debris Avalanche at Soufriere Hills Volcano, Montserrat. In: Druitt, T. and Kokelaar, P., Eds., *The Eruption of Soufriere Hills Volcano, Montserrat, from* 1995 *to* 1999, Geological Society, Memoirs, London, 363-408.

[48] Sparks, S. and Young, S. (2002) The Eruption of Soufriere Hills Volcano, Montserrat (1995-1999): Overview of Scientific Results. In: Druitt, T. and Kokelaar, P., Eds., *The Eruption of Soufriere Hills Volcano, Montserrat, from* 1995 *to* 1999, Geological Society, Memoirs, London, 45-70.

CHAPTER FIVE

CRUSTAL DIFFERENTIATION PROCESSES AT CERRO UTURUNCU, ANDEAN CENTRAL VOLCANIC ZONE, SW BOLIVIA: INSIGHTS FROM IN SITU SR ISOTOPIC ANALYSES OF PLAGIOCLASE PHENOCRYSTS

Contribution of Authors and Co-Authors

Manuscript in Chapter 5

Author: Gary S. Michelfelder

Contributions: Performed geochemical analyses, field work sample preparation, and performed computer modeling. Wrote manuscript with input on data from co-authors.

Co-Author: Todd C. Feeley

Contributions: Aided in the preparation of the manuscript and figures.

Manuscript Information Page

Michelfelder, G.S., and Feeley, T.C.
Geosphere
Status of Manuscript:
__x_ Prepared for submission to a peer-reviewed journal
____ Officially submitted to a peer-review journal
____ Accepted by a peer-reviewed journal
____ Published in a peer-reviewed journal

Geophere, PLUTONS Special Issue, Geological Society of America

Crustal differentiation processes at Cerro Uturuncu, Andean Central Volcanic Zone, SW Bolivia: Insights from in situ Sr isotopic analyses of plagioclase phenocrysts

The following work is currently in progress to be submitted for publication

Gary S. Michelfelder; and Todd C. Feeley

Department of Earth Sciences, Montana State University, Bozeman, MT, USA

ABSTRACT

Cerro Uturuncu is an andesitic to dacitic composite volcano located in the back-arc of the Andean Central Volcanic Zone, SW Bolivia. We present new major and trace element and Sr isotopic data of plagioclase phenocrysts combined with whole rock Sr isotope ratio ($^{87}Sr/^{86}Sr$= 0.71009-0.71653) from Uturuncu lavas and domes.

The isotopic, textural and compositional characteristic of plagioclase phenocrysts in Uturuncu magmas suggest that these crystals were inherited from isotopically more evolved continental crust, which was periodically recharged by higher- temperature, lower $^{87}Sr/^{86}Sr$ ratio magmas. We identified distinct plagioclase phenocryst populations reflecting assimilation of continental crust and mixing with less evolved magmas. Consistent core to rim decreases in $^{87}Sr/^{86}Sr$ ratios and coincident increases in Sr concentrations in plagioclase phenocrysts with maximum $^{87}Sr/^{86}Sr$ ratios of 0.7139-0.7276 are found in the cores. Minimum ratios of 0.7105-0.7138 are found in rims in contact with glass. These data demonstrate that open-system processes operating at shallow crustal depths modified Uturuncu magmas, regardless of the nature of mantle or crustal sources. Calculated crystal residence times suggests that observed isotopic crystal heterogeneities could not have existed for more than a few thousand years (20-5500

years) at inferred magmatic temperatures (790-920°C). The chemical and isotopic variability observed in Uturuncu plagioclase phenocrysts within single lava flows or domes suggest that although shallow crustal assimilation and magma mixing appear to have had limited effects on whole rock chemistry, a complex, late-stage petrogenetic history is recorded within the magmatic cargo of crystals and andesite composition magmatic inclusions.

INTRODUCTION

Volcanism in the central Andes (Central Volcanic Zone, CVZ) of Bolivia, Chile, Peru and northwestern Argentina constitutes the most dramatic example of volcanic arc magmas modified by thick, continental crust. Few composite volcanoes in the arc have been studied in detail, and even fewer studies have focused on back-arc centers where the continental crust may be as thick as 80 km (Beck and Zandt, 2002) and where volumes of intruded magmas are drastically less than along the arc-front (Baker and Francis, 1978). Of the studies that are available on back-arc centers, interpretations of processes, sources and contaminants have largely relied on bulk-rock isotopic and trace element compositions (Wörner et al., 1988; Ginibre and Wörner, 2007, Mamani et al., 2008; 2010). Bulk compositions of volcanic rocks represent the sum of the components and integrated effects that define the magmatic system from the source rock to final crystallization and eruption (Tepley et al., 1999; 2000; Ramos et al., 2005a; 2005b). However, bulk rock compositions impose inherent limitations on petrologic interpretations. While it is straightforward to distinguish components in a suite with bulk-mineral or bulk-rock data, it is difficult to determine where in the crust magmatic process

occurred, time-scales of the process, and order of events when multiple processes and events are suspected (Tepley, 1999; Davidson et al., 2006; 2007b; Ramos and Tepley, 2008).

Differentiated and hybridized magmas often acquire isotopic signatures prior to, and during differentiation and hybridization in early formed, well-preserved crystal cores and rims (Davidson et al., 2005; 2007a; Tepley et al., 1999, 2000; Ramos and Reid, 2005; Ramos and Tepley, 2008). Studies of crystal isotope stratigraphy (CIS; textural, chemical and isotopic analyses of single crystals and growth zones within crystals) have shown that sub-mineral scale-trace element compositions and isotopic ratios express more variation within a single unit than observed in the entire suite of rocks from individual centers (Tepley et al., 1999; 2000; Davidson et al., 2001; 2007a; 2007b; Ramos and Tepley, 2008). Isotopic and trace element analyses of individual mineral components in volcanic rocks have been shown to be extremely valuable in identifying and isolating the effects of magmatic processes (Davidson et al., 2007; Wolff et al., 1999; Ramos et al., 2005; Ramos and Tepley, 2008; Ginibre and Davidson, 2014), and record detailed information on the processes affecting crystallization relative to bulk-rock analyses (Francalanci et al., 2012). Until recently, CIS studies have focused on large volcanic systems (i.e. flood basalts and ignimbrites; Ramos and Reid, 2005; Ramos and Tepley, 2008; Ramos et al. 2013) or systems with simple crystal cargos producing aphyric lava and pyroclastic flows (Tepley et al., 1999; 2000; Davidson et al., 2005; Ginibre and Davidson, 2014). The plumbing systems for these systems represent simplistic histories compared to their complex continental arc counterparts. Nevertheless, CIS studies of

these systems have revealed hidden complexities and complex internal magmatic architectures (Font et al., 2008; Jerram and Widdowson, 2008) that were previously unrecognized through bulk-rock geochemistry alone by incorporating textural information and variation in trace element and isotopic compositions recorded in a single mineral (Davidson et al., 2005; 2007a; Ramos and Tepley, 2008; Ginibre and Davidson, 2014).

In this study we present CIS data on plagioclase phenocrysts in volcanic rocks from Cerro Uturuncu (22.15 ° S) in the back-arc of the Andean Central Volcanic Zone (Fig. 1). The purpose is to investigate, through the application of *in situ* Sr isotope analyses, the differentiation pathways that plagioclase phenocrysts record to help define the dynamics and time-scales of crystal exchange in a complex continental back-arc system. This paper presents detailed textural studies of plagioclase phenocrysts in Uturuncu lava flows and domes, together with in situ Sr isotope ratios, to assess compositional variability and the process of magma differentiation, generation, and migration.

TECTONIC AND REGIONAL BACKGROUND

Late Cenozoic to modern volcanic rocks in the CVZ are divided into three groups based on similarities in composition and eruptive style (Thorpe et al., 1982; Feeley et al., 1993). First, between 21-24° S, large-volume, regionally extensive (~70,000 km^2) ignimbrites erupted from large caldera complexes on the Altiplano and Western Cordillera (Coira et al., 1982; de Silva, 1989; de Silva et al., 2006). These rocks are calc-alkaline, homogeneous dacites to rhyolites. Second, basaltic andesitic to dacitic lava

flows erupted from 23 Ma to the present. At 21 °–22 ° S, the largest volumes of these magmas erupted from composite volcanoes that form the peaks of the Western Cordillera. Baker and Francis (1978) estimated that the Western Cordillera contains ~3000 km^3 of these lavas between 21° and 22° S latitude. Lavas associated with composite volcanoes extend for ~200 km eastward onto the Altiplano, although volumes decrease sharply to <800 km^3. Uturuncu is associated with this group. Third, volumetrically minor alkali basalts erupted from small monogenetic centers to the east of the arc-front on the Altiplano north of 21° S (de Silva et al., 1993; Davidson and de Silva, 1995).

Recent magmatism directly underlying Uturuncu involved the regionally extensive ignimbrites erupted from calderas associated with the Altiplano-Puna Volcanic Complex (APVC) of de Silva (1989). Located in the center of the CVZ, the APVC erupted more ~15,000 km^3 of crystal-rich ignimbrite over the last 10 m.y. distributed over an area of ~70,000 km^2 (de Silva et al., 2006; Ward et al., 2014). Geochemical studies of these ignimbrites suggest they are similar in their processes and generation to magmas erupted at Uturuncu. Mixing of mantle-derived and crustal melts in the middle crust (15-30 km depth) and subsequent mixing at 4-8 km depth created homogeneous composition dacites (Schilling et al., 2006; de Silva et al., 2006; Kay et al., 2010). Geophysical studies suggest that at 4-15 km depth a laterally extensive (~60,000 km^2) seismic low-velocity zone (LVZ) is centered beneath the APVC known as the Altiplano-Puna Magmatic Body (APMB; Chmielowski et al., 1999; Zandt et al., 2003; Leidig and Zandt, 2003; Ward et al., 2013; 2014). The APMB has been argued to be of similar volume to

the APVC ignimbrites, but could be has large as 500,000 km^3 (Ward et al., 2014). Modern surface uplift directly beneath Uturuncu has been modeled to be related to magma movement from the APMB to the upper crust (Pritchard and Simons, 2002; 2004; Fialko and Pearse, 2012; Hickey et al., 2012; del Potro et al., 2013; Muir et al., 2014b).

McLeod et al. (2013) described a series of xenoliths and magmatic inclusions from the Altiplano north of Cerro Uturuncu expressing the diverse compositions of crustal basement in the CVZ. Xenoliths described in this study include sillimante-gneisses, diorites, garnet granulites, granites and garnet quartzites. Sr isotopic ratios for these xenoliths range from 0.710 to 0.738. The diorites and granites range from 0.710 to 0.713 and the quartzites and schists range from 0.720 to 0.738. A gap in isotopic composition exists between 0.724 and 0.730 (McLeod et al., 2013).

Cerro Uturuncu

Cerro Uturuncu is a composite volcano located at 22° 15’ S (Fig. 1) in the CVZ of southwest Bolivia, 125 km behind the modern arc-front. Eruptions from the center were effusive, producing ~105 geochemically distinct lava flows and domes over ~800,000-year eruptive history (Muir et al., 2014b). The volcano overlies Miocene and younger volcanic rocks and folded and faulted mid-Miocene and older volcanic and sedimentary rocks (Sparks et al., 2008).

Sparks et al. (2008), Muir et al. (2014a; 2014b), and Michelfelder et al. (2014) have discussed the volcanic history of Uturuncu in detail. Uturuncu volcanic rocks are crystal-rich andesites to dacites that dominantly contain plagioclase and orthopyroxene (OPX) phenocrysts. Muir et al. (2014a) determined from volatile concentrations of

plagioclase melt inclusions that magma storage ranged from 50-119 MPa, and these authors suggested this storage system was well homogenized. Magmatic temperatures for the shallow crustal chamber ranges from 790 to 920° C calculated using Fe-Ti oxide geothermometry (Sparks et al., 2008; Muir et al., 2014a).

Magma mixing and mingling dominates the petrogenic processes at Cerro Uturuncu based on bulk rock major- and trace- element trends (Sparks et al., 2008). Observations by Sparks et al. (2008) of reversely zoned OPX phenocrysts and complex chemical zoning in plagioclase provided further evidence to these authors that magma mixing was important in the generation of Uturuncu magma, but could not constrain the location or timescales of the events. In combination with geophysical evidence from current deformation, a hot zone/ MASH zone (Hildreth and Moorebath, 1988; Annen et al., 2006) beneath the volcano was suggested to be the location where mixing occurred. These authors suggested that dacitic magmas accumulate at the top of the hot zone and periodically rise to form shallow chambers at 4-8 km depth (Sparks et al., 2008; Henderson et al., 2013; Muir et al., 2014a; 2014b).

RESULTS

Petrography and Bulk-Rock Geochemistry of Uturuncu Lavas and Domes

Texturally, Uturuncu lava flows and domes are porphyritic to seriate. Domes are occasionally hiatal. Some lava flows have ophitic and poikilitic textures observed in orthopyroxene (OPX) and plagioclase phenocrysts. Glomerocrysts containing OPX, Fe-Ti oxides and plagioclase with rare olivine are present in some lava flows. Modal compositions of Uturuncu volcanic rocks are variable in crystal content but restricted in

mineral assemblage (Fig. 2). In all lava flows and domes, phenocrysts volumes range from 30-53% total volume. Phenocrysts include plagioclase (An_{42-94}) > OPX (En_{45-83}) > biotite >> quartz, Fe-Ti oxides, and trace clinopyroxene (CPX), and hornblende and olivine in quenched micro-inclusions (Fig. 2). Nearly all OPX crystals show some zoning. Chemically unzoned OPX are only associated with glomerocrysts and in groundmass crystals. OPX crystals are Ca- poor at (Wo_{06} or less) and represent two zoned populations (Sparks et al., 2008). The first contains Mg-poor cores (En_{55}) and reverse zoned rims (En_{65-75}), and the second population contains Mg- rich cores (En_{65-80}) and normally zoned rims (En_{50-705}). Reaction rims of Fe-Ti oxides and OPX typically surrounds biotite phenocrysts over 0.5 mm. Quartz and olivine phenocrysts and microphenocrysts typically exhibit resorption textures suggesting they are most likely xenocrysts or antecrysts.

Groundmass of the lava flows and domes are hyalopilitic with mineral phases similar to phenocryst phases. Additional phases in the groundmass include glass, trace zircon, apatite, and occasional olivine. Groundmass plagioclase (An_{45-85}) crystals do not exhibit sieving observed in phenocrysts. Groundmass plagioclase and OPX (En_{46-75}) crystals occasionally show zoning and dissolution surfaces. Vesicles comprise approximately 8-23 % of the mode in domes interiors and 0-12 % in lava flows. Sparks et al. (2008), Michelfelder et al. (2014) and Muir et al. (2014b) describe the textural differences between the lava flows and domes in detail, and as such these are not discussed here.

Figures 3, 4 and 5 illustrates bulk rock major- and trace- element compositions of lava flows, domes and inclusions. The suite as a whole define a high-K, calc-alkaline suite (Figs. 3 & 4). SiO_2 ranges from 61-67 wt.% for the lava flows and domes, 53-64 wt.% for the magmatic inclusions and 78-79 wt.% for the xenoliths (Fig. 3). For the suite as a whole, contents of CaO, FeO*, MgO, TiO_2, MnO, Yb, Sr and Cr decrease, whereas Na_2O, K_2O, P_2O_5, La, Zr, Ba and Rb increase with increasing SiO_2 contentss (Figs. 4 & 5). LIL-element concentrations for Uturuncu volcanic rocks are enriched compared to other centers well-studied composite volcanoes in the CVZ (Mamani et al., 2008; 2010; Michelfelder et al., 2013; 2014).

The compositional variation and trends observed highlight petrologic processes affecting the evolution of Uturuncu magmas. The linear trends observed in major element compositions and the divergent linear trends in MgO, La, Sr, Y and Yb suggest multiple sources during magma evolution (Michelfelder et al., 2014). The linear trends are interpreted to reflect magma mixing as the dominant process in the generation of compositional diversity of lavas and domes at Uturuncu. Magmatic inclusion compositions are an extension of this trend at lower SiO_2 contents.

Table 1 presents and Figure 6 illustrates radiogenic bulk-rock Sr and Nd isotopic ratios of lavas and domes. The range in $^{87}Sr/^{86}Sr$ (0.71009-0.71653) and $^{143}Nd/^{144}Nd$ (0.51215-0.51225) isotopic ratios for Uturuncu rocks is small compared to the range observed across the CVZ (Davidson et al. 1990; Mamani et al., 2008; 2010). In comparison with other individual CVZ composite volcanoes, Uturuncu rocks have higher $^{87}Sr/^{86}Sr$ ratios and lower $^{143}Nd/^{144}Nd$ ratios. These lava flows and domes are more

similar to ignimbrites erupted from Cerro Panizos on the eastern Altiplano (Ort et al., 1996; Schmitt et al., 2001; de Silva et al., 2006). The $^{87}Sr/^{86}Sr$ isotopic compositions for the inclusions overlap the lowest ratios measured in the host lavas and domes (Fig. 6) suggesting extensive crustal contamination of the most mafic magmas present at this volcano.

Magmatic Inclusions

A common occurrence in Uturuncu volcanic rocks is the presence of magmatic inclusions. Individual lava flows vary greatly in the volume of magmatic inclusions ranging from ~0- 4%. Three general populations of inclusions exist in Uturuncu lava flows and domes. Mineralogically and petrographically inclusions exhibit similar modes to the lavas and domes. With the exception of inclusions defining population 3, inclusions typically lack quartz and biotite and contain a higher volume of CPX and olivine compared to the host lava flows and domes.

The first population of inclusions is ellipsoidal with a porphyritic to hiatal texture and contains a thick, vesicle-free, glassy rim with vesiculated interiors. These inclusions are characterized by euhedral to subhedral parageneitcally early phenocrysts of OPX and plagioclase in varying proportions. Plagioclase phenocrysts range in size from 0.25 mm to 1.5 mm along the long axis. Large plagioclase phenocrysts are interpreted as xenocrysts or antecrysts because they contain cores riddled with abundant, irregular shaped glass inclusions and euhedral rims and oscillatory zoning patterns similar to those observed in the host lava flows and domes. The groundmasses of these inclusions are hyalopilitic and are composed of microlite- sized (<0.25 mm) plagioclase crystals and Fe-

Ti oxides in a glassy matrix. These inclusions are the most common type observed, and range in size from micro-inclusions (<3 mm) to ~5 cm in diameter although occasional larger inclusions were observed.

The second population of inclusions are non-vesiculated basaltic-andesite clots, containing plagioclase > OPX > Fe- Ti oxides > olivine > amphibole $\pm$ clinopyroxene. Hiatal to intergranular crystal sizes dominate this population of inclusions. The second population of inclusions lack glassy rims in contact with the host lava flow or dome as described above. The contacts of the inclusions are angular and defined by crystal boundaries. Crystal sizes range from microlite- size to crystals ~1.5 mm along the long axis. Inclusion size varies from micro- inclusions (<3 mm) to ~10 cm in diameter. Hand specimen size samples of this inclusion population were only observed in two lava flows, although these inclusions may have been overlooked due to their similarity in color to the host lavas when weathered. Two additional lava flows and one dome contain micro-inclusions of this population.

Non-vesiculated micro-inclusions are distinct from the glomerocrysts observed lava flows and domes due to their crystal size and presence of rare amphibole. OPX phenocrysts are similar in size to the plagioclase though chemical zoning is not present. Some plagioclase phenocrysts show sieving and dissolution surfaces and all crystals over 0.5 mm contain growths zones. A reaction rim of OPX typically surrounds olivine phenocrysts. The groundmasses of the non-vesiculated inclusions are intergranular to hyalopilitic and are composed of microlite-sized acicular lath of plagioclase and blocky OPX.

Vesiculated and non-vesiculated magmatic inclusions (population 1 and 2) are common features observed in CVZ volcanic rocks as well as at other intermediate composition volcanic systems around the world (Bacon, 1986; Feeley et al., 1993; 2008). Magmatic inclusions, with or without vesiculation, are suggested to represent blobs of mafic magma quenched in cooler, more silicic magma due to the processes of magma mixing and mingling (Bacon, 1986; Michelfelder et al., 2014).

The third population of inclusions observed does not exhibit the same mineralogy as the host lavas and domes. This population is dominantly hypidiomorphic to allotriomorphic granular with trace to rare glass (0-0.5 %). Plagioclase and quartz dominate the mode of these inclusions with trace OPX and biotite. Plagioclase crystals are clear with no growth zones or dissolution surfaces observed. Quartz crystals show resorption along the corners of the crystals. Margins of these inclusions are angular and defined by the crystal boundaries. Textures observed in this population of inclusions suggest the inclusions are xenoliths (Michelfelder et al., 2014).

Sparks et al. (2008) described two additional xenolith populations have a similar textures to inclusions in population 3 of this study. These authors interpreted observed quartz-rich xenoliths to represent crustal partial melting of rocks trapped in a MASH zone (Annen et al., 2006). It is our interpretation that xenoliths observed in this study represent basement rocks interacting with Uturuncu magmas during migration and differentiation. These xenoliths may represent the residue of a granodiorite or Paleozoic sedimentary crustal contaminant beneath Uturuncu.

A fourth inclusion population described by Sparks et al. (2008) and was not observed in this study. These authors describe a noritic composition xenolith population found in multiple lava flows sampled in the study. These xenoliths contain mineral assemblages and a similar mineral composition to those observed in the lava flows and domes (Sparks et al., 2008). The adcumulate textures observed in these xenoliths suggested to these authors that these xenoliths represent adcumulates of early-formed crystals that segregated from hotter, less evolved residual magma related to the Uturuncu magmas (Sparks et al., 2008).

Nomarski Interferometry

Nomarski interference contrast imaging (NDIC) is a powerful tool for visualizing textural and zoning patterns in plagioclase phenocrysts and microphenocrysts (Anderson, 1983). The imaging techniques uses plane polarized reflected light to enhance surface relief created by etching plagioclase with compositional zoning. NDIC images of typical Uturuncu plagioclase phenocrysts presented in Figure 7. They reveal four textures common in the crystal history (1) crystal growth zones, (2) resorption surfaces characterized by rounding of edges and corners and partial to complete removal of growth surfaces, (3) partial resorption (sieving) in the core or rim of a phenocryst, and (4) partial resorption in both the core and rims of the phenocryst. Dissolution surfaces in plagioclase phenocrysts are characterized by a sequence of crystal boundaries with rounding of euhedral crystals to complete removal of crystal faces. Incomplete dissolution results in a sieved-texture where micrometer- scale channels of glass cut through the crystal, resulting in the appearance of pitting or glass in the crystal (Tepley et

al., 1999; 2000; Davidson and Tepley, 2003). Growth zones reflect crystallization under equilibrium or near equilibrium conditions.

Three examples of plagioclase phenocrysts from a single lava flow represent the variety of textures observed in plagioclase phenocrysts from Uturuncu volcanic rocks. The largest crystal of the three [DM15P5; 2.3 mm] exhibits complete and incomplete dissolution surfaces and subsequent growth zones. Dissolution surfaces are irregular, and on some surfaces, truncation of growth zones by dissolution creates an asymmetrical appearance to the crystal (Fig. 7). Sieving in the core represents partial dissolution immediately following the crystal being added to the melt or growth of the crystal. The growth zone in contact with surrounding glass is clear and sharp (no sieve textures) and with only minor dissolution at the corners of the crystal.

The medium sized crystal [DM15P9; 0.4 mm] exhibits multiple irregular dissolution surfaces suggesting multiple periods in thermal disequilibrium with the host melt (Fig. 7). Micron-scale growth rims are only present in the rims closest to the glass. No sieving is present in the core of the crystal. A single dissolution surface is observed between the core and clear growth rims in the smallest crystal of the three [DM15P3; 0.25 mm]. Closer examination, however, reveals rolling crystal surfaces overlain by faceted growth zones that tend to restore a euhedral to subhedral crystal shape (Fig. 7).

Electron-Microprobe Analysis (EMPA)

One of the most distinctive features observed in EMPA traverses across zoned plagioclase crystals is punctuated changes in anorthite (An) content (McGee et al., 1987; Tepley et al., 2000). Figure 8 illustrates and Table 2 presents a compilation of

representative traverses across plagioclase phenocrysts. Most crystals show sharp variations in An content along the traverse (Fig. 8). Variation is randomly spaced and variable in magnitude. There is no correlation between crystal size, number of zones and magnitude of An variation.

Compositions of phenocryst cores range from An_{42} to An_{94} and are heterogeneous within a single lava flow or dome (Fig. 9) and show no correlation of size of the crystal core and An composition (Fig. 8). Phenocryst rims typically show more variation in a single lava flow or dome than is observed in cores from the same unit ranging from An_{39} to An_{87}. Plagioclase phenocrysts can be assigned to one of four textural and compositional types: (1) normally zoned; (2) reversely zoned; (3) oscillatory zoned; or (4) unzoned. Normally zoned phenocrysts have cores ranging from An_{46} to An_{94} and decrease in An content toward the rims (An_{39} to An_{80}). Reversely zoned crystals contain the lowest An contents in the cores (An_{42} to An_{75}) and higher An content toward the rim in contact with glass (An_{60} to An_{87}). Crystals exhibiting an oscillatory zoning pattern range in composition from An_{46} to An_{94} and show no trends in composition from core to rim.

$^{87}Sr/^{86}Sr$ Crystal Isotope Stratigraphy

Table 2 and Figures 8, 10 and 11 presents Sr isotopic variation in Uturuncu plagioclase phenocrysts. Plagioclase phenocrysts from Uturuncu lava flows and domes have variable Sr concentrations, and $^{87}Sr/^{86}Sr$ ratios are in disequilibrium with the bulk rock and across the volcanic history (Table 2; Fig. 11). Similar studies of large magmatic systems, plagioclase phenocrysts cores, show more variation within a unit than is seen in

bulk-rock analyses for the volcanic suite (Davidson et al., 2007b). The variation observed is remarkable because Sr isotope ratios in Uturuncu phenocrysts exhibit in a single lava flow than is observed in the suite of Uturuncu bulk-rock Sr isotope compositions (Fig. 11; Feeley and Davidson, 1994; Grunder et al., 2008; Mamani et al., 2008; 2010; Ginibre and Wörner, 2007). Bulk-rock Sr isotopic ratios typically fall in the range observed in the phenocryst cores for a given unit (Fig. 11).

Two units show a unique relationship of the bulk-rock Sr isotopic composition to the plagioclase Sr isotopic composition. Units UTDM90 (Figs. 10 & 11) and GSM29 (Fig. 11) contain plagioclase cores and rims that are restricted ranging from $^{87}Sr/^{86}Sr$=0.7123 to 0.7135 and $^{87}Sr/^{86}Sr$=0.7131 to 0.7140 respectively. The bulk-rock ratios for these units are $^{87}Sr/^{86}Sr$= 0.710088$\pm$11 and $^{87}Sr/^{86}Sr$= 0.711490$\pm$09. The rims of these crystals exhibit the greatest range of isotopic disequilibrium with the bulk-rock observed. Each of the crystals analyzed by EMPA and LA-MC-ICP-MS exhibit dissolution surfaces with no new growth zones on the outer edge of the crystal. This unit also contains abundant micro-inclusions and glomerocrysts containing olivine and CPX. Olivine and CPX are phases that are rare Uturuncu lava flows and domes. The second distinct population of crystals, observed in unit UTDM108, displays a bimodal distribution of isotopic ratios within the crystals rims and cores. The populations are distinct from the bulk-rock and each other, and contain only minor variation within a population. The first population contains lower Sr isotopic ratios ranging from $^{87}Sr/^{86}Sr$= 0.7105-0.7107 with the core and rim for each crystal within analytical error (Fig. 10). The

second population contains higher $^{87}Sr/^{86}Sr$ ratios ($^{87}Sr/^{86}Sr$= 0.7130-0.7139) with the cores and rims of each crystal within analytical error.

Four different core to rim profiles are observed. Core Sr isotopic compositions range from $^{87}Sr/^{86}Sr$=0.7098 to 0.720 with a dominant population ranging from $^{87}Sr/^{86}Sr$=0.7129 to 0.7139 (Fig. 12). Observed in phenocryst rim profiles are four general trends: normal zoned, reverse zoned, oscillatory zoned, and isotopically unzoned. Normal zoned profiles contain the lowest $^{87}Sr/^{86}Sr$ ratio in the close to the core and ratios become higher towards the rim in contact with the melt. Reverse zoned profiles are opposite of normally zoned profiles with the highest ratio close to the core and the lowest ratio in contact with the melt. Oscillatory zoned profiles oscillate between higher and lower ratios from the core to the rim in contact with the melt. The final profile trend are isotopically unzoned phenocrysts that are within analytical error between the core and the rim. These four trends do not necessarily correlate to the trend observed in the major elements for the same crystal; and suggest that the trends observed in both the major elements and the Sr isotopic ratios are produced by magmatic process and not as a result of diffusion.

DISCUSSION

Assimilation Fractional Crystallization and Magma Mixing/ Mingling Modeling

Whole Rock Modeling

The lavas and domes have a large range of $^{87}Sr/^{86}Sr$ ratios for a narrow range of $^{143}Nd/^{144}Nd$ ratios (Fig. 6). Assimilation of crustal rocks with high $^{87}Sr/^{86}Sr$ ratios but similar $^{143}Nd/^{144}Nd$ ratios explains the observed trend. Figure 13 illustrates six scenarios

using different composition contaminants and different partition coefficients dependent on the crustal composition.

There is very little information about the composition of the crust beneath Cerro Uturuncu. Michelfelder et al. (2013) suggest that the composition must be old (Paleozoic or older), felsic composition crust that is plagioclase-stable and garnet-unstable. These conclusions were based on high bulk-rock $^{87}Sr/^{86}Sr$ ratios (0.71009-0.71653), low $^{143}Nd/^{144}Nd$ ratios (0.51215-0.51225) and low LIL/HFS element ratios (ex. Sr/Y<20; Michelfelder et al., 2013). Based on these conclusions, two crustal contaminants were selected, one representing a lower crustal composition and the second an upper crustal composition. The compositions of these contaminants used in the model are presented in Table 3. The lower crustal contaminant composition used is a garnet-sillimanite-gneiss xenolith described by McLeod et al. (2013) from the southern CVZ. This composition was selected because of petrographic and geochemical similarities to the sillimanite-gneiss xenoliths described by Sparks et al. (2008) in Uturuncu lavas. The upper crustal contaminant used in the models is Paleozoic granite from Sierra de Moreno described by Lucassen et al. (1999). These granites are petrographically similar to a xenolith described by Michelfelder et al. (2014) and expresses crustal isotopic signatures and LIL/HFS element ratios that are within the compositional range required by the Michelfelder et al. (2013) model for the contamination of Uturuncu magmas. Two primitive basalt compositions were contaminated with lower and upper crustal compositions: one from Davidson and de Silva (1995) for basalts from the central Altiplano. The second basalt composition was reported by Hernando et al. (2014) for pre-caldera basalts from the

Payún Matrú volcanic field in western Argentina's Southern Volcanic Zone (SVZ). Primitive mafic volcanic rocks in the southern CVZ are extremely rare, but some lava flows and dikes have been described in the central Altiplano by Davidson and de Silva (1995). This study described a primitive basalt from the Chiar Kkollu sill north of Uyuni, Bolivia. This sill is the geographically closest primitive mafic composition rock to Uturuncu, but is much older in age at 22.16 Ma (Davidson and de Silva, 1995). Mafic compositions from the same area that are closer in age to Uturuncu (~1 Ma) are basaltic andesite in composition. When modeled with the compositions described for the upper and lower crust above similar curvilinear trends to the Chiar Kkollu sill forms. The Payún Matrú volcanic field lava described by Hernando et al. (2014) is representative of mafic lava flows and domes erupted in the SVZ. It is assumed that there is little or no along arc variation in the composition of mantle melts between the CVZ and the SVZ in the model.

Model curves labeled AFC (D=1.7) and AFC (D=1.5) simulate the effects of differentiation of two potential parental magma compositions contaminated by a highly evolved crustal contaminant (Fig. 13). Bulk distribution coefficients of 1.5 and 1.7 are high for andesites, but the decrease of Sr content with increasing SiO_2 content and in increase of Rb/Sr ratios with increasing $^{87}Sr/^{86}Sr$ ratios suggest that Sr was compatible during differentiation. The curve AFC (D=0.1) simulates the effects of differentiation in the lower crust compared to curves for the upper crust. A bulk distribution coefficient of 0.1 is considered appropriate for this composition. We suggest this based on regional studies that have shown that increases in Sr/Y ratio associated with decreases in $^{87}Sr/^{86}Sr$

ratios reflects incompatibility of Sr in garnet- stable/ plagioclase- unstable- hybridized crust (Feeley, 1993; Kay et al., 2010; Michelfelder et al., 2013).

$^{87}Sr/^{86}Sr$ and $^{143}Nd/^{144}Nd$ ratios for Uturuncu lavas and domes form an array consistent with assimilation of radiogenic basement rocks with relatively non-radiogenic Nd and radiogenic Sr (Fig. 13). High Rb/Sr ratios suggest that these basement rocks were also felsic in composition as opposed to noritic, as suggested by the presence of noritic composition xenoliths described by Sparks et al. (2008). Subsequent magma mixing between the hybrid magmas after contamination events can account for the limited compositional range observed in Uturuncu lavas and domes and incomplete mixing/mingling accounts for the presence of the magmatic inclusions observed in this study and by Sparks et al. (2008) that are similar in composition to Uturuncu lavas. High silica, quartz-feldspathic xenoliths, observed in this study, and similar to xenoliths interpreted by Sparks et al. (2008) to be remnants of a crustal hot zone could represent this contaminant. However, isotopic compositions of these xenoliths are too similar to the lava and dome ratios for Sr isotopes for this to be a viable hypothesis.

Origin of Major-Element Zonation in Plagioclase Phenocrysts

Variations of An content in plagioclase are a well-documented phenomena that have been described at many CVZ volcanic centers and other arc magmatic systems globally (Feeley and Hacker, 1995; Feeley and Dunagen, 1996; Tepley et al., 2000; Singer et al., 2008; Davidson et al., 2008; Ginibre and Davidson, 2014). Small-scale changes in An content have been proposed to be related to diffusion associated growth at near equilibrium conditions (Singer et al., 1995; Davidson et al., 2001; Zellmer et al.,

1999; 2000; 2003; 2011); while larger-scale variations have been related to open system processes or changes in pressure or volatile contents (Pearce et al., 1987a; Muir et al., 2014a; Davidson et al., 2001; Zellmer et al., 1999; 2000; 2003; 2011). Muir et al. (2014a) suggested that the variation of An content and crystal size distribution of phenocrysts in Uturuncu lavas and domes reflect crystal nucleation and growth in the upper crust, producing crystal compositions that have many short periods of undercooling followed by equilibration. These authors concluded that these processes remained relatively constant throughout the eruptive history of Uturuncu (Muir et al., 2014a).

In principle, closed system processes of fractional crystallization and magma de-volatilization can produce the zoning textures described above and by Muir et al. (2014a) during magma migration through the crust.Without additional information, open system processes cannot be definitively determined by the zoning and An content variation alone (Tepley et al., 2000). However, Sr isotopic ratios, Sr concentration variation across plagioclase phenocrysts and linear bulk rock compositions suggest it is unlikely that closed system processes created the geochemical diversity observed in Uturuncu volcanic rocks and plagioclase phenocrysts. The repetitive large-scale fluctuations in An content across plagioclase phenocrysts indicate open-system, magma mixing and mingling in conjunction with or in isolation of AFC events. The closed system processes suggested by Muir et al. (2014a) may play a role in An content variations but only in response to a magma mixing event on a localized scale.

Origin of Single-Crystal Isotopic Variation

Core- to rim variation of $^{87}Sr/^{86}Sr$ isotopic ratios are observed in many plagioclase phenocrysts from Uturuncu lavas and domes. Few crystals show no variation within analytical error and these are typically found in an individual sample (UTDM90 and GSM29). The presence or lack of isotopic zoning seems to be independent of crystal size, bulk rock composition, or $^{87}Sr/^{86}Sr$ ratios in the core of the phenocryst (Fig. 8). Explanations for these variations between crystals in a single lava flow or dome must account for disequilibrium with the whole rock and explain the textural and compositional features created during crystal growth. Core to rim variation in $^{87}Sr/^{86}Sr$ can be explained three ways: (1) crystal growth in magma periodically recharged with magmas with a lower $^{87}Sr/^{86}Sr$ ratio; (2) crystal growth in a magma contaminated by country- rocks with differing $^{87}Sr/^{86}Sr$ isotopic ratios; and (3) self-mixing of the magma through convection in a heterogeneous magma reservoir.

Crystal Growth in a Periodically Recharged Chamber

Some isotopic variation found in plagioclase phenocrysts record crystal growth in magma with higher $^{87}Sr/^{86}Sr$ ratios to which periodically magma with lower $^{87}Sr/^{86}Sr$ isotopic ratios was added (Fig. 14). The addition of magma with lower $^{87}Sr/^{86}Sr$ ratios could be the cause of the change of volatile concentrations observed in melt inclusions and temperature fluctuations observed by Muir et al. (2014a; 2014b).The same model could also be used for a second crystal population nucleated in the magma with lower $^{87}Sr/^{86}Sr$ isotopic ratios recharging the chamber producing a normally zoned phenocryst population. Major element variations across the crystals record the rapidly

changing magmatic conditions of this mixing process and the dissolution surfaces record that these magmas were in thermal and chemical disequilibrium. Spikes in An content are often interpreted to reflect changes in the compositional and thermal environment during crystallization. These spikes record recharge events with hotter more mafic magma (Tepley et al., 1999; 2000). If the hypothesis that intra-crystalline isotopic variations are the result of crystal growth in a progressively recharged magmatic system is correct, it is reasonable to assume that the largest crystals with the most complex zoning patterns have longer residence times in a shallow magmatic system. In addition to having the longest residence times, the largest, most complex crystals may record processes taking place prior to the recharge event that introduced the crystal to the hybridized chamber such as contamination by the country rock or tracer diffusion and self- mixing in a larger magmatic reservoir. Crystals that are smaller or show less variation nucleated and grew later in the development of the magma relating to a volcanic unit (just prior to eruption) and record the conditions under which that crystal nucleated.

Tepley et al. (2000) proposed a similar model for El Chichón Volcano in Mexico. The magmas that erupted in the 200 ka and the 1982 eruptions are similar in bulk rock compositions, but contain heterogeneous plagioclase phenocrysts that are in disequilibrium with bulk rock compositions. These authors concluded that magma mixing was efficient prior to eruption, and multiple chambers each acted independently in the system then mixed into a single chamber just prior to eruption. The pathways of individual crystals record the isotopic heterogeneity of the zones. Similar to Uturuncu, each unit is unique at El Chichón, but the processes of early wall rock contamination

followed by rapid magma mixing are consistent throughout the lifespan of the volcano (Tepley et al., 2000; Davidson et al. 2007a).

Crystal Growth in Magma Progressively Contaminated by Country-Rock

An alternative explanation to the recharge model is that the core- to rim changes in $^{87}Sr/^{86}Sr$ isotopic ratios result from phenocryst growth in a magma progressively contaminated by an assimilant with higher or lower $^{87}Sr/^{86}Sr$ ratios compared to the magma. The known and plausible contaminants beneath Uturuncu have compositions that vary widely. High-silica quartz-rich xenoliths with bulk rock isotopic ratios ranging from 0.71368 to 0.71455 have been described by Michelfelder et al. (2014) while other xenoliths described by Sparks et al. (2008) and Muir et al. (2014a; 2014b) range from norite to sillimanite gneiss. Currently, no isotopic data is available for these xenoliths. Additionally, pressures of homogenization and storage calculated by Muir et al. (2014a) suggest local ignimbrites with $^{87}Sr/^{86}Sr$ ratios range from 0.7059 to 0.7083 (Schnurr et al., 2007) as a possible contaminant source during ascent. Populations of crystals with an increase in $^{87}Sr/^{86}Sr$ ratios from core to rim could have been produced by assimilation fractional crystallization processes. Fluctuations of these ratios could have been produced by multiple contaminants interacting with the magmas during migration. This process does not account for the dissolution surfaces observed in rims or the sieving textures that occur late in the crystals residence time. The dissolution surfaces between the core and growth zones and sieving in the core would require the cores to be xenocrysts, added to the magma from the contaminant early in the contamination event.

Self-Mixing

An alternative argument is that these crystals nucleated in a large compositionally homogeneous, but isotopically heterogeneous crystal mush reservoir. Crystals migrated slowly through this compositionally zoned body and would require incorporation of the crystals into a shallow hybridized chamber just prior to eruption creating the diversity found in each unit. Crystals that contain these profiles commonly contain dissolution surfaces and sieving in the rims that would require incorporation of the crystal into a hotter isotopically unique magma throughout the crystals residence in the system.

Muir et al. (2014a) attributed local variations in matrix glass and melt inclusion chemistry within Uturuncu lavas and domes to variability in the crystallization pathway of plagioclase, biotite and orthopyroxene in an andesitic crystal mush. These authors attributed this local variation to distributed pockets of melt that do not communicate chemically. Annen et al. (2006) proposed this model for the formation of mid-crustal hot zones. Melt inclusion and glass compositions in Uturuncu lavas and domes determined by Muir et al. (2014a; 2014b) and Sparks et al. (2008) suggest that the glass and mineral compositions reflect only local smaller scale processes while bulk rock trends reflect larger scale processes at greater depths.

Timescales of Magmatic Processes at Cerro Uturuncu

We now address the question of whether repeated sampling of the magma system took place throughout the eruptive history of Uturuncu. Diffusion of Sr acts to eradicate isotopic disequilibria between crystals and melt. Good spatial resolution of $^{87}Sr/^{86}Sr$ ratio and Sr concentration variation may also provide information about time as well as

process. Zellmer et al. (1999; 2003; 2011) suggest that Sr concentrations in plagioclase can be used to determine maximum crystal residence times and similar arguments have been suggested to apply for Sr isotopes (Davidson et al., 2001; Ramos et al., 2005b) with the additional assumption that equilibrium conditions across a crystal are uniform. This method measures the width of the zone across which $^{87}Sr/^{86}Sr$ ratios or Sr concentrations change, and given reasonable estimates of diffusion coefficients; it is possible to obtain residence time (Davidson et al., 2001; equation on page 441). Temperatures of Uturuncu volcanic rocks, measured by Fe-Ti oxide geothermometry, range from 790-920 °C (Muir et al., 2014a). Appropriate Sr diffusion coefficients (D_{Sr}) for andesite to dacite melts are between 9.92×10^{-15} and 1.42×10^{-13} cm^2s^{-1} (Giletti and Casserly, 1994; Cherniak and Watson, 1994) for plagioclase compositions ranging from An_{40} to $An_{90.}$ Using the relationship between D_{Sr}, time and distance between compositional variation, residence times between magma mixing events (represented by dissolution surfaces) range from 20-1500 years for zoned plagioclase phenocrysts in Uturuncu lavas and dome. A calculated total residence for the crystals are between 5000 and 6000 years which is in agreement the calculated repose interval between eruptions suggested by Michelfelder et al. (2014) of ~6000 years. The variability in estimates reflects uncertainty in magmatic temperatures between events and therefore variation in D_{Sr}. It is possible that these crystals could have been held at magmatic temperatures for hundreds of years prior to local equilibration resulting in a more defined dissolution surface and marked change in $^{87}Sr/^{86}Sr$ ratios and subsequent shorter calculated timescales. These residence times though constrain plagioclase to a maximum of a few thousand years at magmatic

temperatures and suggest that assimilation of thermally mature crust occurs on short timescales. These timescales agree with the conclusions by Muir et al. (2014a; 2014b) that mixing events occurred on short timescales. These authors concluded that the variable temperatures recorded in Fe-Ti oxides require mixing triggering eruption within weeks to months of the event to prevent re-equilibration of the Fe-Ti oxides.

Short timescales between magmatic events with or without eruptions associated with complex mineral zoning patterns particularly in plagioclase is common. Other young silicic centers in the CVZ have similar short timescales producing large crystals. Crystal residence times a few hundred years based on Sr diffusion in potassium feldspar megacrysts were described at Taapaca Volcano in northern Chile (Zellmer, 2003). Ramos et al. (2013) found that residence time for plagioclase in the various members of the Columbia River Flood Basalts exists for only 5-50 years prior to eruption.

Model of Contamination and Recharge

A model for the magmatic plumbing system beneath Cerro Uturuncu requires changing isotopic conditions between eruptive units and the plagioclase compositional and isotopic data. The simplest explanation for the similarity in bulk rock isotopic ratios and heterogeneity in plagioclase phenocrysts is that phenocrysts resided in multiple interconnected magma chambers and mixed into a single shallow chamber just prior to eruption. Isotopic disequilibrium between zones within a single phenocryst and between multiple phenocrysts in the same unit reflect nucleation, growth and dissolution at various times in magma of changing isotopic and chemical composition as the magma migrates through the crust.

An implication of this model is that processes within each chamber are similar and that each is initiated and maintained for a finite time, by similar composition recharging magmas. We assume that mafic recharge magmas with low $^{87}Sr/^{86}Sr$ ratios, similar to mafic lava flows observed at volcanic centers north of 21 °S, continually migrate through the crust, reach buoyancy equilibrium, and starts the contamination-hybridization process anew. The plumbing system beneath Uturuncu is a system with multiple magma chambers, some active, and some in repose as the system evolves. The diversity of the crystal compositions requires that some of these chambers are interconnected with magma passing through one to another creating a complex magmatic system while maintaining restricted bulk rock compositions.

Given that crustal heating must have accompanied more than 25 m.y. of volcanism in the CVZ, significantly more evolved and more radiogenic Uturuncu lavas and domes bulk rock compositions relative to the arc-front centers suggest greater amounts of differentiation. Highly radiogenic plagioclase phenocryst core and rim compositions observed in multiple lava flows and domes across the eruptive history require the presence of a radiogenic contaminant throughout the migration pathway. Such materials are rare for APVC ignimbrites, but common are in Paleozoic granites in NW Argentina and northern Chile (Lucassen et al. 1999; 2001). Plagioclase isotopic signatures, however, indicate the transition between less radiogenic $^{87}Sr/^{86}Sr$ ratios and more radiogenic signatures and vice versa. Bulk-rock isotopic ratios of Uturuncu lavas, domes and inclusions overlap the range of plagioclase phenocrysts for all but two lava flows and are presumably the result of assimilation of radiogenic crust prior to and during

mixing. This observation supports the assertion that Uturuncu magmas represent a continuation of geochemical and isotopic modification of CVZ magmas resulting from continued crustal assimilation (Fig. 13; Michelfelder et al., 2013).

Ramos et al. (2013) suggests that plagioclase phenocrysts are predictive in nature, and more radiogenic phenocryst compositions become signatures of the future bulk rock. Short residence times of phenocrysts support a petrogenic history in which Uturuncu magmas did not spend sufficient time at shallow depths that would allow for significant crystal fractionation. In contrast to plagioclase phenocrysts with short residence times and complex zoning textures, crystals with homogeneous internal $^{87}Sr/^{86}Sr$ ratios (UTDM90; Fig. 10) experience greater residence times at crustal depths where diffusional re-equilibration of $^{87}Sr/^{86}Sr$ ratios occurred and eliminated pre-existing $^{87}Sr/^{86}Sr$ variations, if a variation existed at all.

It is also possible that heterogeneity in crystal compositions could be created by one single, irregularly shaped, partially crystalline chamber with pockets of isolated magmas that are not in good communication with each other. Pockets of magma isolated from contact with other parts of the chamber have been suggested to be remobilized by injection of mafic melt into the base of crystal mushes due to additional heat and volatiles added to the system (Bachman et al., 2002). Muir et al. (2014a) suggested this model for the magmatic system beneath Uturuncu and has been suggested for other intermediate magmatic systems based on detailed petrographic and stratigraphically constrained geochemical observations (Gamble et al., 1999; Hobden et al., 1999; Tepley et al., 2000).

Figure 15 presents a schematic model for the magmatic plumbing system beneath Uturuncu. We envision that, during the early stages of emplacement of differentiated basaltic andesite into the crust, assimilation of continental crust with high $^{87}Sr/^{86}Sr$ ratios raised the $^{87}Sr/^{86}Sr$ ratios of the magma. Recharge of magma with lower $^{87}Sr/^{86}Sr$ ratios from deeper levels of the magmatic system systematically lowered the $^{87}Sr/^{86}Sr$ ratios of the contaminated magma.

The introduction of volatiles with recharge may be responsible for ultimately triggering eruption, but in any case would likely disturb plagioclase crystallization equilibria. The associated changes in plagioclase $^{87}Sr/^{86}Sr$ ratios cannot, however, be naturally produced by eruption-associated changes in pressure,temperature or X_{H_2O}, but instead require a simultaneous recharge by a magma distinct in isotope composition from which the crystals are growing. We suggest that this recharge suppresses the solidus of plagioclase, which in turn causes dissolution of the existing crystal population(s), modifying the Sr concentrations and $^{87}Sr/^{86}Sr$ ratios of the magma accordingly. Growth recommences from this modified magma crystallizing crystal rims and a new population of crystal cores that is representative of the new hybridized magma. Because there is no isolation of magma from wall rock interaction during migration, it is suggested that subsequent assimilation in chambers between magma mixing events introduces a higher $^{87}Sr/^{86}Sr$ source into the system, recording core-to- rim increases in $^{87}Sr/^{86}Sr$ ratios. Similar models have been proposed for El Chichón volcano and Lassen Volcanic Center for plagioclase phenocrysts that exhibit similar textures (Tepley et al., 1999; 2000; Davidson et al., 2001; 2007a).

CONCLUSIONS

Plagioclase phenocrysts from Uturuncu lavas and domes show large- magnitude changes in An content, textural discontinuities, and variation of $^{87}Sr/^{86}Sr$ ratios from core to rim. The observed variation result from open-system processes that occur during residence in or transport through continental crust and could not have existed at magmatic temperatures for more than a few thousand years. It is likely that different compositions of phenocrysts derive from different locations in the magmatic system and mixed just prior to eruption. We infer that Uturuncu magmas initially assimilated country rock with a higher $^{87}Sr/^{86}Sr$ ratio than the magmas and the magmas evolved subsequently through frequent recharge events of magmas with lower $^{87}Sr/^{86}Sr$ ratio. A typical Uturuncu andesitic or dacitic magma (melt plus crystals) therefore only attain its final geochemical identity just before and during eruption. Though Sr isotopic plagioclase isotopic data for the central Andean crustal basement and APVC ignimbrites is not currently available, it is clear that shallow-level mixing is an important process producing differentiated magmas. This process was only interrupted by the process of quenching due to eruption.

APPENDIX 1- METHODS

Bulk-rock samples of Uturuncu volcanic rocks were analyzed for major and trace element compositions at Washington State University, Pullman. Major and trace element compositions for 121 samples were acquired by X-ray fluorescence spectrometry (XRF) on a ThermoARL Advant'XP+ automated sequential wavelength spectrometer. Methods and errors for XRF analyses are described in Johnson et al. (1999). Additional trace

element compositions, including the rare earth elements, for 45 samples, were acquired by inductively coupled plasma mass spectrometry (ICP-MS) on an Agilent 7700 ICP-MS. Methods and errors for trace element analyses are presented in detail in Jarvis (1988). Methods for bulk rock major- and trace- element and Sr and Nd isotopic analyses are present in Michelfelder et al. (2013). Major and trace element compositions of plagioclase microphenocrysts and phenocrysts were determined on a JEOL JXA-8500F field emission electron microprobe/scanning electron microscope with an acceleration voltage of 15 KV at Washington State University, Pullman using the methods described in Ellis et al. (2010). Ten to fifteen phenocrysts and five to ten microphenocrysts from each eruptive unit were selected to reduce sample bias. Transects included the core and any rim 15 microns or larger.

In this paper, we describe the results of crystal-isotope stratigraphy performed on various crystals in rocks spanning the eruptive history of Uturuncu. We focused on plagioclase phenocrysts from lava flows and domes for the following reasons. First, plagioclase is a ubiquitous mineral phase in Uturuncu rocks. Second, the phase typically crystallizes over a broad temperature range, and, therefore, potentially records a significant part of the cooling history of the magmas. Third, plagioclase commonly has high Sr contents (partitioning coefficient of 2.84 to 5.28 for dacite and andesite respectively; Ewart and Griffin, 1994) allowing for isotopic analysis by laser ablation inductively coupled plasma mass spectrometry. Lastly, plagioclase crystals are usually large and display textural features such as growth zones, dissolution surfaces, and overgrowths that are readily identifiable allowing for detailed micro-sampling strategies

(Sparks et al., 2008; Charlier et al., 2006; Davidson et al., 2007; Ramos and Tepley, 2008).

Laser ablation multi-collector inductively coupled plasma mass spectrometry (LA-MC-ICPMS) analysis to determine in situ Sr isotopic ratios of plagioclase phenocrysts were performed at Washington State University, Pullman. The analyses were performed using a New Wave^{TM} UP 213 nm Nd: YAG laser ablation system (Jackson, 2001; Neufeld and Roy, 2004) in conjunction with a double focusing Thermo-Finnegan Neptune^{TM} MC-ICPMS equipped with nine Faraday collectors and 10^{-11} Ω resistors. Ablation trenches of 80 microns in diameter and 800 microns long by approximately 15 microns deep for each analysis. Precision of Sr isotopic ratios is within 0.00001 (Ramos et al., 2004). An in-house reference sample, SRP-1 ($^{87}Sr/^{86}Sr$= 0.70671) was used for calibration and corrections. Analytical procedures for in situ Sr isotope analysis and discussion of data quality and corrections have been addressed by Ramos et al. (2004). EPMA of zones within plagioclase larger than 80 micron in width containing Sr concentrations between 300 and 1000 ppm allowed analysis of zones for the highest quality data (Ramos et al., 2004; Ramos and Tepley, 2008). Whenever possible we combined NDIC imaging (Anderson, 1983; Feeley and Davidson, 1994; Pearce et al., 1987a; 1987b) and electron microprobe traverses with laser ablation pits to relate textural features, major element chemistry and isotopic compositions.

ACKNOWLEDGEMENTS

The authors wish to thank Frank Ramos for use of and assistance with the thermal ionization mass spectrometer at New Mexico State University; the staff at the

Geoanalyitical lab at Washington State University and all members of the PLUTONS Research group for insightful discussions. Jamie Kern for assistance mapping and collecting samples in the field, and the residents of Quetena Chico, Bolivia and Lipiko Tours for logistical support and hospitality. Support for this work came from the U.S. National Science Foundation EAR-0901148 to TCF and grants to GSM from the Department of Earth Sciences at Montana State University.

FIGURES

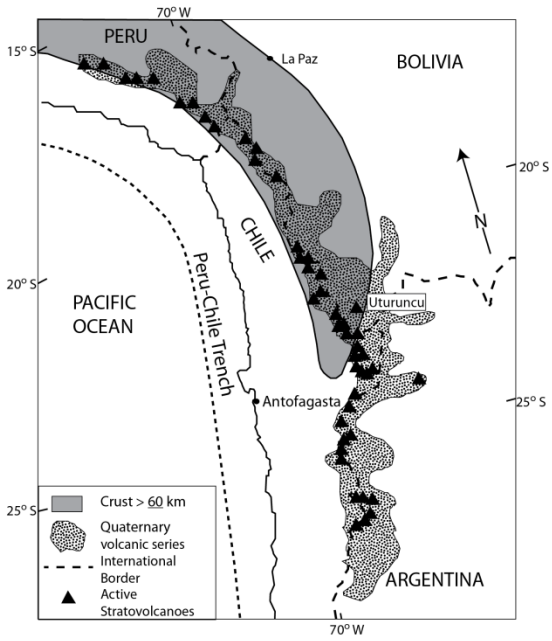

Figure 1. Map showing location of Andean Central Volcanic Zone (CVZ). Shaded area shows the region where crustal thickness exceeds 60 km (James, 1971; Beck and Zandt, 2002); stippled region illustrates distribution of Quaternary volcanic rocks. Modified from Feeley and Hacker (1995).

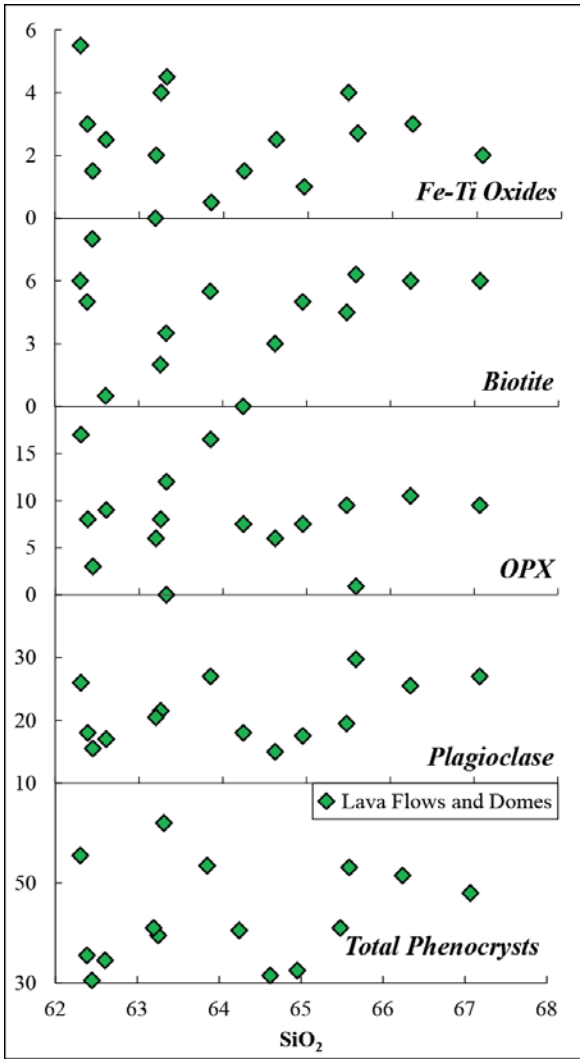

Figure 2. Modal percent of mineral phases in select Uturuncu volcanic lava flows and domes.

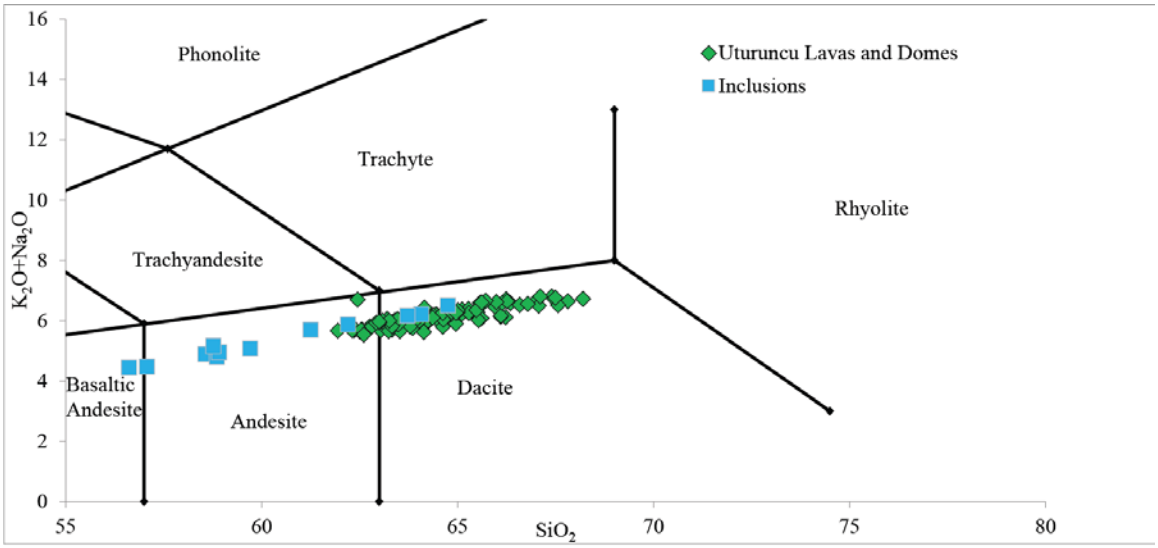

Figure 3. Total alkali versus silica (TAS) diagram for Uturuncu volcanic rocks.

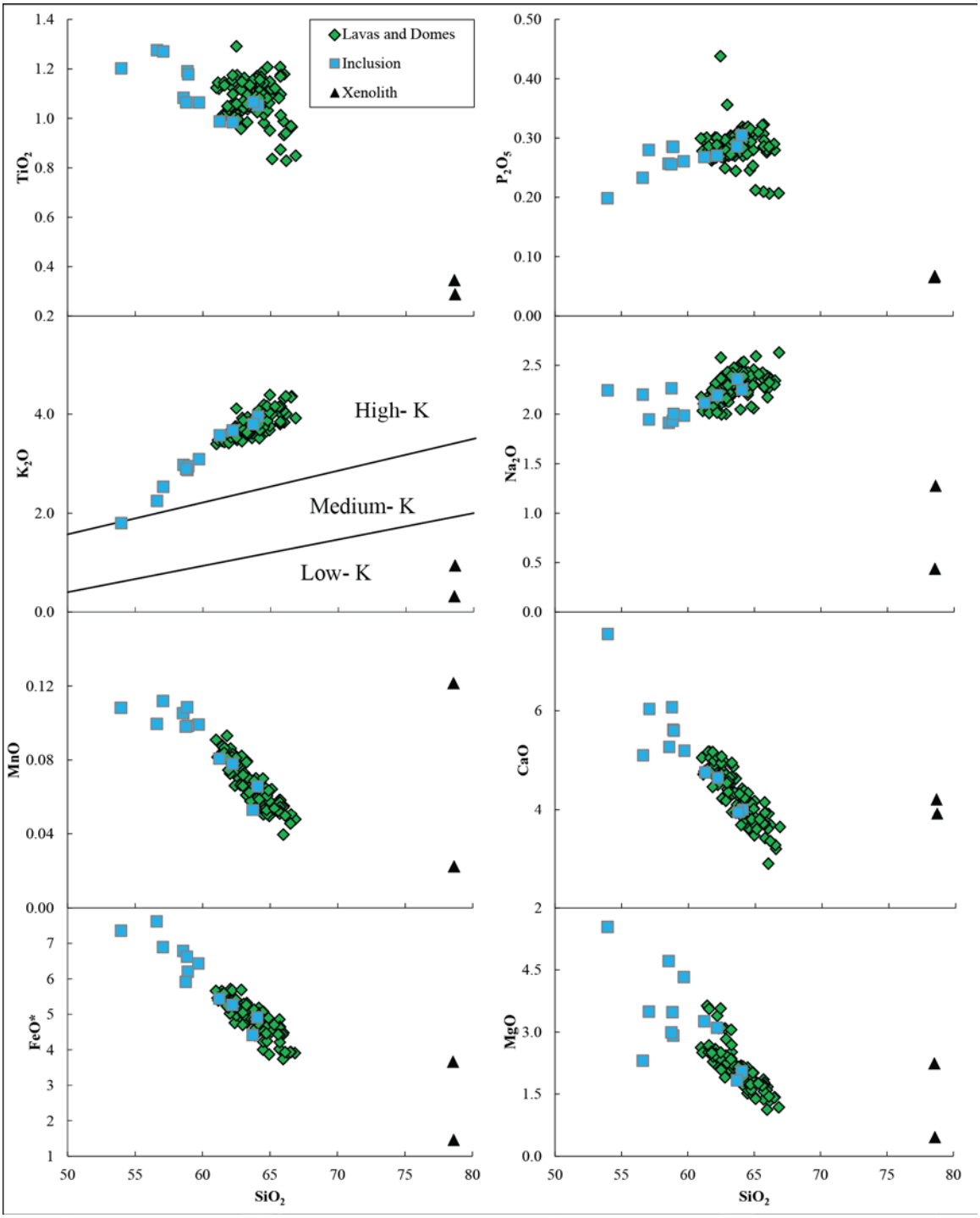

Figure 4. Major-element oxide concentrations versus SiO_2 for Uturuncu lavas and domes, inclusions and xenoliths.

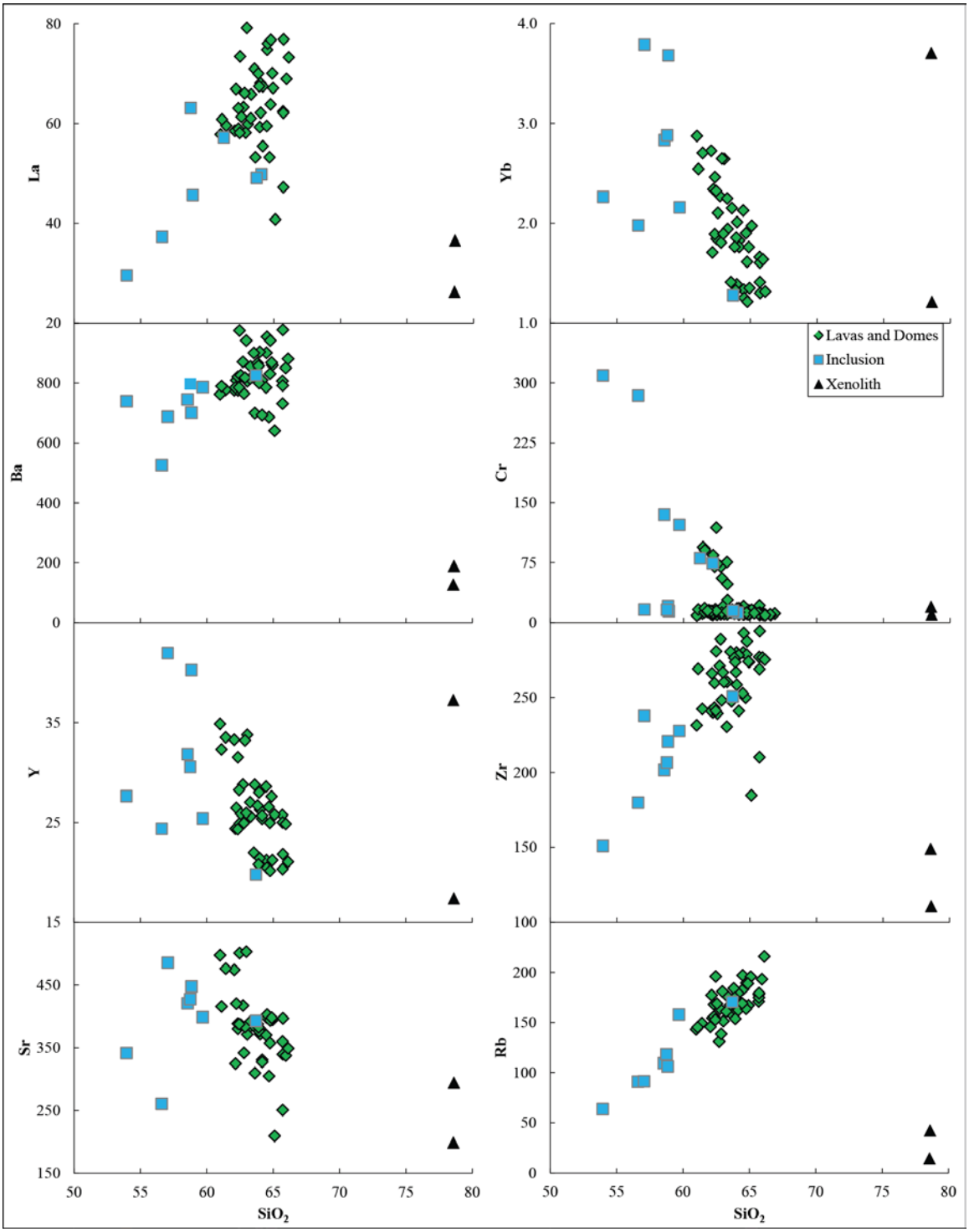

Figure 5. Trace-element concentrations versus SiO_2 for Uturuncu lavas and domes, inclusions and xenoliths.

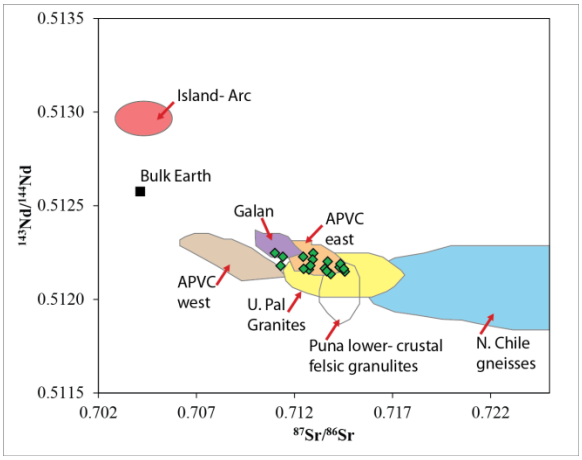

Figure 6. $^{143}Nd/^{144}Nd$ ratios versus $^{87}Sr/^{86}Sr$ ratios for Uturuncu volcanic rocks. Shaded areas represent compositions from CVZ igneous and metamorphic rocks (de Silva et al., 2006). Analytical errors are with the size of the data point.

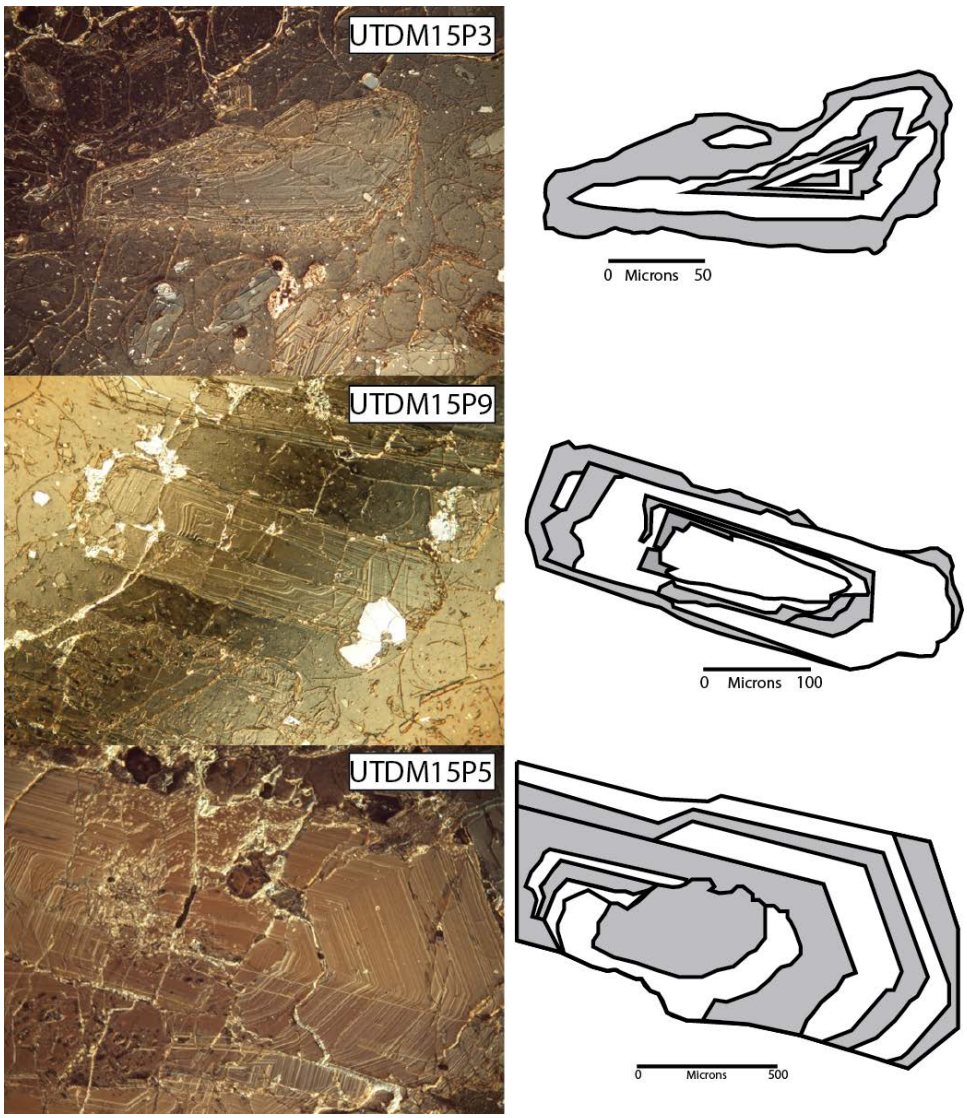

Figure 7. Nomarski differential interference contrast (NDIC) images and interpretative line drawings of representative plagioclase crystals from rocks of Cerro Uturuncu. The images demonstrate the variety of equilibrium and disequilibrium textures associated with this complex magmatic system. The line drawings illustrate dissolution surfaces or zones. See text for description for each crystal.

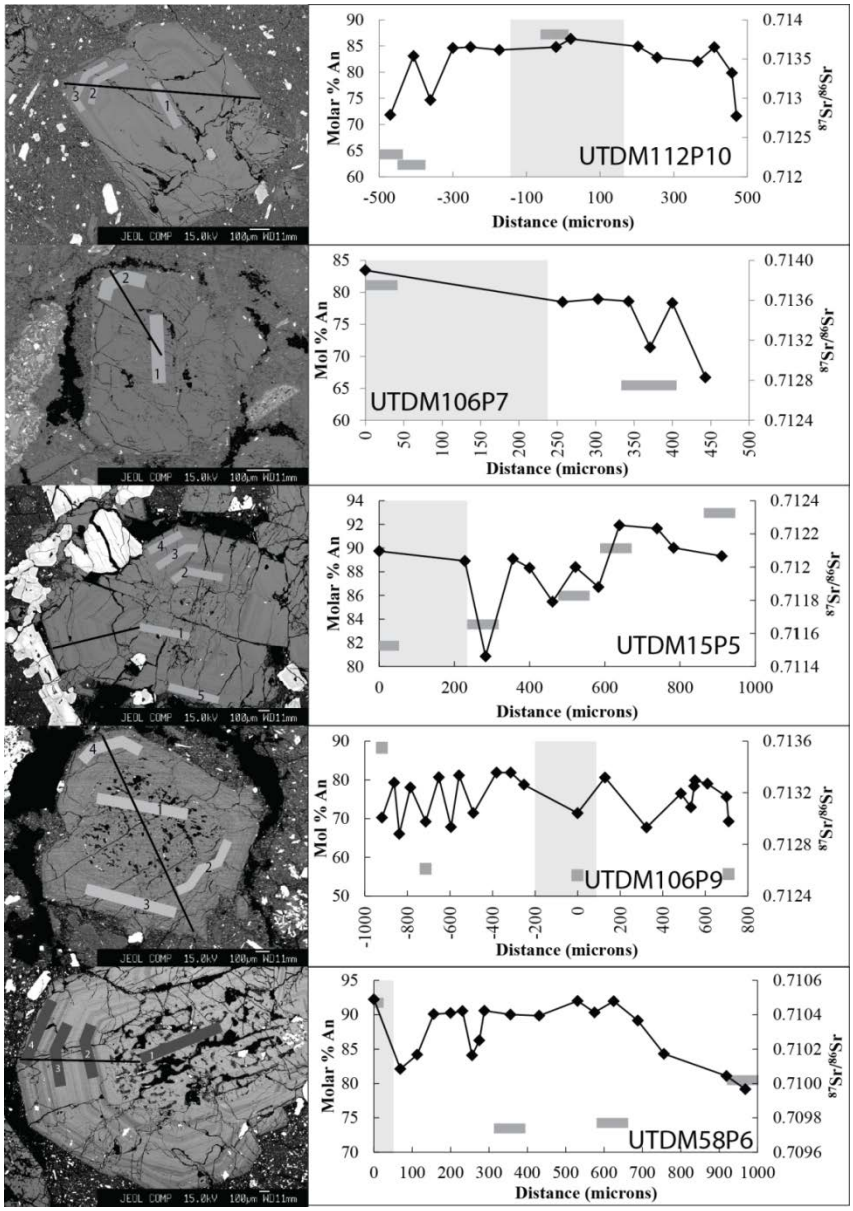

Figure 8. Laser ablation and EMPA data shown for traverses across five Cerro Uturuncu plagioclase phenocrysts. Black lines represent approximate traverse by EMPA. Grey lines represent approximate laser ablation troughs. Graphs are comparison diagrams of $^{87}Sr/^{86}Sr$ ratios and molar % An. Grey shaded areas in graphs represent approximate core of the crystal. Molar percent An=◆. $^{87}Sr/^{86}Sr$ ratios are approximate width of trough on plot. $^{87}Sr/^{86}Sr$=▭. Uncertainty in the $^{87}Sr/^{86}Sr$ ratios are represented by the thickness of the bar.

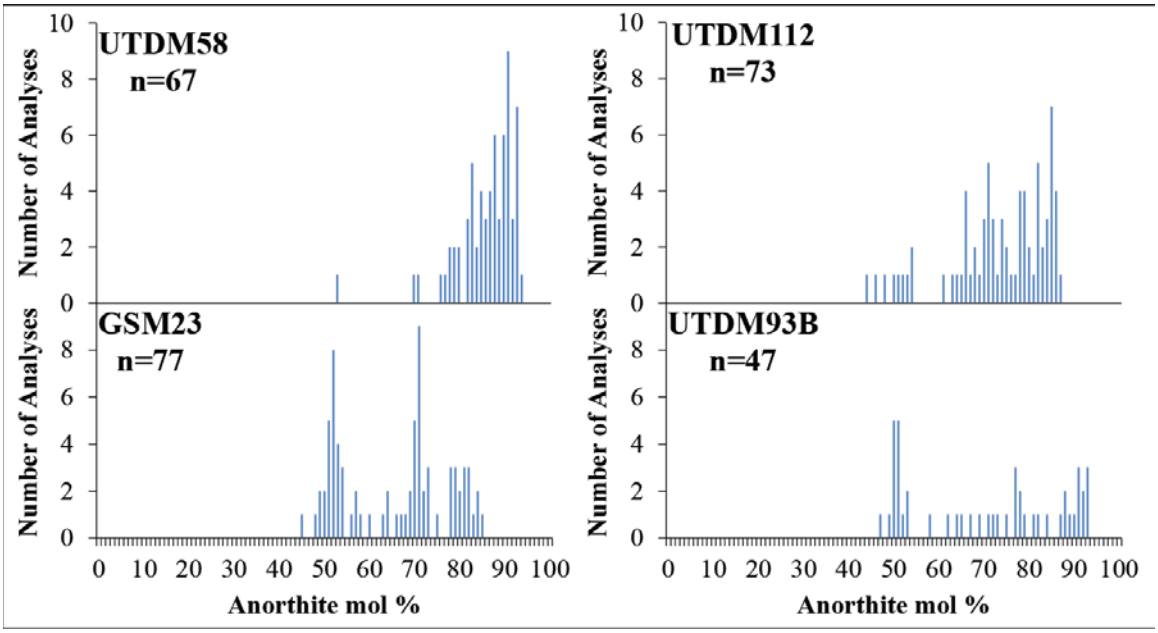

Figure 9. Histograms of anorthite mole percent showing the distribution of plagioclase rim and core anorthite compositions for representative lava flows and domes.

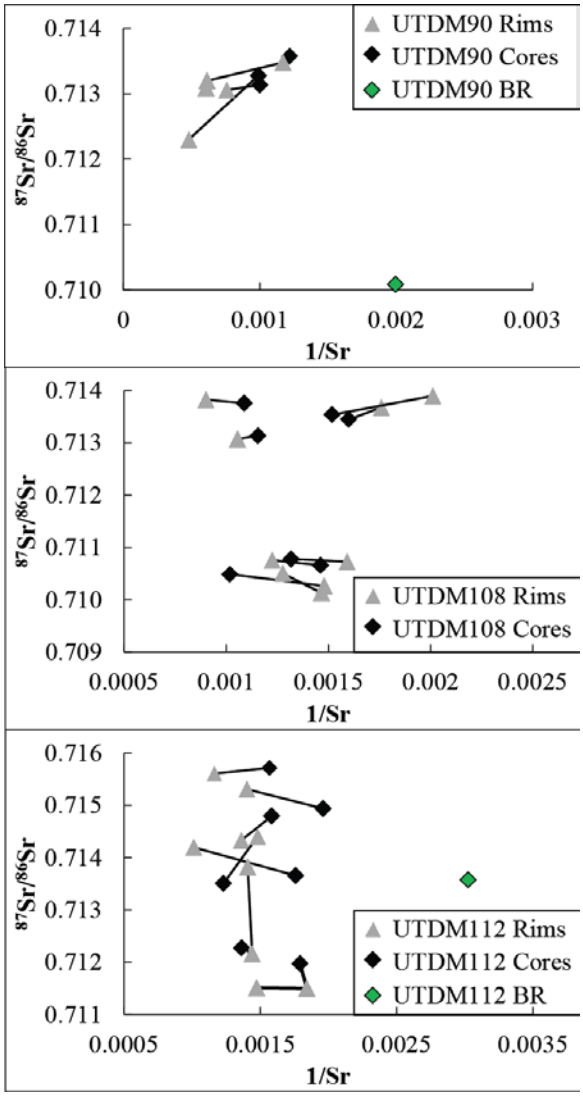

Figure 10. Plot of $^{87}Sr/^{86}Sr$ ratios versus 1/Sr ratios for microanalysis traverses in plagioclase phenocrysts and bulk-rock analyses. Analytical errors are with the size of the data point.

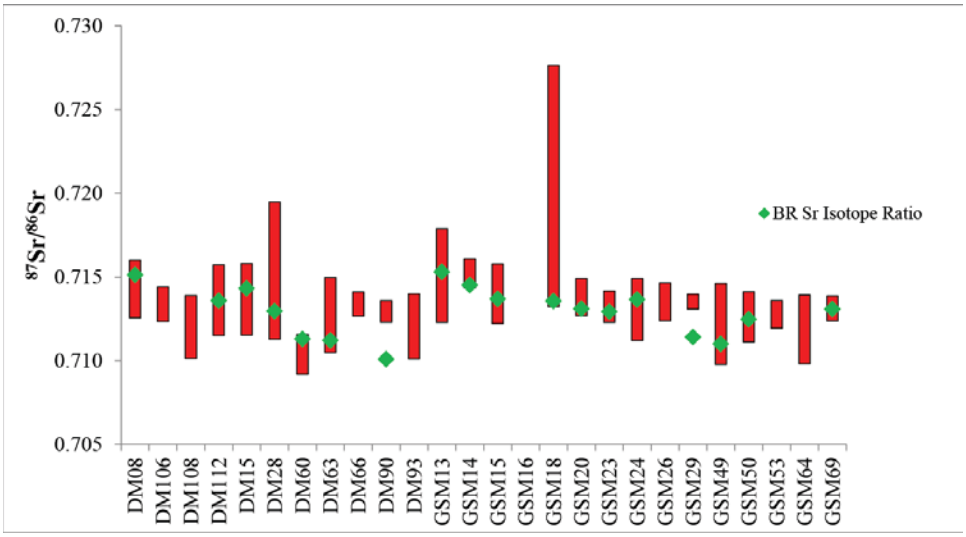

Figure 11. Bulk rock $^{87}Sr/^{86}Sr$ ratios compared to the range of $^{87}Sr/^{86}Sr$ ratios measured in the plagioclase phenocrysts contained in the bulk rock sample. Diamonds represent the bulk rock $^{87}Sr/^{86}Sr$ ratio. Grey bars represent the range in $^{87}Sr/^{86}Sr$ ratios observed in phenocryst cores and rims. Analytical errors are with the size of the data point.

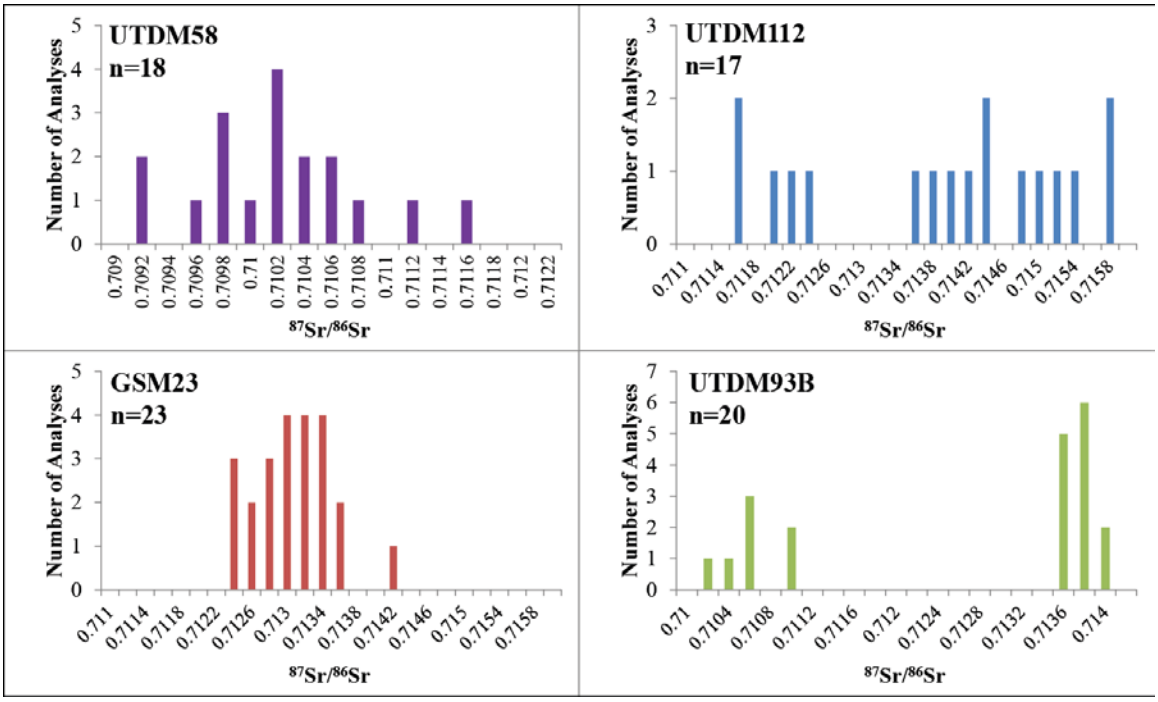

Figure 12. Histograms of Sr isotopic ratios of plagioclase rims and cores from representative lava flows and domes.

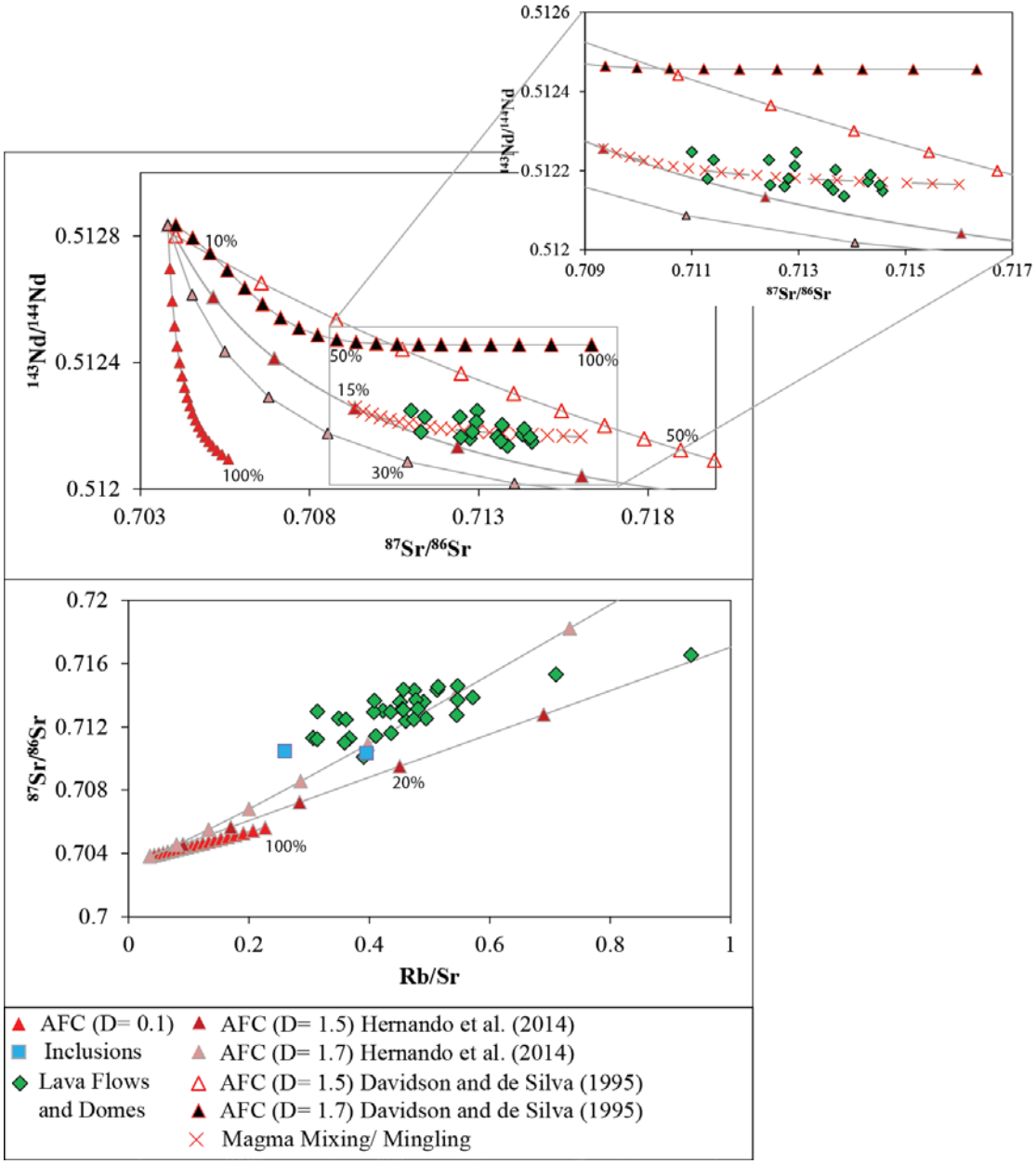

Figure 13. (A) Nd Isotope and Sr isotope constraints on bulk mixing and assimilation fractional crystallization (AFC; DePaolo, 1981) models for Uturuncu lava flows and domes. (B) $^{87}Sr/^{86}Sr$ ratios versus Rb/Sr ratios for Uturuncu lavas, domes and inclusions with AFC models primary melts discussed in text. Analytical errors are with the size of the data point.

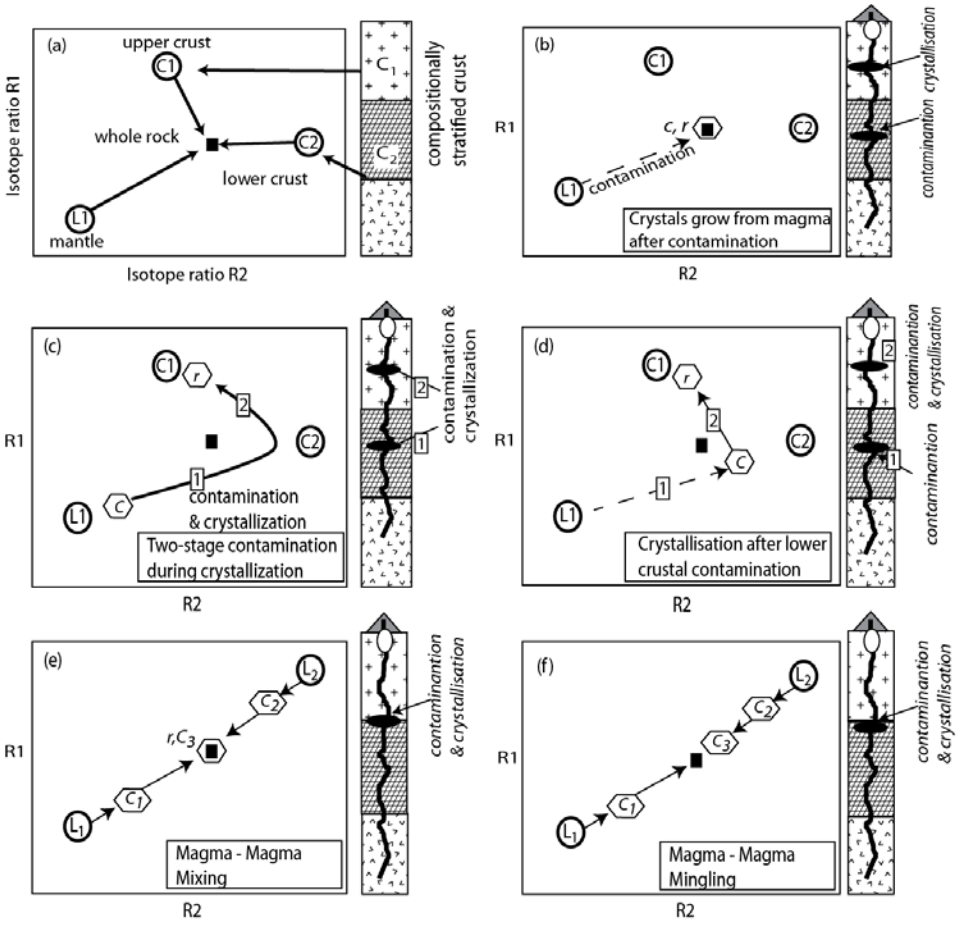

Figure 14. Cartoon model illustrating possible processes creating the isotopic diversity observed in the crystal cargo and lack of diversity observed in bulk-rock isotopic compositions. R1 and R2 represent hypothetical isotopic ratios. L_1 and L_2 represent the starting magmatic compositions and C_1 and C_2 in the circles represent the composition of the contaminant and C_n and r in the polygons represents the compositions of the cores in the crystal cargo in each melt.

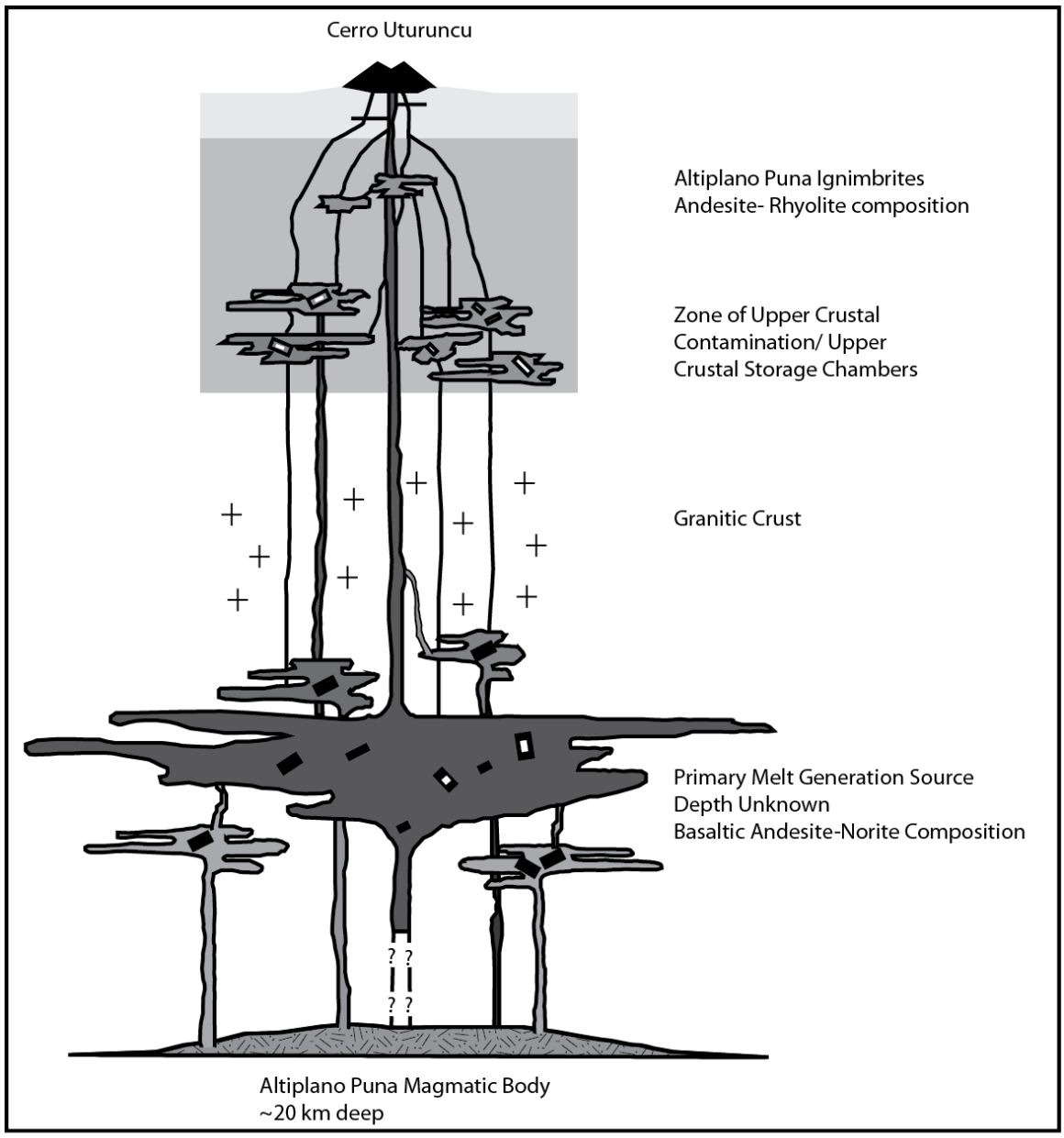

Figure 15. Cartoon illustrating a hypothetical magmatic plumbing system beneath Cerro Uturuncu that would account for the diversity of compositions in the crystal cargo. Modified for Cerro Uturuncu from Gardner et al. (2013).

Table1. Representative bulk-rock major-, trace- element concentrations and isotopic ratios analyses of Uturuncu lavas and domes.

	SiO_2	Sr	$^{87}Sr/^{86}Sr$	$^{144}Nd/^{143}Nd$
UTDM05	66.35	398	0.712520	0.512166
UTDM10	65.55	305	0.714570	0.512148
UTDM15	64.95	309	0.714317	
UTDM28	63.33	417	0.712956	0.512246
UTDM29	62.76	420	0.711270	
UTDM52	64.27	384	0.712358	
UTDM58	62.30	474	0.711294	0.512179
UTDM60	62.39	476	0.711207	
UTDM63	61.95	498	0.710976	0.512193
UTDM66	62.51	416	0.712519	0.512232
UTDM73	63.04	325	0.712738	0.512159
UTDM90	62.45	501	0.710088	
UTDM93	63.85	371	0.712920	0.512162
UTDM101	65.61	360	0.714300	0.512172
UTDM106	64.73	381	0.713126	0.512135
UTDM108	63.20	389	0.712073	0.512167
UTDM112	64.54	331	0.713576	
GSM10	65.53	358	0.714343	0.512189
GSM13	67.07	251	0.715303	
GSM14	66.10	340	0.714519	0.512163
GSM15	64.24	342	0.713687	
GSM16	66.24	209	0.716530	
GSM17	66.59	338	0.713850	0.512135
GSM18	66.14	397	0.713551	0.512164
GSM20	65.59	403	0.713106	
GSM21	66.26	394	0.713125	
GSM22	65.00	327	0.713692	0.512202
GSM23	64.78	384	0.712928	0.512212
GSM24	64.62	376	0.713649	0.512150
GSM28	63.52	387	0.711591	
GSM29	63.65	391	0.711409	0.512227
GSM49	64.15	503	0.711002	0.512247
GSM50	64.84	388	0.712468	0.512163
GSM60	63.24	383	0.712446	0.512227
GSM69	65.48	382	0.713075	

Table 2. EMPA and LA-MC-ICPMS analyses of select plagioclase phenocrysts.

	UTDMI15													
	UTDMI15P3				UTDMI15P5									
	Core	Growth Zone	Growth Zone	Growth Zone	Growth Zone	Growth Zone	Growth Zone	Growth Zone	Growth Zone	Core	Growth Zone	Growth Zone	Growth Zone	Growth Zone
SiO_2	50.60	47.78	50.95	50.75	45.91	46.18	47.92	46.14	46.36	47.15	46.03	46.76	45.34	
Al_2O_3	31.61	33.99	32.24	32.22	35.57	35.02	33.17	35.18	34.47	34.21	34.93	34.26	35.11	
FeO	0.22	0.25	0.18	0.22	0.35	0.42	0.45	0.45	0.43	0.38	0.42	0.38	0.36	
CaO	14.06	16.22	14.66	14.55	18.39	18.17	16.43	18.24	17.98	17.47	17.99	17.67	18.64	
K_2O	0.30	0.16	0.23	0.26	0.08	0.10	0.18	0.11	0.12	0.13	0.11	0.12	0.08	
Na_2O	3.48	2.32	3.21	3.25	1.25	1.42	2.04	1.40	1.55	1.63	1.36	1.59	1.03	
Total	100.4	100.8	101.6	101.4	101.7	101.5	100.4	101.7	101.1	101.1	101.0	100.9	100.8	
Sr (ppm)	762	467	798	866	759	709	661	608	698	672	760	613	871	
$^{87}Sr/^{86}Sr$	0.71408				0.71153		0.71165				0.71183		0.71211	
Sr_M	508	311	532	577	506	472	441	405	465	448	507	408	580	

	UTDMI15													
	UTDMI15P5				UTDMI15P9						UTDM58P6			
	Growth Zone	Growth Zone	Growth Zone	Core	Growth Zone	Growth Zone	Growth Zone	Growth Zone	Growth Zone	Growth Zone	Growth Zone	Growth Zone	Growth Zone	Growth Zone
SiO_2	45.48	46.15	46.18	50.76	52.58	51.02	50.75	49.07	48.59	45.58	48.17	47.67	46.11	
Al_2O_3	35.46	34.70	34.95	32.01	30.15	31.96	32.67	33.31	33.91	35.65	33.72	34.04	34.94	
FeO	0.31	0.40	0.40	0.16	0.53	0.22	0.17	0.21	0.21	0.40	0.53	0.47	0.51	
CaO	18.70	18.35	18.23	14.30	13.23	14.39	14.59	15.73	16.40	18.87	16.87	17.27	18.40	
K_2O	0.09	0.12	0.10	0.25	0.76	0.24	0.28	0.17	0.16	0.07	0.17	0.15	0.08	
Na_2O	1.15	1.37	1.23	3.48	3.01	3.57	3.40	2.50	2.54	0.87	2.05	1.73	1.28	
Total	101.4	101.3	101.2	101.1	100.8	101.5	102.0	101.1	101.9	101.6	101.7	101.5	101.5	
Sr (ppm)	718	622	569	692	694	721	792	766	863	864	1040	1115	878	
$^{87}Sr/^{86}Sr$			0.71233	0.71454					0.71481	0.71047				
Sr_M	479	415	379	462	463	481	528	511	576	576	693	743	585	

Table 2 Continued. EMPA and LA-MC-ICPMS analyses of select plagioclase phenocrysts.

	UTDM106													
	UTDM106P9													
	Growth Zone	Growth Zone	Growth Zone	Growth Zone	Core	Growth Zone	Growth Zone	Growth Zone	Growth Zone	Growth Zone	Growth Zone	Growth Zone	Growth Zone	Growth Zone
SiO_2	48.65	50.68	48.28	47.83	48.99	51.33	48.64	49.60	47.11	48.42	46.59	46.26	46.57	49.84
Al_2O_3	33.50	31.57	33.41	33.46	32.76	31.61	33.38	29.26	31.00	30.20	31.26	31.42	31.25	29.79
FeO	0.49	0.46	0.42	0.38	0.44	0.45	0.41	0.51	0.31	0.37	0.48	0.36	0.45	0.44
CaO	16.72	14.76	16.76	16.90	16.13	14.70	16.67	13.47	15.69	14.63	16.00	16.45	16.12	14.15
K_2O	0.16	0.30	0.16	0.13	0.18	0.28	0.14	0.38	0.22	0.24	0.21	0.15	0.17	0.34
Na_2O	2.04	3.07	1.94	1.98	2.29	3.07	2.13	3.30	2.52	2.85	2.30	2.20	2.26	3.25
Total	101.7	101.0	101.1	100.9	100.9	101.6	101.5	96.8	96.9	96.8	97.1	97.0	96.9	98.0
Sr (ppm)	442	322	373	487	690	473	360	508	495	569	746	440	555	625
$^{87}Sr/^{86}Sr$						0.71256								0.71257
Sr_M	294	215	249	325	460	315	240	339	330	379	497	293	370	417

	UTDM112													
	UTDM112P10													
	Growth Zone	Growth Zone	Growth Zone	Growth Zone	Growth Zone	Growth Zone	Core	Growth Zone	Growth Zone	Growth Zone	Growth Zone	Growth Zone	Growth Zone	Growth Zone
SiO_2	49.76	47.29	49.79	46.54	46.88	47.08	47.25	46.87	46.84	47.79	48.18	47.09	48.28	
Al_2O_3	31.72	33.89	32.00	34.03	33.62	33.90	34.04	35.30	34.04	33.80	33.67	33.96	33.36	
FeO	0.67	0.50	0.43	0.46	0.41	0.32	0.19	0.25	0.43	0.42	0.45	0.48	0.53	
CaO	14.54	16.96	15.00	17.34	17.22	17.27	17.28	17.48	17.16	16.76	16.61	17.30	16.06	
K_2O	0.26	0.14	0.23	0.11	0.14	0.15	0.15	0.13	0.11	0.16	0.17	0.11	0.19	
Na_2O	2.98	1.81	2.66	1.67	1.61	1.69	1.62	1.44	1.62	1.82	1.90	1.65	2.12	
Total	100.1	100.8	100.3	100.3	100.1	100.6	100.6	101.6	100.4	101.0	101.2	100.8	100.7	
Sr (ppm)	735	694	776	577	692	844	711	657	728	843	769	755	667	
$^{87}Sr/^{86}Sr$	0.71228	0.71216					0.71382							
Sr_M	490	463	517	385	462	563	474	438	485	562	513	503	445	

Table 3. Bulk-rock trace element concentrations and isotopic ratios of basement rocks and primary basalts used in geochemical modeling.

	Sample Type	Location	Rb	Sr	Nd	$^{87}Sr/^{86}Sr$	$^{143}Nd/^{144}Nd$	Reference
Py-5	Basalt	Payún Matrú volcanic field	27	751	24.4	0.703813	0.512834	Hernando et al. (2008)
4/23	Granite	Sierra de Moreno	173	40	11.7	0.76261	0.512456	Lucassen et al. (1999)
BC93PAX12	Grt-sill gneiss	Bolivia	27.3	18.5	22.8	0.717314	0.511966	McLeod et al. (2013)
BC9016a	Basalt	Central Altiplano	23	936	40.1	0.704052	0.512801	Davidson and de Silva (1995)

REFERENCES

Allmendinger, R. W., Jordan, T. E., Kay, S. M. and Isacks, B. L., 1997, The evolution of the Altiplano-Puna plateau of the central Andes: Annual Reviews in Earth and Planetary Science, v. 25, p. 139–174.

Anderson, A. T., 1983, Oscillatory Zoning of Plagioclase - Nomarski Interference Contrast Microscopy of Etched Polished Sections: American Mineralogist, v. 68, no. 1-2, p. 125-129.

Bachmann, O., Dungan, M.A., and Lipman, P.W., 2002, The Fish Canyon Magma Body, San Juan Volcanic Field, Colorado: rejuvenation and eruption of an upper crustal batholith: Journal of Petrology, v. 43, no. 8, p. 1469- 1503.

Bacon, C.J. (1986) Magmatic Inclusions in Silicic and Intermediate Volcanic Rocks: Journal of Geophysical Research: Solid Earth, v. 91, p. 6091-6112. http://dx.doi.org/10.1029/JB091iB06p06091

Baker, M.C.W., and Francis, P.W., 1978, Upper Cenozoic volcanism in Central Andes-Ages and volumes: Earth and Planetary Science Letters, v. 41, p. 175-187.

Beck, S.L., and Zandt, G., 2002, The nature of orogenic crust in the Central Andes: Journal of Geophysical Research: Solid Earth, v. 107.

Camp, V.E., and Hanan, M.E., 2008, A plume-triggered delamination origin for the Columbia River Basalt Group: Geosphere, v. 4, p. 480-495.

Charlier, B. L. A., Ginibre, C., Morgan, D., Nowell, G. M., Pearson, D. G., Davidson, J. P., and Ottley, C. J., 2006, Methods for the microsampling and high-precision analysis of strontium and rubidium isotopes at single crystal scale for petrological and geochronological applications: Chemical Geology, v. 232, no. 3-4, p. 114-133.

Chakraborty, S., and Costa, F., 2004, Fast diffusion of Si and O in San Carlos olivine under hydrous conditions: Geochimica Et Cosmochimica Acta, v. 68, no. 11, p. A275-A275.

Cherniak, D. J., and Watson, E. B., 1994, A Study of Strontium Diffusion in Plagioclase Using Rutherford Backscattering Spectroscopy: Geochimica Et Cosmochimica Acta, v. 58, no. 23, p. 5179-5190.

Coira, B., Davidson, J., Mpodozis, C. and Ramos, V., 1982, Tectonic and magmatic evolution of the Andes of northern Argentina and Chile: Earth-Sci. Research Letters, v. 18, p. 303-332.

Costa, F., and Chakraborty, S., 2004a, Decadal time gaps between mafic intrusion and silicic eruption obtained from chemical zoning patterns in olivine. Earth and Planetary Science Letters, v. 227, p. 3-4, 517-530.

Costa, F., and Chakraborty, S., 2004b, Time scales of igneous differentiation obtained from diffusion modeling of compositional zoning in olivine: Geochimica Et Cosmochimica Acta, v. 68, no. 11, p. A642.

Davidson, J.P., McMillan, N. J., Moorbath, S. Worner, G., Harmon, R.S., and Lopez-Escobar, L., 1990),The Nevados de Payachata volcanic region (18° S, 69° W, N. Chile) II: Evidence or widespread crustal involvement in Andean magmatism: Contributions to Mineralogy and Petrology, v. 105, p. 412-432.

Davidson, J.P., and de Silva, S.L., 1995, Late Cenozoic magmatism of the Bolivian Altiplano: Contributions to Mineralogy and Petrology, v.119, p. 387-408.

Davidson, J. P., and Tepley, F. J., 1997, Recharge in volcanic systems: Evidence from isotope profiles of phenocrysts: Science, v. 275, no. 5301, p. 826-829.

Davidson, J., Tepley, F., Palacz, Z., and Meffan-Main, S., 2001, Magma recharge, contamination and residence times revealed by in situ laser ablation isotopic analysis of feldspar in volcanic rocks: Earth and Planetary Science Letters, v. 184, p. 427-442.

Davidson, J. P., Font, L., Charlier, B. L. A., and Tepley, F. J., 2006, Mineral-scale Sr isotope variation in plutonic rocks - a tool for unravelling the evolution of magma systems: Transactions of the Royal Society of Edinburgh-Earth Sciences, v. 97, p. 357-367.

Davidson, J. P., Hora, J. M., Garrison, J. M., and Dungan, M. A., 2005, Crustal forensics in arc magmas: Journal of Volcanology and Geothermal Research, v. 140, no. 1-3, p. 157-170.

Davidson, J. P., Morgan, D. J., and Charlier, B. L. A., 2007a, Isotopic microsampling of magmatic rocks: Elements, v. 3, no. 4, p. 253-259.

Davidson, J. P., Morgan, D. J., Charlier, B. L. A., Harlou, R., and Hora, J. M., 2007b, Microsampling and isotopic analysis of igneous rocks: Implications for the study of magmatic systems: Annual Review of Earth and Planetary Sciences, v. 35, p. 273-311.

Davidson, J. P., Turner, S. P., and Macpherson, C. G., 2008, Water storage and amphibole control in arc magma differentiation: Geochimica Et Cosmochimica Acta, v. 72, no. 12, p. A201.

de Silva, S.L., 1989, Altiplano-Puna volcanic complex of the central Andes: Geology, v. 17, p. 1102-1106.

de Silva, S.L. and Francis, P.W., 1991, Volcanoes of the Central Andes: New York, Springer-Verlag, 216 p.

de Silva, S.L., Self, S., Francis, P.W., Drake, R.E., Carlos Ramirez, R., 1994, Effusive silicic volcanism in the Central Andes: The Chao dacite and other young lavas of the Altiplano- Puna Volcanic Complex. Journal of Geophysical Research, v. 99, no. B9, p. 17805-17825.

de Silva, S.L., Zandt, G., Trumbull, R., Viramonte, J., Salas, G., and Jiminez, N., 2006, Large ignimbrite eruptions and volcano-tectonic depressions in the Central Andes: a thermomechanical perspective, *in* Troise, C., De Natale, G., Kilburn, C.R.J., eds., Mechanisms of activity and unrest at large calderas: Geological Society, London Special Publication No. 269, p. 47–63.

del Potro, R., Diez, M., Blundy, J., Gottsmann, J. and Camacho, A., 2013, Diapiric ascent of silicic magma beneath the Bolivian Altiplano: Journal of Geophysical Research, v. 40, p. 2044-2048.

Ellis, B.S., Barry, T.L., Branney, M.J., Wolff, J.A., Bindeman, I., Bonnichsen, B., and Wilson, R., 2010, Petrologic constraints on the development of a large-volume, high temperature, silicic magma system: The Twin Falls eruptive center, central Snake River Plain: Lithos, v. 120, p. 475–489.

Feeley, T.C., Davidson, J.P., and Armendia, A., 1993, The volcanic and magmatic evolution of Volcán Ollagüe, a hig-K, late Quaternary stratovolcano in the Andean Central Volcanic Zone: Journal of Volcanology and Geothermermal Research, v. 54, p. 221-245.

Feeley, T. C., and Davidson, J. P., 1994, Petrology of Calc-Alkaline Lavas at Volcan-Ollague and the Origin of Compositional Diversity at Central Andean Stratovolcanoes: Journal of Petrology, v. 35, no. 5, p. 1295-1340.

Francalanci, L., Avanzinelli, R., Nardini, I., Tiepolo, M., Davidson, J.P., and Vannucci, R., 2012, Crystal recycling in the steady-state system of the active Stromboli volcano: a 2.5-ka story inferred from insitu Sr isotope and trace element data: Contributions to Mineralogy and Petrology, v. 163, p. 109-131.

Gamble, J.A., Wood, C.P., Price, R.C., Smith, I.E.M., Stewart, R.B., and Waight, T., 1999, A fifty year perspective of the magmatic evolution of Ruapehu Volcano, New Zealand: verification of open system behavior in an arc volcano: Earth and Planetary Science Letters, v. 170, p. 301-314.

Gardner, M. F., Troll, V. R., Gamble, J. A., Gertisser, R., Hart, G. L., Ellam, R. M., Harris, C., and Wolff, J. A., 2013, Crustal Differentiation Processes at Krakatau Volcano, Indonesia: Journal of Petrology, v. 54, no. 1, p. 149-182.

Giletti, B. J., and Casserly, J. E. D., 1994, Strontium Diffusion Kinetics in Plagioclase Feldspars: Geochimica Et Cosmochimica Acta, v. 58, no. 18, p. 3785-3793.

Ginibre, C., and Worner, G., 2007, Variable parent magmas and recharge regimes of the Parinacota magma system (N. Chile) revealed by Fe, Mg and Sr zoning in plagioclase: Lithos, v. 98, p. 118-140.

Ginibre, C., and Davidson, J.P., 2014, Sr isotope zoning in plagioclase from Prainacota Volcano (Northern Chile): Quantifying magma mixing and crustal contamination: Journal of Petrology, v. 55, no. 6, p. 1203-1238.

Henderson, S.T. and Pritchard, M.E., 2013, Decadal volcanic deformation in the Central Andes Volcanic Zone revealed by InSAR time series: Geochemistry, Geophysics, Geosystems, v. 15, no 5, p. 1358-1374.

Hernando, I.R., Aragon, E., Frei, R., Gonzalez, P.D., and Spakman, W., 2014, Constraints on the origin and evolutions of magmas in the Puyun Matru Volcanic Field, Quaternary Andean Back-arc of Western Argentina: Journal of Petrology, v. 55, no. 1, p. 209-239.

Hildreth, W.; Moorbath, S., 1988, Crustal contributions to arc magmatism in the Andes of central Chile: Contributions Mineralogy and Petrology, v. 98, p. 455–489.

Hobden, B.J., Houghton, B.F., Davidson, J.P., and Weaver, S.D., 1999, Small short-lived magma batches at composite volcanoes: time windows at Tongariro volcano, New Zealand: Journal of the Geologic Society, London, v. 156, p. 865-868.

Jackson, S. E., 2001, The application of Nd:YAG lasers in LA-ICPMS, *in* Sylvester, P. J., eds., Laser Ablation ICP- Mass Spectrometry in the Earth Sciences: Principles and Application: Mineralogical Association of Canada Volume 29, p. 29-45.

Jarvis, K.E., 1988, Inductively coupled plasma mass spectrometry, a new technique for the rapid or ultra-trace level determination of the rare-earth elements in geological materials: Chemical Geology, v. 68, p. 31-39.

Johnson, D.M., Hooper P.R., and Conrey, R.M., 1999, GeoAnalytical Lab, Washington State University: Advances in X-ray Analysis, v. 41, p. 843-867.

Knesel, K.M, Davidson, J.P., and Duffield, W.A., 1999, Open-system evolution of silicic magma by assimilation followed by recharge: evidence from Sr isotopes in sanidine phenocrysts, Taylow Creek Rhyolite, NM: Journal of Petrology, v. 40, p. 773-786.

Lucassen, F., Franz, G., Thirlwall, M.F., and Mezger, K., 1999, Crustal recycling of metamorphic basement: Late Paleozoic granites of northern Chile (~22° S). Implications for the composition of the Andean crust: Journal of Petrology, v. 40, n. 10, p. 1527-1551.

Lucassen, F., Becchio, R., Harmon, R., Kasemann, S., Franz, G., Trumbull, R., Wilke, H. G., Romer, R. L., and Dulski, P., 2001, Composition and density model of the continental crust at an active continental margin - the Central Andes between 21 degrees and 27 degrees S: Tectonophysics, v. 341, no. 1-4, p. 195-223.

McLeod, C.L., Davidson, J.P., Nowell, G.M., de Silva, S.L., and Schmitt, A.K., 2013, Characterizing the continental basement of the Central Andes: Constraints form Bolivian crustal xenoliths: Geological Society of America Bulletin, v. 125, no. 5-6, p. 985-997.

McGee, J.J., Tilling, R.I., and Duffield, W.A., 1987, Petrologic characteristics of the 1982 and pre- 1982 eruptive products of El Chichon volcano, Chiapas, Mexico: Geofisica Internacional, v. 26, no. 1, p. 85-108.

Michelfelder, G.S., Feeley, T.C., Wilder, A.D., and Klemetti, E.W., 2013, Modification of the continental crust by subduction zone magmatism and vice-versa: Across- strike geochemical variation of silicic lavas from individual eruptive centers in the Andean Central Volcanic Zone. Geosciences, v. 3, no. 4, p. 633-667.

Michelfelder, G.S., Feeley, T.C., and Wilder, A.D., 2014, The Volcanic Evolution of Cerro Uturuncu: A High-K, Composite Volcano in the Back-Arc of the Central Andes of SW Bolivia: International Journal of Geosciences, v. 5, no. 11, p. 1263-1282.

Muir, D. D., Blundy, J., Hutchinson, M. C., and Rust, A. C., 2014, Petrological imaging of an active pluton beneath Cerro Uturuncu, Bolivia: Contributions to Mineralogy and Petrology, v. 167, p. 980.

Muir, D. D., Blundy, J., Rust, A. C. and Hickey, J., 2014, Experimental Constraints on Dacite Pre-eruptive Magma Storage Conditions beneath Uturuncu Volcano: Journal of Petrology, v. 55, no. 4, p. 749-767.

Neufeld, L., and Roy, J., 2004, Laser ablation solid sampling plasma spectrochemistry - The importance of matching the hardware to the application: Spectroscopy, v. 19, no. 1, p. 16-28.

Pearce, T. H., Griffin, M. P., and Kolisnik, A. M., 1987a, Magmatic Crystal Stratigraphy and Constraints on Magma Chamber Dynamics - Laser Interference Results on Individual Phenocrysts: Journal of Geophysical Research-Solid Earth and Planets, v. 92, no. B13, p. 13745-13752.

Pearce, T. H., Russell, J. K., and Wolfson, I., 1987b, Laser-Interference and Nomarski Interference Imaging of Zoning Profiles in Plagioclase Phenocrysts from the May 18, 1980, Eruption of Mount-St-Helens, Washington: American Mineralogist, v. 72, no. 11-12, p.1131-1143.

Ramos, F. C., and Reid, M. R.., 2005, Distinguishing melting of heterogeneous mantle sources from crustal contamination: Insights from Sr isotopes at the phenocryst scale, Pisgah Crater, California: Journal of Petrology, v. 46, no. 5, p. 999-1012.

Ramos, F. C., and Tepley, F. J., 2008, Inter- and Intracrystalline Isotopic Disequilibria: Techniques and Applications, *in* Putirka, K.D, and Tepley, F.J., eds., Minerals, Inclusions and Volcanic Processes: Reviews in Mineralogy and Geochemistry v. 69, p. 403-443.

Ramos, F. C., and Wolff, J. A., 2005, In situ Sr isotopes measured by LA-MC-ICPMS: Utility for the average Joe: Geochimica Et Cosmochimica Acta, v. 69, no 10, p. A376-A376.

Ramos, F. C., Wolff, J. A., and Tollstrup, D. L., 2004, Measuring Sr-87/Sr-86 variations in minerals and groundmass from basalts using LA-MC-ICPMS: Chemical Geology, v. 211, no. 1-2, p. 135-158.

Ramos, F. C., Wolff, J. A., and Gill, J. B., 2005a, Open-system processes and rhyolites: What isotope systems can we trust, and for what?: Geochimica Et Cosmochimica Acta, v. 69, no. 10, p. A235-A235.

Ramos, F. C., Wolff, J. A., and Gill, J. B., 2005b, Sr isotope disequilibrium in Columbia River flood basalts: Evidence for rapid shallow-level open-system processes: Geology, v. 33, no. 6, p. 457-460.

Ramos, F.C., Wolff, J.A., Starkel, W., Eckberg, A., Tollstrup, D.L., and Scott, S., 2013, The changing nature of sources associated with Columbia River flood basalts: Evidence from strontium isotope ratio variations in plagioclase phenocrysts, *in* Reidel, S.P., Camp, V.E., Ross, M.E., Wolff, J.A., Martin, B.S., Tolan, T.L., and Wells, R.E., eds., The Columbia River Flood Basalt Province: Geological Society of America Special Paper 497, p. 231-257.

Schnurr, W.B.W, Trumbull, R.B., Clavero, J., Hahne, K., Siebel, W., and Gardeweg, M., 2007, Twenty- five million years of silicic volcanism in the southern central volcanic zone of the Andes: Geochemistry and magma genesis of ignimbrites from 25 to 27° S, 67 to 72° W: Journal of Volcanology and Geothermal Research, v. 166, p. 17-46.

Schmitt, A.K., de Silva, S.L., Trumbull, R. and Emmermann, R., 2001, Magma Evolution in the Purico Ignimbrite Complex, Northern Chile: Evidence for Zoning of a Dacitic Magma by Injection of Rhyolitic Melts Following Mafic Recharge: Contributions to Mineralogy and Petrology, v. 140, p. 680-700. http://dx.doi.org/10.1007/s004100000214

Sparks, R.S.J., Folkes, C.B., Humphreys, M.C.S., Barfod, D.N., Clavero, J., Sunagua, M.C., McNutt, S.R., and Pritchard, M.E., 2008, Uturuncu volcano, Bolivia: Volcanic

unrest due to mid-crustal magma intrusion: American Journal of Science, v. 308, p. 727-769, DOI: 10.2475/06.2008.01

Tepley, F. J., Davidson, J. P., and Clynne, M. A., 1999, Magmatic Interactions as Recorded in Plagioclase Phenocrysts of Chaos Crags, Lassen Volcanic Center, California: Journal of Petrology, v. 40, no. 5, p. 787-806.

Tepley, F. J., Davidson, J. P., Tilling, R. I., and Arth, J. G., 2000, Magma mixing, recharge and eruption histories recorded in plagioclase phenocrysts from El Chichon Volcano, Mexico: Journal of Petrology, v. 41, no. 9, p. 1397-1411.

Thorpe, R.S., Potts, P.J., Hammill, M., and Baker, M.C.W., 1982, The Andes, *in*. Thorpe, R.S ed., Andesites: New York, Wiley, p. 187-205.

Ward, K. M., Porter, R.C., Zandt, G., Beck, S., Wagner, L.S., Mnaya, E., Tavera, H., 2013, Ambient noise tomography across the Central Andes: Geophysical Journal International, v. 194, p. 1559-1573.

Ward, K.M.; Zandt, G., Beck, S., Christiansen, D.H., 2014, Seismic imaging of the magmatic underpinnings beneath the Altiplano-Puna volcanic complex from the joint inversion of surface wave dispersion and receiver functions: Earth and Planetary Science Letters, v. 404, p. 43-53.

Wolff, J. A., Ramos, F. C., and Davidson, J. P., 1999, Sr isotope disequilibrium during differentiation of the Bandelier Tuff: Constraints on the crystallization of a large rhyolitic magma chamber: Geology, v. 27, no. 6, p. 495-498.

Zellmer, G.F., Blake, S., Vance, D., Hawkesworth, C., and Turner, S., 1999, Plagioclase residence times at two island arc volcanoes (Kameni islands, Santorini, and Soufriere, St. Vincent) determined by Sr diffusion systematics: Contributions to Mineralogy and Petrology, v. 136, no. 4, p. 345–357.

Zellmer, G.F., Turner, S.P., and Hawkesworth, C.J., 2000, Timescales of destructive plate margin magmatism: new insights from Santorini, Aegean volcanic arc: Earth Planetary Science Letters, v. 174, no. 3-4, p.265-282.

Zellmer, G.F., Sparks, R.S.J., Hawkesworth, C.J. and Wiedenbeck, M., 2003, Magma emplacement and remobilization timescales beneath Montserrat: insights from Sr and Ba zonation in plagioclase phenocrysts: Journal of Petrology, v. 44, p. 1413-1431.

Zellmer, G.F. and Clavero, J., 2006, Using trace element correlation patterns to decipher a sanidine crystal growth chronology: an example from Taapaca volcano, Central Andes: Journal of Volcanology and Geothermal Research, v. 156, p. 291–301.

Zellmer, G.F., Rubin, K.H., Dulski, P., Iizuka, Y., Goldstein, S.L., and Perfit, M.R., 2011, Crystal growth during dike injection of MOR basaltic melts: evidence from

preservation of local Sr disequilibria in plagioclase: Contributions to Mineralogy and Petrology, v. 161, p. 153-173.

CHAPTER SIX

MODIFICATION OF THE CONTINENTAL CRUST BY SUBDUCTION ZONE MAGMATISM AND VICE-VERSA: ACROSS-STRIKE GEOCHEMICAL VARIATIONS OF SILICIC LAVAS FROM INDIVIDUAL ERUPTIVE CENTERS IN THE ANDEAN CENTRAL VOLCANIC ZONE

Contribution of Authors and Co-Authors

Manuscript in Chapter 6

Author: Gary S. Michelfelder

Contributions: Performed geochemical analyses, field work sample preparation, and performed computer modeling. Wrote manuscript with input on data from co-authors.

Co-Author: Todd C. Feeley

Contributions: Aided in the preparation of the manuscript and figures.

Co-Author: Alicia D. Wilder

Contributions: Aided in the preparation of the manuscript and figures. Worked in the field as a field assistant and contributed by performing geochemical analyses.

Co-Author: Erik C. Klemetti

Contributions: Provided data.

Manuscript Information Page

Michelfelder, G.S.; Feeley, T.C.; Wilder, A.D., and Klemetti, E.W.
Geosciences
Status of Manuscript:
____ Prepared for submission to a peer-reviewed journal
____ Officially submitted to a peer-review journal
____ Accepted by a peer-reviewed journal
_X__Published in a peer-reviewed journal

Citation:

Michelfelder, G.S.; Feeley, T.C.; Wilder, A.D., and Klemetti, E.W., 2013, Modification of the continental crust by subduction zone magmatism and vice-versa: across-strike geochemical variations of silicic lavas from individual eruptive centers in the Andean Central Volcanic Zone: Geosciences, v. 3, p. 633-667; doi:10.3390/geosciences3040633.

Geosciences **2013**, *3*, 633-667; doi:10.3390/geosciences3040633

OPEN ACCESS

geosciences

ISSN 2076-3263

www.mdpi.com/journal/geosciences

Article

Modification of the Continental Crust by Subduction Zone Magmatism and *Vice-Versa*: Across-Strike Geochemical Variations of Silicic Lavas from Individual Eruptive Centers in the Andean Central Volcanic Zone

Gary S. Michelfelder [1,*,†], Todd C. Feeley [1], Alicia D. Wilder [1] and Erik W. Klemetti [2]

[1] Department of Earth Sciences, Montana State University, Bozeman, MT 59717, USA; E-Mails: tfeeley@montana.edu (T.C.F.); alicia.wilder@msu.montana.edu (A.D.W.)

[2] Department of Geosciences, Denison University, Granville, OH 43023, USA; E-Mail: klemettie@denison.edu

[†] Present Address: Department of Geography, Geology and Planning, Missouri State University, Springfield, MO 65897, USA.

* Author to whom correspondence should be addressed; E-Mail: gary.michelfelder@msu.montana.edu; Tel.: +1-406-994-6916; Fax: +1-406-994-6923.

Received: 2 May 2013; in revised form: 8 November 2013 / Accepted: 14 November 2013 / Published: 27 November 2013

Abstract: To better understand the origin of across-strike K_2O enrichments in silicic volcanic rocks from the Andean Central Volcanic Zone, we compare geochemical data for Quaternary volcanic rocks erupted from three well-characterized composite volcanoes situated along a southeast striking transect between 21° and 22° S latitude (Aucanquilcha, Ollagüe, and Uturuncu). At a given SiO_2 content, lavas erupted with increasing distance from the arc front display systematically higher K_2O, Rb, Th, Y, REE and HFSE contents; Rb/Sr ratios; and Sr isotopic ratios. In contrast, the lavas display systematically lower Al_2O_3, Na_2O, Sr, and Ba contents; Ba/La, Ba/Zr, K/Rb, and Sr/Y ratios; Nd isotopic ratios; and more negative Eu anomalies toward the east. We suggest that silicic magmas along the arc front reflect melting of relatively young, mafic composition amphibolitic source rocks and that the mid- to deep-crust becomes increasingly older with a more felsic bulk composition in which residual mineralogies are progressively more feldspar-rich toward the east. Collectively, these data suggest the continental crust becomes strongly hybridized beneath frontal arc localities due to protracted intrusion of primary, mantle-derived basaltic

magmas with a diminishing effect behind the arc front because of smaller degrees of mantle partial melting and primary melt generation.

Keywords: across-strike geochemical variation; Central Volcanic Zone; Aucanquilcha; Ollagüe; Uturuncu

1. Introduction

Continental arc volcanoes represent a dramatic surface expression of one of the most significant and fundamental phenomena in global tectonics: subduction of an oceanic plate beneath a more buoyant continental plate. The subduction of an oceanic plate results in recycling of crustal material into the convecting mantle, partial melting, and primary basalt production. Moreover, during passage through thick continental crust, subduction zone magmas may substantially differentiate and melt crustal rocks giving rise to the great diversity of igneous lithologies characteristic of Earth. These are important processes that must be understood in detail in order to interpret the long-term evolution of subduction zone systems on Earth and the generation of continental crust.

Although exceptions exist, one of the most remarkable features of arc magmatism is the systematic increase in the contents of K_2O and other incompatible trace elements in volcanic rocks erupted with increasing vertical distance to the Benioff zone [1–4]. Understanding the significance of these trends has long been a major objective of petrologists due to the broader implications for regional tectonic complexities and magma generation processes, in addition to advancing understanding of arc magmatism. Despite decades of intense study, the origins of across-strike geochemical variations in intra-oceanic arcs are still vigorously debated; they are considerably less understood in continental arcs. As emphasized by Dickinson [5], interpreting the origin of these variations is inherently difficult in continental arcs due to the scarcity of primary, or near-primary basalts and the complicating effects of crustal contamination. For these reasons most of the better studied examples are from arcs underlain by relatively thin and, or, young continental crust where the potential for contamination is reduced [3,6–19].

Much has been learned about arc magmatism since publication of Gill's [2] classic book on the subject, although much remains to be learned. Because of its exceptionally thick continental crust and numerous well preserved volcanic centers, the Central Volcanic Zone (CVZ) presents a unique opportunity to advance understanding of fundamental problems such as how silicic magmas are generated in continental arcs, how the continental crust may modify the compositions of primary arc magmas in space and time [7,17,20–22], and how arc magmas may, in turn, spatially and temporally modify the composition of the crust through which these magmas ascend and differentiate [23–27].

In this study we examine and interpret across-arc geochemical trends of <1 Ma silicic volcanic rocks (andesites to dacites) erupted from three composite volcanoes in the Andean Central Volcanic Zone (CVZ) of northern Chile and southwest Bolivia (21°–22° S latitude; Figure 1) and use this information to shed light on how the continental crust may influence across-arc trends in magma chemistry. Associated with active eastward subduction of the oceanic Nazca plate beneath the continental South American plate, the CVZ represents an end member in subduction zone systems on

Earth because the continental crust is thicker (70–80 km) than at any other convergent margin setting [28–35]. The centers examined in this study were selected because of the young and limited range in ages (<1 Ma), quality and availability of comprehensive data sets (including isotopic data), and similarity in eruptive histories (*i.e.*, effusive eruptions from andesitic to dacitic composite cones). In addition, we selected centers that span the range of volcanic activity in the arc, but show a small N-S coverage area, in order to minimize potential along-arc variations in magma sources and processes. Other volcanic centers are present within the study area that fit some of the above mentioned criteria, but no other centers were identified that fit all three of the controls. These restrictions allow for a more focused examination relative to larger regional studies (*i.e.*, [22,36,37]). Previous regional-scale studies of magmatism in the southern Altiplano region documented eastward increases in K_2O and related incompatible trace elements virtually identical to across-strike geochemical trends observed at many oceanic island arcs and continental arcs constructed on thin crust [38–45].

Figure 1. Map showing location of Andean Central Volcanic Zone (CVZ). Shaded area shows the region where crustal thickness exceeds 60 km [30,32,33,46]; stippled region illustrates distribution of Quaternary volcanic rocks. Modified from Feeley and Hacker [47]. Red box highlights the region illustrated in Figure 2.

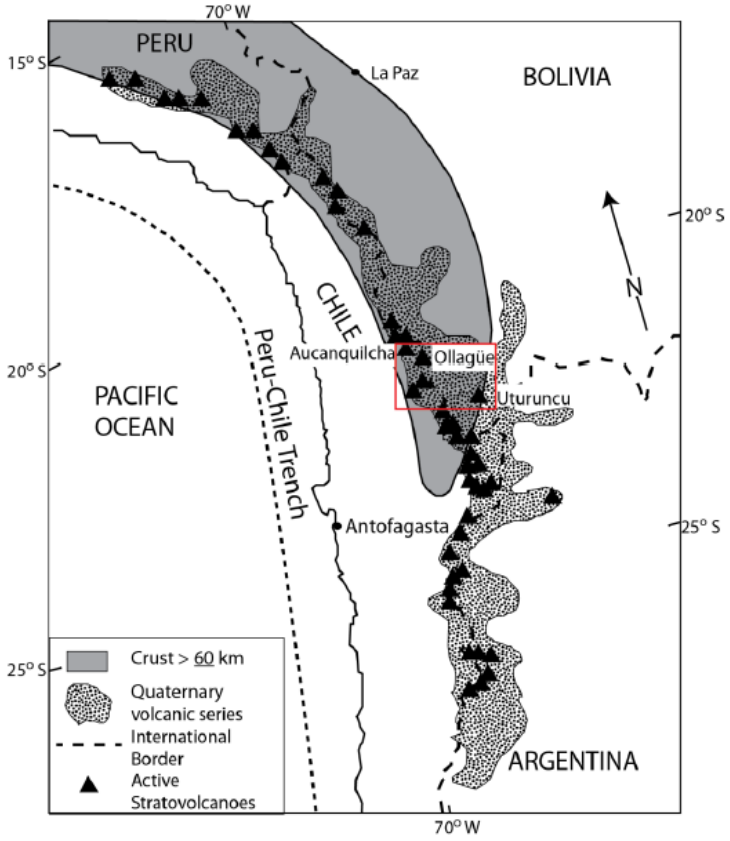

Figure 2. Simplified geologic map of the southern Altiplano and surrounding region (modified from Sparks *et al.* [48]). Only potentially active volcanoes as defined by de Silva and Francis [49] and volcanoes on the southern Altiplano are illustrated. Labeled volcanic centers are those considered in this study due to the quality of data sets available for other volcanic centers within the study area. The thick dashed line trending NW-SE across the Bolivian-Argentine border is interpreted from Allmendinger *et al.* [28] and is considered to be the general boundary between the Bolivian Altiplano (north) and the Argentine Puna (south).

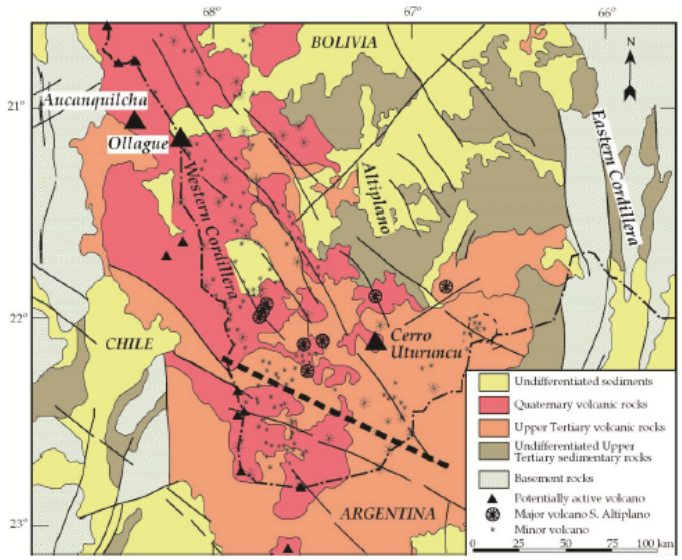

2. Background: Tectonic and Geologic Setting

2.1. Regional Setting

The Andes are generally considered the classic example of a modern Cordilleran type orogen formed by long-term subduction of oceanic lithosphere beneath continental lithosphere. The central Andes, in particular, represent the type locality for this process owing to the great width of the orogen and immense crustal thicknesses (up to 70–80 km; [29]) and high elevations (~4–6 km; [50]) that occur over vast areas (Figure 1). The region composes one of the youngest and largest active silicic volcanic provinces on Earth with recent caldera formation. It contains over 20 calderas and numerous ignimbrites (large ash flow sheets) less than 10 Ma as well as an estimated 50 active or recently active composite volcanoes [51–53].

The modern central Andes at 21°–22° S latitude are divided into three north- to north-west striking geological and upper crustal provinces. From west to east these are: (1) the Western Cordillera: an active volcanic arc bounded on the west by a westward dipping monocline; (2) the Altiplano: a broad, elevated plateau (>3800 m) where undeformed late-Miocene and younger volcanic rocks overlie variably folded and faulted mid-Miocene and older sedimentary and volcanic rocks; and (3) the Eastern Cordillera: a major east-verging thrust complex involving Paleozoic to Mesozoic sedimentary

and metamorphic rocks. The largest volumes of intermediate composition lavas at 21°–22° S latitude erupted from composite volcanoes that form the peaks of the Western Cordillera. Baker and Francis [53] estimated that the Western Cordillera contains ~3000 km^3 of these lavas between 21° and 22° S latitude. Lavas associated with composite volcanoes extend for ~200 km eastward onto the Altiplano, although volumes decrease sharply to <800 km^3 [53].

The youngest rocks in the southern Altiplano region of the CVZ were erupted following relatively recent changes in the subduction history of the CVZ. These changes are related to breakup of the Farallon plate into the Cocos and the Nazca plates, which increased the rate of subduction beneath the South American plate [16,54–56]. Between 15° and 28° S latitude the present day subduction angle of ~30° allows for an expression of magmatism that is absent from 2° to 15° S where the subduction angle is between 5° and 10° [57]. Uplift of the Altiplano and thickening of the CVZ crust are believed to be related, in part, to the recent steepening of the subducting slab [16,58,59]. In this study we focus on compositional variations of rocks on and behind the Quaternary arc-front that erupted after the last major episode of regional crustal thickening and shortening in the region.

2.2. Individual Volcanic Centers

Aucanquilcha is a long lived (11 Ma) volcanic complex located on the volcanic front in northern Chile (Figures 1 and 2; [27]). The Aucanquilcha Volcanic Complex consists of 4 distinct volcanic groups: the Alconcha Group (11 to 8 Ma), the Gordo Group (6 to 4 Ma), the Polan Group (~4 to 2 Ma), and Volcán Aucanquilcha (<1 Ma; [27,60]). There are long hiatuses between the Aconcha and Gordo Groups and between the Polan Group and Volcán Aucanquilcha. This paper focuses exclusively on the eruptive products of Volcán Aucanquilcha.

Eruptive products from Volcán Aucanquilcha range in age from 1.04 to 0.24 Ma [60]. Volcán Aucanquilcha experienced four stages of growth as defined by Klemetti and Grunder [60]: the Azufrera, Rodado, Cumbre Negra and Angulo stages. These stages are not uniquely distinguished on the basis of location or time, and all are dominantly dacitic in composition. Eruptive units of the Azufrera stage (1.04 to 0.94 Ma) make up the main edifice of the volcano [60]. These units are mainly blocky two-amphibole (with the exception of the Rodado Stage) plus biotite dacitic lava flows [60,61]. Nearly all lavas contain undercooled basaltic andesitic to andesitic magmatic inclusions that compose 1%–10% of the total volume of the lavas [27,60].

Volcán Ollagüe straddles the Bolivia-Chile border approximately 25 km to the east of the arc front (Figures 1 and 2; [41]). It is a composite volcano with no Holocene eruptions [62]. Feeley *et al.* [63] described four eruptive series (Vinta Loma, Chasca Orkho, La Celosa, and post-collapse) and a debris avalanche deposit resulting from sector collapse of the western flank of the volcano. These series were subsequently sub-divided into ten sequences by Wörner *et al.* [64], Clavero *et al.* [65], and Vezzoli *et al.* [66].

Ollagüe was primarily active between 1.2 Ma and 130 ka. Currently the volcano shows signs of activity through active degassing of fumaroles that vent from a young dacitic dome on the upper western flank [63,65]. Compositions of eruptive products range from basaltic andesitic to dacitic lava flows and domes covering an estimated area of ~230 km^2 with a volume of ~85 km^3 [63]. In addition, basaltic andesitic to andesitic magmatic inclusions are present in varying proportions in nearly all lava

flows, although they are more abundant in younger units. The volcano is built upon 8 to 5 Ma ignimbrite deposits [47].

Cerro Uturuncu is an andesitic to mainly dacitic composite volcano located in the southern Altiplano region of the CVZ in southwest Bolivia, approximately 120 km east of the arc front (Figures 1 and 2; [48]). The volcano was primarily active between 890 and 271 ka. Eruptive products define two series as described by Sparks *et al.* [48]. The first series is more extensive older material ranging from 890 to 549 ka. These flows and domes rest directly on approximately 5 Ma ignimbrites [49]. The second series consists of younger flows covering about 10 km^2, mostly located on the upper flanks of the edifice. These flows range from 427 to 271 ka and are built upon the first series flows and domes [48]. Most flows and domes sampled by Sparks *et al.* [48] and in this study contain undercooled andesitic magmatic inclusions that compose no more than a few volume percent of the host rocks. In many older rocks magmatic inclusions are rarer [48]. This relationship is similar to that seen at Aucanquilcha [60] and Ollagüe [63] where magmatic inclusions are typically more abundant in younger lavas.

3. Methods

New whole rock analyses for Uturuncu rocks were performed at Washington State University, Pullman. Major and trace element analyses on 121 samples were performed by X-ray Fluorescence Spectrometry (XRF) on a ThermoARL Advant'XP+ automated sequential wavelength spectrometer (ThermoARL, Waltham, MA, USA). Methods and errors for the XRF analyses are described in Johnson *et al.* [67]. 65 distinct geochemical samples were further analyzed for trace elements, including the rare earth elements, by Inductively Coupled Plasma Mass Spectrometry (ICP-MS) on an Agilent Technologies 7700 ICP-MS (Agilent Technologies, Conesus, NY, USA). Methods and errors for trace element analyses are detailed in Jarvis [68].

Whole rock Nd and Sr isotopic analyses on 30 samples were acquired by Thermal Ionization Mass Spectrometry (TIMS) on a VG Sector 54 (VG, Santa Clara, CA, USA) and analyzed by five Faraday collectors in dynamic mode at New Mexico State University, Las Cruces. Calibration of $^{87}Sr/^{86}Sr$ ratios was calculated using the $^{86}Sr/^{88}Sr$ ratio analyzed at 3.0 V aiming intensity and normalized to 0.1194 using NBS 987 Standard (0.710298 + 0.000010) to monitor the precision of the analyses. Sr was isolated using Sr-Spec resin column chromatography by the method described in Ramos and Reid [69]. Nd was separated using REE resin column chromatography using the digested split of prepared sample for Sr chromatography. Nd isotopes were normalized to $^{146}Nd/^{144}Nd = 0.7219$ and results for JNDi-1 were $^{146}Nd/^{144}Nd = 0.512137 \pm 0.000009$ for five analyses. Pb isotopes were separated from the same digested samples used for Sr and Nd isotope ratios. Pb separations used ~2 mL of anion exchange resin in a high-aspect ratio glass column with an eluent of 1*N* HBr and 7*N* HNO_3. Purified samples were then dried and re-dissolved in 1 mL of 2% HNO_3 containing 0.01 ppm Tl. Samples were analyzed on a ThermoFinnigan Neptune multi-collector ICP-MS (ThermoFinnigan, Waltham, MA, USA) equipped with nine Faraday collectors and an ion counter. The standard NBS 981 ($^{208}Pb/^{204}Pb \approx 36.662 \pm 0.002$, $^{207}Pb/^{204}Pb \approx 15.462 \pm 0.001$, $^{206}Pb/^{204}Pb \approx 16.928 \pm 0.001$) was used for accuracy corrections and to monitor precision of the analyses. The values measured for NBS 981 were within the error of published ratios for NBS 981 [70] and therefore corrections were not applied to unknown sample

ratios. Given the young ages of all rocks examined in this study, no age corrections were performed for the radiogenic isotope data.

$\delta^{18}O$ values were determined for 30 Ututuncu samples by the laser fluorination method described by Takeuchi and Larsen [71] at Washington State University, Pullman. Quartz and plagioclase phenocryst separates were analyzed twice to insure reproducibility. The standard UWG-2 was measured with a difference of 0.2‰ from the published value of 5.89‰ [71,72]. Data are illustrated in figures and presented in Table 1 in permil using standard delta notation relative to Vienna Standard Mean Ocean Water (VSMOW).

Table 1. Representative new whole rock samples from Cerro Ututuncu.

Sample	DM10A	DM58A2	GSM17	GSM29	GSM-50
SiO_2	65.55	62.30	66.59	63.65	64.84
TiO_2	1.08	1.13	1.00	0.99	1.08
Al_2O_3	16.16	17.19	15.84	16.11	16.25
FeO*	4.81	5.73	4.47	5.24	4.93
MnO	0.07	0.09	0.06	0.07	0.07
MgO	1.87	2.60	1.61	3.07	2.11
CaO	4.14	4.95	3.64	4.69	4.11
Na_2O	2.37	2.21	2.41	2.23	2.29
K_2O	3.70	3.49	4.11	3.67	4.01
P_2O_5	0.25	0.30	0.28	0.28	0.32
LOI (%)	0.99	0.43	0.53	0.51	0.95
Sum	100.00	100.00	100.00	100.00	100.00
La	53	59	69	61	70
Ce	109	118	140	120	141
Pr	13	14	17	15	17
Nd	50	53	61	54	62
Sm	10	10	11	10	11
Eu	1.80	1.98	1.89	1.90	1.97
Gd	7.68	8.23	8.10	7.79	8.36
Tb	1.11	1.25	1.11	1.10	1.18
Dy	5.89	6.96	5.65	5.74	6.07
Ho	1.03	1.31	0.93	1.03	1.04
Er	2.44	3.29	2.18	2.63	2.40
Tm	0.33	0.45	0.29	0.37	0.31
Yb	1.90	2.72	1.64	2.25	1.76
Lu	0.27	0.40	0.24	0.33	0.25
Ba	686	776	850	814	866
Th	19	19	25	20	25
Nb	18	21	19	19	22
Y	27	33	25	27	27
Hf	6.6	6.4	7.3	6.4	7.3
Ta	1.4	1.5	1.4	1.3	1.5
Rb	167	146	193	161	184
Sr	305	474	338	391	388
Zr	250	241	277	230	276

Note: Total Fe reported as FeO*.

4. Results

4.1. Summary of Petrology and Petrogenetic Processes at 21°–22° S Latitude

Rocks from all three centers are porphyritic with 30% to 60% by volume phenocrysts (average ~40%). Plagioclase is the most abundant phenocryst phase in all samples, accounting for 50% to 75% of the mineral assemblage in many of the samples. Other phenocryst phases are present in variable amounts and include orthopyroxene, clinopyroxene, amphibole, biotite, quartz, magnetite, and ilmenite. In general, phenocryst assemblages are similar for rocks from the three centers, except that amphibole and clinopyroxene are typically more abundant in young rocks from Aucanquilcha, whereas biotite is progressively more abundant in young rocks from Ollagüe and Uturuncu. The latter probably reflects the higher K_2O contents of Ollagüe and Uturuncu rocks relative to rocks from Aucanquilcha.

Petrographic similarities such as those described above and the presence of undercooled magmatic inclusions that are slightly more mafic than the host lavas, suggest that Uturuncu magmas experienced similar petrogenetic processes to magmas erupted at Ollagüe and Aucanquilcha. Specifically, recent geochemical modeling of Uturuncu rocks suggests that the magmas were produced by complex processes involving magma mixing and mingling with more mafic magmas following assimilation of crustal rocks coupled with fractional crystallization (AFC) in multiple reservoirs within both the mid-deep and shallow crust [73,74]. This is consistent with the work of Sparks *et al.* [48] who, on the basis of geochemical and petrologic data, concluded that dacitic magmas at Uturuncu formed by fractional crystallization of andesite forming norite cumulates and involving partial melting and assimilation of the continental crust. Furthermore, phenocryst compositions and zoning patterns indicate that more detailed compositional variations of the dacites reflect magma mixing with silicic andesite at shallow crustal levels. The latter conclusion is supported by geophysical evidence that indicates magma accumulation and seismicity clusters at sea level beneath Uturuncu (6 km depth; [75–77]).

The petrologic model for Uturuncu rocks [48,73,74] is nearly identical to those proposed by Feeley and Davidson [25] and Feeley and Hacker [47] for production of magmas at Ollagüe and Klemetti and Grunder [60] and Walker *et al.* [78] for production of magmas at Aucanquilcha. These authors argue that magma mixing with a component of mid-deep crustal AFC were responsible for producing the rock compositions observed at these two centers. Therefore, mid-deep crustal AFC is considered the dominant process in producing the dacitic rocks erupted at the three centers followed by mixing and mingling with more mafic melts and undercooled inclusions, respectively, in shallow reservoirs to produce rocks lower in SiO_2 contents. The most silicic rocks erupted at the three centers are thus all considered to contain a significant crustal component derived from melting and assimilation of mid-deep crustal local basement lithologies.

4.2. Across-Arc Geochemical Variations

In this section we describe across-arc geochemical and isotopic variations of silicic volcanic rocks (*i.e.*, >60 wt % SiO_2) erupted from the three centers. We focus on silicic rocks because more mafic rocks are generally rare or non-existent at the three centers and the silicic rocks better record the compositions of crustal rocks through which the magmas ascended and interacted. Data for magmas erupted at Ollagüe and Aucanquilcha are in Feeley and Davidson [25], Feeley and Hacker [47], Feeley and Sharp [26],

Mattoli *et al.* [79], Grunder *et al.* [27], Klemetti and Grunder [60], and Vezzoli *et al.* [66]. New whole rock and isotopic data are illustrated in this paper for Uturuncu rocks with representative analyses presented in Tables 1–3. A complete dataset for new analyses is available in the supplementary information. Additional major and trace element data for Uturuncu rocks are in Sparks *et al.* [48].

Table 2. Representative new whole rock trace element ratios from Cerro Uturuncu.

Sample	DM10A	DM58A2	GSM17	GSM29	GSM-50
$K_2O + Na_2O$	5.99	5.68	6.46	5.87	6.20
Rb/Sr	0.55	0.31	0.57	0.41	0.47
Sr/Y	11.48	14.25	13.59	14.48	14.54
Ce/Y	4.09	3.56	5.63	4.43	5.29
Ce/Yb	57.24	43.43	85.38	53.23	80.06
Ba/La	12.91	13.27	12.34	13.34	12.37
Ba/Zr	2.75	3.22	3.07	3.53	3.13
K/Rb	184.42	199.17	176.59	189.74	180.83
Nb/Zr	0.07	0.09	0.07	0.08	0.08
Dy/Dy*	0.81	0.73	0.80	0.68	0.81
Dy/Yb_N	2.01	1.66	2.24	1.66	2.23
La/Yb_N	18.87	14.47	28.36	18.29	26.75
Eu Anomaly	0.57	0.58	0.56	0.58	0.63

Note: $Dy/Dy^* = Dy_N/(La_N^{4/13}Yb_N^{9/13})$.

Table 3. Representative new whole rock Sr, Nd, Pb whole rock isotopic ratios and $^{18}O/^{16}O$ ratios from mineral separates from Cerro Uturuncu.

Sample	DM10A	DM58A2	GSM17	GSM29	GSM-50
$^{87}Sr/^{86}Sr$	0.71457	0.711294	0.71385	0.71141	0.71247
$^{144}Nd/^{143}Nd$	0.51215	0.512179	0.51214	0.51223	0.51216
$^{208/204}Pb$	38.94	38.92	38.94	38.9	38.93
$^{207/204}Pb$	15.65	15.65	15.65	15.65	15.64
$^{206/204}Pb$	18.87	18.84	18.84	18.84	18.86
$\delta^{18}O$-QTZ	7.26	8.95	–	7.60	7.98
$\delta^{18}O$-PLG	–	9.32	–	–	8.75

Notes: $\delta^{18}O$-QTZ represents mineral separate analyses of quartz phenocrysts; $\delta^{18}O$-PLG represents mineral separate analyses of plagioclase phenocrysts.

Volcanic rocks at Aucanquilcha, Ollagüe, and Uturuncu are high-K, calc-alkaline andesites/trachyandesites and dacites/trachytes, together with less abundant basaltic andesites (Figure 3). Total alkali concentrations of rocks from Aucanquilcha and Ollagüe with 61–68 wt % SiO_2 are restricted, ranging from 5.1 to 7.9 wt %, such that they plot along the border of the andesite-dacite/trachyte-trachyandesite fields (Figure 3; [27,60]). Ollagüe also contains a few rocks that plot in the trachyte and trachyandesite fields, but these are rare (Figure 3; [23,25]). Silicic rocks at Uturuncu with SiO_2 contents from 61 to 68 wt % have lower total alkali concentrations of 5.5–6.7 wt %

(as a result of low Na_2O concentrations; see below); classifying them as andesitic to dacitic (Figure 3; [23,25,48]).

Figure 3. Total alkalis *vs.* SiO_2 contents and classification of silicic rocks from Aucanquilcha, Ollagüe and Ututuncu [80].

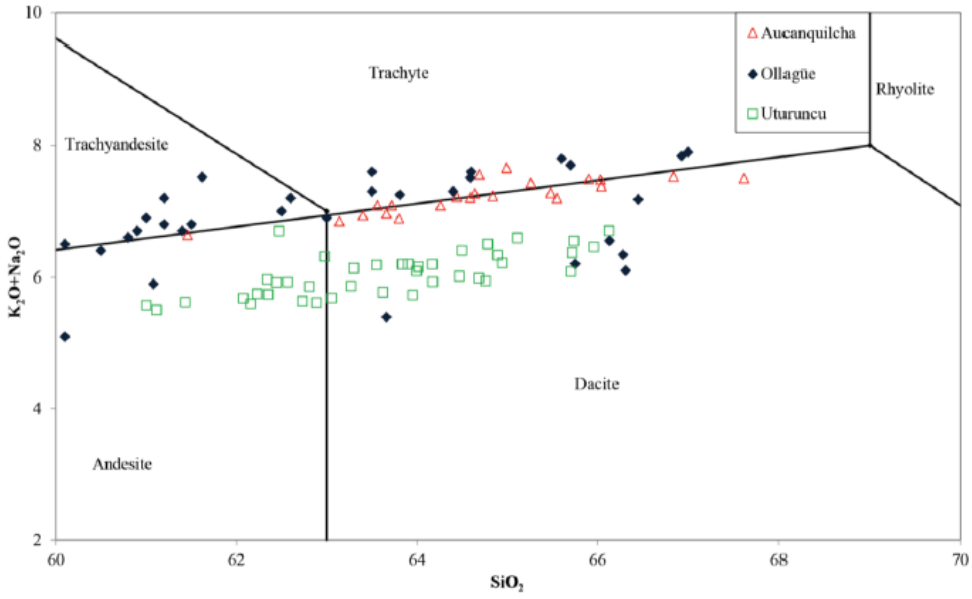

Systematic differences exist in the major and trace element compositions of rocks erupted with increasing distance from the arc front. At a given SiO_2 content, K_2O, FeO, P_2O_5, and TiO_2 concentrations increase toward the east, particularly in the most silicic composition rocks, with the highest concentrations in rocks at Ututuncu (Figure 4). In contrast, contents of CaO, Al_2O_3, and, particularly, Na_2O, decrease in concentration toward the east, with very low concentrations of the latter in Ututuncu rocks (Figure 4). In more detail, trends for P_2O_5 and TiO_2 decrease with increasing SiO_2 for lavas from Aucanquilcha and Ollagüe, whereas they increase with increasing SiO_2 for lavas from Ututuncu.

At a given SiO_2 content, all trace elements analyzed increase in rocks erupted progressively toward the east with the exception of Sr and Ba (Figure 5). In contrast, Sr (and to a lesser degree, Ba) concentrations decrease toward the east at a given SiO_2 concentration (Figure 5). Chondrite-normalized REE patterns for rocks from Aucanquilcha and Ollagüe have similar slopes, although Ollagüe rocks have higher concentrations of REE compared to Aucanquilcha (Figure 6). In contrast, Ututuncu REE patterns have steeper slopes for middle to heavy REE compared to patterns for Ollagüe or Aucanquilcha rocks and higher concentrations (Figure 6). In these regards, with increasing SiO_2 contents, $(La/Yb)_n$ (when "*n*" refers to chondrite normalized values) ratios increase for rocks from all centers and broadly overlap (although the most silicic rocks from Ututuncu have the highest ratios; Figure 7). In contrast, with increasing SiO_2 concentrations, trends for $(Dy/Yb)_n$ ratios are variable: they decrease in Aucanquilcha rocks, are roughly constant for the Ollagüe suite, and increase for Ututuncu rocks (Figure 7). Furthermore, negligible Eu anomalies are observed in REE patterns for rocks from

Aucanquilcha (0.8–0.85) compared to small negative Eu anomalies in Ollagüe rocks (0.61–0.88; ratios close to one are considered small). Relatively large negative Eu anomalies (0.49–0.69) are observed for all Uturuncu rocks (Figures 6 and 7; Table 2).

Figure 4. Major element diagrams for volcanic rocks from Aucanquilcha, Ollagüe and Uturuncu rocks *vs.* SiO_2.

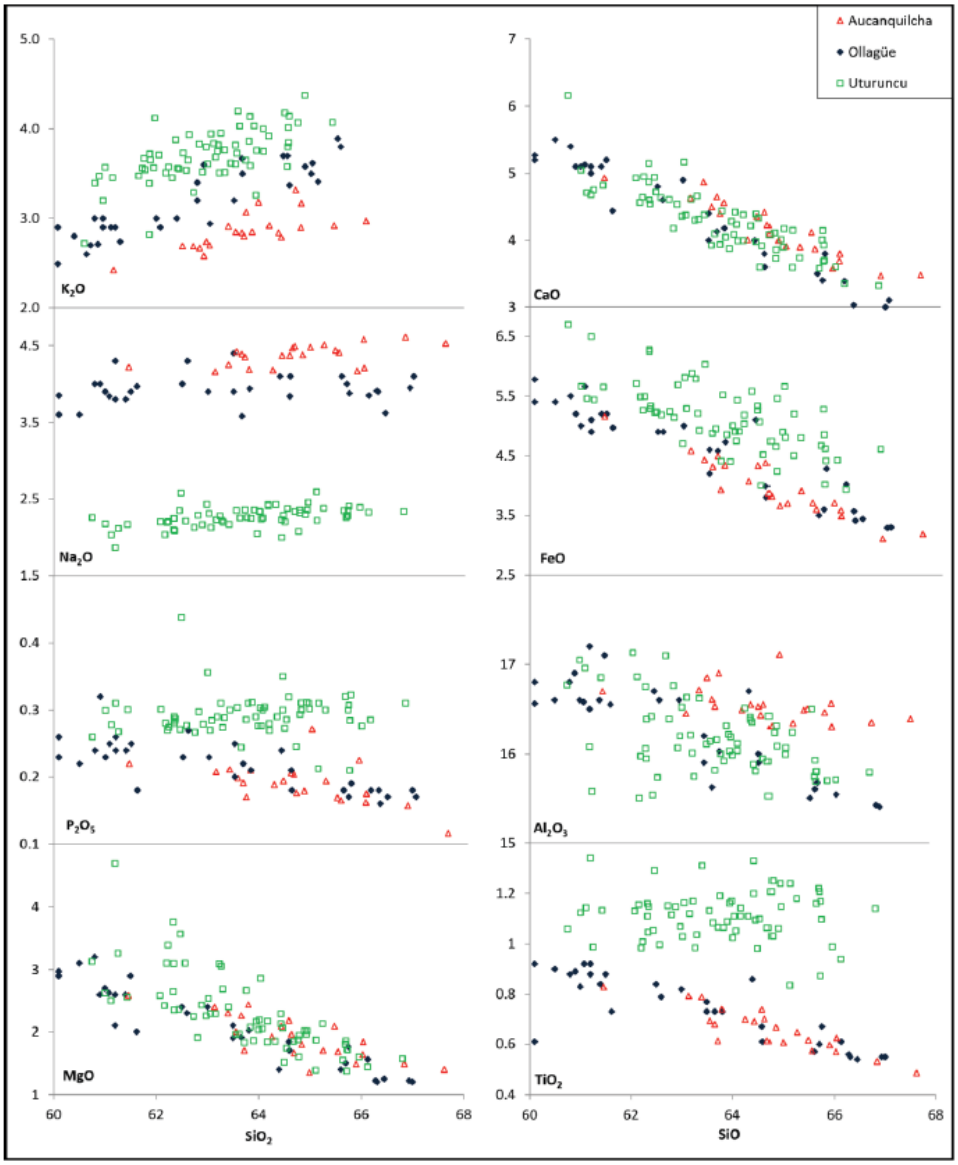

Figure 5. Plots of selected trace element compositions of Aucanquilcha, Ollagüe, and Uturuncu rocks *vs.* SiO_2.

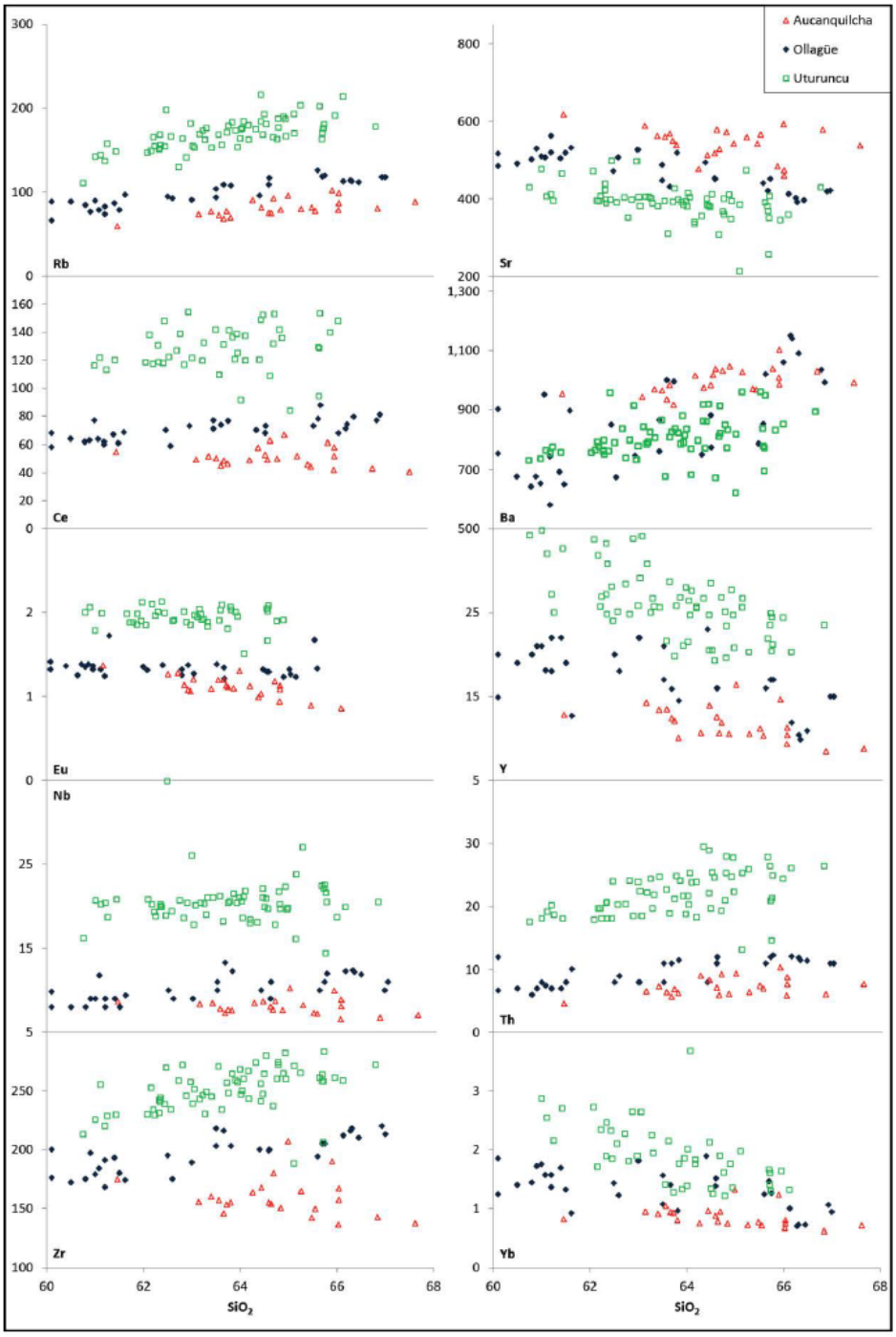

Figure 6. Rare earth element fields for whole rock samples from each volcanic center. Chondrite normalization values from Sun and Mcdonough [81].

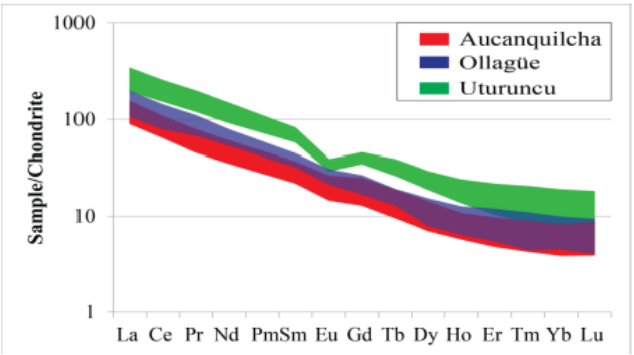

LILE to HFSE ratios (e.g., Ba/Zr and Rb/Nb; the latter not illustrated), K/Rb, Ba/La, and Eu/Eu* decrease toward the east for a given SiO_2 (Figure 7). Nb/Zr and Rb/Sr ratios increase toward the east with the highest ratios observed in Uturuncu rocks for a given SiO_2 (Figure 7). Aucanquilcha rocks contain the highest Sr/Y ratios for a given Y concentration (Figure 8). This ratio is lower in Ollagüe rocks and the lowest ratios are observed in Uturuncu rocks. Ratios of La/Ta show no correlation with distance from the arc front with the exception that there are no observed ratios for Aucanquilcha that fall below La/Ta = 40. Ba/Ta ratios decrease towards the east. Ba/La ratios for all observed rocks from Aucanquilcha and most rocks for Ollagüe are above the Ba/La = 20 ratio indicative of their arc affiliation [17,82].

Across-arc variations in Sr, Nd, and O isotope ratios generally parallel those observed for K_2O and incompatible trace elements (with the exceptions of Sr and Ba), particularly for the most silicic rocks erupted at any given center. In this regard, $^{87}Sr/^{86}Sr$ and $^{18}O/^{16}O$ ratios of Uturuncu rocks (Table 3) are highly elevated and become progressively lower in rocks erupted towards the arc front, whereas $^{143}Nd/^{144}Nd$ ratios increase (Figure 9). In detail, with increasing SiO_2 contents, Sr and Nd isotopic ratios of rocks from Aucanquilcha decrease and increase, respectively, show small variations for rocks from Ollagüe, and increase and decrease, respectively, for rocks from Uturuncu.

On a plot of $^{143}Nd/^{144}Nd$ *vs.* $^{87}Sr/^{86}Sr$, rocks from all three centers form a slightly scattered curvilinear array, becoming isotopically more "crustal-like" (*i.e.*, plotting lower and further to the right from Bulk Earth (BE; $^{143}Nd/^{144}Nd = 0.51263$; $^{87}Sr/^{86}Sr = 0.7052$; [83])) with increasing distance from the arc front (Figure 10). This is a long observed trend in the CVZ as outlined by Kay *et al.* [17] and references within. Furthermore, on Figure 10, there is a distinct gap between magmas erupted at Uturuncu *versus* those erupted on or just to the east of the arc front. In a similar manner, $\delta^{18}O$ values for the rocks as a group are elevated relative to generally accepted mantle values [24,84–86], thus requiring the incorporation of a significant crustal component during the petrogenesis of all studied suites. $\delta^{18}O$ values of mineral separates are extremely variable for Uturuncu rocks ($\delta^{18}O$ = 7.3‰–9.6‰) compared to Ollagüe ($\delta^{18}O$ = 7.3‰–8.3‰) and Aucanquilcha rocks ($\delta^{18}O$ = 7‰–7.3‰), in part reflecting that values for both plagioclase and quartz are illustrated for Uturuncu rocks. Nevertheless, Aucanquilcha rocks contain the lowest $\delta^{18}O$ values and, while values for Uturuncu and Ollagüe overlap, $^{18}O/^{17}O$ ratios become on-average more crustal-like toward the east (Figure 9).

Figure 7. Plots of selected trace element abundance ratios for Aucanquilcha, Ollagüe, and Ututuncu rocks *vs.* SiO_2. Lines through data points without arrowheads illustrate inferred trends for individual eruptive centers.

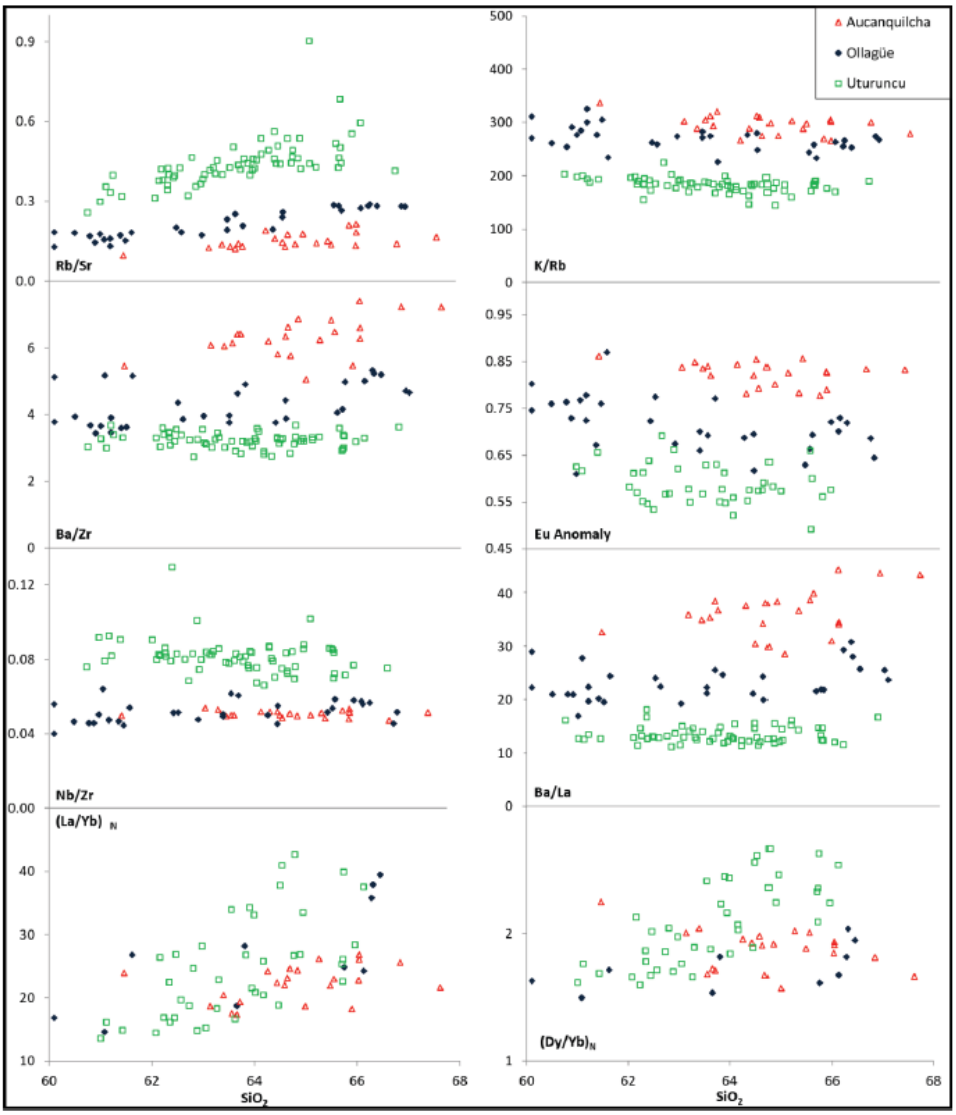

Figure 8. Plots of trace element ratios for Aucanquilcha, Ollagüe, and Uturuncu rocks *vs.* Y, La contents and La/Yb ratios.

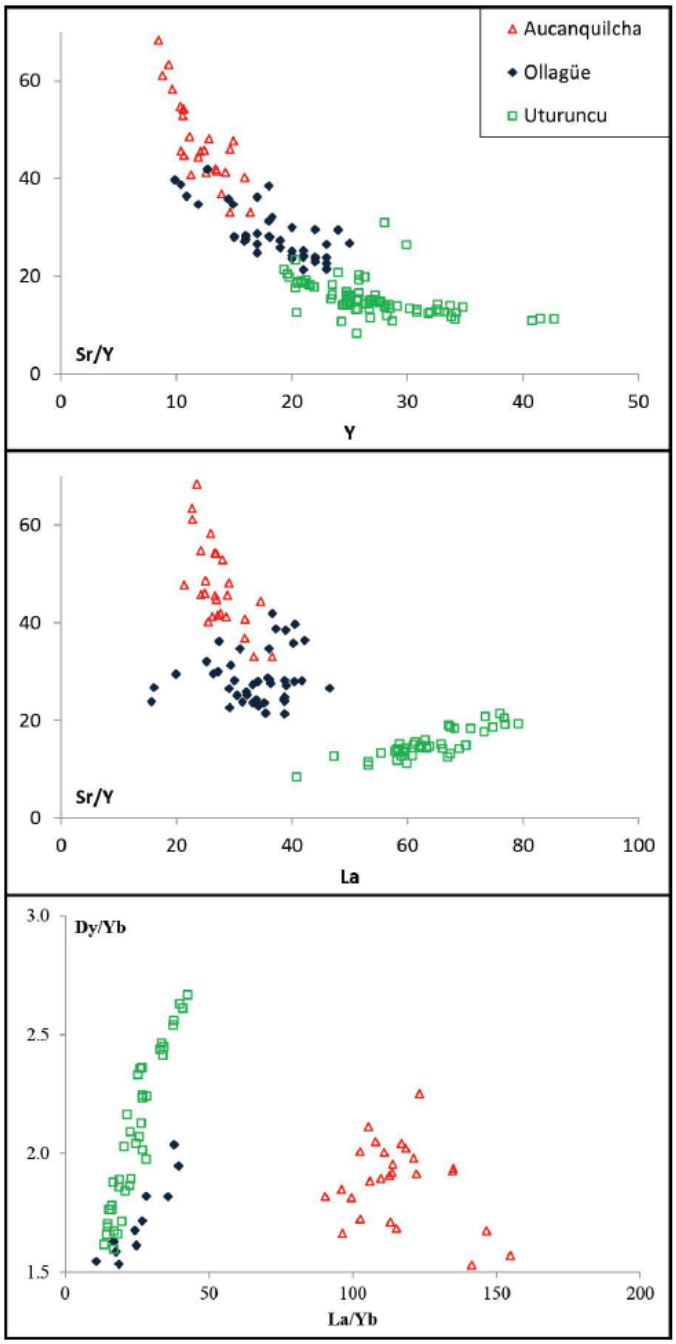

Figure 9. Plots of $^{87}Sr/^{86}Sr$, $^{143}Nd/^{144}Nd$, and $^{18}O/^{16}O$ (as $\delta^{18}O$ values of mineral separates) ratios of Aucanquilcha, Ollagüe and Uturuncu rocks *vs.* SiO_2. Lines through data points illustrate inferred trends for individual eruptive centers.

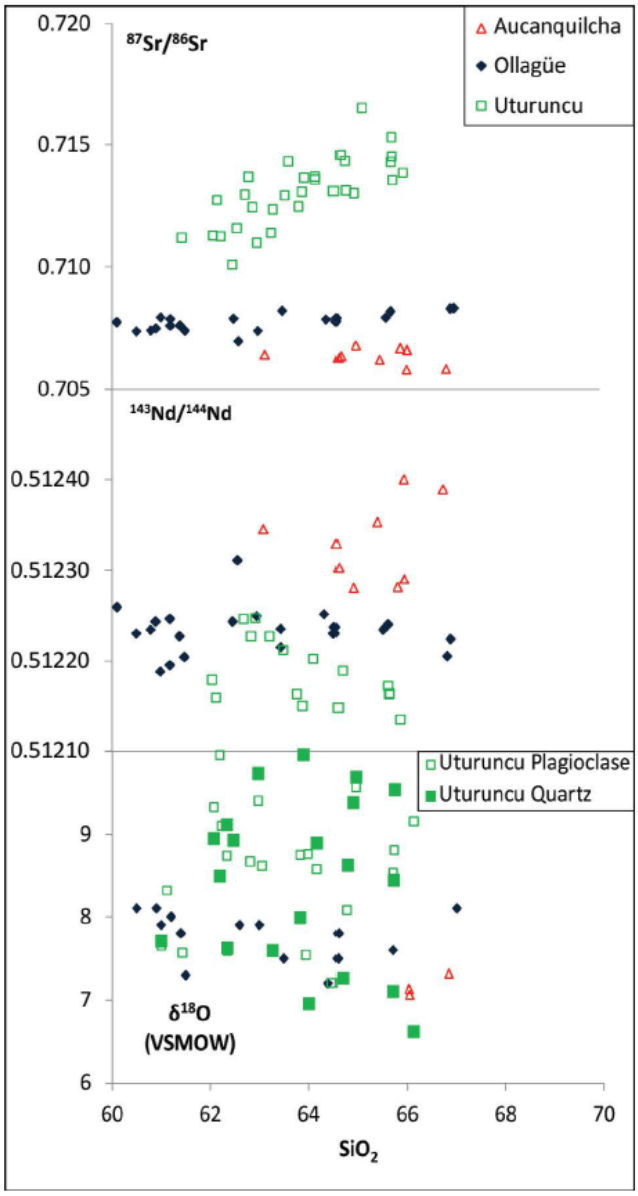

Figure 10. (**a**) $^{143}Nd/^{144}Nd$ *vs.* $^{87}Sr/^{86}Sr$ ratios of Aucanquilcha, Ollagüe and Uturuncu rocks. Arrow labeled BE illustrates direction toward position of "Bulk Earth", which plots off of figure; (**b**) $^{87}Sr/^{86}Sr$ *vs.* Sr/Y ratios of Aucanquilcha, Ollagüe and Uturuncu rocks.

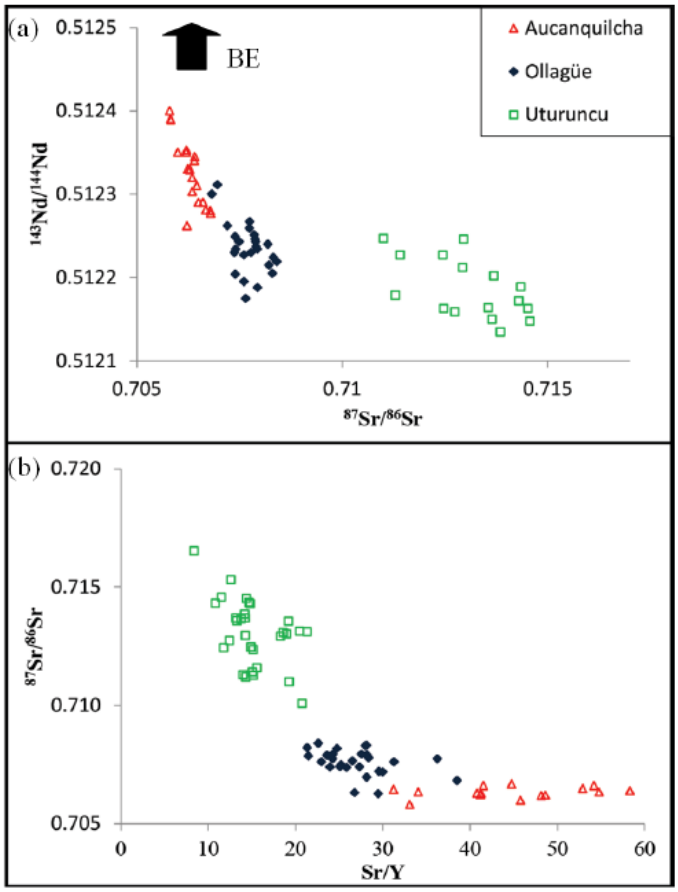

Rocks from Aucanquilcha and Ollagüe have extremely variable Pb isotopic ratios and show no distinct arrays with varying SiO_2 concentrations (not shown). Uturuncu rocks (Table 3) have very restricted $^{207}Pb/^{204}Pb$, $^{208}Pb/^{204}Pb$, and $^{206}Pb/^{204}Pb$ ratios, although they are higher on average than for Ollagüe or Aucanquilcha rocks (Figure 11).

Pb isotopic ratios for all three centers lie within the southern sector Pb isotopic domain defined by Wörner *et al.* [22]. Aucanquilcha and Ollagüe Pb isotopic values lie in the Southern Altiplano Pb isotopic domains ($^{207}Pb/^{204}Pb > 15.64$, $^{208}Pb/^{204}Pb < 38.89$ but >38.5 and $^{206}Pb/^{204}Pb > 18.6$) defined by Aitcheson *et al.* [87] and Uturuncu lies within the Eastern Cordilleran domain ($^{207}Pb/^{204}Pb > 15.64$, $^{208}Pb/^{204}Pb > 38.9$ and $^{206}Pb/^{204}Pb > 18.6$).

Figure 11. $^{208}Pb/^{204}Pb$ *vs.* $^{206}Pb/^{204}Pb$ and $^{207}Pb/^{204}Pb$ *vs.* $^{206}Pb/^{204}Pb$. Pb isotopic ratios for all three centers lie within the southern Altiplano Pb isotopic domain defined by Wörner *et al.* [22] and Aitcheson *et al.* [87]. Grey field defines the boundary between the Eastern Cordilleran domain and the Southern Altiplano domain [87].

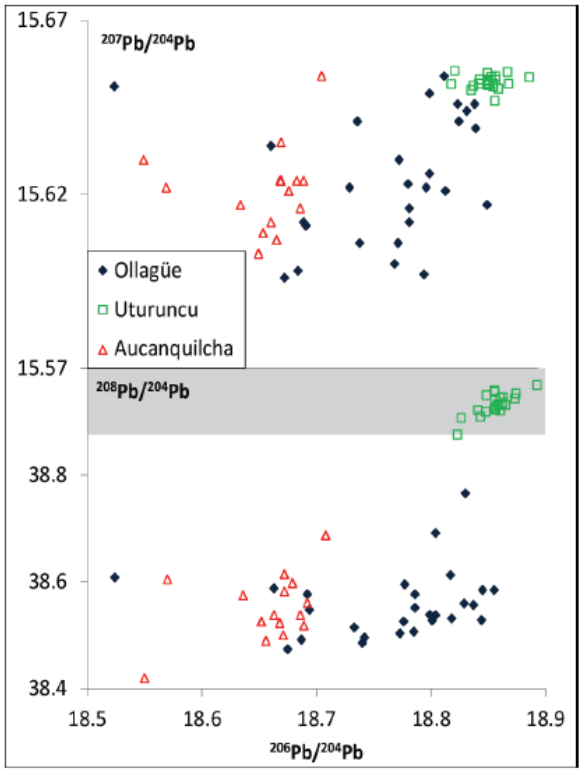

5. Discussion: Origin of Across-Arc Geochemical Variations in the Central Andes at 21°–22° S Latitude

Major and trace element across-arc variations at 21°–22° S latitude described in the previous section are similar in several respects to trends observed at many other convergent margin settings where there is thin (Southern Andes) or no overlying continental crust (oceanic arcs; as described by Gill [2]; p. 209, and Tatsumi and Eggins [4]; pp. 80–81). These include increases in K_2O and most incompatible trace elements with increasing distance from the active arc front. Notable exceptions are that whole rock Na_2O, Sr, and Ba contents decrease to the east for a given SiO_2 concentration (Figures 4 and 5). These trends are contrary to the across-arc behavior of these elements observed at other oceanic arcs (e.g., New Zealand, Java, Japan, and the Aleutians; [2–5,88]).

It has been repeatedly demonstrated that K and incompatible trace elements tend to increase in arc magmas with distance behind the volcanic front (there is, however, no general rule for isotopic ratios [2–5,89]). Much of our perspective on the origin of these trends comes from study of intra-oceanic arcs or arcs constructed over young, thin continental crust [6,90–92]. In these settings,

across-arc geochemical trends are nearly always linked to systematic changes in mantle source compositions, degrees of partial melting, and, or, slab dehydration reactions. This is because they are typically expressed in the most primitive rocks of any given suite and they frequently correlate with other petrologic features such as inferred primary magmatic H_2O contents [11,12,93–95].

The Andean CVZ offers the opposite perspective to island arcs: thick continental crust producing or enhancing across-arc trace element variations in subduction zone magmas. A result of the anomalously thick crust beneath the CVZ is that the across-arc increases in K_2O and incompatible trace element concentrations do not *directly* reflect variations in mantle source compositions or degrees of partial melting. Baseline Sr and O isotopic ratios of the volcanic rocks are highly elevated relative to primitive intra-oceanic arc magmas, implying a contribution from the continental crust during magma petrogenesis [96]. Furthermore, $^{87}Sr/^{86}Sr$ and $^{18}O/^{16}O$ ratios become more variable and increase towards the east for a given SiO_2 concentration while $^{143}Nd/^{144}Nd$ ratios decrease (Figure 9). These trends parallel the incompatible trace element trends for each of the three volcanic centers (Figures 5–7). This suggests that the sources become more variable/complex towards the east. The thick continental crust thus modifies primary arc magmas generated across the transect (Figures 10 and 11), yet many of the universal across-arc trace element trends observed at oceanic arcs are maintained (Figure 5). How is this possible?

A variety of models have been proposed to account for the across-arc trace element trends at 21°–22° S latitude. However, until recently these models have been difficult to test due to the absence of a comprehensive data set on magmas erupted from suitable back-arc locations. This is important in order to constrain the processes and contaminants that influence magmatic differentiation to a singular location rather than using multiple locations that may have undergone different processes or assimilated different crustal contaminants. Using data from multiple centers representing a "zone" would require additional analyses and comparison of the centers. Fernández *et al.* [42], Kussmaul *et al.* [44], Avila-Salinas [38], and Feeley [41] demonstrated that rocks with the highest K_2O contents also have the highest $^{87}Sr/^{86}Sr$ ratios. These authors proposed that the eastward enrichments of incompatible trace elements require the involvement of some form of crustal melting or contamination. Further to the south, Kay *et al.* [17] suggested that the ignimbrites located on the Puna plateau are controlled by basement contaminants during the earliest stages of volcanism. Overtime, this contribution diminishes and compositions become increasingly controlled by mantle source compositions. Fernández *et al.* [42] and Kussmaul *et al.* [44] suggested that the observed compositional trends may reflect crustal melting or contamination of more mafic magmas at increasingly shallower depths eastward. These conclusions were reached without comprehensive trace element data, which was later suggested to play key roles in modeling the mineralogies and source compositions during magma differentiation and migration [41,97,98]. Avila-Salinas [38] suggested the trends may reflect an eastward increase in the degree of upper-crustal contamination, although little evidence was discussed to support this idea. Feeley [41] argued the trends may reflect assimilation of progressively less hybridized mid-deep crustal rocks eastward (e.g., Figure 5). Diminishing hybridization of the continental crust east of the volcanic front was inferred to reflect diminishing intrusion of subduction-derived basaltic magmas due to progressively lower degrees of mantle partial melting. In contrast to these models, Dostal *et al.* [99] suggested a more traditional model where the across-arc spatial variations were attributed to the degree of mantle partial melting with increasing depths to the Benioff zone and possibly systematic variations

in mantle source compositions as a result of hydrous fluid fluxing. The temporal geochemical evolution of the Central Andes was discussed by Mamani *et al.* [36,37]. These authors used Sr/Y, Dy/Yb and Sm/Yb to describe changes in arc magma composition from the Triassic to the recent and discussed the observed changes these ratios have during arc migration. These authors suggested that along-strike variations from 18° to 28° S over time were caused by the onset of crustal thickening and changes in the depth of assimilation at ~30 Ma and again at ~3 Ma. The variation caused by the onset of crustal thickening at ~30 Ma resulted in higher ratios of Dy/Yb and Sm/Yb reflecting increased lithospheric pressures at the time of differentiation and crust-magma interaction. These depths were suggested to be where garnet and amphibole are stable [37].

The model by Kay *et al.* [17] is a hybrid model. In the early stages of eruption of the Puna ignimbrites the composition of the ignimbrites are controlled by variation in the crustal composition. Over time, these authors suggest that the composition of the crust becomes less important, and the controlling factor in the compositional variation between the back arc and the arc front volcanic rocks is variation in the mantle source and slab fluxes. Early stages of this model suggest hybridization and crustal assimilation similar to the model presented by Feeley [41], but does not suggest how geochemical variation occurs at a single point in time. The model of Kay *et al.* [17] requires a temporal component to observe similar across arc variations seen at 21°–22°.

Our preferred explanation for the across-arc geochemical and isotopic trends described in the previous section is that magmas assimilate continental crust that becomes increasingly more mafic toward the arc-front because of relatively recent intrusion and hybridization by primary, subduction-derived basaltic magmas. Several lines of evidence collectively support this hypothesis. First, the curvilinear array formed by $^{87}Sr/^{86}Sr$ and $^{143}Nd/^{144}Nd$ ratios on Figure 10, with magmas becoming isotopically more crustal-like with increasing distance from the arc front, cannot reflect a continuous differentiation trend formed by a common petrogenetic process given the similar bulk compositions (*i.e.*, SiO_2 and MgO contents) of the rocks at the three centers (a similar argument can be made for the across-arc trend in Sr *vs.* O isotope ratios). Instead, it is more likely related to local isotopic differences in the composition of the mid- deep-continental crust. In this regard, it is possible that magmas at Uturuncu assimilated crustal rocks similar in composition to un-hybridized Paleozoic granites and gneisses exposed in northwestern Argentina. These rocks have $^{87}Sr/^{86}Sr$ ratios between 0.71 and 0.80 [100–104]. Assimilation fractional crystallization modeling of Uturuncu magmatic inclusions and contaminants of similar composition to the Paleozoic granites described by Lucassen [36,37,73,100,102,103,105–110] suggest that very little contamination is required to produce the high Sr isotopic ratios while maintaining the moderate Sr concentrations observed at Uturuncu. Increasing Rb/Sr ratios (Figure 7) toward the east can thus be directly related to assimilation of progressively older, less-hybridized crustal rocks toward the east with high $^{87}Sr/^{86}Sr$ ratios due to protracted in-growth of radiogenic ^{87}Sr in assimilated lithologies.

Second, across-arc increases in K_2O, Rb, Th, Y, REE and HFSE contents can be interpreted to reflect assimilation of more silicic lithologies with higher incompatible trace element contents in which residual mineralogies are progressively more feldspar-rich. In the latter regard it is important to note that contrary to across-arc geochemical trends commonly observed at other arcs, the CVZ rocks display systematically lower Na_2O, CaO, Al_2O_3, Sr, and Ba contents toward the east; stoichiometric components or trace elements with relatively high partition coefficients in feldspar-rich assemblages [83]. Furthermore,

with increasing distance from the arc-front, the rocks have progressively more negative Eu anomalies (Figure 7), also consistent with more feldspar-rich residual mineralogies. In a similar manner, across-arc increases in $\delta^{18}O$ can be interpreted to indicate assimilation of rocks with increasingly higher proportions of more silicic, ^{18}O-concentrating minerals toward the east.

Third, more feldspar-rich residual mineralogies toward the east are supported by experimental studies. Specifically, Huang and Wyllie [111] demonstrated in tonalite melting experiments at low-H_2O and high pressures (~15 kbar), similar to conditions assumed for the mid-deep crust beneath the southern CVZ, that K_2O-rich silicic melts are produced with residual plagioclase and garnet. In contrast, during melting of mafic amphibolite under similar conditions, plagioclase becomes unstable, increasing Sr concentrations in the melt [20,98]. Moreover, high-pressure (e.g., ≥15 kbar) melting experiments by Litvinovsky *et al.* [112] on a variety of Archean silicic rock compositions (e.g., charnokite, granodiorite, and leuco-granite) under both wet and fluid-absent conditions in all cases produced silicic melts in equilibrium with residual garnet, Na-rich feldspar, and clinopyroxene. At low to moderate melt fractions (e.g., 5%–25%), derivative melts are characterized by low Na_2O, but high K_2O contents. Collectively, these experiments demonstrate that partial melting of mafic protoliths at high pressures leads to production of melts with high Sr/Y ratios, whereas high pressure melting of more silicic compositions leads to production of melts with low Sr/Y ratios (largely due to low Sr contents) and Na_2O contents, but high K_2O contents. The smooth, curvilinear array on Figure 8 with Sr/Y ratios decreasing with increasing Y contents to the east is therefore consistent with a progressive change to melting of more silicic bulk composition crustal rocks eastward and more feldspar-rich residual mineralogies (alternatively, this trend has also been ascribed to melting at progressively lower pressures in the absence of residual garnet, but we discount this below).

Kay *et al.* [17] suggested that the low Na_2O concentrations observed in the Puna ignimbrites (Grandada-Orosmayo, Panizos, and Vilama) combined with high $^{87}Sr/^{86}Sr$ ratios (0.709861–0.715048; [113,114]) and $\delta^{18}O$ (9.05–10.24; [113,114]) ratios are the result of crustal contamination by old shale-like components with similar interpretations for the Altiplano ignimbrites (e.g., Morococala; [115]). This is a possible alternative to the model described above, but still supports the model that the composition of the continental crust changes eastward.

Finally, observations by Baker and Francis [53] indicate that the greatest volumes of late Cenozoic, subduction-related rocks are located along the arc-front and decrease systematically toward the east. This may indicate that recent intrusion of subduction-derived mafic melts has been greatest in the mid- to deep-crust beneath the arc front and diminishes in a regular manner toward the east. A straightforward interpretation of this result is that the continental crust is likely younger and more mafic beneath the arc-front as a result of hybridization due to protracted intrusion of subduction-derived, primary basaltic magmas. A further implication of the higher magma volumes along the arc-front is that the degree of mantle partial melting and thus melt production may be greatest along the arc-front.

We discount other models to explain the observed across-arc geochemical trends. For example, Fernández *et al.* [42] and Kussmaul *et al.* [44] suggested the trends may reflect crustal melting or contamination of more mafic magmas at increasingly shallower depths eastward. This hypothesis is unlikely because Y and Yb contents, although high in Uturuncu rocks, probably as a result of assimilation of more incompatible element-enriched silicic crustal source rocks, decrease with

increasing SiO_2 contents for rocks from all centers (Figure 5). This suggests that garnet was in the high-pressure melt residue after assimilation for all three suites, consistent with the experimental studies cited above involving a wide-range of crustal source rock compositions [17]. Furthermore, with increasing SiO_2 contents, $(La/Yb)_n$ ratios increase for rocks from all centers and broadly overlap or are higher in Uturuncu rocks, consistent with similar amounts of garnet in the residue during crustal melting for all centers and, by extension, comparable depths of differentiation (Figure 7; [116]). This is also consistent with the similar petrographic features of the rocks from all centers, which indicates comparable petrogenetic histories. There is thus no evidence for shallower depths of melting toward the east. In contrast, with increasing SiO_2 contents, $(Dy/Yb)_n$ ratios (calculated by the method of [116]) decrease in Aucanquilcha rocks, are roughly constant for the Ollagüe suite, and increase for Uturuncu rocks (Figure 7). Similar trends are seen for TiO_2 *vs.* SiO_2 for rocks from Aucanquilcha and Uturuncu (Figure 4). Furthermore, FeO contents increase eastward at a given SiO_2 content. Collectively these trends can be explained by more mafic, Ti- amphibole-rich lithologies (and residual mineralogies) in the mid-deep crust beneath the arc-front relative to the mid- to deep-crust beneath the back-arc, given that partition coefficients for middle-REE (e.g., Dy) are higher than for heavy-REE (e.g., Yb) in amphibole (see [116,117]). As a result, the trend of smoothly decreasing Sr/Y ratios with increasing Y contents and increasing Eu anomalies from west to east (Figures 5 and 8) are best explained by assimilation in the mid- to deep-crust of progressively more felsic, incompatible trace element enriched crustal compositions (e.g., [118]), as opposed to progressively shallower depths of assimilation.

The presence of plagioclase, either in the source as a residual phase or as a result of fractionation during melt migration, plays a key role in controlling the variations observed in the Sr contents for all three centers. By normalizing Sr to an element such as Y we can observe the effects of plagioclase in the source or during melt migration. The increasing Eu anomalies observed from west to east suggest that beneath the arc front plagioclase is neither retained in the source or fractionated during melt migration. This can be explained by either the stability of plagioclase in the melt or in the source. As suggested by the middle-REE patterns for rocks from Aucanquilcha, a mafic amphibole-rich source explains why fractionation or retention of plagioclase is not observed in either the Sr/Y ratio or the Eu anomaly for these rocks. In contrast, at Uturuncu more pronounced Eu anomalies, lower Sr/Y ratios and middle-REE patterns are observed suggesting fractionation or retention of plagioclase is present either in the source or during migration of the melt.

La/Ta ratios show little correlation with distance from the arc front at 21°–22° S similar to the model proposed by Kay *et al.* [17] for the Puna ignimbrites. When Ba/Ta ratios are compared to Ta concentrations for the three centers, the highest Ba/Ta ratios coincide with the lowest Ta concentrations (Figure 12). Uturuncu rocks for a given SiO_2 have lower Ba concentrations than observed at Aucanquilcha. This relationship further supports the inference made from the Sr/Y ratios that the source beneath Uturuncu is compositionally different than beneath Aucanquilcha. Ba/Ta ratios for Ollagüe overlap with both Uturuncu and Aucanquilcha suggesting that the variation may be more controlled by the Ta concentration of the rocks than the Ba concentration.

Figure 12. Ba/Ta ratios *vs.* La/Ta ratios. The Ba/La ratio for rocks sampled at the three centers decreases with distance from the arc front. The grey shaded area labeled arc are the lower limits of ratios among La, Ba and Ta in mafic southern Andean volcanic arc rocks as interpreted by Hickey *et al.* [82] as inferred from Kay *et al.* [17]. Ratios observed at Uturuncu are similar to ratios observed by Kay *et al.* [17] for northern Puna small volume ignimbrites.

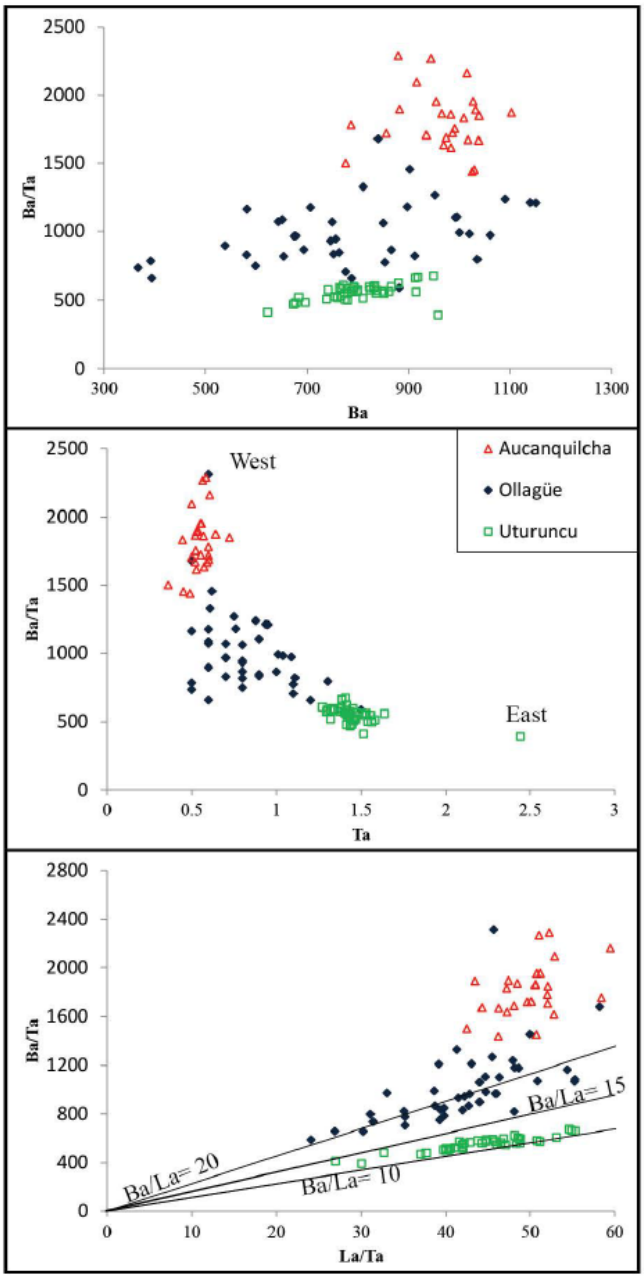

Finally, Dostal *et al.* [99] suggested a more traditional model to explain the across-arc geochemical variations at 21°–22° S latitude. This model is similar in many respects to models often invoked for oceanic island arc settings or arcs constructed over thin continental crust [6,94,118]. Specifically, Dostal *et al.* [99] suggested that the proportion of a LILE-enriched hydrous fluid added to the mantle source region for the volcanic rocks decreases across the strike of the arc. Ultimately, this fluid is derived from the subducting, dehydrating Nazca plate. Concomitant with the across-arc decrease in the proportion of a slab-derived fluid is a decrease in the degree of mantle partial melting. This suggestion stems from the well-documented decrease in mantle solidus temperatures with progressive hydration (e.g., [119–121]). This model is initially attractive because it can account for the strongly west to east decreasing primary magma production rates as reflected in decreasing eruption volumes of the composite cones at 21°–22° S latitude. This, of course, assumes that magma production rates in the mantle and eruption rates at the surface correlate with the degree of mantle partial melting.

The geochemical implications of decreasing west to east fluid fluxing are two-fold. First, because contents of trace elements with low crystal/liquid partition coefficients (e.g., LILE, REE, HFSE) in primary basaltic melts are a strong function of the degree of partial melting of the mantle source, primary melts generated behind the arc-front will have progressively higher contents of incompatible elements, relative to arc-front magmas, because they derive from smaller degrees of partial melting (this accounts for the K-*h* relationship). Second, superposed on these first-order variations will be across-arc variations in the LILE contents of the mantle source due to their selective transport and enrichment in slab-derived hydrous fluids [12,122,123]. The LILE enrichments are highest at the arc-front where the proportion of fluid is greatest and they diminish behind the arc. The net effect of these two processes is to produce primary melts with relatively low incompatible trace element contents but high LILE/HFSE and LILE/REE along the arc-front where the mantle is fluxed by larger amounts of slab-derived fluid and partially melts to a greater extent than behind the arc (e.g., [8]). Further, there may also be additional complexities introduced by inherent across-arc variations in mantle source compositions, particularly radiogenic isotopic ratios, prior to or during slab dehydration- or melt-related metasomatism [124].

Any subcrustal model such as that described above is inherently difficult to test and quantitatively model, given the strongly crustal isotopic compositions of the volcanic rocks at 21°–22° S latitude and lack of knowledge of deep-crustal compositions in the CVZ. Interaction of the silicic magmas with thick continental crust is thus expected to mask most of the influence of the slab dehydration fluids and any pre-metasomatic isotopic variations [118]. Geochemical variations consistent with such a model include lower LILE/HFSE and LILE/REE ratios at a given SiO_2 content toward the east at the three centers (Figure 7). However, in more detail this model cannot account for numerous other features such as lower Na_2O, Ba, and Sr contents (Figures 4 and 5) and higher Sr/Y (where Sr is considered to be more fluid-mobile than Y) and $^{18}O/^{16}O$ ratios (Figure 8) ratios in Uturuncu rocks relative to those erupted on or slightly behind the arc-front. A subcrustal model invoking an across-arc variation in degrees of mantle partial melting also cannot account for relatively high Nb/Zr ratios in Uturuncu rocks relative to those at Aucanquilcha and Ollagüe, as the degrees of incompatibility between Nb and Zr in mantle solid assemblages are very small (D_{Nb} and D_{Zr} are estimated to be 0.04 and 0.08, respectively; [125]). Thus, this ratio is not expected to vary strongly with different degrees of mantle partial melting and is instead controlled by the crustal contaminant. Therefore, although decreasing

degrees of mantle partial melting with increased distance from the arc front are expected to produce geochemical variations in parental magmas at 21°–22° S latitude (*i.e.*, [126]), we consider the across-arc geochemical and isotopic variations documented for silicic rocks in this study to be largely, if not mostly, crustal in origin. We acknowledge, however, that the more "arc-like" nature (e.g., higher LILE/HFSE ratios) of the silicic rocks erupted on or just east of the arc-front may, in fact, partially reflect greater volumetric intrusion of primary mafic magmas with high LILE/HFSE beneath the arc-front relative to the back-arc, lowering the compositional distinctions between primary magmas and the arc-front crust with time.

Wörner *et al.* [22] and Harmon *et al.* [127] observed similar along-strike geochemical trends within the CVZ to the across strike trends. The northern CVZ has been shown to be more radiogenic compared to the south. These authors proposed that this relationship is a function of thicker crust and varying composition of the crust beneath the arc front of the northern CVZ compared to the southern CVZ. Across-arc geochemical variation at 21°–22° S latitude shows a similar relationship to the along-arc variations described by previous authors [22,36,37,96,128] in that variation in the continental crust composition and thickness of the crust is expressed in the volcanic products with increasing distance away from the arc front. Toward the east as the continental crust thickens the volcanic rocks record more radiogenic isotopic signatures inherited from the assimilation of older, less hybridized basement rocks. The source rock composition at the arc-front is less radiogenic as a direct result of intrusion of mafic magmas during the formation of the modern arc-front.

6. Broader Implications

An intriguing result of this study is that on first inspection across-arc geochemical variations at volcanic arcs constructed over thick continental crust, such as increasing K_2O and incompatible trace element contents, resemble those observed at island arcs and arcs constructed over thin continental crust. However, on closer inspection there are significant differences, particularly involving systematic variations in isotopic ratios and other geochemical features that reflect interaction with variable composition continental crust with distance from the arc-front. This contrasts with the results of studies of island arcs where the occurrence of K_2O-rich magmas in back-arc regions is often ascribed to decreasing additions of slab-derived, LILE-rich hydrous fluids to mantle source regions with concomitant decreases in the degree of mantle partial melting and volumetric production of primary mafic magmas. However, we argue based on the geochemical data presented in this paper and geologic relationships [53] that although across-arc geochemical variations at island arcs and arcs constructed over thick continental crust are produced by apparently fundamentally different processes, ultimately they are both related, directly and indirectly, respectively, to mantle processes associated with the subduction process itself. Specifically, at continental volcanic arcs greater time-integrated primary melt production beneath frontal arc regions has the potential to produce younger, more mafic crustal compositions due to repeated intrusion and hybridization by primary mantle-derived melts. Smaller degrees of mantle partial melting and volumetric melt production in back arc regions results in progressively less hybridized or modified continental crust that retains to a larger degree its more silicic, isotopically evolved composition. Production of intermediate to silicic composition magmas in continental arcs with more "arc-like" chemical (e.g., higher LILE/HFSE) and isotopic features (lower

$^{87}Sr/^{86}Sr$) in frontal-arc localities relative to back-arc magmas is therefore ultimately linked to higher degrees of mantle partial melting and melt production, as is inferred for island arcs as well. Thus, although subduction zone magmas may be substantially modified by the continental crust resulting in systematic across-arc geochemical trends, these trends are a manifestation that the continental crust has also been substantially modified by fundamental subduction zone processes similar to those proposed for island arcs. In short, the crust thus modifies the compositions of subduction zone magmas, but complimentary to this, subduction zone magmas modify the composition of the continental crust.

7. Conclusions

In an effort to better understand the origin of systematic across-arc geochemical variations in silicic volcanic rocks (60–68 wt % SiO_2) from the Andean Central Volcanic Zone, we compared geochemical and isotopic compositions of Quaternary (<1.0 Ma) lava flows erupted at three well-characterized composite volcanoes situated along a narrow southeast striking transect between 21° and 22° S. Trends observed include the following. At a given SiO_2 content lavas erupted with increasing distance from the arc-front display systematically higher K_2O, P_2O_5, TiO_2, Rb, Th, Y, REE and HFSE contents; Rb/Sr elemental ratios; and Sr and O isotopic ratios. In contrast, the lavas display systematically lower Al_2O_3, Na_2O, Sr, and Ba contents; Ba/Nb, K/Rb, and Sr/Y elemental ratios; and Nd isotopic ratios. In addition, Eu anomalies become progressively more negative toward the east.

These variations are interpreted to indicate that mid- to deep-crustal source rocks for the lavas become progressively older and more feldspar-rich with increasing distance from the arc front. In this regard, silicic magmas erupted along the arc-front reflect melting of relatively young, mafic composition amphibolitic source rocks with garnet-rich, but feldspar-poor residual mineralogies. Towards the east, the lower crust becomes increasingly older with a more felsic bulk composition in which residual mineralogies are progressively more feldspar-rich. The implication of this interpretation is that large-scale regional trends in magma compositions at continental volcanic arcs may reflect a process wherein the continental crust becomes strongly hybridized beneath frontal arc localities due to protracted intrusion of subduction-derived basaltic magmas, with a diminishing effect behind the arc front because of smaller degrees of mantle partial melting and primary melt generation.

Acknowledgments

The authors wish to thank Frank Ramos for use of and assistance with the thermal ionization mass spectrometer at New Mexico State University; Peter Larson at Washington State University for assistance with the O-isotope analyses; Shan de Silva, Duncan Muir, and all members of the PLUTONS working group for insightful discussions; Jamie Kern for field assistance; and the residents of Quetena Chico, Bolivia, and Lipiko Tours for logistical support and hospitality. We thank three anonymous reviews for detailed comments that substantially improved this manuscript. We also thank David Foster for efficient handling of this paper. This work was supported by U.S. National Science Foundation grant EAR-0901148 to TCF and grants to GSM from the Department of Earth Sciences at Montana State University.

Conflicts of Interest

The authors declare no conflict of interest.

References

1. Dickinson, W.R.; Hatherton, T. Andesitic volcanism and seismicity around pacific. *Science* **1967**, *157*, 801–803.
2. Gill, J.B. *Orogenic Andesites and Plate Tectonics*; Springer-Verlag: Berlin, Germany, 1981.
3. Jakes, P.; White, A.J.R. Major and trace-element abundances in volcanic-rocks of orogenic areas. *Geol. Soc. Am. Bull.* **1972**, *83*, 29–40.
4. Tatsumi, Y.; Eggins, S. *Subduction Zone Magmatism*; Blackwell Science: Oxford, UK, 1995.
5. Dickinson, W.R. Potash-depth (K-*h*) relations in continental-margin and intra-oceanic magmatic arcs. *Geology* **1975**, *3*, 53–56.
6. Churikova, T.; Dorendorf, F.; Worner, G. Sources and fluids in the mantle wedge below Kamchatka, evidence from across-arc geochemical variation. *J. Petrol.* **2001**, *42*, 1567–1593.
7. Feeley, T.C. Origin and tectonic implications of across-strike geochemical variations in the Eocene Absaroka volcanic province, United States. *J. Geol.* **2003**, *111*, 329–346.
8. Hickey-Vargas, R.; Roa, H.M.; Escobar, L.L.; Frey, F.A. Geochemical variations in Andean basaltic and silicic lavas from the Villarrica-Lanin volcanic chain (39.5° S): An evaluation of source heterogeneity, fractional crystallization and crustal assimilation. *Contrib. Mineral. Petrol.* **1989**, *103*, 361–386.
9. Leeman, W.P.; Smith, D.R.; Hildreth, W.; Palacz, Z.; Rogers, N. Compositional diversity of Late Cenozoic basalts in a transect across the southern Washington Cascades: Implications for subduction zone magmatism. *J. Geophys. Res. Solid* **1990**, *95*, 19561–19582.
10. Patino, L.C.; Carr, M.J.; Feigenson, M.D. Cross-arc geochemical variations in volcanic fields in Honduras CA: Progressive changes in source with distance from the volcanic front. *Contrib. Mineral. Petrol.* **1997**, *129*, 341–351.
11. Ryan, J.G.; Morris, J.; Tera, F.; Leeman, W.P.; Tsvetkov, A. Cross-arc geochemical variations in the Kurile Arc as a function of slab depth. *Science* **1995**, *270*, 625–627.
12. Stolper, E.; Newman, S. The role of water in the petrogenesis of Mariana Trough magmas. *Earth Planet. Sci. Lett.* **1994**, *121*, 293–325.
13. Walker, J.A.; Carr, M.J.; Patino, L.C.; Johnson, C.M.; Feigenson, M.D.; Ward, R.L. Abrupt change in magma generation processes across the Central-American arc in southeastern Guatemala: Flux dominated melting near the base of the wedge to decompression melting near the top of the wedge. *Contrib. Mineral. Petrol.* **1995**, *120*, 378–390.
14. Coira, B.; Kay, S.M. Implications of Quaternary volcanism at Cerro Tuzgle for crustal and mantle evolution of the Puna Plateau, Central Andes, Argentina. *Contrib. Mineral. Petrol.* **1993**, *113*, 40–58.
15. Caffe, P.J.; Trumbull, R.B.; Coira, B.L.; Romer, R.L. Petrogenesis of Early Neogene magmatism in the northern Puna; Implications for magma genesis and crustal processes in the Central Andean Plateau. *J. Petrol.* **2002**, *43*, 907–942.

16. Kay, S.M.; Mpodzis, C.; Coria, B. Neogene Magmatism, Tectonism, and Mineral Deposits of the Central Andes (22° to 33° S Latitude). In *Geology and Ore Deposits of the Central Andes*; Skinner, B.J., Ed.; Society of Economic Geologists: Littleton, CO, USA, 1999; pp. 27–59.
17. Kay, S.M.; Coira, B.L.; Caffe, P.J.; Chen, C.H. Regional chemical diversity, crustal and mantle sources and evolution of Central Andean Puna Plateau ignimbrites. *J. Volcanol. Geotherm. Res.* **2010**, *198*, 81–111.
18. Schnurr, W.B.W.; Trumbull, R.B.; Clavero, J.; Hahne, K.; Siebel, W.; Gardeweg, M. Twenty-five million years of silicic volcanism in the southern Central Volcanic Zone of the Andes: Geochemistry and magma genesis of ignimbrites from 25° to 27° S, 67° to 72° W. *J. Volcanol. Geotherm. Res.* **2007**, *166*, 17–46.
19. Trumbull, R.D.; Wittenbrink, R.; Hahne, K.; Emmermann, R.; Busch, W.; Gerstenberger, H.; Siebel, W. Evidence for Late Miocene to recent contamination of arc andesites by crustal melts in the Chilean Andes (25–26° S) and its geodynamic implications. *J. S. Am. Earth Sci.* **1999**, *12*, 135–155.
20. Hildreth, W.; Moorbath, S. Crustal contributions to arc magmatism in the Andes of central Chile. *Contrib. Mineral. Petrol.* **1988**, *98*, 455–489.
21. Plank, T.; Langmuir, C.H. An evaluation of the global variations in the major element chemistry of arc basalts. *Earth Planet. Sci. Lett.* **1988**, *90*, 349–370.
22. Worner, G.; Moorbath, S.; Harmon, R.S. Andean Cenozoic volcanic centers reflect basement isotopic domains. *Geology* **1992**, *20*, 1103–1106.
23. Feeley, T.C. Volcan Ollagüe: Volcanology, Petrology and Geochemistry of a Major Quaternary Stratovolcano in the Andean Central Volcanic Zone. Ph.D. Thesis, University of California, Los Angeles, CA, USA, June 1993.
24. Feeley, T.C.; Clynne, M.A.; Winer, G.S.; Grice, W.C. Oxygen isotope geochemistry of the Lassen Volcanic Center, California: Resolving crustal and mantle contributions to continental arc magmatism. *J. Petrol.* **2008**, *49*, 971–997.
25. Feeley, T.C.; Davidson, J.P. Petrology of calc-alkaline lavas at Volcan Ollagüe and the origin of compositional diversity at Central Andean stratovolcanoes. *J. Petrol.* **1994**, *35*, 1295–1340.
26. Feeley, T.C.; Sharp, Z.D. $^{18}O/^{16}O$ isotope geochemistry of silicic lava flows erupted from Volcan Ollagüe, Andean Central Volcanic Zone. *Earth Planet. Sci. Lett.* **1995**, *133*, 239–254.
27. Grunder, A.L.; Klemetti, E.W.; Feeley, T.C.; McKee, C.M. Eleven million years of arc volcanism at the Aucanquilcha volcanic cluster, northern Chilean Andes: Implications for the life span and emplacement of plutons. *Trans. Roy. Soc. Ed. Earth* **2006**, *97*, 415–436.
28. Allmendinger, R.W.; Jordan, T.E.; Kay, S.M.; Isacks, B.L. The evolution of the Altiplano-Puna Plateau of the Central Andes. *Annu. Rev. Earth Planet. Sci.* **1997**, *25*, 139–174.
29. Beck, S.L.; Zandt, G.; Myers, S.C.; Wallace, T.C.; Silver, P.G.; Drake, L. Crustal-thickness variations in the Central Andes. *Geology* **1996**, *24*, 407–410.
30. James, D.E. Plate Tectonic model for evolution of Central Andes. *Geol. Soc. Am. Bull.* **1971**, *82*, 3325–3346.
31. Schmitz, M.; Heinsohn, W.D.; Schilling, F.R. Seismic, gravity and petrological evidence for partial melt beneath the thickened Central Andean crust (21–23° S). *Tectonophysics* **1997**, *270*, 313–326.

32. Beck, S.L.; Zandt, G. The nature of orogenic crust in the Central Andes. *J. Geophys. Res. Solid Earth* **2002**, *107*, doi:10.1029/2000JB000124.
33. McGlashan, N.; Brown, L.; Kay, S.M. Crustal thickness in the Central Andes from teleseismically recorded depth phase precursors. *Geophys. J. Int.* **2008**, *175*, 1013–1022.
34. Yuan, X.; Sobolev, S.V.; Kind, R.; Oncken, O.; Bock, G.; Asch, G.; Schurr, B.; Graeber, F.; Rudloff, A.; Hanka, W.; *et al*. Subduction and collision processes in the Central Andes constrained by converted seismic phases. *Nature* **2000**, *408*, 958–961.
35. Yuan, X.; Sobolev, S.V.; Kind, R. Moho Topography in the Central Andes and its geodynamic implications. *Earth Planet. Sci. Lett.* **2002**, *199*, 389–402.
36. Mamani, M.; Tassara, A.; Woerner, G. Composition and structural control of crustal domains in the Central Andes. *Geochem. Geophys. Geosyst.* **2008**, *9*, doi:10.1029/2007GC001925.
37. Mamani, M.; Worner, G.; Sempere, T. Geochemical variations in igneous rocks of the Central Andean orocline (13° S to 18° S): Tracing crustal thickening and magma generation through time and space. *Geol. Soc. Am. Bull.* **2010**, *122*, 162–182.
38. Avila-Salinas, W. Petrological and Tectonic Evolution of Cenozoic Volcanism in the Bolivian Western Andes. In *Andean Magmatism and Its Tectonic Setting*; Geological Society of America Special Paper; Harmon, R.S., Rapela, C.W., Eds.; Geological Society of America: Boulder, CO, USA, 1991; Volume 265, pp. 245–258.
39. Deruelle, B. Calc-alkaline and shoshonitic lavas from 5 Andean volcanos (between latitudes 21°45' S and 24°30' S) and distribution of Plio-Quaternary volcanism of south-Central and Southern Andes. *J. Volcanol. Geotherm. Res.* **1978**, *3*, 281–298.
40. Du Bray, E.A.; Ludington, S.; Brooks, W.E.; Gamble, B.M.; Ratte, J.C.; Richter, D.H.; Soria-Escalante, E. *Compositional Characteristics of Middle to Upper Tertiary Volcanic Rocks of the Bolivian Altiplano*; U.S. Geological Survey: Reston, VA, USA, 1995.
41. Feeley, T.C. Crustal modification during subduction-zone magmatism: Evidence from the southern Salar De Uyuni region (20°–22° S), Central Andes. *Geology* **1993**, *21*, 1019–1022.
42. Fernandez, C.; Horman, P.K.; Kussmaul, S.; Meave, J.; Pichler, H.; Subieta, T. First petrologic data on young volcanic rocks of SW-Bolivia. *Tsch. Mineral. Petrogr. Mitt.* **1973**, *19*, 149–172.
43. Klerkx, J.; Deutsch, S.; Pichler, H.; Zeil, W. Strontium isotopic composition and trace-element data bearing on origin of Cenozoic volcanic-rocks of Central and Southern Andes. *J. Volcanol. Geotherm. Res.* **1977**, *2*, 49–71.
44. Kussmaul, S.; Hormann, P.K.; Ploskonka, E.; Subieta, T. Volcanism and structure of southwestern Bolivia. *J. Volcanol. Geotherm. Res.* **1977**, *2*, 73–111.
45. Thorpe, R.S.; Francis, P.W. Variations in Andean andesite compositions and their petrogenetic significance. *Tectonophysics* **1979**, *57*, 53–70.
46. Lamb, S.H.; Hoke, L.; Kennan, L.; Dewey, J. Cenozoic Evolution of the Central Andes in Bolivia and Northern Chile. In *Orogeny Through Time*; Geological Society Special Publication No. 121; Burg, J.P., Ford, M., Eds.; The Geologic Society: London, UK, 1997; pp. 237–264.
47. Feeley, T.C.; Hacker, M.D. Intracrustal derivation of Na-rich andesitic and dacitic magmas: An example from Volcan Ollagüe, Andean Central Volcanic Zone. *J. Geol.* **1995**, *103*, 213–225.

48. Sparks, R.S.J.; Folkes, C.B.; Humphreys, M.C.S.; Barfod, D.N.; Clavero, J.; Sunagua, M.C.; McNutt, S.R.; Pritchard, M.E. Uturuncu Volcano, Bolivia: Volcanic unrest due to mid-crustal magma intrusion. *Am. J. Sci.* **2008**, *308*, 727–769.
49. De Silva, S.L.; Francis, P.W. *Volcanoes of the Central Andes*; Springer-Verlag: New York, NY, USA, 1991.
50. Zandt, G.; Leidig, M.; Chmielowski, J.; Baumont, D.; Yuan, X.H. Seismic detection and characterization of the Altiplano-Puna Magma Body, Central Andes. *Pure Appl. Geophys.* **2003**, *160*, 789–807.
51. De Silva, S.L.; Zandt, G.; Trumbull, R.; Viramonte, J.; Salas, G.; Jiminez, N. Large Ignimbrite Eruptions and Volcano-Tectonic Depressionsin the Central Andes: A Thermomechanical Perspective. In *Mechanisms of Activity and Unrest at Large Calderas*; Geological Society Special Publication No. 269; Troise, C., De Natale, G., Kilburn, C.R.J., Eds.; The Geologic Society: London, UK, 2006; pp. 47–63.
52. De Silva, S.L. Altiplano-Puna Volcanic Complex of the Central Andes. *Geology* **1989**, *17*, 1102–1106.
53. Baker, M.C.W.; Francis, P.W. Upper Cenozoic volcanism in Central Andes—Ages and volumes. *Earth Planet. Sci. Lett.* **1978**, *41*, 175–187.
54. Gradstein, F.M.; Ogg, J.G.; Smith, A.G. *A Geologic Time Scale 2004*; Cambridge University Press: Cambridge, UK, 2004.
55. Somoza, R.; Ghidella, M.E. Convergencia en el margen occidental de América del Sur durante el Cenozoico: Subducción de las Placas de Nazca, Farallon y Phoenix. *Rev. Assoc. Geol. Argent.* **2005**, *60*, 797–809, (in Spanish).
56. Somoza, R.; Ghidella, M.E. Late Cretaceous to recent plate motioins in western South America revisited. *Earth Planet. Sci. Lett.* **2012**, *331–332*, 152–163.
57. Gregory-Wodzicki, K.M. Uplift history of the Central and Northern Andes: A review. *Bull. Geol. Soc. Am.* **2000**, *112*, 1091–1105.
58. Isacks, B.L. Uplift of the Central Andean Plateau and bending of the Bolivian orocline. *J. Geophys. Res. Solid* **1988**, *93*, 3211–3231.
59. Kay, S.M.; Coira, B.L.; Kay, R.W. Central Andean Galan Ignimbrites: Magma evolution from the mantle to eruption in a thickened crust. *Geochim. Cosmochim. Acta* **2009**, *73*, A630.
60. Klemetti, E.W.; Grunder, A.L. Volcanic evolution of Volcan Aucanquilcha: A long-lived dacite volcano in the Central Andes of northern Chile. *Bull. Volcanol.* **2008**, *70*, 633–650.
61. Klemetti, E.W. Constraining the Magmatic Evolution of the Andean Arc at 21° S Using the Volcanic and Petrologic History of Volcán Aucanquilcha, Central Volcanic Zone, Northern Chile. Ph.D. Thesis, Oregon State University, Corvalis, OR, USA, February 2005.
62. Simkin, T.; Siebert, S.L. *Volcanoes of the World: a Regional Directory, Gazetteer, and Chronology of Volcanism During the Last 10,000 Years*; Geosciences Press: Tucson, AZ, USA, 1994.
63. Feeley, T.C.; Davidson, J.P.; Armendia, A. The volcanic and magmatic evolution of Volcan Ollagüe, a high-K, Late Quaternary stratovolcano in the Andean Central Volcanic Zone. *J. Volcanol. Geotherm. Res.* **1993**, *54*, 221–245.

64. Worner, G.; Lezaun, J.; Beck, A.; Heber, V.; Lucassen, F.; Zinngrebe, E.; Rossling, R.; Wilke, H.G. Precambrian and Early Paleozoic evolution of the Andean basement at Belen (northern Chile) and Cerro Uyarani (western Bolivia Altiplano). *J. S. Am. Earth Sci.* **2000**, *13*, 717–737.
65. Clavero, J.; Polanco, E.; Godoy, E.; Aguilar, G.; Sparks, R.S.J.; van Wykde Vries, B.; Pérez de Arce, C.; Matthews, S. Substrata influence in the transport and emplacement mechanism of the Ollagüe debris avalanche (northern Chile). *Acta Vulcanol.* **2004**, *16*, 59–76.
66. Vezzoli, L.; Tibaldi, A.; Renzulli, A.; Menna, M.; Flude, S. Faulting-assisted lateral collapses and influence on shallow magma feeding systems at Ollagüe volcano (Central Volcanic Zone, Chile-Bolivia Andes). *J. Volcanol. Geotherm. Res.* **2008**, *171*, 137–159.
67. Johnson, D.M.; Hooper, P.R.; Conrey, R.M. XRF Analysis of rocks and minerals for major and trace elements on a single low dilution Li-tetraborate fused bead. *Adv. X-Ray Anal.* **1999**, *41*, 843–867.
68. Jarvis, K.E. Inductively coupled plasma mass-spectrometry: A new technique for the rapid or ultra-trace level determination of the rare-earth elements in geological-materials. *Chem. Geol.* **1988**, *68*, 31–39.
69. Ramos, F.C.; Reid, M.R. Distinguishing melting of heterogeneous mantle sources from crustal contamination: Insights from Sr isotopes at the phenocryst scale, Pisgah Crater, California. *J. Petrol.* **2005**, *46*, 999–1012.
70. Todt, W.; Cliff, R.A.; Hanser, A.; Hofmann, A.W. Evaluation of a ^{202}Pb-^{205}Pb Double Spike for High-Precision Lead Isotope Analysis. In *Earth Processes: Reading the Isotope Code*; Hart, S.R., Basu, A., Eds.; American Geophysical Union: Washington, DC, USA, 1996; Volume 95, pp. 429–437.
71. Takeuchi, A.; Larson, P.B. Oxygen isotope evidence for the Late Cenozoic development of an orographic rain shadow in eastern Washington, USA. *Geology* **2005**, *33*, 313–316.
72. Valley, J.W.; Kitchen, N.; Kohn, M.J.; Niendorf, C.R.; Spicuzza, M.J. UWG-2, A garnet standard for oxygen isotope ratios: Strategies for high precision and accuracy with laser heating. *Geochim. Cosmochim. Acta* **1995**, *59*, 5223–5231.
73. Michelfelder, G.S.; Feeley, T.C.; Wilder, A.D.; Thacker, J. Mixing Following Assimilation-Fractional Crystallization at Cerro Uturuncu, Andean Central Volcanic Zone, SW Bolivia as Revealed from *in Situ* Laser Ablation Isotopic Analysis of Plagioclase. In Proceedings of International Association of Volcanology and Chemistry of the Earth's Interior (IAVCEI) 2013 Scientific Assembly, Kagoshima, Japan, 20–24 July 2013; pp. 1847–1841.
74. Muir, D.D.; Blundy, J.; Hutchinson, M.C.; Rust, A.C. Petrological imaging of an active pluton beneath Cerro Uturuncu, Bolivia. *Contrib. Mineral. Petrol.* **2013**, submitted for publication.
75. Fialko, Y.; Pearse, J. Sombrero uplift above the Altiplano-Puna Magma Body: Evidence of a ballooning mid-crustal diapir. *Science* **2012**, *338*, 250–252.
76. Henderson, S.T.; Pritchard, M.E. Decadal volcanic deformation in the Central Andes Volcanic Zone revealed by InSAR time series. *Geochem. Geophys. Geosyst.* **2013**, *14*, 1358–1374.

77. Jay, J.A.; Pritchard, M.E.; West, M.E.; Christensen, D.; Haney, M.; Minaya, E.; Sunagua, M.; McNutt, S.R.; Zabala, M. Shallow seismicity, triggered seismicity, and ambient noise tomography at the long-dormant Uturuncu Volcano, Bolivia. *Bull. Volcanol.* **2012**, *74*, 817–837.
78. Walker, B.A., Jr.; Klemetti, E.W.; Grunder, A.L.; Dilles, J.H.; Tepley, F.J.; Gile, D. Crystal reaming during the assembly, maturation, and waning of an eleven-million-year crustal magma cycle: Thermobarometry of the Aucanquilcha Volcanic Cluster. *Contrib. Mineral. Petrol.* **2013**, *165*, 663–682.
79. Mattioli, M.; Renzulli, A.; Menna, M.; Holm, P.M. Rapid ascent and contamination of magmas through the thick crust of the CVZ (Andes, Ollague region): Evidence from a nearly aphyric high-K andesite with skeletal olivines. *J. Volcanol. Geotherm. Res.* **2006**, *158*, 87–105.
80. Le Maitre, R.W. *Igneous Rocks, A Classification and Glossary of Terms*; Cambridge University Press: Cambridge, UK, 2002.
81. Sun, S.S.; McDonough, W.F. Chemical and isotopic systematics of oceanic basalts: Implications for mantle compositions and processes. *Geol. Soc. Lond. Spec. Publ.* **1989**, *42*, 313–345.
82. Hickey, R.L.; Frey, F.A.; Gerlach, D.C.; Lopez-Escobar, L. Multiple sources for basaltic arc rocks from the Southern Volcanic Zone of the Andes (34°–41° S): Trace element and isotopic evidence for contributions from subducted oceanic crust, mantle, and continental crust. *J. Geophys. Res. Solid Earth* **1986**, *91*, 5963–5983.
83. Rollinson, H.R. *Using Geochemical Data: Evaluation, Presentation, Interpretation*; John Wiley and Sons: New York, NY, USA, 1993.
84. Bindeman, I.N.; Eiler, J.M.; Yogodzinski, G.M.; Tatsumi, Y.; Stern, C.R.; Grove, T.L.; Portnyagin, M.; Hoernle, K.; Danyushevsky, L.V. Oxygen isotope evidence for slab melting in modern and ancient subduction zones. *Earth Planet. Sci. Lett.* **2005**, *235*, 480–496.
85. Bindeman, I.N.; Ponomareva, V.V.; Bailey, J.C.; Valley, J.W. Volcanic arc of Kamchatka: A province with high-$\delta^{18}O$ magma sources and large-scale $^{18}O/^{16}O$ depletion of the upper crust. *Geochim. Cosmochim. Acta* **2004**, *68*, 841–865.
86. Valley, J.W. Stable isotope thermometry at high temperatures. *Rev. Mineral. Geochem.* **2001**, *43*, 365–413.
87. Aitcheson, S.J.; Harmon, R.S.; Moorbath, S.; Schneider, A.; Soler, P.; Soriaescalante, E.; Steele, G.; Swainbank, I.; Worner, G. Pb isotopes define basement domains of the Altiplano, Central Andes. *Geology* **1995**, *23*, 555–558.
88. Elburg, M.A.; van Bergen, M.; Hoogewerff, J.; Foden, J.; Vroon, P.; Zulkarnain, I.; Nasution, A. Geochemical trends across an arc-continent collision zone: Magma sources and slab-wedge transfer processes below the Pantar Strait Volcanoes, Indonesia. *Geochim. Cosmochim. Acta* **2002**, *66*, 2771–2789.
89. Dreher, S.T.; Macpherson, C.G.; Pearson, D.G.; Davidson, J.P. Re-Os isotope studies of Mindanao Adakites: Implications for sources of metals and melts. *Geology* **2005**, *33*, 957–960.
90. Ayers, J. Trace element modeling of aqueous fluid—Peridotite interaction in the mantle wedge of subduction zones. *Contrib. Mineral. Petrol.* **1998**, *132*, 390–404.
91. Brenan, J.M.; Shaw, H.F.; Ryerson, F.J.; Phinney, D.L. Mineral-aqueous fluid partitioning of trace-elements at 900 °C and 2.0 GPa—Constraints on the trace-element chemistry of mantle and deep-crustal fluids. *Geochim. Cosmochim. Acta* **1995**, *59*, 3331–3350.

92. Schmidt, M.W.; Poli, S. Experimentally based water budgets of dehydrating slabs and consequencesfor arc magma generation. *Earth Planet. Sci. Lett.* **1998**, *163*, 361–379.
93. Danyushevsky, L.V.; Falloon, T.J.; Sobolev, A.V.; Crawford, A.J.; Carroll, M.; Price, R.C. The H_2O content of basalt glasses from southwest Pacific back-arc basins. *Earth Planet. Sci. Lett.* **1993**, *117*, 347–362.
94. Newman, S.; Stolper, E.; Stern, R. H_2O and CO_2 in magmas from the Mariana arc and back arc systems. *Geochem. Geophys. Geosyst.* **2000**, *1*, doi:10.1029/1999GC000027.
95. Shibata, T.; Nakamura, E. Across-arc variations of isotope and trace element compositions from Quaternary basaltic volcanic rocks in northeastern Japan: Implications for interaction between subducted oceanic slab and mantle wedge. *J. Geophys. Res. Solid Earth* **1997**, *102*, 8051–8064.
96. Davidson, J.P.; Hannon, R.S.; Womer, G. The Source of Central Andean Magmas: Some Considerations. In *Andean Magmatism and Its Tectonic Setting*; Hannon, R.S., Rapela, C.W., Eds.; Geological Society of America: Denver, CO, USA, 1991; pp. 825–843.
97. Hawkesworth, C.J.; Clarke, C.B. Partial Melting in the Lower Crust: New Constraints on Crustal Contamination Processes in the Central Andes. In *Tectonics of the Southern Central Andes*; Reutter, K.J., Scheurber, E., Wigger, P.J., Eds.; Springer-Verlag: New York, NY, USA, 1994; pp. 93–101.
98. Sen, C. Subduction Related Petrologic Processes: 1—Dehydration Melting of a Basaltic Composition Amphibolites. 2—Mantle Metasomatism. Ph.D. Thesis, University of New Brunswick, New Brunswick, Canada, February 1994.
99. Dostal, J.; Zentilli, M.; Caelles, J.C.; Clark, A.H. Geochemistry and origin of volcanic-rocks of Andes (26°–28° S). *Contrib. Mineral. Petrol.* **1977**, *63*, 113–128.
100. Lucassen, F.; Becchio, R.; Wilke, H.G.; Franz, G.; Thirlwall, M.F.; Viramonte, J.; Wemmer, K. Proterozoic-Paleozoic development of the basement of the Central Andes (18–26° S)—A mobile belt of the South American craton. *J. S. Am. Earth Sci.* **2000**, *13*, 697–715.
101. Lucassen, F.; Franz, G.; Laber, A. Permian high pressure rocks—The basement of the Sierra de Limon Verde in northern Chile. *J. S. Am. Earth Sci.* **1999**, *12*, 183–199.
102. Lucassen, F.; Kramer, W.; Bartsch, V.; Wilke, H.G.; Franz, G.; Romer, R.L.; Dulski, P. Nd, Pb, and Sr isotope composition of juvenile magmatism in the Mesozoic large magmatic province of northern Chile (18°–27° S): Indications for a uniform subarc mantle. *Contrib. Mineral. Petrol.* **2006**, *152*, 571–589.
103. Lucassen, F.; Lewerenz, S.; Franz, G.; Viramonte, J.; Mezger, K. Metamorphism, isotopic ages and composition of lower crustal granulite xenoliths from the Cretaceous Salta Rift, Argentina. *Contrib. Mineral. Petrol.* **1999**, *134*, 325–341.
104. Perez, W.A.; Kawashita, K. K-Ar and Rb-Sr geochronology of igneous rocks from the Sierra de Paiman, northwestern Argentina. *J. S. Am. Earth Sci.* **1992**, *5*, 251–264.
105. Lucassen, F.; Becchio, R.; Harmon, R.; Kasemann, S.; Franz, G.; Trumbull, R.; Wilke, H.G.; Romer, R.L.; Dulski, P. Composition and density model of the continental crust at an active continental margin—The Central Andes between 21° and 27° S. *Tectonophysics* **2001**, *341*, 195–223.
106. Lucassen, F.; Franz, G.; Thirlwall, M.F.; Mezger, K. Crustal recycling of metamorphic basement: Late Palaeozoic granitoids of northern Chile (similar to 22° S). Implications for the composition of the Andean crust. *J. Petrol.* **1999**, *40*, 1527–1551.

107. Lucassen, F.; Harmon, R.; Franz, G.; Romer, R.L.; Becchio, R.; Siebel, W. Lead evolution of the pre-Mesozoic crust in the Central Andes (18–27° S): Progressive homogenisation of Pb. *Chem. Geol.* **2002**, *186*, 183–197.
108. Lucassen, F.; Escayola, M.; Romer, R.L.; Viramonte, J.; Koch, K.; Franz, G. Isotopic composition of late Mesozoic basic and ultrabasic rocks from the Andes (23–32° S)—Implications for the Andean mantle. *Contrib. Mineral. Petrol.* **2002**, *143*, 336–349.
109. Lucassen, F.; Franz, G.; Romer, R.L.; Schultz, F.; Dulski, P.; Wemmer, K. Pre-Cenozoic intra-plate magmatism along the Central Andes (17–34° S): Composition of the mantle at an active margin. *Lithos* **2007**, *99*, 312–338.
110. Lucassen, F.; Franz, G.; Viramonte, J.; Romer, R.L.; Dulski, P.; Lang, A. The Late Cretaceous lithospheric mantle beneath the Central Andes: Evidence from phase equilibria and composition of mantle xenoliths. *Lithos* **2005**, *82*, 379–406.
111. Huang, W.L.; Wyllie, P.J. Phase-relationships of gabbro-tonalite-granite-water at 15-kbar with applications to differentiation and anatexis. *Am. Mineral.* **1986**, *71*, 301–316.
112. Litvinovsky, B.A.; Steele, I.M.; Wickham, S.M. Silicic magma formation in overthickened crust: Melting of charnockite and leucogranite at 15, 20 and 25 kbar. *J. Petrol.* **2000**, *41*, 717–737.
113. Ort, M.H.; Coira, B.L.; Mazzoni, M.M. Generation of a crust-mantle magma mixture: Magma sources and contamination at Cerro Panizos, Central Andes. *Contrib. Mineral. Petrol.* **1996**, *123*, 308–322.
114. Soler, M.M.; Caffe, P.J.; Coira, B.L.; Onoe, A.T.; Kay, S.M. Geology of the Vilama caldera: A new interpretation of a large-scale explosive event in the Central Andean plateau during the Upper Miocene. *J. Volcanol. Geotherm. Res.* **2007**, *164*, 27–53.
115. Morgan, G.B.; London, D.; Luedke, R.G. Petrochemistry of Late Miocene peraluminous silicic volcanic rocks from the Morococala field, Bolivia. *J. Petrol.* **1998**, *39*, 601–632.
116. Davidson, J.; Turner, S.; Handley, H.; Macpherson, C.; Dosseto, A. Amphibole "sponge" in arc crust? *Geology* **2007**, *35*, 787–790.
117. Davidson, J.; Turner, S.; Plank, T. Dy/Dy*: variations arising from mantle sources and petrogenetic processes. *J. Petrol.* **2013**, *54*, 525–537.
118. Defant, M.J.; Drummond, M.S. Derivation of some modern arc magmas by melting of young subducted lithosphere. *Nature* **1990**, *347*, 662–665.
119. Melzer, S.; Wunder, B. Island-arc basalt alkali ratios: Constraints from phengite-fluid partitioning experiments. *Geology* **2000**, *28*, 583–586.
120. Kushiro, I.; Nakamura, Y.; Haramura, H.; Akimoto, S.I. Crystallization of some lunar mafic magmas and generation of rhyolitic liquid. *Science* **1970**, *167*, 610–612.
121. Kushiro, I.; Syono, Y.; Akimoto, S.I. Melting of a peridotite nodule at high pressures and high water pressures. *J. Geophys. Res.* **1968**, *73*, 6023–6029.
122. Kushiro, I.; Yoder, H.S.; Nishikaw, M. Effect of water on melting of enstatite. *Geol. Soc. Am. Bull.* **1968**, *79*, 1685–1692.
123. Tatsumi, Y.; Hamilton, D.L.; Nesbitt, R.W. Chemical characteristics of fluid phase released from a subducted lithosphere and origin of arc magmas: Evidence from high-pressure experiments and natural rocks. *J. Volcanol. Geotherm. Res.* **1986**, *29*, 293–309.

124. Mcculloch, M.T.; Gamble, J.A. Geochemical and geodynamical constraints on subduction zone magmatism. *Earth Planet. Sci. Lett.* **1991**, *102*, 358–374.
125. Heydolph, K.; Hoernle, K.; Hauff, F.; van den Bogaard, P.; Portnyagin, M.; Bindeman, I.; Garbe-Schonberg, D. Along and across arc geochemical variations in NW Central America: Evidence for involvement of lithospheric pyroxenite. *Geochim. Cosmochim. Acta* **2012**, *84*, 459–491.
126. Hofmann, A.W. Chemical Differentiation of the Earth: The relationship between mantle, continental crust, and oceanic crust. *Earth Planet. Sci. Lett.* **1988**, *90*, 297–314.
127. Harmon, R.S.; Barreiro, B.A.; Moorbath, S.; Hoefs, J.; Francis, P.W.; Thorpe, R.S.; Deruelle, B.; Mchugh, J.; Viglino, J.A. Regional O-isotope, Sr-isotope, and Pb-isotope relationships in Late Cenozoic calc-alkaline lavas of the Andean Cordillera. *J. Geol. Soc. Lond.* **1984**, *141*, 803–822.
128. Davidson, J.P.; de Silva, S.L. Volcanic-rocks from the Bolivian Altiplano: insights into crustal structure, contamination, and magma genesis: Comment and reply. *Geology* **1992**, *21*, 1147–1149.

CHAPTER SEVEN

CONCLUSIONS

The manuscripts presented here examine the petrogenic processes and magmatic evolution of Cerro Uturuncu and the connection of the volcanic center to the central Andes. This project sought to answer three primary questions about the evolution of Cerro Uturuncu and the centers role in the CVZ. First, how did the magma chamber evolve over time and what processes affected magma composition during the magmatic evolution of the system? Second, what extent does Uturuncu represents a manifestation of Altiplano-Puna Volcanic Complex (APVC) magmatism and is large-scale hybridization of the continental crust by intrusion beneath long-lived volcanic centers a continental dynamic phenomenon of general importance? Finally, how does this volcanic center relate to the big picture of magmatism in the CVZ?

This work shows that over the 800,000 year lifespan of Uturuncu bulk-rock magma chemistry is highly restricted, and eruptions from the center occurred roughly every 6000 to 8000 years. Linear trends in bulk-rock chemistry suggest that magma mixing played a major role in the evolution of the bulk-rock major- and trace-element and isotopic trend, but the crystal cargo, specifically plagioclase, provides more information about magmatic processes that occurred prior to the final mixing event.

The chapters presented in this dissertation provides and important perspective on the evolution of a continental back-arc volcanic system, and provides the first application of micro-analytical isotopic techniques to a CVZ system that has been significantly

modified by the continental crust. The work also provides a first attempt in applying these micro-analytical techniques to the entirety of a complex continental back-arc system. While a quantitative model of the evolution of the system was not able to be presented, the work does provide more detailed information about processes occurring prior to the final mixing event producing a variety of textures and compositions in the plagioclase crystal cargo of an individual eruptive unit and a across the evolution of the system. The significant conclusions of this work about this work are as follows:

1. Cerro Uturuncu erupted uniform, crystal-rich orthopyroxene, biotite dacite and andesite lavas for ~800,000 years. Field relationships between the lava flows and domes suggest eruptions are effusive with an average repose interval between 6000 and 8000 years. Sparks et al. (2008) identified 50 lava flows; we have identified an additional 45 lava flows and 10 domes with the total number of erupted units to 105. Erupted volumes ranged between 0.1 km^3 and ~10 km^3 per eruption with a total volume erupted of ~89 km^3. Construction of the edifice took place in one stage in the volcanic history.
2. Typical phenocryst assemblage is plagioclase > OPX > biotite >> Fe-Ti oxides and quartz. Micro-inclusions and glomerocrysts contain trace olivine. Lava flows and domes were erupted with a limited compositional range (61 wt% -67 wt% SiO_2) of magma for ~800,000 years. Xenocrysts/antecrysts of olivine and quartz in both the magmatic inclusion and the lava flows and domes, and the presence of quartz-rich xenoliths suggest crustal contamination is an important process in magma genesis. Lavas and domes at Uturuncu show abundant evidence for

thermal and chemical disequilibrium through the presence of sieved and zoned phenocryst phases and magmatic inclusions.

3. Magma mixing controlled the limited compositional range observed in Uturuncu volcanic rocks. It is possible to explain the geochemical trends of the andesite and dacite volcanic rocks by differentiation in old, Sr radiogenic, Nd non-radiogenic felsic basement rock. The variation in isotopic composition suggests large amounts of assimilation fractional crystallization during differentiation.
4. Plagioclase phenocrysts from Uturuncu lavas and domes show large- magnitude changes in An content, textural discontinuities, and variation of isotopic ratios from core to rim. The observed variation result from open-system processes that occur during residence in or transport through continental crust and could not have existed at magmatic temperatures for more than a few thousand years. It is likely that different compositions of phenocrysts derived from different locations in the magmatic system and mixed just prior to eruption. Cerro Uturuncu magmas initially assimilated country rock with a higher $^{87}Sr/^{86}Sr$ ratio than the magmas and the magmas evolved subsequently through frequent recharge events of magma with a lower $^{87}Sr/^{86}Sr$ ratio. A typical Uturuncu andesitic or dacitic magma (melt plus crystals) therefore only attain its final geochemical identity just before and during eruption. Though currently, Sr isotopic plagioclase isotopic data for the central Andean crustal basement and APVC ignimbrites is not available, it is clear that shallow-level mixing is an important process producing

differentiated magmas. This process was only interrupted by the process of quenching because of eruption.

5. In the regional context of the CVZ, Cerro Uturuncu contains systematically higher K_2O, P_2O_5, TiO_2, Rb, Th, Y, REE and HFSE contents; Rb/Sr elemental ratios; and Sr and O isotopic ratios. In contrast, the lavas display systematically lower Al_2O_3, Na_2O, Sr, and Ba contents; Ba/Nb, K/Rb, and Sr/Y elemental ratios; and Nd isotopic ratios compared to volcanic centers of similar age, composition, and eruptive at the same latitude (21-22° S) at the arc-front. In addition, Eu anomalies become progressively more negative toward Uturuncu.
6. These variations are interpreted to indicate that mid- to deep-crustal source rocks for the lavas become progressively older and more feldspar-rich with increasing distance from the arc front. In this regard, silicic magmas erupted along the arc-front reflect melting of relatively young, mafic composition amphibolitic source rocks with garnet-rich, but feldspar-poor residual mineralogies. Towards the east, the lower crust becomes increasingly older with a more felsic bulk composition in which residual mineralogies are progressively more feldspar-rich. The implication of this interpretation is that large-scale regional trends in magma compositions at continental volcanic arcs may reflect a process wherein the continental crust becomes strongly hybridized beneath frontal arc localities due to protracted intrusion of subduction-derived basaltic magmas, with a diminishing effect behind the arc front because of smaller degrees of mantle partial melting and primary melt generation.

7. An intriguing result of this study is that on first inspection across-arc geochemical variations at volcanic arcs constructed over thick continental crust, such as increasing K_2O and incompatible trace element contents, resemble those observed at island arcs and arcs constructed over thin continental crust. However, on closer inspection there are significant differences, particularly involving systematic variations in isotopic ratios and other geochemical features that reflect interaction with variable composition continental crust with distance from the arc-front. This contrasts with the results of studies of island arcs where the occurrence of K_2O-rich magmas in back-arc regions is often ascribed to decreasing additions of slab-derived, LILE-rich hydrous fluids to mantle source regions with concomitant decreases in the degree of mantle partial melting and volumetric production of primary mafic magmas. However, we argue based on the geochemical data presented in this paper and geologic relationships (Baker and Francis, 1978) that although across-arc geochemical variations at island arcs and arcs constructed over thick continental crust are produced by apparently fundamentally different processes, ultimately they are both related, directly and indirectly, respectively, to mantle processes associated with the subduction process itself. Specifically, at continental volcanic arcs greater time-integrated primary melt production beneath frontal arc regions has the potential to produce younger, more mafic crustal compositions due to repeated intrusion and hybridization by primary mantle-derived melts. Smaller degrees of mantle partial melting and volumetric melt production in back arc regions results in progressively less hybridized or modified

continental crust that retains to a larger degree its more silicic, isotopically evolved composition. Production of intermediate to silicic composition magmas in continental arcs with more “arc-like” chemical (e.g., higher LILE/HFSE) and isotopic features (lower $^{87}Sr/^{86}Sr$) in frontal-arc localities relative to back-arc magmas is therefore ultimately linked to higher degrees of mantle partial melting and melt production, as is inferred for island arcs as well. Thus, although subduction zone magmas may be substantially modified by the continental crust resulting in systematic across-arc geochemical trends, these trends are a manifestation that the continental crust has also been substantially modified by fundamental subduction zone processes similar to those proposed for island arcs. In short, the crust thus modifies the compositions of subduction zone magmas, but complimentary to this, subduction zone magmas modify the composition of the continental crust.

References

Baker, M.C.W., and Francis, P.W., 1978, Upper Cenozoic volcanism in Central Andes-Ages and volumes: Earth and Planetary Science Letters, v. 41, p. 175-187.

Sparks, R.S.J., Folkes, C.B., Humphreys, M.C.S., Barfod, D.N., Clavero, J., Sunagua, M.C., McNutt, S.R., and Pritchard, M.E., 2008, Uturuncu volcano, Bolivia: Volcanic unrest due to mid-crustal magma intrusion: American Journal of Science, v. 308, p. 727-769, DOI: 10.2475/06.2008.01

REFERENCES

Aitcheson, S. J., Harmon, R. S., Moorbath, S., Schneider, A., Soler, P., Soriaescalante, E., Steele, G., Swainbank, I., and Worner, G., 1995, Pb Isotopes Define Basement Domains of the Altiplano, Central Andes: Geology, v. 23, no. 6, p. 555-558.

Allmendinger, R. W., Jordan, T. E., Kay, S. M., and Isacks, B. L., 1997, The evolution of the Altiplano-Puna plateau of the Central Andes: Annual Review of Earth and Planetary Sciences, v. 25, p. 139-174.

Anderson, A. T., 1983, Oscillatory Zoning of Plagioclase - Nomarski Interference Contrast Microscopy of Etched Polished Sections: American Mineralogist, v. 68, no. 1-2, p. 125-129.

Avila- Salinas, W., 1991, Petrological and tectonic evolution of Cenozoic volcanism in the Bolivian western Andes: In: Harmon, R.S. and Rapela, C.W. (Eds.), Andean Magmatism and its Tectonic Setting, Geological Society of America Special Paper 265, p. 245-258.

Ayers, J., 1998, Trace element modeling of aqueous fluid - peridotite interaction in the mantle wedge of subduction zones: Contributions to Mineralogy and Petrology, v. 132, no. 4, p. 390-404.

Bachmann, O., Charlier, B. L. A., and Lowenstern, J. B., 2007, Zircon crystallization and recycling in the magma chamber of the rhyolitic Kos Plateau Tuff (Aegean arc): Geology, v. 35, no. 1, p. 73-76.

Bachmann, O., and Dungan, M. A., 2002, Temperature-induced Al-zoning in hornblendes of the Fish Canyon magma, Colorado: American Mineralogist, v. 87, no. 8-9, p. 1062-1076.

Bacon, C. R., 1986, Magmatic inclusions in silicic and intermediate volcanic rocks: Journal of Geophysical Research: Solid Earth (1978–2012), v. 91, no. B6, p. 6091-6112.

Baker, M. C. W., and Francis, P. W., 1978, Upper Cenozoic Volcanism in Central Andes - Ages and Volumes: Earth and Planetary Science Letters, v. 41, no. 2, p. 175-187.

Beck, S. L., and Zandt, G., 2002, The nature of orogenic crust in the central Andes: Journal of Geophysical Research-Solid Earth, v. 107, no. B10.

Beck, S. L., Zandt, G., Myers, S. C., Wallace, T. C., Silver, P. G., and Drake, L., 1996, Crustal-thickness variations in the central Andes: Geology, v. 24, no. 5, p. 407-410.

Bindeman, I. N., Eiler, J. M., Yogodzinski, G. M., Tatsumi, Y., Stern, C. R., Grove, T. L., Portnyagin, M., Hoernle, K., and Danyushevsky, L. V., 2005, Oxygen isotope

evidence for slab melting in modem and ancient subduction zones: Earth and Planetary Science Letters, v. 235, no. 3-4, p. 480-496.

Bindeman, I. N., Ponomareva, V. V., Bailey, J. C., and Valley, J. W., 2004, Volcanic arc of Kamchatka: a province with high-delta ^{18}O magma sources and large-scale $^{18}O/^{16}O$ depletion of the upper crust: Geochimica Et Cosmochimica Acta, v. 68, no. 4, p. 841-865.

Brenan, J. M., Shaw, H. F., Ryerson, F. J., and Phinney, D. L., 1995, Mineral-Aqueous Fluid Partitioning of Trace-Elements at 900-Degrees-C and 2.0 Gpa - Constraints on the Trace-Element Chemistry of Mantle and Deep-Crustal Fluids: Geochimica Et Cosmochimica Acta, v. 59, no. 16, p. 3331-3350.

Caffe, P. J., Trumbull, R. B., Coira, B. L., and Romer, R. L., 2002, Petrogenesis of early neogene magmatism in the northern Puna; Implications for magma genesis and crustal processes in the Central Andean Plateau: Journal of Petrology, v. 43, no. 5, p. 907-942.

Camp, V. E., and Hanan, B. B., 2008, A plume-triggered delamination origin for the Columbia River Basalt Group: Geosphere, v. 4, no. 3, p. 480-495.

Chakraborty, S., and Costa, F., 2004, Fast diffusion of Si and O in San Carlos olivine under hydrous conditions: Geochimica Et Cosmochimica Acta, v. 68, no. 11, p. A275-A275.

Charlier, B. L. A., Ginibre, C., Morgan, D., Nowell, G. M., Pearson, D. G., Davidson, J. P., and Ottley, C. J., 2006, Methods for the microsampling and high-precision analysis of strontium and rubidium isotopes at single crystal scale for petrological and geochronological applications: Chemical Geology, v. 232, no. 3-4, p. 114-133.

Cherniak, D. J., and Watson, E. B., 1994, A Study of Strontium Diffusion in Plagioclase Using Rutherford Backscattering Spectroscopy: Geochimica Et Cosmochimica Acta, v. 58, no. 23, p. 5179-5190.

Chlieh, M., De Chabalier, J., Ruegg, J., Armijo, R., Dmowska, R., Campos, J., and Feigl, K., 2004, Crustal deformation and fault slip during the seismic cycle in the North Chile subduction zone, from GPS and InSAR observations: Geophysical Journal International, v. 158, no. 2, p. 695-711.

Churikova, T., Dorendorf, F., and Worner, G., 2001, Sources and fluids in the mantle wedge below Kamchatka, evidence from across-arc geochemical variation: Journal of Petrology, v. 42, no. 8, p. 1567-1593.

Clavero, J., Polanco, E., Godoy, E., Aguilar, G., Sparks, R.S.J., van Wykde Vries, B., Pérez de Arce, C., Matthews, S., 2004, Substrata influence in the transport and

emplacement mechanism of the Ollagüe debris avalanche (northern Chile): Acta Vulcanologica, v. 16, p. 59-76.

Clavero, J. E., Sparks, R. S. J., Pringle, M. S., Polanco, E., and Gardeweg, M. C., 2004, Evolution and volcanic hazards of Taapaca Volcanic Complex, Central Andes of Northern Chile: Journal of the Geological Society, v. 161, p. 603-618.

Coira, B., Davidson, J., Mpodozis, C., and Ramos, V., 1982, Tectonic and magmatic evolution of the Andes of northern Argentina and Chile: Earth-Science Reviews, v. 18, no. 3, p. 303-332.

Coira, B., and Kay, S. M., 1993, Implications of Quaternary Volcanism at Cerro Tuzgle for Crustal and Mantle Evolution of the Puna Plateau, Central Andes, Argentina: Contributions to Mineralogy and Petrology, v. 113, no. 1, p. 40-58.

Coira, B., Kay, S. M., and Viramonte, J., 1993, Upper Cenozoic magmatic evolution of the Argentine Puna—a model for changing subduction geometry: International Geology Review, v. 35, no. 8, p. 677-720.

Costa, F., and Chakraborty, S., 2004a, Decadal time gaps between mafic intrusion and silicic eruption obtained from chemical zoning patterns in olivine: Earth and Planetary Science Letters, v. 227, no. 3-4, p. 517-530.

-, 2004b, Time scales of igneous differentiation obtained from diffusion modeling of compositional zoning in olivine: Geochimica Et Cosmochimica Acta, v. 68, no. 11, p. A642-A642.

Danyushevsky, L. V., Falloon, T. J., Sobolev, A. V., Crawford, A. J., Carroll, M., and Price, R. C., 1993, The H_2O Content of Basalt Glasses from Southwest Pacific Back-Arc Basins: Earth and Planetary Science Letters, v. 117, no. 3-4, p. 347-362.

Davidson, J., Tepley, F., Palacz, Z., and Meffan-Main, S., 2001, Magma recharge, contamination and residence times revealed by in situ laser ablation isotopic analysis of feldspar in volcanic rocks: Earth and Planetary Science Letters, v. 184, no. 2, p. 427-442.

Davidson, J., Turner, S., Handley, H., Macpherson, C., and Dosseto, A., 2007a, Amphibole "sponge" in arc crust?: Geology, v. 35, no. 9, p. 787-790.

Davidson, J., Turner, S., and Plank, T., 2013, Dy/Dy*: variations arising from mantle sources and petrogenetic processes: Journal of Petrology, v. 54, no. 3, p. 525-537.

Davidson, J. P., and de Silva, S. L., 1992, Volcanic-Rocks from the Bolivian Altiplano - Insights into Crustal Structure, Contamination, and Magma Genesis - Reply: Geology, v. 21, no. 12, p. 1148-1148.

-, 1995, Late Cenozoic Magmatism of the Bolivian Altiplano: Contributions to Mineralogy and Petrology, v. 119, no. 4, p. 387-408.

Davidson, J. P., Hannon, R.S., and Womer, G., 1991, The source of central Andean magmas; some considerations, *in* Hannon, R. S., and Rapela, C.W., ed., Andean magmatism and its tectonic setting, Volume 265: Denver, Geological Society of America, p. 825-843.

Davidson, J. P., Hora, J. M., Garrison, J. M., and Dungan, M. A., 2005, Crustal forensics in arc magmas: Journal of Volcanology and Geothermal Research, v. 140, no. 1-3, p. 157-170.

Davidson, J. P., Mcmillan, N. J., Moorbath, S., Worner, G., Harmon, R. S., and Lopezescobar, L., 1990, The Nevados-De-Payachata Volcanic Region (18-Degrees-S 69-Degrees-W, N Chile) .2. Evidence for Widespread Crustal Involvement in Andean Magmatism: Contributions to Mineralogy and Petrology, v. 105, no. 4, p. 412-432.

Davidson, J. P., and Morgan, D. J., 2006, Crystal isotope stratigraphy; time constraints on magmatic processes: Geochimica Et Cosmochimica Acta, v. 70, no. 18, p. A130-A130.

Davidson, J. P., Morgan, D. J., and Charlier, B. L. A., 2007b, Isotopic microsampling of magmatic rocks: Elements, v. 3, no. 4, p. 253-259.

Davidson, J. P., Morgan, D. J., Charlier, B. L. A., Harlou, R., and Hora, J. M., 2007c, Microsampling and isotopic analysis of igneous rocks: Implications for the study of magmatic systems: Annual Review of Earth and Planetary Sciences, v. 35, p. 273-311.

Davidson, J. P., and Tepley, F. J., 1997, Recharge in volcanic systems: Evidence from isotope profiles of phenocrysts: Science, v. 275, no. 5301, p. 826-829.

de Silva, S., Salas, G., and Schubring, S., 2008, Triggering explosive eruptions—The case for silicic magma recharge at Huaynaputina, southern Peru: Geology, v. 36, no. 5, p. 387-390.

de Silva, S. L., 1989, Altiplano-Puna Volcanic Complex of the Central Andes: Geology, v. 17, no. 12, p. 1102-1106.

de Silva, S. L., Davidson, J. P., Croudace, I. W., and Escobar, A., 1993, Volcanological and Petrological Evolution of Volcan Tata Sabaya, Sw Bolivia: Journal of Volcanology and Geothermal Research, v. 55, no. 3-4, p. 305-335.

de Silva, S. L., and Francis, P. W., 1991, Volcanoes of the Central Andes, New York, Springer-Verlag, p. 216.

de Silva, S. L., and Gosnold, W. D., 2007, Episodic construction of batholiths: Insights from the spatiotemporal development of an ignimbrite flare-up: Journal of Volcanology and Geothermal Research, v. 167, no. 1-4, p. 320-335.

de Silva, S. L., Self, S., Francis, P. W., Drake, R. E., and Ramirez, C., 1994, Effusive Silicic Volcanism in the Central Andes - the Chao Dacite and Other Young Lavas of the Altiplano-Puna Volcanic Complex: Journal of Geophysical Research-Solid Earth, v. 99, no. B9, p. 17805-17825.

de Silva, S. L., Zandt, G., Trumbull, R., Viramonte, J., Salas, G., Jiminez, N., 2006, Large ignimbrite eruptions and volcano-tectonic depressions in the Central Andes: a thermomechanical perspective, *in* Troise, C., De Natale, G., Kilburn, C.R.J. , ed., Mechanisms of activity and unrest at large calderas, Geological Society Special Publication No. 269, Volume 269: London, The Geologic Society, p. 47-63.

Defant, M. J., and Drummond, M. S., 1990, Derivation of Some Modern Arc Magmas by Melting of Young Subducted Lithosphere: Nature, v. 347, no. 6294, p. 662-665.

Deruelle, B., 1978, Calc-Alkaline and Shoshonitic Lavas from 5 Andean Volcanos (between Latitudes 21^{o} 45's and 24^{o} 30's) and Distribution of Plio-Quaternary Volcanism of South-Central and Southern Andes: Journal of Volcanology and Geothermal Research, v. 3, no. 3-4, p. 281-298.

Dickinson, W. R., 1975, Potash-Depth (K-H) Relations in Continental-Margin and Intra-Oceanic Magmatic Arcs: Geology, v. 3, no. 2, p. 53-56.

Dickinson, W. R., and Hatherton, T., 1967, Andesitic Volcanism and Seismicity around Pacific: Science, v. 157, no. 3790, p. 801-803.

Dostal, J., Zentilli, M., Caelles, J. C., and Clark, A. H., 1977, Geochemistry and Origin of Volcanic-Rocks of Andes (26^{o} - 28^{o} S): Contributions to Mineralogy and Petrology, v. 63, no. 2, p. 113-128.

Dreher, S. T., Macpherson, C. G., Pearson, D. G., and Davidson, J. P., 2005, Re-Os isotope studies of Mindanao adakites: Implications for sources of metals and melts: Geology, v. 33, no. 12, p. 957-960.

du Bray, E. A., Ludington, S., Brooks, W.E., Gamble, B.M., Ratte, J.C., Richter, D.H., and Soria-Escalante, E., 1995, Compositional characteristics of middle to upper Tertiary volcanic rocks of the Bolivian Altiplano, U.S. Geological Survey Bulletin Volume 2119, U.S. Geological Survey, p. 30.

Elburg, M. A., van Bergen, M., Hoogewerff, J., Foden, J., Vroon, P., Zulkarnain, I., and Nasution, A., 2002, Geochemical trends across an arc-continent collision zone: magma sources and slab-wedge transfer processes below the Pantar Strait

volcanoes, Indonesia: Geochimica Et Cosmochimica Acta, v. 66, no. 15, p. 2771-2789.

Ellis, B. S., Barry, T., Branney, M. J., Wolff, J. A., Bindeman, I., Wilson, R., and Bonnichsen, B., 2010, Petrologic constraints on the development of a large-volume, high temperature, silicic magma system: The Twin Falls eruptive centre, central Snake River Plain: Lithos, v. 120, no. 3, p. 475-489.

Ewart, A., and Griffin, W., 1994, Application of proton-microprobe data to trace-element partitioning in volcanic rocks: Chemical Geology, v. 117, no. 1, p. 251-284.

Feeley, T. C., 1993a, Volcan Ollagüe: volcanology, petrology and geochemistry of a major Quaternary stratovolcano in the Andean Central Volcanic Zone [PhD: University of California, Los Angeles, USA.

- 1993b, Crustal Modification during Subduction-Zone Magmatism: Evidence from the Southern Salar De Uyuni Region (20^{o} -22^{o} S), Central Andes: Geology, v. 21, no. 11, p. 1019-1022.

-, 2003, Origin and tectonic implications of across-strike geochemical variations in the Eocene Absaroka volcanic province, United States: Journal of Geology, v. 111, no. 3, p. 329-346.

Feeley, T. C., Clynne, M. A., Winer, G. S., and Grice, W. C., 2008a, Oxygen isotope geochemistry of the Lassen Volcanic Center, California: Resolving crustal and mantle contributions to continental arc magmatism: Journal of Petrology, v. 49, no. 5, p. 971-997.

Feeley, T. C., and Davidson, J. P., 1994, Petrology of Calc-Alkaline Lavas at Volcan-Ollague and the Origin of Compositional Diversity at Central Andean Stratovolcanoes: Journal of Petrology, v. 35, no. 5, p. 1295-1340.

Feeley, T. C., Davidson, J. P., and Armendia, A., 1993, The Volcanic and Magmatic Evolution of Volcan Ollague, a High-K, Late Quaternary Stratovolcano in the Andean Central Volcanic Zone: Journal of Volcanology and Geothermal Research, v. 54, no. 3-4, p. 221-245.

Feeley, T. C., and Hacker, M. D., 1995, Intracrustal Derivation of Na-Rich Andesitic and Dacitic Magmas: an Example from Volcan Ollague, Andean Central Volcanic Zone: Journal of Geology, v. 103, no. 2, p. 213-225.

Feeley, T. C., and Sharp, Z. D., 1995, $^{18}O/^{16}O$ Isotope Geochemistry of Silicic Lava Flows Erupted from Volcan Ollague, Andean Central Volcanic Zone: Earth and Planetary Science Letters, v. 133, no. 3-4, p. 239-254.

Feeley, T. C., Wilson, L. F., and Underwood, S., 2008b, Distribution and compositions of magmatic inclusions in the Mount Helen dome, Lassen Volcanic Center, California: Insights into magma chamber processes: Lithos, v. 106, no. 1-2, p. 173-189.

Fernandez, C., Horman, P.K., Kussmaul, S., Meave, J., Pichler, H., and Subieta, T. , 1973, First petrologic data on young volcanic rocks of SW-Bolivia: Tschermaks Mineralogische und Petrographische Mitteilungen, v. 19, p. 149-172.

Fialko, Y., and Pearse, J., 2012, Sombrero Uplift Above the Altiplano-Puna Magma Body: Evidence of a Ballooning Mid-Crustal Diapir: Science, v. 338, no. 6104, p. 250-252.

Francalanci, L., Avanzinelli, R., Nardini, I., Tiepolo, M., Davidson, J. P., and Vannucci, R., 2012, Crystal recycling in the steady-state system of the active Stromboli volcano: a 2.5-ka story inferred from in situ Sr-isotope and trace element data: Contributions to Mineralogy and Petrology, v. 163, no. 1, p. 109-131.

Gamble, J., Wood, C., Price, R., Smith, I., Stewart, R., and Waight, T., 1999, A fifty year perspective of magmatic evolution on Ruapehu Volcano, New Zealand: verification of open system behaviour in an arc volcano: Earth and Planetary Science Letters, v. 170, no. 3, p. 301-314.

Gardner, M. F., Troll, V. R., Gamble, J. A., Gertisser, R., Hart, G. L., Ellam, R. M., Harris, C., and Wolff, J. A., 2013, Crustal Differentiation Processes at Krakatau Volcano, Indonesia: Journal of Petrology, v. 54, no. 1, p. 149-182.

Giletti, B. J., and Casserly, J. E. D., 1994, Strontium Diffusion Kinetics in Plagioclase Feldspars: Geochimica Et Cosmochimica Acta, v. 58, no. 18, p. 3785-3793.

Gill, J. B., 1981, Orogenic andesites and plate tectonics, Berlin, Springer-Verlag, 390 p.:

Ginibre, C., and Davidson, J., 2014, Sr Isotope Zoning in Plagioclase from Parinacota Volcano (Northern Chile): Quantifying Magma Mixing and Crustal Contamination: Journal of Petrology, v. 55, no. 6, p. 1203-1238.

Ginibre, C., and Wörner, G., 2007, Variable parent magmas and recharge regimes of the Parinacota magma system (N. Chile) revealed by Fe, Mg and Sr zoning in plagioclase: Lithos, v. 98, no. 1, p. 118-140.

Glazner, A., Bartley, J. M., Coleman, D. S., Gray, W., and Taylor, R. Z., 2004, Are plutons assembled over millions of years by amalgamation from small magma chambers?: GSA Today, v. 14, no. 4/5, p. 4-11.

Gregory-Wodzicki, K. M., 2000, Uplift history of the Central and Northern Andes: a review: Geological Society of America Bulletin, v. 112, no. 7, p. 1091-1105.

Grunder, A. L., Klemetti, E. W., Feeley, T. C., and McKee, C. M., 2006, Eleven million years of arc volcanism at the Aucanquilcha Volcanic Cluster, Northern Chilean Andes: implications for the life span and emplacement of plutons: Transactions of the Royal Society of Edinburgh-Earth Sciences, v. 97, p. 415-436.

Harford, C., Pringle, M., Sparks, R., and Young, S., 2002, The volcanic evolution of Montserrat using 40Ar/39Ar geochronology: Geological Society, London, Memoirs, v. 21, no. 1, p. 93-113.

Harmon, R. S., Barreiro, B. A., Moorbath, S., Hoefs, J., Francis, P. W., Thorpe, R. S., Deruelle, B., Mchugh, J., and Viglino, J. A., 1984, Regional O-Isotope, Sr-Isotope, and Pb-Isotope Relationships in Late Cenozoic Calc-Alkaline Lavas of the Andean Cordillera: Journal of the Geological Society, v. 141, no. Sep, p. 803-822.

Hawkesworth, C. J., and Clarke, C.B., 1994, Partial melting in the lower crust: new constraints on crustal contamination processes in the central Andes, *in* Reutter, K. J., Scheurber, E, and Wigger, P. J. , ed., Tectonics of the Southern Central Andes, Springer-Verlag, p. 93-101.

Hayes, G. P., Wald, D. J., and Johnson, R. L., 2012, Slab1. 0: A three-dimensional model of global subduction zone geometries: Journal of Geophysical Research: Solid Earth (1978–2012), v. 117, no. B1.

Henderson, S., and Pritchard, M., 2013, Decadal volcanic deformation in the Central Andes Volcanic Zone revealed by InSAR time series: Geochemistry, Geophysics, Geosystems, v. 14, no. 5, p. 1358-1374.

Hernando, I., Aragón, E., Frei, R., González, P., and Spakman, W., 2014, Constraints on the origin and evolution of magmas in the Payún Matrú Volcanic Field, Quaternary Andean back-arc of western Argentina: Journal of Petrology, v. 55, no. 1, p. 209-239.

Heydolph, K., Hoernle, K., Hauff, F., van den Bogaard, P., Portnyagin, M., Bindeman, I., and Garbe-Schonberg, D., 2012, Along and across arc geochemical variations in NW Central America: Evidence for involvement of lithospheric pyroxenite: Geochimica Et Cosmochimica Acta, v. 84, p. 459-491.

Hickey- Vargas, R., Roa, H. M., Escobar, L. L., and Frey, F. A., 1989, Geochemical Variations in Andean Basaltic and Silicic Lavas from the Villarrica-Lanin Volcanic Chain (39.5^{o} S): an Evaluation of Source Heterogeneity, Fractional Crystallization and Crustal Assimilation: Contributions to Mineralogy and Petrology, v. 103, no. 3, p. 361-386.

Hickey, R. L., Frey, F. A., Gerlach, D. C., and Lopez-Escobar, L., 1986, Multiple sources for basaltic arc rocks from the southern volcanic zone of the Andes (34–41 S):

trace element and isotopic evidence for contributions from subducted oceanic crust, mantle, and continental crust: Journal of Geophysical Research: Solid Earth (1978–2012), v. 91, no. B6, p. 5963-5983.

Hildreth, W., 1981, Gradients in Silicic Magma Chambers - Implications for Lithospheric Magmatism: Journal of Geophysical Research, v. 86, no. Nb11, p. 153-192.

Hildreth, W., and Moorbath, S., 1988, Crustal Contributions to Arc Magmatism in the Andes of Central Chile: Contributions to Mineralogy and Petrology, v. 98, no. 4, p. 455-489.

Hobden, B. J., Houghton, B. F., Davidson, J. P., and Weaver, S. D., 1999, Small and short-lived magma batches at composite volcanoes: time windows at Tongariro volcano, New Zealand: Journal of the Geological Society, v. 156, p. 865-868.

Hofmann, A. W., 1988, Chemical differentiation of the Earth: the relationship between mantle, continental crust, and oceanic crust: Earth and Planetary Science Letters, v. 90, p. 297-314.

Huang, W. L., and Wyllie, P. J., 1986, Phase-Relationships of Gabbro-Tonalite-Granite-Water at 15-Kbar with Applications to Differentiation and Anatexis: American Mineralogist, v. 71, no. 3-4, p. 301-316.

Huber, C., Bachmann, O., and Dufek, J., 2011, Thermo-mechanical reactivation of locked crystal mushes: Melting-induced internal fracturing and assimilation processes in magmas: Earth and Planetary Science Letters, v. 304, no. 3-4, p. 443-454.

Iriarte, R., 2012, The Cerro Guacha caldera complex: an upper Miocene-Pliocene polycyclic volcano-tectonic structure in the Altiplano Puna Volcanic Complex of the Central Andes of Bolivia.

Isacks, B. L., 1988, Uplift of the Central Andean Plateau and Bending of the Bolivian Orocline: Journal of Geophysical Research-Solid Earth and Planets, v. 93, no. B4, p. 3211-3231.

Jackson, S. E., 2001, The application of Nd:YAG lasers in LA-ICPMS, *in* Sylvester, P. J., ed., Laser Ablation ICP- Mass Spectrometry in the Earth Sciences: Principles and Application, Volume 29, Mineralogical Association of Canada, p. 29-45.

Jakes, P., and White, A. J. R., 1972, Major and Trace-Element Abundances in Volcanic-Rocks of Orogenic Areas: Geological Society of America Bulletin, v. 83, no. 1, p. 29-40.

James, D. E., 1971, Plate Tectonic Model for Evolution of Central Andes: Geological Society of America Bulletin, v. 82, no. 12, p. 3325-3346.

Jarvis, K. E., 1988, Inductively Coupled Plasma Mass-Spectrometry - a New Technique for the Rapid or Ultra-Trace Level Determination of the Rare-Earth Elements in Geological-Materials: Chemical Geology, v. 68, no. 1-2, p. 31-39.

Jay, J. A., Pritchard, M. E., West, M. E., Christensen, D., Haney, M., Minaya, E., Sunagua, M., McNutt, S. R., and Zabala, M., 2012, Shallow seismicity, triggered seismicity, and ambient noise tomography at the long-dormant Uturuncu Volcano, Bolivia: Bulletin of Volcanology, v. 74, no. 4, p. 817-837.

Johnson, D. M., Hooper P.R., and Conrey, R.M., 1999, GeoAnalytical Lab, Washington State University: Advances in X-ray Analysis, v. 41, p. 843-867.

Kay, S. M., Coira, B. L., Caffe, P. J., and Chen, C. H., 2010, Regional chemical diversity, crustal and mantle sources and evolution of central Andean Puna plateau ignimbrites: Journal of Volcanology and Geothermal Research, v. 198, no. 1-2, p. 81-111.

Kay, S. M., Coira, B. L., and Kay, R. W., 2009, Central Andean Galan Ignimbrites: Magma evolution from the mantle to eruption in a thickened crust: Geochimica Et Cosmochimica Acta, v. 73, no. 13, p. A630-A630.

Kay, S. M., Mpodzis, C., and Coria, B., 1999, Neogene magmatism, tectonism, and mineral deposits of the Central Andes (22° to 33°S latitude), *in* Skinner, B. J., ed., Geology and Ore deposits of the Central Andes, Volume 7, Society of Economic Geologists, p. 27-59.

Kendrick, E., Bevis, M., Smalley, R., and Brooks, B., 2001, An integrated crustal velocity field for the central Andes: Geochemistry, Geophysics, Geosystems, v. 2, no. 11.

Klemetti, E. W., 2005, Constraining the Magmatic Evolution of the Andean Arc at 21°S Using the Volcanic and Petrologic History of Volcán Aucanquilcha, Central Volcanic Zone, Northern Chile [PhD: Oregon State University.

Klemetti, E. W., and Grunder, A. L., 2008, Volcanic evolution of Volcan Aucanquilcha: a long-lived dacite volcano in the Central Andes of northern Chile: Bulletin of Volcanology, v. 70, no. 5, p. 633-650.

Klerkx, J., Deutsch, S., Pichler, H., and Zeil, W., 1977, Strontium Isotopic Composition and Trace-Element Data Bearing on Origin of Cenozoic Volcanic-Rocks of Central and Southern Andes: Journal of Volcanology and Geothermal Research, v. 2, no. 1, p. 49-71.

Klotz, J., Khazaradze, G., Angermann, D., Reigber, C., Perdomo, R., and Cifuentes, O., 2001, Earthquake cycle dominates contemporary crustal deformation in Central

and Southern Andes: Earth and Planetary Science Letters, v. 193, no. 3, p. 437-446.

Knesel, K. M., and Davidson, J. P., 1999, Sr isotope systematics during melt generation by intrusion of basalt into continental crust: Contributions to Mineralogy and Petrology, v. 136, no. 3, p. 285-295.

Kushiro, I., 1968, Compositions of Magmas Formed by Partial Zone Melting of Earths Upper Mantle: Journal of Geophysical Research, v. 73, no. 2, p. 619-&.

Kushiro, I., Nakamura, Y., Haramura, H., and Akimoto, S. I., 1970, Crystallization of Some Lunar Mafic Magmas and Generation of Rhyolitic Liquid: Science, v. 167, no. 3918, p. 610-612.

Kushiro, I., Yoder, H. S., and Nishikaw.M, 1968, Effect of Water on Melting of Enstatite: Geological Society of America Bulletin, v. 79, no. 12, p. 1685-1692.

Kussmaul, S., Hormann, P. K., Ploskonka, E., and Subieta, T., 1977, Volcanism and Structure of Southwestern Bolivia: Journal of Volcanology and Geothermal Research, v. 2, no. 1, p. 73-111.

Lamb, S. H., Hoke, L., Kennan, L., and Dewey, J., 1997, Cenozoic evolution of the Central Andes in Bolivia and northern Chile: Orogeny Through Time, *in* Burg, J. P., and Ford, M ed., Geological Society Special Publication No. 121: London, The Geologic Society, p. 237-264.

Le Friant, A., Lock, E., Hart, M., Boudon, G., Sparks, R., Leng, M., Smart, C. W., Komorowski, J.-C., Deplus, C., and Fisher, J., 2008, Late Pleistocene tephrochronology of marine sediments adjacent to Montserrat, Lesser Antilles volcanic arc: Journal of the Geological Society, v. 165, no. 1, p. 279-289.

Le Maitre, R. W., 2002, Igneous Rocks. A Classification and Glossary of Terms, New York, Cambridge University Press, 236 p.:

Leeman, W. P., Smith, D. R., Hildreth, W., Palacz, Z., and Rogers, N., 1990, Compositional Diversity of Late Cenozoic Basalts in a Transect across the Southern Washington Cascades - Implications for Subduction Zone Magmatism: Journal of Geophysical Research-Solid Earth and Planets, v. 95, no. B12, p. 19561-19582.

Lindsay, J. M., de Silva, S., Trumbull, R., Emmermann, R., and Wemmer, K., 2001a, La Pacana caldera, N. Chile: a re-evaluation of the stratigraphy and volcanology of one of the world's largest resurgent calderas: Journal of Volcanology and Geothermal Research, v. 106, no. 1-2, p. 145-173.

Lindsay, J. M., Schmitt, A. K., Trumbull, R. B., De Silva, S. L., Siebel, W., and Emmermann, R., 2001b, Magmatic evolution of the La Pacana caldera system, Central Andes, Chile: Compositional variation of two cogenetic, large-volume felsic ignimbrites: Journal of Petrology, v. 42, no. 3, p. 459-486.

Lipman, P. W., 2007, Incremental assembly and prolonged consolidation of Cordilleran magma chambers: Evidence from the Southern Rocky Mountain volcanic field: Geosphere, v. 3, no. 1, p. 42-70.

Litvinovsky, B. A., Steele, I. M., and Wickham, S. M., 2000, Silicic magma formation in overthickened crust: Melting of charnockite and leucogranite at 15, 20 and 25 kbar: Journal of Petrology, v. 41, no. 5, p. 717-737.

Lowenstern, J. B., Charlier, B. L. A., Clynne, M. A., and Wooden, J. L., 2006, Extreme U-Th disequilibrium in rift-related basalts, rhyolites and granophyric granite and the timescale of rhyolite generation, intrusion and crystallization at Alid volcanic center, Eritrea: Journal of Petrology, v. 47, no. 11, p. 2105-2122.

Lucassen, F., Becchio, R., Wilke, H. G., Franz, G., Thirlwall, M. F., Viramonte, J., and Wemmer, K., 2000, Proterozoic-Paleozoic development of the basement of the Central Andes (18-26^{o} S) - a mobile belt of the South American craton: Journal of South American Earth Sciences, v. 13, no. 8, p. 697-715.

Lucassen, F., Escayola, M., Romer, R. L., Viramonte, J., Koch, K., and Franz, G., 2002a, Isotopic composition of Late Mesozoic basic and ultrabasic rocks from the Andes (23-32^{o} S) - implications for the Andean mantle: Contributions to Mineralogy and Petrology, v. 143, no. 3, p. 336-349.

Lucassen, F., Franz, G., and Laber, A., 1999a, Permian high pressure rocks - the basement of the Sierra de Limon Verde in Northern Chile: Journal of South American Earth Sciences, v. 12, no. 2, p. 183-199.

Lucassen, F., Franz, G., Romer, R. L., Schultz, F., Dulski, P., and Wemmer, K., 2007, Pre-Cenozoic intra-plate magmatism along the Central Andes (17-34^{o} S): Composition of the mantle at an active margin: Lithos, v. 99, no. 3-4, p. 312-338.

Lucassen, F., Franz, G., Thirlwall, M. F., and Mezger, K., 1999b, Crustal recycling of metamorphic basement: Late palaeozoic granitoids of northern chile (similar to 22^{o} S). Implications for the composition of the Andean crust: Journal of Petrology, v. 40, no. 10, p. 1527-1551.

Lucassen, F., Franz, G., Viramonte, J., Romer, R. L., Dulski, P., and Lang, A., 2005, The late Cretaceous lithospheric mantle beneath the Central Andes: Evidence from phase equilibria and composition of mantle xenoliths: Lithos, v. 82, no. 3-4, p. 379-406.

Lucassen, F., Harmon, R., Franz, G., Romer, R. L., Becchio, R., and Siebel, W., 2002b, Lead evolution of the Pre-Mesozoic crust in the Central Andes (18-27^{o}): progressive homogenisation of Pb: Chemical Geology, v. 186, no. 3-4, p. 183-197.

Lucassen, F., Kramer, W., Bartsch, V., Wilke, H. G., Franz, G., Romer, R. L., and Dulski, P., 2006, Nd, Pb, and Sr isotope composition of juvenile magmatism in the Mesozoic large magmatic province of northern Chile (18-27 degrees S): indications for a uniform subarc mantle: Contributions to Mineralogy and Petrology, v. 152, no. 5, p. 571-589.

Lucassen, F., Lewerenz, S., Franz, G., Viramonte, J., and Mezger, K., 1999c, Metamorphism, isotopic ages and composition of lower crustal granulite xenoliths from the Cretaceous Salta Rift, Argentina: Contributions to Mineralogy and Petrology, v. 134, no. 4, p. 325-341.

Mamani, M., Tassara, A., and Woerner, G., 2008, Composition and structural control of crustal domains in the central Andes: Geochemistry Geophysics Geosystems, v. 9.

Mamani, M., Worner, G., and Sempere, T., 2010, Geochemical variations in igneous rocks of the Central Andean orocline (13^{o} S to 18^{o} S): Tracing crustal thickening and magma generation through time and space: Geological Society of America Bulletin, v. 122, no. 1-2, p. 162-182.

Mason, B. G., Pyle, D. M., and Oppenheimer, C., 2004, The size and frequency of the largest explosive eruptions on Earth: Bulletin of Volcanology, v. 66, no. 8, p. 735-748.

Mattioli, M., Renzulli, A., Menna, M., and Holm, P. M., 2006, Rapid ascent and contamination of magmas through the thick crust of the CVZ (Andes, Ollague region): Evidence from a nearly aphyric high-K andesite with skeletal olivines: Journal of Volcanology and Geothermal Research, v. 158, no. 1-2, p. 87-105.

Mcculloch, M. T., and Gamble, J. A., 1991, Geochemical and Geodynamical Constraints on Subduction Zone Magmatism: Earth and Planetary Science Letters, v. 102, no. 3-4, p. 358-374.

McGee, J. J. T., R.I.; Duffield W.A. , 1987, Petrologic characteristics of the 1982 and pre-1982 eruptive products of El Chichon volcano, Chiapas, Mexico: Geophysical Journal International, v. 26, no. 1, p. 85-108.

McGlashan, N., Brown, L., and Kay, S. M., 2008, Crustal thickness in the central Andes from teleseismically recorded depth phase precursors: Geophysical Journal International, v. 175, no. 3, p. 1013-1022.

McLeod, C. L., Davidson, J. P., Nowell, G. M., de Silva, S. L., and Schmitt, A. K., 2013, Characterizing the continental basement of the Central Andes: Constraints from Bolivian crustal xenoliths: Geological Society of America Bulletin, v. 125, no. 5-6, p. 985-997.

Melzer, S., and Wunder, B., 2000, Island-arc basalt alkali ratios: Constraints from phengite-fluid partitioning experiments: Geology, v. 28, no. 7, p. 583-586.

Michelfelder, G. S., Feeley, T. C., and Wilder, A. D., 2014, The Volcanic Evolution of Cerro Uturuncu: A High-K, Composite Volcano in the Back-Arc of the Central Andes of SW Bolivia: International Journal of Geosciences, v. 5, no. 11, p. 1263.

Michelfelder, G. S., Feeley, T. C., Wilder, A. D., and Klemetti, E. W., 2013, Modification of the continental crust by subduction zone magmatism and vice-versa: across-strike geochemical variations of silicic lavas from individual eruptive centers in the Andean Central Volcanic Zone: Geosciences, v. 3, no. 4, p. 633-667.

Michelfelder, G. S., Feeley, T. C., Wilder, A. D., and Thacker, J., in preparation Evidence for multi-stage mixing after assimilation fractional crystallization during the magma chamber evolution at Cerro Uturuncu, Central Volcanic Zone, SW Bolivia: Magma recharge, contamination and residence times revealed from in situ laser ablation isotopic analysis of plagioclase

Morgan, G. B., London, D., and Luedke, R. G., 1998, Petrochemistry of late Miocene peraluminous silicic volcanic rocks from the Morococala field, Bolivia: Journal of Petrology, v. 39, no. 4, p. 601-632.

Muir, D. D., Blundy, J. D., Hutchinson, M. C., and Rust, A. C., 2014a, Petrological imaging of an active pluton beneath Cerro Uturuncu, Bolivia: Contributions to Mineralogy and Petrology, v. 167, no. 3, p. 1-25.

Muir, D. D., Blundy, J. D., Rust, A. C., and Hickey, J., 2014b, Experimental constraints on dacite pre-eruptive magma storage conditions beneath Uturuncu volcano: Journal of Petrology, v. 55, no. 4, p. 749-767.

Neufeld, L., and Roy, J., 2004, Laser ablation solid sampling plasma spectrochemistry - The importance of matching the hardware to the application: Spectroscopy, v. 19, no. 1, p. 16-+.

Newman, S., Stolper, E., and Stern, R., 2000, H_2O and CO_2 in magmas from the Mariana arc and back arc systems: Geochemistry Geophysics Geosystems, v. 1.

Ort, M. H., Coira, B. L., and Mazzoni, M. M., 1996, Generation of a crust-mantle magma mixture: Magma sources and contamination at Cerro Panizos, central Andes: Contributions to Mineralogy and Petrology, v. 123, no. 3, p. 308-322.

Patino, L. C., Carr, M. J., and Feigenson, M. D., 1997, Cross-arc geochemical variations in volcanic fields in Honduras CA: progressive changes in source with distance from the volcanic front: Contributions to Mineralogy and Petrology, v. 129, no. 4, p. 341-351.

Pearce, T. H., Griffin, M. P., and Kolisnik, A. M., 1987a, Magmatic Crystal Stratigraphy and Constraints on Magma Chamber Dynamics - Laser Interference Results on Individual Phenocrysts: Journal of Geophysical Research-Solid Earth and Planets, v. 92, no. B13, p. 13745-13752.

Pearce, T. H., Russell, J. K., and Wolfson, I., 1987b, Laser-Interference and Nomarski Interference Imaging of Zoning Profiles in Plagioclase Phenocrysts from the May 18, 1980, Eruption of Mount-St-Helens, Washington: American Mineralogist, v. 72, no. 11-12, p. 1131-1143.

Perez, W. A., and Kawashita, K., 1992, K-Ar and Rb-Sr Geochronology of Igneous Rocks from the Sierra De Paiman, Northwestern Argentina: Journal of South American Earth Sciences, v. 5, no. 3-4, p. 251-264.

Plank, T., and Langmuir, C. H., 1988, An Evaluation of the Global Variations in the Major Element Chemistry of Arc Basalts: Earth and Planetary Science Letters, v. 90, no. 4, p. 349-370.

Pritchard, M. E., and Simons, M., 2002, A satellite geodetic survey of large-scale deformation of volcanic centres in the central Andes: Nature, v. 418, no. 6894, p. 167-171.

Ramos, F. C., and Reid, M. R., 2005, Distinguishing melting of heterogeneous mantle sources from crustal contamination: Insights from Sr isotopes at the phenocryst scale, Pisgah Crater, California: Journal of Petrology, v. 46, no. 5, p. 999-1012.

Ramos, F. C., and Tepley, F. J., 2008, Inter- and Intracrystalline Isotopic Disequilibria: Techniques and Applications: Minerals, Inclusions and Volcanic Processes, v. 69, p. 403-443.

Ramos, F. C., and Wolff, J. A., 2005, In situ Sr isotopes measured by LA-MC-ICPMS: Utility for the average Joe: Geochimica Et Cosmochimica Acta, v. 69, no. 10, p. A376-A376.

Ramos, F. C., Wolff, J. A., and Gill, J. B., 2005a, Open-system processes and rhyolites: What isotope systems can we trust, and for what?: Geochimica Et Cosmochimica Acta, v. 69, no. 10, p. A235-A235.

Ramos, F. C., Wolff, J. A., Starkel, W., Eckberg, A., Tollstrup, D. L., and Scott, S., 2013, The changing nature of sources associated with Columbia River flood basalts:

Evidence from strontium isotope ratio variations in plagioclase phenocrysts: Geological Society of America Special Papers, v. 497, p. 231-257.

Ramos, F. C., Wolff, J. A., and Tollstrup, D. L., 2004, Measuring Sr-87/Sr-86 variations in minerals and groundmass from basalts using LA-MC-ICPMS: Chemical Geology, v. 211, no. 1-2, p. 135-158.

-, 2005b, Sr isotope disequilibrium in Columbia River flood basalts: Evidence for rapid shallow-level open-system processes: Geology, v. 33, no. 6, p. 457-460.

Rollinson, H. R., 1993, Using Geochemical Data: Evaluation, Presentation, Interpretation, New York, John Wiley and Sons, p. 352.

Ryan, J. G., Morris, J., Tera, F., Leeman, W. P., and Tsvetkov, A., 1995, Cross-Arc Geochemical Variations in the Kurile Arc as a Function of Slab Depth: Science, v. 270, no. 5236, p. 625-627.

Schmidt, M. W., and Poli, S., 1998, Experimentally based water budgets of dehydrating slabs and consequences for arc magma generation: Earth and Planetary Science Letters, v. 163, p. 361-379.

Schmitt, A. K., de Silva, S. L., Trumbull, R. B., and Emmermann, R., 2001, Magma evolution in the Purico ignimbrite complex, northern Chile: evidence for zoning of a dacitic magma by injection of rhyolitic melts following mafic recharge: Contributions to Mineralogy and Petrology, v. 140, no. 6, p. 680-700.

Schmitz, M., Heinsohn, W. D., and Schilling, F. R., 1997, Seismic, gravity and petrological evidence for partial melt beneath the thickened Central Andean crust (21-23^{o} S): Tectonophysics, v. 270, no. 3-4, p. 313-326.

Schnurr, W. B. W., Trumbull, R. B., Clavero, J., Hahne, K., Siebel, W., and Gardeweg, M., 2007, Twenty-five million years of silicic volcanism in the southern central volcanic zone of the Andes: Geochemistry and magma genesis of ignimbrites from 25 to 27 degrees S, 67 to 72 degrees W: Journal of Volcanology and Geothermal Research, v. 166, no. 1, p. 17-46.

Self, S., 2006, The effects and consequences of very large explosive volcanic eruptions: Philosophical Transactions of the Royal Society A: Mathematical, Physical and Engineering Sciences, v. 364, no. 1845, p. 2073-2097.

Şen, C., 1994, Subduction related petrologic processes: 1—Dehydration Melting of a Basaltic Composition Amphibolite 2—Mantle Metasomatism: PhD Thesis, University of New Brunswick, New Brunswick-Canada.

Shibata, T., and Nakamura, E., 1997, Across-arc variations of isotope and trace element compositions from Quaternary basaltic volcanic rocks in northeastern Japan:

Implications for Interaction between subducted oceanic slab and mantle wedge: Journal of Geophysical Research-Solid Earth, v. 102, no. B4, p. 8051-8064.

Simkin T, a. S. L., 1994, Volcanoes of the World: a Regional Directory, Gazetteer, and Chronology of Volcanism During the Last 10,000 Years, Tucson, Geosciences Press, p. 368.

Soler, M. M., Caffe, P. J., Coira, B. L., Onoe, A. T., and Kay, S. M., 2007, Geology of the Vilama caldera: A new interpretation of a large-scale explosive event in the Central Andean plateau during the Upper Miocene: Journal of Volcanology and Geothermal Research, v. 164, no. 1-2, p. 27-53.

Somoza, R., and Ghidella, M.E., 2005, Convergencia en el margen occidental de América del Sur durante el Cenozoico: subducción de las placas de Nazca, Farallon y Phoenix: Rev. Asoc. Geol. Argent, v. 60, p. 797-809.

Somoza R., G., M.E., 2012, Late Cretaceous to recent plate motioins in western South America revisited: Earth and Planetary Science Letters, v. 331-332, p. 152-163.

Sparks, R., and Young, S., 2002, The eruption of Soufriere Hills Volcano, Montserrat (1995-1999): overview of scientific results: Geological Society, London, Memoirs, v. 21, no. 1, p. 45-69.

Sparks, R.S.J., Self, S., Grattan, J.P., Oppenheimer, C., Pyle, D.M., and Rymer, H., 2005, Super-eruptions: Global effects and future threats. Report of a Geological Society of London working group, v. 24, London, UK: The Geological Society.

Sparks, R. S. J., Folkes, C. B., Humphreys, M. C. S., Barfod, D. N., Clavero, J., Sunagua, M. C., McNutt, S. R., and Pritchard, M. E., 2008, Uturuncu volcano, Bolivia: Volcanic unrest due to mid-crustal magma intrusion: American Journal of Science, v. 308, no. 6, p. 727-769.

Stolper, E., and Newman, S., 1994, The role of water in the petrogenesis of Mariana trough magmas: Earth and Planetary Science Letters, v. 121, p. 293-325.

Sun, S. s., and McDonough, W.F., 1989, Chemical and isotopic systematics of oceanic basalts: implications for mantle compositions and processes: Geological Society, London, Special Publications, v. 42, p. 313-345.

Takeuchi, A., and Larson, P. B., 2005, Oxygen isotope evidence for the late Cenozoic development of an orographic rain shadow in eastern Washington, USA: Geology, v. 33, no. 4, p. 313-316.

Tatsumi, Y., and Eggins, S., 1995, Subduction Zone Magmatism, Oxford, Blackwell Science, Frontiers in Earth Sciences, p. 211.

Tatsumi, Y., Hamilton, D. L., and Nesbitt, R. W., 1986, Chemical Characteristics of Fluid Phase Released from a Subducted Lithosphere and Origin of Arc Magmas - Evidence from High-Pressure Experiments and Natural Rocks: Journal of Volcanology and Geothermal Research, v. 29, no. 1-4, p. 293-309.

Tepley, F. J., Davidson, J. P., and Clynne, M. A., 1999, Magmatic interactions as recorded in plagioclase phenocrysts of Chaos Crags, Lassen Volcanic Center, California: Journal of Petrology, v. 40, no. 5, p. 787-806.

Tepley, F. J., Davidson, J. P., Tilling, R. I., and Arth, J. G., 2000, Magma mixing, recharge and eruption histories recorded in plagioclase phenocrysts from El Chichon Volcano, Mexico: Journal of Petrology, v. 41, no. 9, p. 1397-1411.

Thorpe, R. S., and Francis, P. W., 1979, Variations in Andean Andesite Compositions and Their Petrogenetic Significance: Tectonophysics, v. 57, no. 1, p. 53-70.

Thorpe, R. S., Francis, P.W., Hammill, M. and Baker. M.C.W., 1982, The Andes, *in* Thorpe, R. S., ed., Andesites: New York, Wiley, p. 187-205.

Todt, W., Cliff, R.A., Hanser, A., and Hofmann, A.W., 1996, Evaluation of a ^{202}Pb- ^{205}Pb double spike for high-precision lead isotope analysis, *in* Hart, S. R., and Basu, A. , ed., Earth processes: Reading the isotope code, Volume 95: Washington D.C., American Geophysical Union, p. 429-437.

Trumbull, R. D., Wittenbrink, R., Hahne, K., Emmermann, R., Busch, W., Gerstenberger, H., and Siebel, W., 1999, Evidence for Late Miocene to Recent contamination of arc andesites by crustal melts in the Chilean Andes (25-26 degrees S) and its geodynamic implications: Journal of South American Earth Sciences, v. 12, no. 2, p. 135-155.

Valley, J. W., 2001, Stable isotope thermometry at high temperatures: Stable Isotope Geochemistry, v. 43, p. 365-413.

Valley, J. W., Kitchen, N., Kohn, M. J., Niendorf, C. R., and Spicuzza, M. J., 1995, UWG-2, a garnet standard for oxygen isotope ratios: Strategies for high precision and accuracy with laser heating: Geochimica Et Cosmochimica Acta, v. 59, no. 24, p. 5223-5231.

Vezzoli, L., Tibaldi, A., Renzulli, A., Menna, M., and Flude, S., 2008, Faulting-assisted lateral collapses and influence on shallow magma feeding systems at Ollague volcano (Central Volcanic Zone, Chile-Bolivia Andes): Journal of Volcanology and Geothermal Research, v. 171, p. 137-159.

Voight, B., Komorowski, J., Norton, G., Belousov, A., Belousova, M., Boudon, G., Francis, P., Franz, W., Heinrich, P., and Sparks, R., 2002, The 26 December (Boxing Day) 1997 sector collapse and debris avalanche at Soufriere Hills

volcano, Montserrat: MEMOIRS-GEOLOGICAL SOCIETY OF LONDON, v. 21, p. 363-408.

Walker, B. A. K., E.W., Grunder, A.L., Dilles, J.H., Tepley, F.J. Gile, D., 2013, Crystal reaming during the assembly, maturation, and waning of an eleven-million-year crustal magma cycle: thermobarometry of the Aucanquilcha Volcanic Cluster: Contributions to Mineralogy and Petrology, v. 165, p. 663-682.

Walker, J. A., Carr, M. J., Patino, L. C., Johnson, C. M., Feigenson, M. D., and Ward, R. L., 1995, Abrupt Change in Magma Generation Processes across the Central-American Arc in Southeastern Guatemala - Flux Dominated Melting near the Base of the Wedge to Decompression Melting near the Top of the Wedge: Contributions to Mineralogy and Petrology, v. 120, no. 3-4, p. 378-390.

Wolff, J. A., Ramos, F. C., and Davidson, J. P., 1999, Sr isotope disequilibrium during differentiation of the Bandelier Tuff: Constraints on the crystallization of a large rhyolitic magma chamber: Geology, v. 27, no. 6, p. 495-498.

Worner, G., Lezaun, J., Beck, A., Heber, V., Lucassen, F., Zinngrebe, E., Rossling, R., and Wilke, H. G., 2000, Precambrian and Early Paleozoic evolution of the Andean basement at Belen (northern Chile) and Cerro Uyarani (western Bolivia Altiplano): Journal of South American Earth Sciences, v. 13, no. 8, p. 717-737.

Worner, G., Moorbath, S., and Harmon, R. S., 1992, Andean Cenozoic Volcanic Centers Reflect Basement Isotopic Domains: Geology, v. 20, no. 12, p. 1103-1106.

Yuan, X., Sobolev, S. V., and Kind, R., 2002, Moho topography in the central Andes and its geodynamic implications: Earth and Planetary Science Letters, v. 199, no. 3-4, p. 389-402.

Yuan, X., Sobolev, S. V., Kind, R., Oncken, O., Bock, G., Asch, G., Schurr, B., Graeber, F., Rudloff, A., Hanka, W., Wylegalla, K., TIbi, R., Haberland, C., Rietbrock, A., Giese, P., Wigger, P., Rower, P., Zandt, G., Beck, S., Wallace, T., Pardo, M., and Comte, D., 2000, Subduction and collision processes in the Central Andes constrained by converted seismic phases: Nature, v. 408, no. 6815, p. 958-961.

Zandt, G., Leidig, M., Chmielowski, J., Baumont, D., and Yuan, X. H., 2003, Seismic detection and characterization of the Altiplano-Puna magma body, central Andes: Pure and Applied Geophysics, v. 160, no. 3-4, p. 789-807.

Zellmer, G., Turner, S., and Hawkesworth, C., 2000, Timescales of destructive plate margin magmatism: new insights from Santorini, Aegean volcanic arc: Earth and Planetary Science Letters, v. 174, no. 3-4, p. 265-281.

Zellmer, G. F., Blake, S., Vance, D., Hawkesworth, C., and Turner, S., 1999, Plagioclase residence times at two island arc volcanoes (Kameni Islands, Santorini, and

Soufriere, St. Vincent) determined by Sr diffusion systematics: Contributions to Mineralogy and Petrology, v. 136, no. 4, p. 345-357.

Zellmer, G. F., and Clavero, J. E., 2006, Using trace element correlation patterns to decipher a sanidine crystal growth chronology: An example from Taapaca volcano, Central Andes: Journal of Volcanology and Geothermal Research, v. 156, no. 3-4, p. 291-301.

Zellmer, G. F., Rubin, K. H., Dulski, P., Iizuka, Y., Goldstein, S. L., and Perfit, M. R., 2011, Crystal growth during dike injection of MOR basaltic melts: evidence from preservation of local Sr disequilibria in plagioclase: Contributions to Mineralogy and Petrology, v. 161, no. 1, p. 153-173.

Zellmer, G. F., Sparks, R. S. J., Hawkesworth, C. J., and Wiedenbeck, M., 2003, Magma emplacement and remobilization timescales beneath Montserrat: Insights from Sr and Ba zonation in plagioclase phenocrysts: Journal of Petrology, v. 44, no. 8, p. 1413-1431.

APPENDIX A

SUPPLEMENTARY DATA

To obtain the supplementary data for chapters 4 and 6 please click on the DOI for the published manuscript. The supplementary data for chapter 5 can be obtained by contacting the author at garymichelfelder@missouristate.edu.